Synthesis of Aminoquinone Derivatives and Development of Electricity Harvesting Cells using Electron Transfer Reactions

A Thesis

Submitted for the Degree of

DOCTOR OF PHILOSOPHY

By

Ramesh E

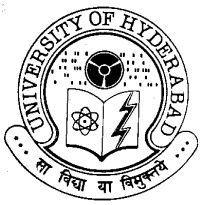

SCHOOL OF CHEMISTRY

UNIVERSITY OF HYDERABAD

HYDERABAD-500 046

INDIA

DECEMBER 2018

Dedicated to

My Teachers and

My Parents

School of Chemistry
University of Hyderabad
Central University P.O.
Hyderabad 500046
Telangana, India

DECLARATION

I, **RAMESH E** hereby declare that this thesis entitled "**Synthesis of Aminoquinone Derivatives and Development of Electricity Harvesting Cells using Electron Transfer Reactions**" submitted by me under the guidance and supervision of **Professor M. Periasamy** is a bonafide research work which is also free from plagiarism. I also declare that it has not been submitted previously in part or in full to this University or any other University or Institution for the award of any degree or diploma. I here by agree that my thesis can deposit in Shodganga/INFLIBNET.

A report on plagiarism statistics from the University Librarian is enclosed.

Date:

Name:

Signature of the Student:

Regd. No.:

Signature of the Supervisor:

School of Chemistry
University of Hyderabad
Central University P.O.
Hyderabad 500046
Telangana, India

CERTIFICATE

This is to certify that the thesis entitled "**Synthesis of Aminoquinone Derivatives and Development of Electricity Harvesting Cells using Electron Transfer Reactions**" submitted by **Mr. Ramesh E** bearing registration number **12CHPH18** in partial fulfillment of the requirements for award of Doctor of Philosophy in the School of Chemistry is a bonafide work carried out by him under my supervision and guidance.

This thesis is free from plagiarism and has not been submitted previously in part or in full to this or any other University or Institution for the award of any degree or diploma. Further the student has four publications before the submission of his thesis.

Parts of this thesis have been published in the following two publications:

1. Periasamy, M.; Edukondalu, A.; Ramesh, E. ***Chemistryselect.***, **2017**, *2*, 3937.

He has also made presentations in the following conferences:

1. Synthesis of Aminoquinone derivatives via Electron Transfer Reactions; Poster Presentation in the *Chemfest-2017* held at School of Chemistry, University of Hyderabad, INDIA.
2. Oxidative Coupling of 2-Naphthols using I_2/O_2 Reagent; Poster Presentation in the *Chemfest-2018* held at School of Chemistry, University of Hyderabad, INDIA.

Further the student has passed the following courses towards fulfillment of coursework requirement for Ph.D.

	Course	Title	Credits	Pass/Fail
1.	CY-801	Research Proposal	3	Pass
2.	CY-805	Instrumental Methods A	3	Pass
3.	CY-806	Instrumental Methods B	3	Pass
4.	CY-821	Organic Reactions and Mechanisms	3	Pass

Hyderabad
Date:

Prof. M. Periasamy
(Thesis Supervisor)

Dean
School of Chemistry
University of Hyderabad
Hyderabad 500 046
INDIA

Ackonwledgements

I take immense pleasure in expressing my heartfelt gratitude and indebtedness to my thesis supervisor **Prof. M. Periasamy** for his constant guidance, inspirations, encouragements and support throughout my tenure here.

I extend my heartfelt thanks toProf. D. Basavaiah, Prof. M. V. Rajasekharan, Prof.M. Durga Prasadand Prof. T. P. Radhakrishan Deans, School of Chemistry, for providing all the necessary facilities to carry out my research work.I am thankful to my doctoral committee members Prof. D. B. Ramachary and Prof. R. Balamuragan for their generous support.

I would like to thank. Mr. C S Reddy. inspiring teaching and encouragement during my MSC, i take this opportunity to thank Mr. Sridhar sir. inspiring teaching during my B.Sc., Chemistry in Jyothi Academy i also thank Mr. chakravarthy (Lecturer) during my inter college Gayathri Vidhyaparashid junior college. I also thanks to K.K.V. Prasad babu excellent teaching. during my School days in St.Peters high School

I wish to thank my senior colleague Dr. A. Edukondalu for his help during the initial stages of my research. I extend my sincere thanks to my past and present labmates Mr. M. Ramusagar, Mr. B. Uday Kumar, Dr. Mallesh Beesu, Dr. Guru Brahmam, Dr. Manasi Dalai, Mr. V. Harish, Mr. G. Ananda rao, Mr. L. Mohan, Mr. E. Ramesh, Mr. Yesu and Mr. Srinivas for creating a pleasant working atmosphere.

All the research scholar of the school of chemistry has been extremely helpful, I thank them all. I specially thank Mr. Majji Shankar, Mr. Koilapu Rambabu, Dr. Ramu Yadav, Dr. Trn Prasad, Mr. Chaithanya, Dr. Shivprasad, Dr. Naveen, Dr. Madhavachary, Dr. Thirupathi, Dr. Lingaiah, Dr. Narendra babu, Mr. Srikanth, Mr. Vinodh, Mr. Surya Narayana, Ms. Laxmipriya, Ms. Kavya joseph and A to Z are to mention.I also thank all my Tamil friends of University of Hyderabad.

All the non-teaching staff of the School has been helpful, I thank them all. Mr. Shetty, Mr. S. Satyanarayana, Mrs. Vijaya Lakshmi, Mr. V. Bhaskar Rao, Mr. Asia Parwez, Mr. Vijaya Bhaskar, Mr. K. R. V. Prasad, Mr. Ramana, Mr. Joseph, Mr. Santoshand, Mr. Sambasiva Rao are a few to mention.

I specially thank all of my M.Sc classmates for their help and thoughtful discussion during my M.Sc., days. Dr. P. Srinivas, K. Jagan Mohan, Vinodh Kumar, Dr. Shankar, Dr. Keshav,

I wish to express my gratitude to my parents Mr. E. Ramadandu and Mrs. E. Mangamma for their support, affections and caring throughout my life. I cannot end without thanking my brothers Mr. D. Govinda naidu, and D. Gopala Krishna, for their love, support and encouragement. and i also thanks to.my sweet sisters Ms. K. Radhamani and Mrs. E. Sandhya for their affections and caring. I specially thank my wife E. Haritha for her affection and caring. I also thank my uncle K.M. Naidu and K.Srinivas Reshita, Teju, Joshivika and family members for their affection.

I wish to extend my sincere thanks to the University authorities for providing all the necessary facility for this work. The X-ray crystallography data were collected in the National Single Crystal X-ray facility funded by DST, New Delhi.

Finally, I would like to thank the UGC, New Delhi for the financial support during my tenure. Also, financial assistance from the research grant of DST-SERB and DST-JC BOSE National fellowship of Prof. M. Periasamy is gratefully acknowledged.

Ramesh E

Contents

Chapter 2

Synthetic Methods based on Electron Transfer Reactions

Chapter 3

Construction of Electricity Harvesting electrochemical cell using *p*-Chloranil, tertiary amines and sulfones

Chapter 4

Electricity Harvesting cell based on reversible electron transfer reaction of *p*-Chloranil with DMSO.

Abbreviations

$[\alpha]_D^{25}$	specific rotation at 25 °C, λ = 589 nm
Ac	acetyl
Al	aluminium
anhyd.	anhydrous
aq.	aqueous
Ar	aryl
Bn	benzyl
BQ	1,4-benzoquinone
BINOL	2,2' bi-2-naphthol
br	broad (in spectroscopy)
CC	cell configuration
cat.	catalytic
Cm^{-1}	wavenumber(s)
CT	charge transfer
CAN	ceric ammonium nitrate
DABCO	1,4-diazabicyclo[2.2.2]octane
DDQ	2,3-dichloro-5,6-dicyano-p-benzoquinone
DiPrBA	*N*,*N*-diisopropylbenzamide
DIPEA	*N*, *N*-diisopropylethylamine
d	doublet (in spectroscopy)
dd	doublet of doublet (in spectroscopy)
de	diastereomeric excess
dr	diastereomeric ratio
DEPT	distortionless enhancement by polarization transfer
DCM	dichloromethane
DMF	*N*,*N*-dimethylformamide
DMSO	dimethyl sulfoxide
ee	enantiomeric excess
EC	ethylene carbonate
EI	electrn impact (in mass spectrometry)
EPR	electron paramagnetic resonance
ET	electron transfer

Et	ethyl
equiv	equivalent
ESI-MS	electronspray ionization mass spectrometry
Et	ethyl
FF	fill factor
h	hour(s)
HMPA	hexamethylphosphoramide
i	iso
IR	infrared
J	coupling constant (in NMR spectroscopy)
liq	liquid
lit.	literature
m	multiplet (in spectroscopy)
Me	methyl
MHz	megahertz
min	minute(s)
mp	melting point
MS	mass spectrum
M.S.	molecular sieves
NMP	N-methyl-2-pyrrolidone
NMR	nuclear magnetic resonance
NQ	1,4-naphthaquinone
ORTEP	Oak Ridge Thermal Ellipsoid Plot
^{i}Pr	isopropyl
PC	propylene carbonate
PEO	polyethylene oxide
Nu	nucleophile
Ph	phenyl
$PhNEt_2$	*N*,*N*-diethylaniline
ppm	parts per million
Pr	propyl
q	quartet (in spectroscopy)
ref	reference number
rt	room temperature

s	singlet (in spectroscopy)
sat.	saturated
sec	secondary
SET	single electron transfer
soln	solution
SS	stainless steel
T	temperature
t	tertiary
t	triplet (in spectroscopy)
THF	tetrahydrofuran
TMPDA	*N,N,N',N'*-tetramethylethylenediamine
TPA	triphenylamine
TMS	trimethylsilyl
TFA	trifluoroaceticacid
UV	ultraviolet
y	yield

Abstract

This thesis entitled "**Synthesis of Aminoquinone Derivatives and Development of Electricity Harvesting Cells using Electron Transfer Reactions**" comprises of four chapters. The work described in this thesis is exploratory in nature. The first chapter describes the **General Introduction**, **References** on electron transfer reactions in organic chemistry. The second, third and fourth chapters are subdivided into four sections namely **Introduction, Results and Discussion**, **Conclusions** and **Experimental section** along with **References.**

The second chapter deals with the results and discussion of the studies undertaken on the synthesis of amino quinones based on electron transfer reactions of *p*-chloranil with amine derivatives.

We have developed a method for the synthesis of monosubstituted *N*,*N* - dialkyl-1-naphthylaminoquinone derivatives **3** by the reaction of *N*,*N*-dialkylnapthalene derivatives **2** with *p*-chloranil **1a** (Scheme 1).

Scheme 1

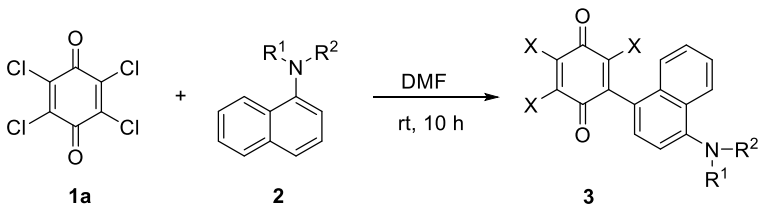

1a **2** **3**

2a) R^1,R^2 = CH_3
2b) R^1,R^2 = C_2H_5
2c) R^1 = CH_3 R^2 = C_2H_5

up to 84% yield

Similarly *N*,*N*-dialkyl naphthalene derivatives **2** react with 3,4,5,6-tetrachloro-1,2-napthoquinone **4** to give the aryloxy products **5** in 58-75% yields (Scheme 2).

Scheme 2

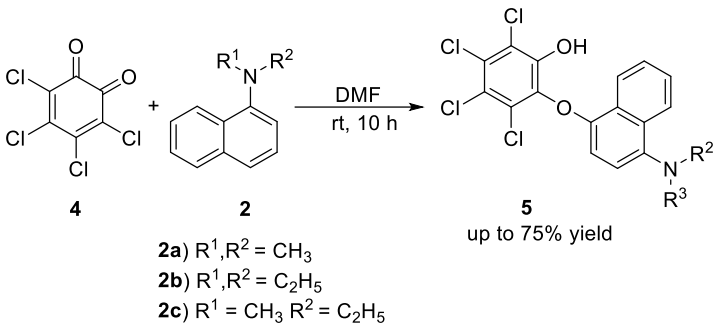

We have developed a method for the synthesis of fused aminoquinone and piperazine derivatives **7a-c** in 30-82% yields by the reaction of *p*-chloranil **1a** with *N*,*N*-dimethyl amino ethanol **6a** and *N*,*N*-dimethylethylenediamine **6b** (Scheme 3).

Scheme 3

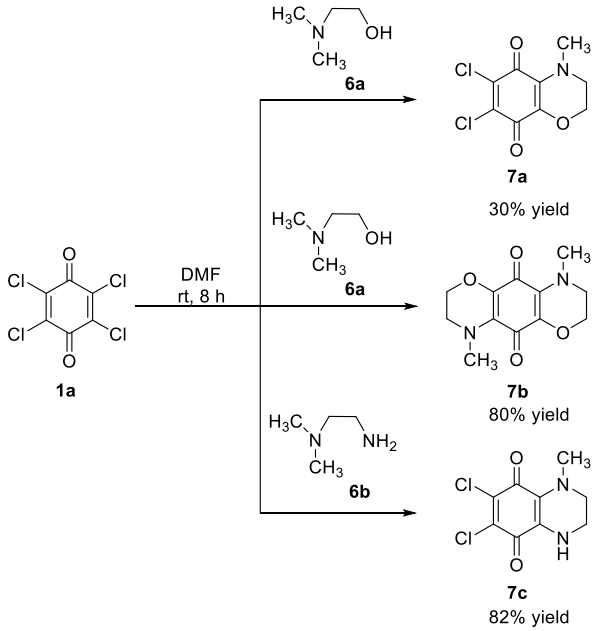

Similarly fused aminoquinone and piperazine derivatives **9a-b** were synthesized by the reaction of 2,3-dichloronaphthaquinone **8a** with *N*,*N*-dimethyl amino ethanol **6a** and *N*,*N*-dimethylethylenediamine **6b** (Scheme 4).

Scheme 4

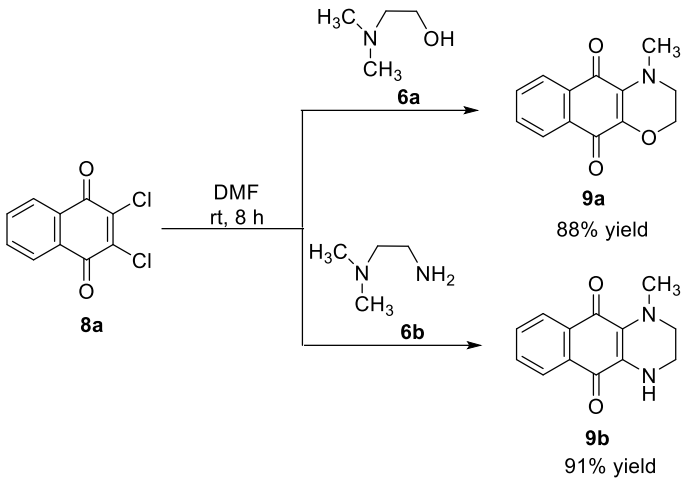

We have also developed a method for the synthesis of chiral tricyclic products **11** in 60-81% yields using quinone derivatives **1** with different cyclic secondary amino alcohols **10** (Scheme 5).

Scheme 5

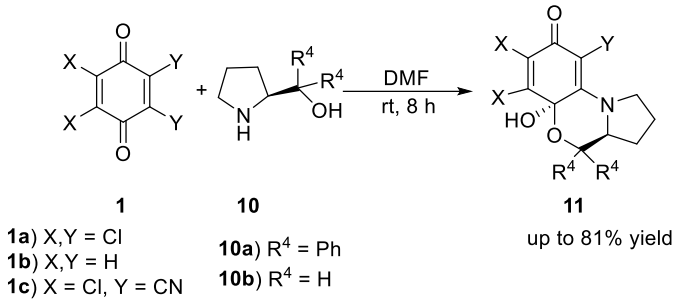

Also, when 2,3-dichloronaphthaquinone **8a** and 1,4-naphthaquinone **8b** was reacted with (*S*)-DPP **10a** in DMF solvent similar tricyclic products **12** were obtained in 62-73% yields (Scheme 6).

Scheme 6

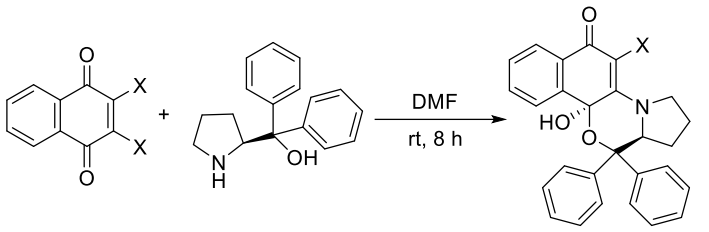

8 **10a** **12**

8a) X = Cl
8b) X = H

62-73% yield

The tricyclic product **13** reacted with TFA to give the aminoquinol product **14** (Scheme 7).

Scheme 7

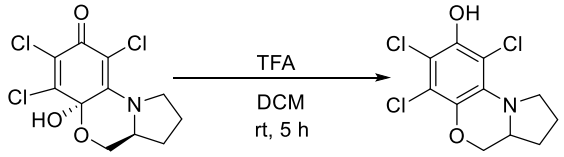

13 **14**

81% yield

The 2-naphthol **15** reacts with *p*-chloranil **1a** and triflouroacetic acid to give bi-2-naphthol **16** in 80% yield (Scheme 8).

Scheme 8

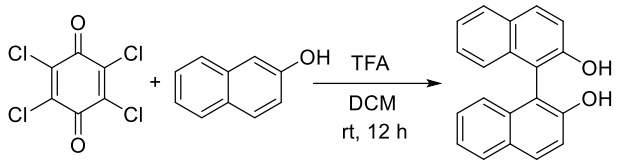

1a **15** **16**

80% yield

We have also developed a method for synthesis of meso-2,3-diphenylpiperazine **20** system (Scheme 9) and examined its use as donor in the electron transfer reaction with *p*-chloranil.

Scheme 9

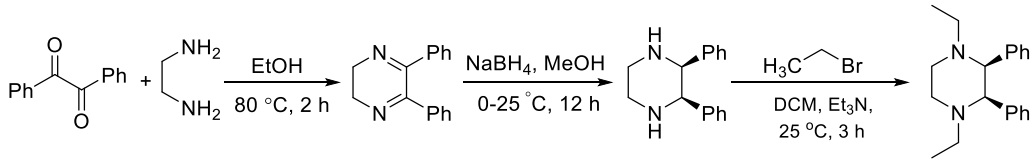

17 **18** **19** **20** (±)-**21**

86% y 90% y

In chapter 3, research efforts toward the construction of electrochemical cells based on the reversible electron transfer reaction of tertiary amines, with *p*-chloranil as electron acceptor and dimethyl sulfone as electron transporter are described (Scheme 10).

Scheme 10

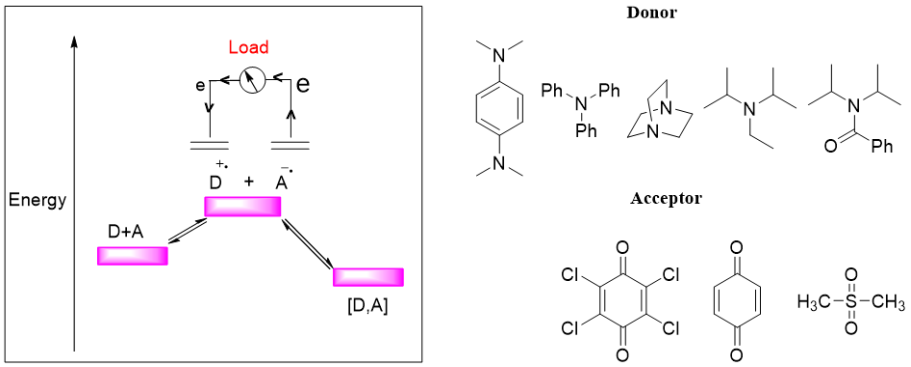

In chapter 4, efforts on the construction of electrochemical cells using DMSO as electron donor and *p*-chloranil as electron acceptor with benzoquinone (BQ) and dimethyl sulfone as electron transporter are described. The results are presented and discussed considering the intermediates and mechanisms involved in these transformations. Experimental and spectral data are provided in the experimental sections in chapters 2, 3 and 4.

Representative ^{1}H-NMR, ^{13}C-NMR spectra, are presented in Appendix-I and the X-ray crystallographic data are listed in Appendix-II

Note: Scheme numbers and compound numbers given in this abstract are different from those given in the chapters.

Chapter 1

General Introduction to Electron Transfer Reactions

1.1 Introduction

Electron transfer reactions play key role in many biological processes, like drug activation, metabolism, respiration and photosynthesis.[1] Such reactions involve the transfer of an electron from donor to an acceptor. Electron transfer reactions can take place thermally and photochemically.[2] There are two main processes involving transfer of charges in chemical and biological reactions.[3-5] One is a polar process and another is a single electron transfer (SET) process. The electron transfer reactions are also very important in the development of semiconductors,[6] polymers[7] and for solar energy conversion.[8]

1.1.1 Redox reactions through electron transfer

Samarium iodide (SmI_2), is a unique one electron transfer reducing agent. It is used as a versatile reducing agent in several organic reactions. In these reactions, radicals are generated through the reduction of organohalides or carbonyl compounds as outlined in Chart 1.[9]

Chart 1

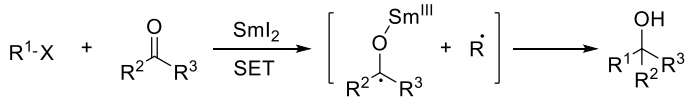

1 **2** **3** **4**

R^1, R^2, R^3 =Alkyl
X= Br,I

Chart 1 (continued.)

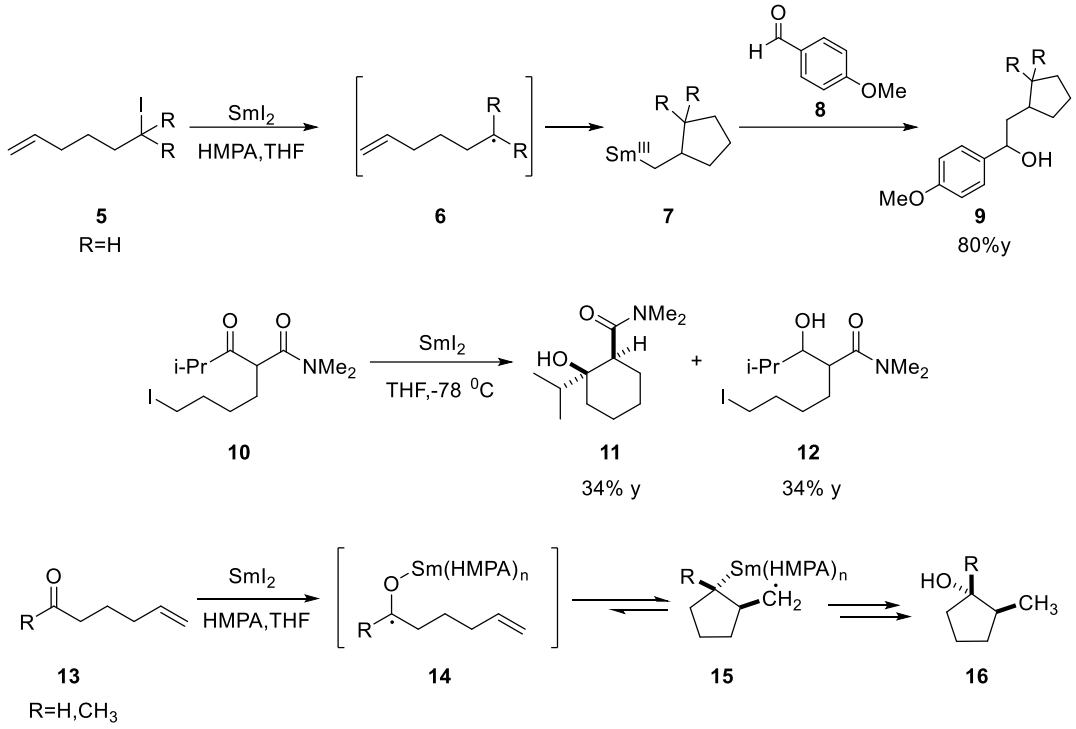

Recently, MacMillan *et al* reported several organic transformations using ceric ammonium nitrate (CAN) which take place through single electron transfer (SET) mechanisim Chart 2.[10-13]

Chart 2

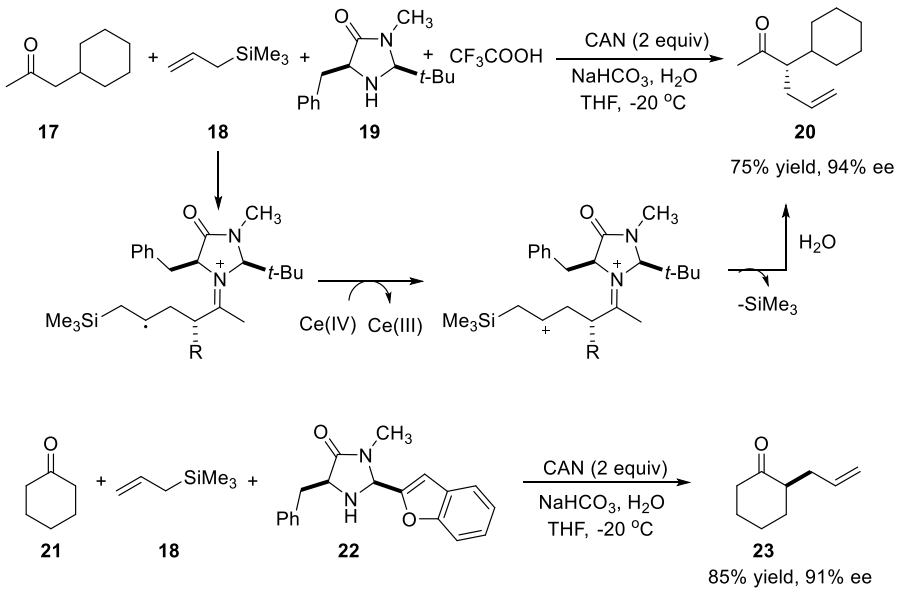

Chart 2 (continued.)

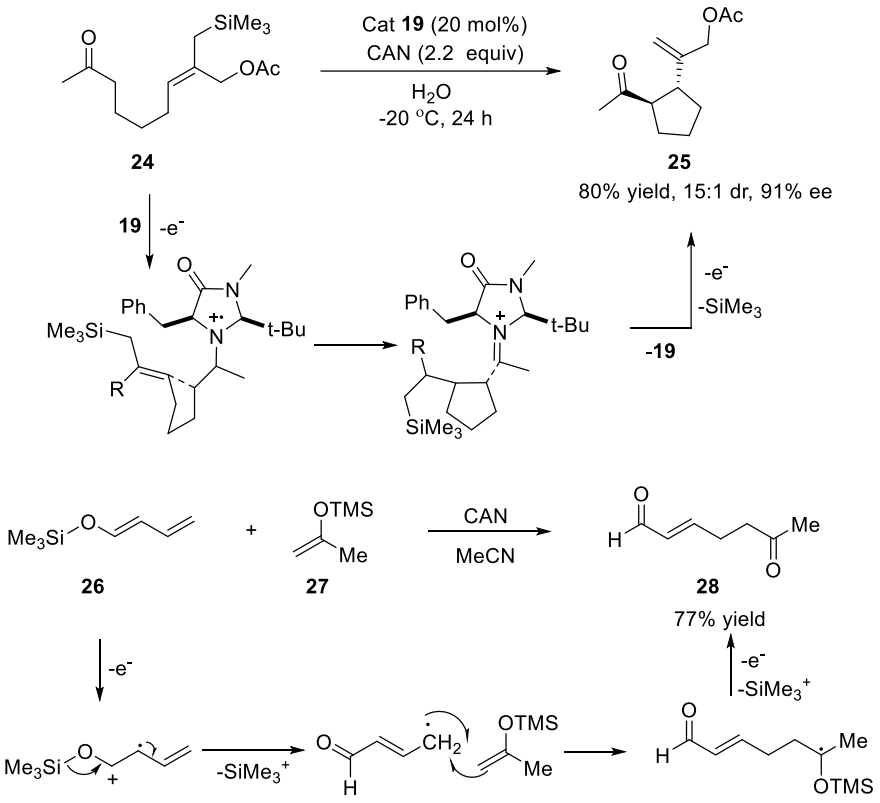

1.1.2 SET reactions involving metal hydrides

Ashby *et al.* reported[14] the SET reduction of primary halides by metal hydrides. They observed that the reaction of 1-iodo-5-hexene **29** with $LiAlH_4$ in THF solvent gave 1-hexene **30** but in the reaction of 1-iodo-2,2-dimethyl-5-hexene **32** with $LiAlH_4$, the cyclized product **36** was obtained as major product besides the minor product 5,5-dimethyl-1-hexene **35.** They proposed SET mechanism for the formation of cyclized product (Scheme 1).

Scheme 1

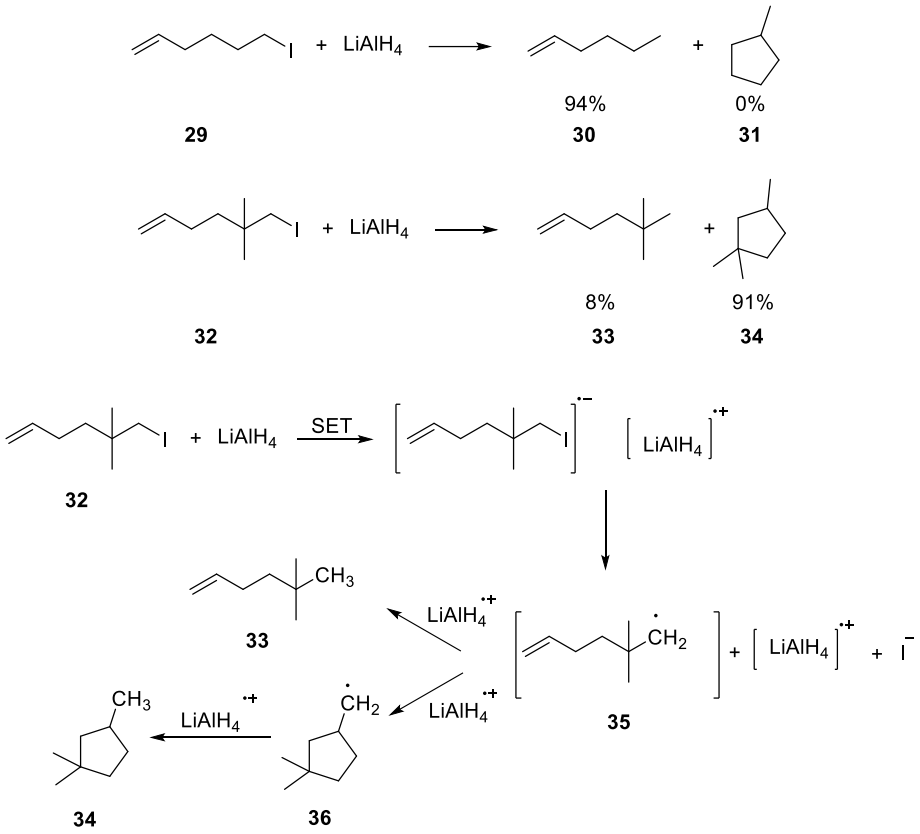

1.1.3 Electron transfer reactions in electrochemical processes

In 1834, Faraday first reported the production of ethane by the electrolysis of aqueous acetate solution. Kolbe observed that the anodic oxidation of carboxylate lead to decarboxylation and the radical intermediates combined to form a hydrocarbon (Scheme 2).[15]

Scheme 2

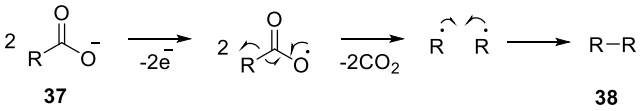

The anodic and cathodic processes were utilized in the synthesis of some useful organic products including biologically active compounds (Chart 3).[16-26]

Chart 3

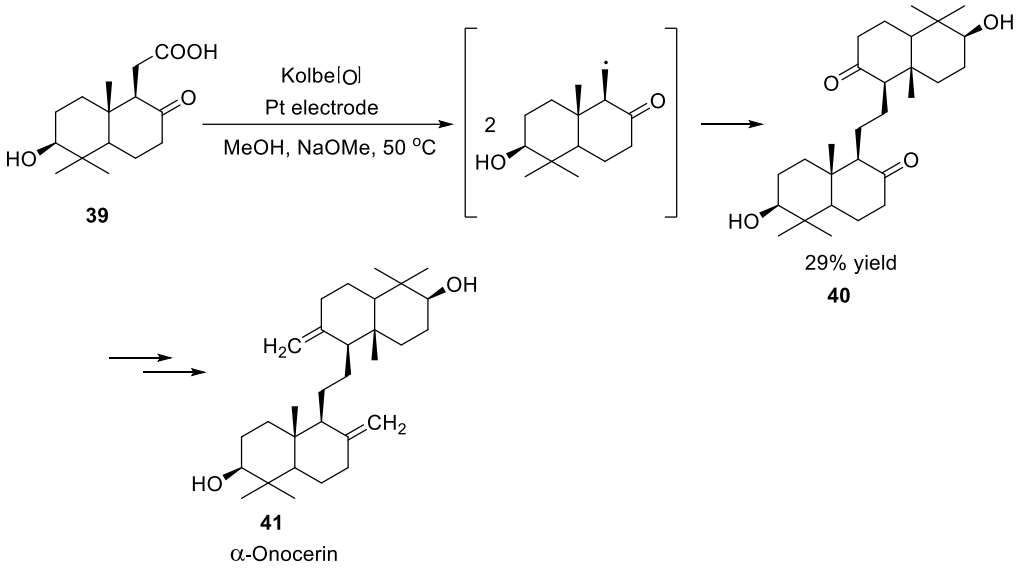

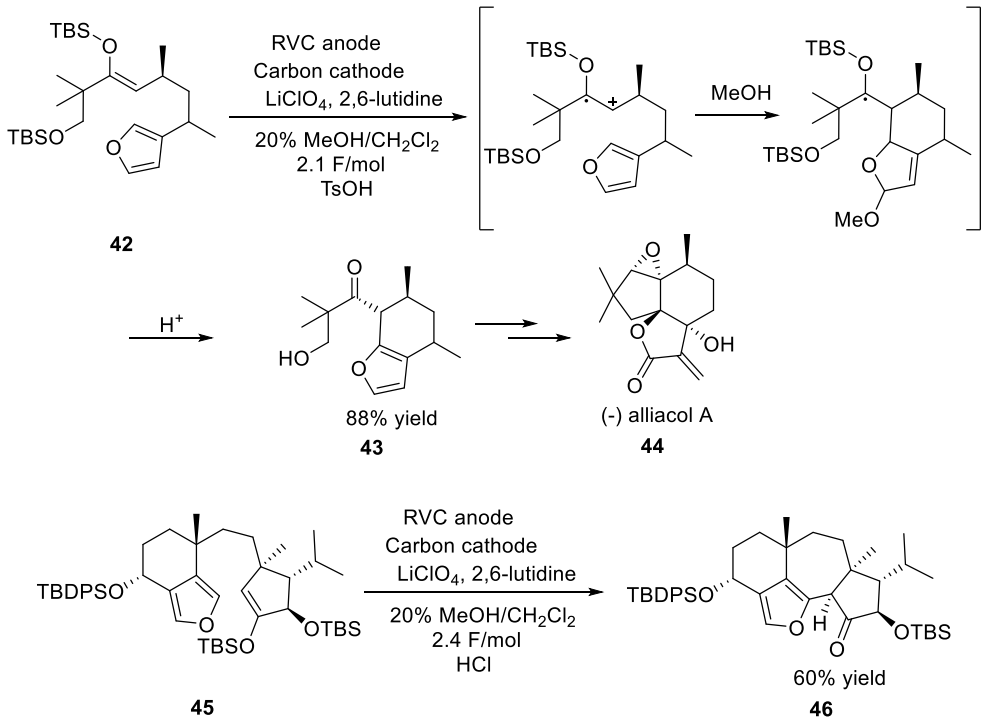

Chart 3 (continued.)

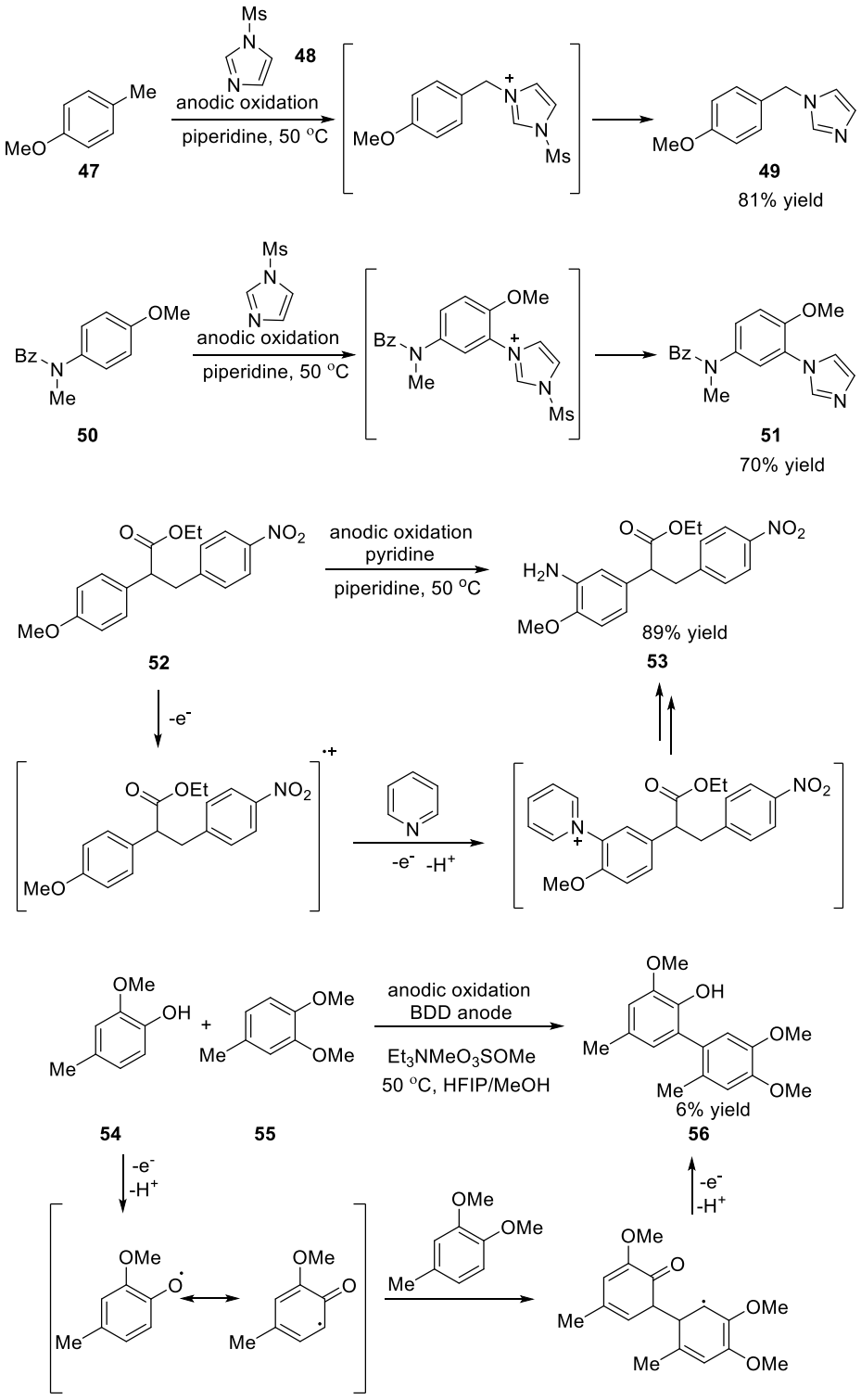

Chart 3 (continued.)

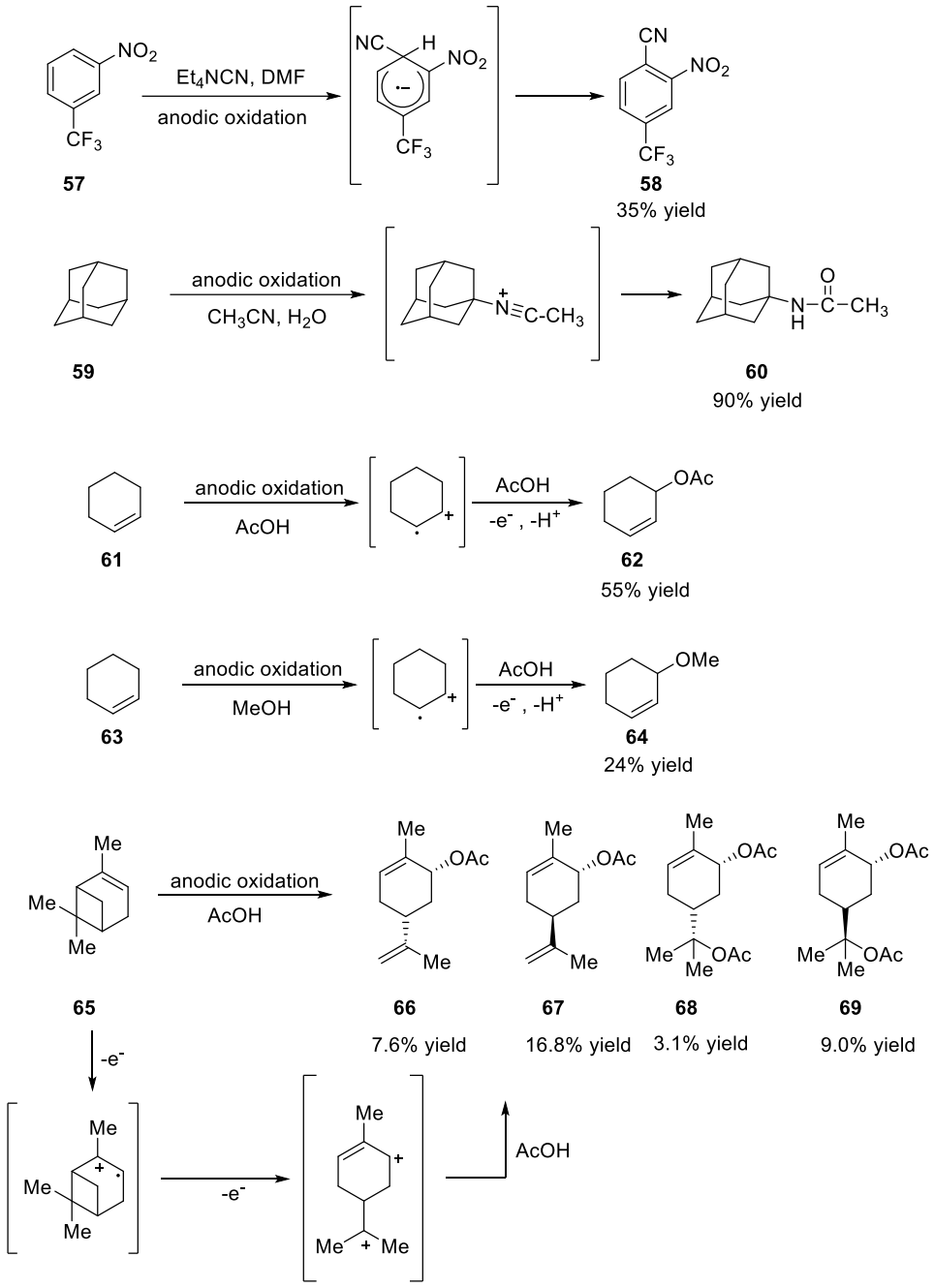

Chart 3 (continued.)

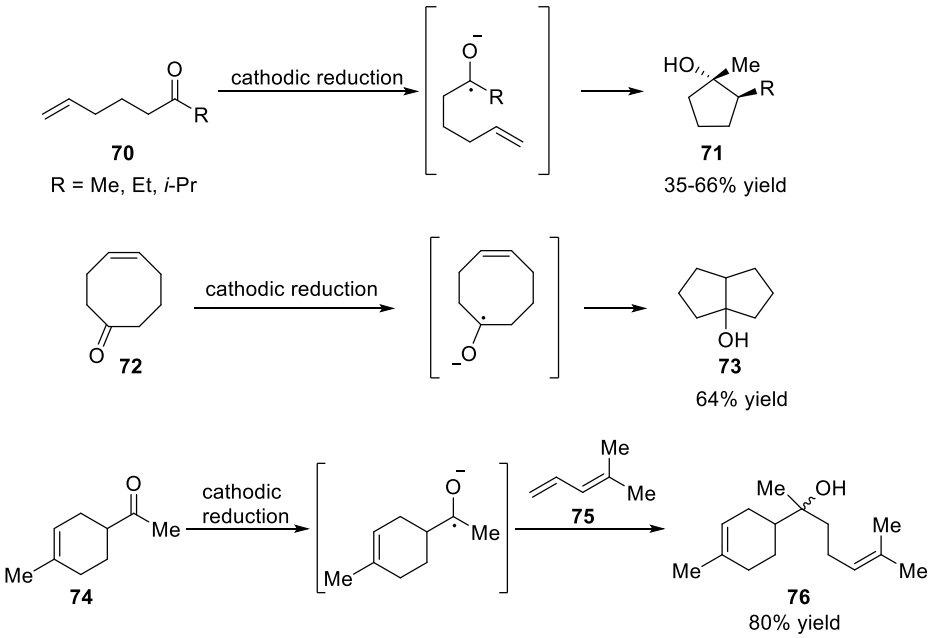

1.1.4 Electron transfer reactions in photochemical processes

Recently, there have been several reports on the application of electron transfer reactions in organic synthesis using amines under photoredox catalysis Chart 4.[27-31]

Chart 4

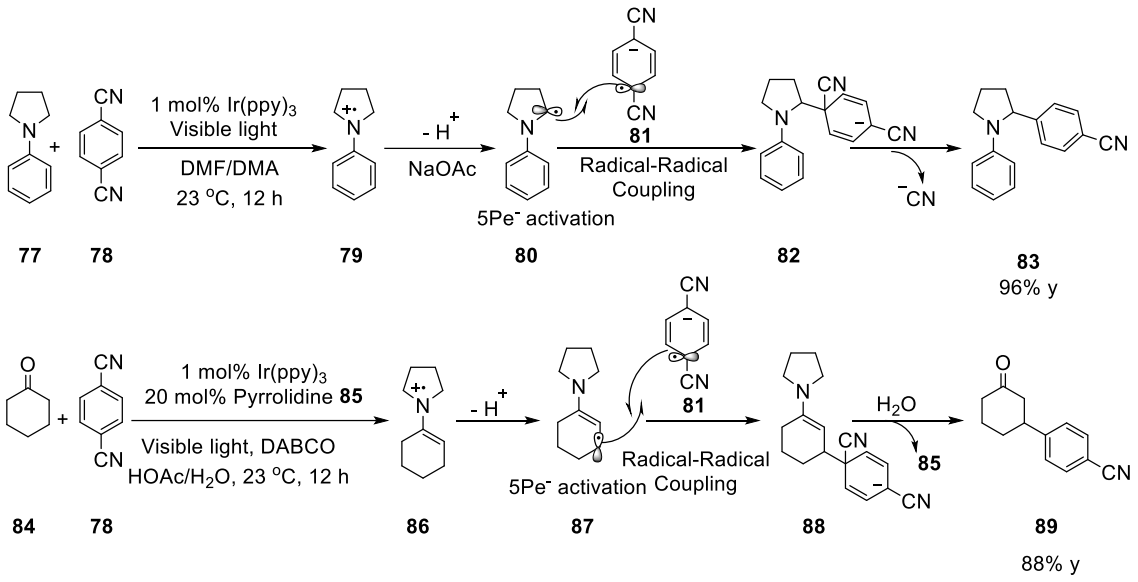

Chart 4 (continued.)

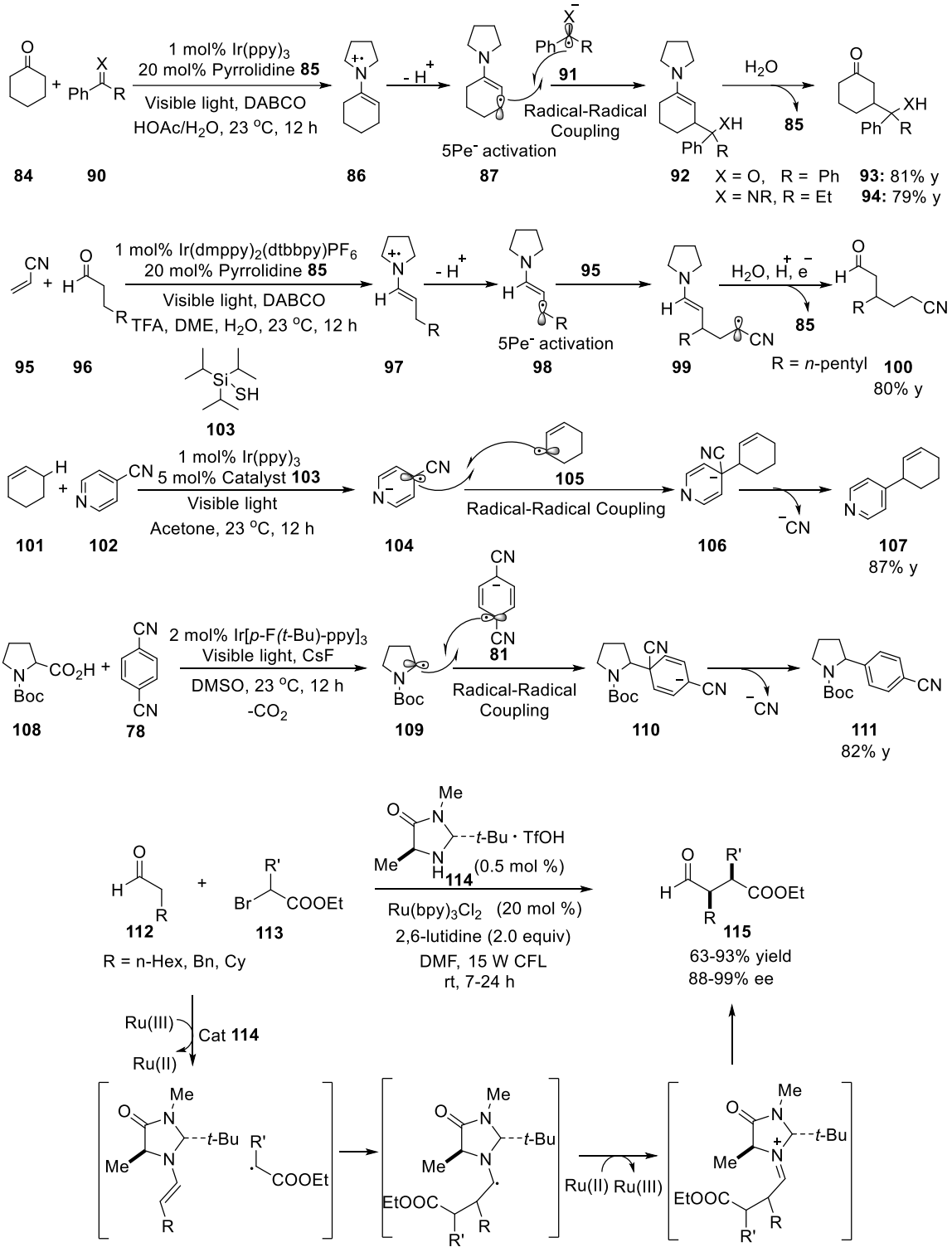

Chart 4 (continued.)

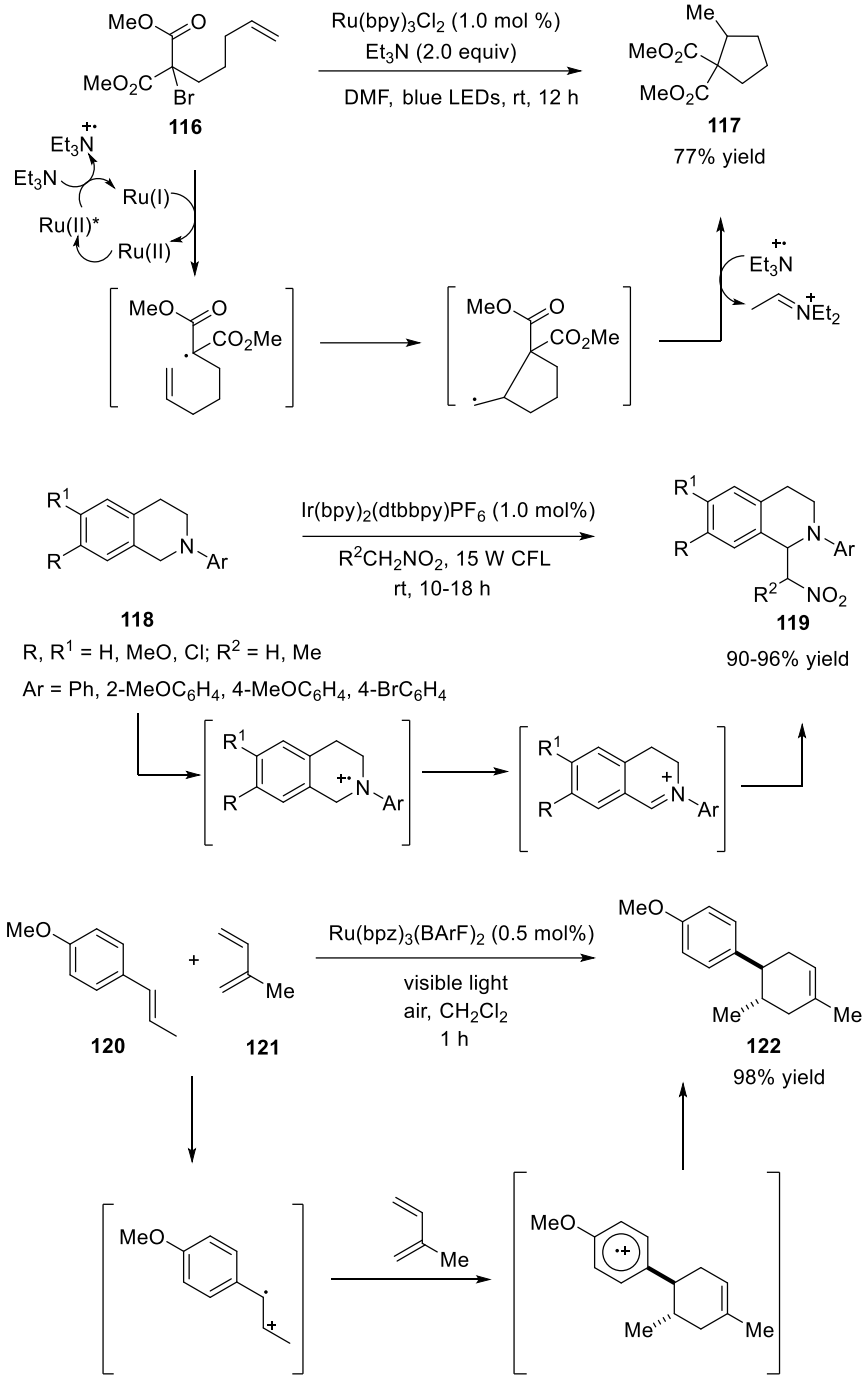

1.1.5 SET reactions in Grignard reagent formation

Alkyl halides react with magnesium to give Grignard reagents. The reaction proceeds through a SET process (Scheme 3).[32]

Scheme 3

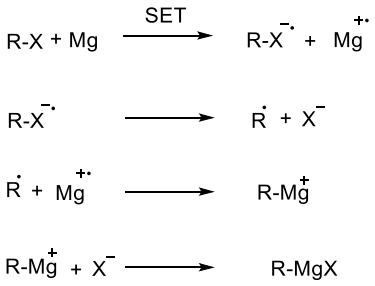

Carbonyl compounds react with Grignard reagent to give the corresponding alcohols. The reactions go through SET mechanism, especialy when there is steric hindrance (Chart 5).[33-36]

Chart 5

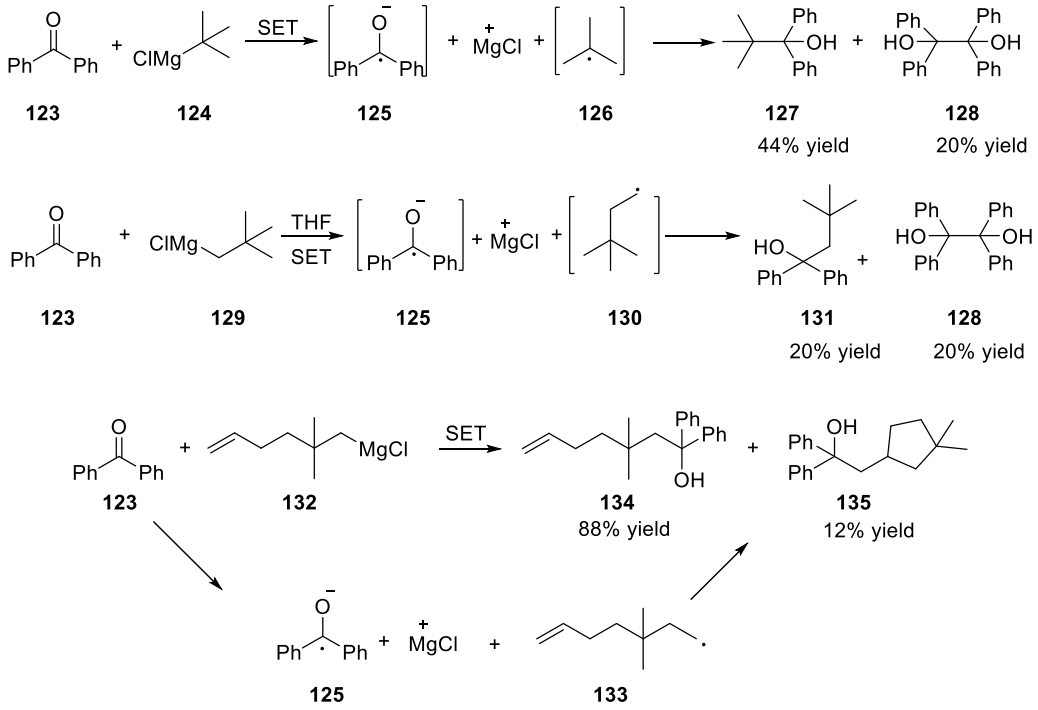

Chart 5 (continued.)

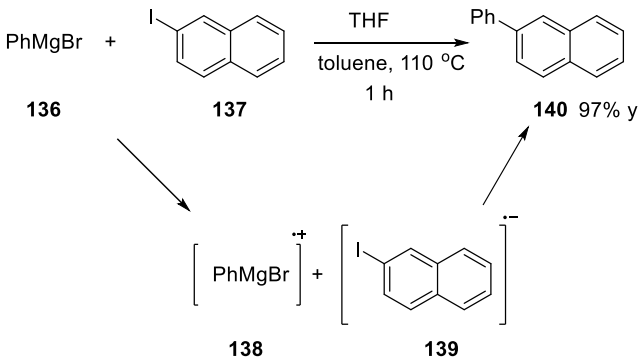

1.1.6 SET process in Aldol Condensasition

Generally, Aldol condensasition takes place through polar mechanism but when there is steric hindrance the reaction goes through single electron transfer pathway as reported by Ashby *et al*. (Scheme 4).[37]

Scheme 4

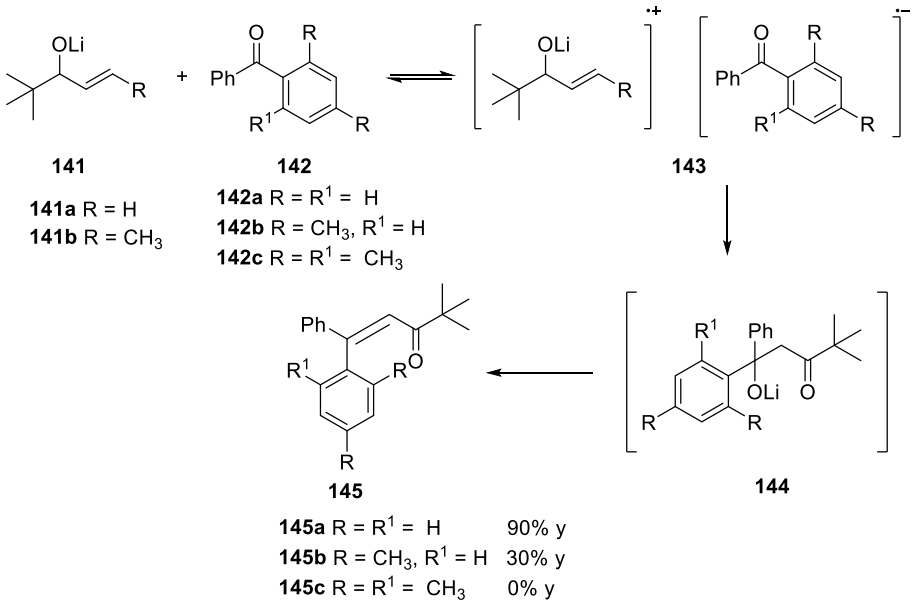

1.1.7 SET reactions in Cannizzaro reaction

The Cannizzaro reaction is a redox reaction in which two molecules of benzaldhyde **146** react with a strong base (e.g. KOH) to produce benzyl alcohol **148** and potassium benzoate **149** (Scheme 5).[38]

Scheme 5

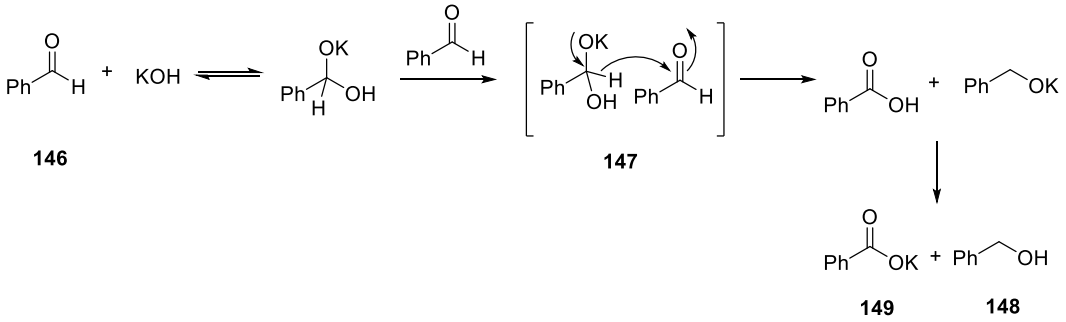

146 **147** **149** **148**

Ashby *et a.l*[39] provided evidence for formation of paramagnetic intermediates and for radical cyclization in Cannizzaro reactions. For example, the reaction of two molecules of 2-methyl benzaldehyde **150** with sodium hydroxide base leads to the formation of 2-methyl benzylalcohol **152**, 2-methyl benzoicacid **151** and along with cyclized product **153** (Scheme 6).

Scheme 6

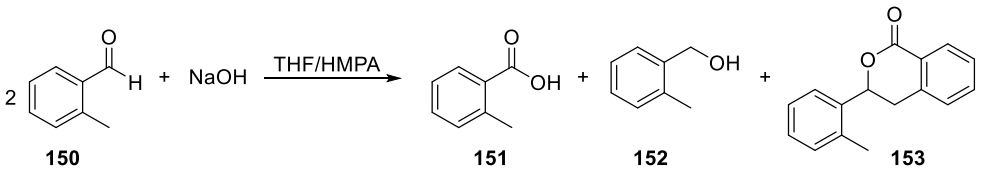

150 **151** **152** **153**

The lactone product **153** is formed through SET mechanism as outlined in Scheme 7.

Scheme 7

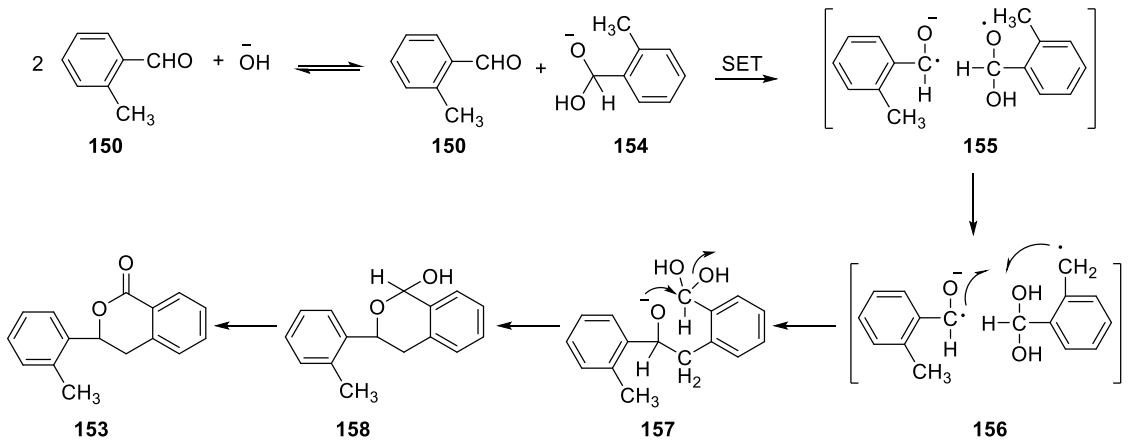

1.1.8. SET reactions in Claisen condensation

The Claisen condensation reaction of two ester molecules with an alkoxide base gives a *β*-ketoester (Scheme 8).[40]

Scheme 8

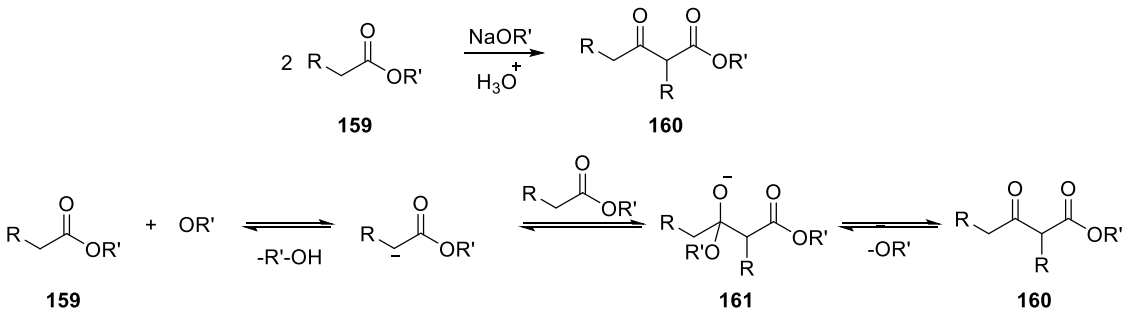

In 1983, Ashby *et al.* reported[41] that the Claisen condensation reaction of ethyl *p*-benzoate **162** with lithium enolate of pinacolone **163** gave the product **165** and the intermediacy of paramagnetic species **164** was confirmed by epr experiments (Scheme 9).

Scheme 9

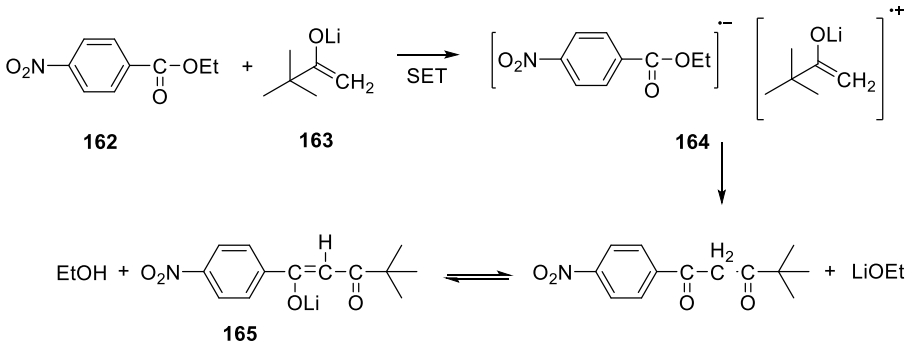

1.1.9 SET reactions in Birch reduction

Birch *et al.* reported [42] that substituted benzene derivatives react with Na metal in liquid ammonia to give the corresponding unconjugated cyclohexadienes (Scheme 10).

Scheme 10

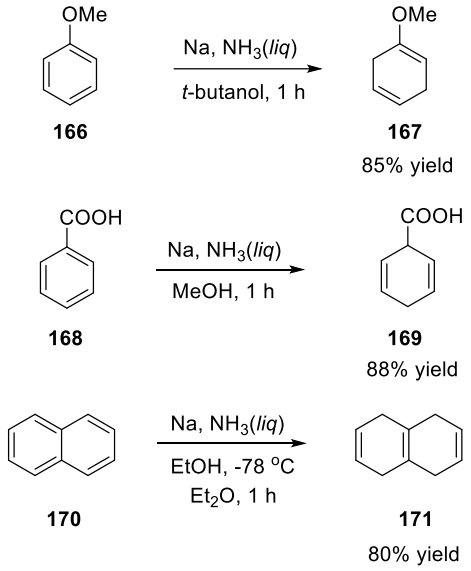

The Birch reaction goes through a SET process. The electron transfer from Na metal to the benzene ring **172** would give a radical anion **173** which after protonation by alcohol followed by further reduction and protonolysis lead to the formation of 1, 4-cyclohexadiene **174** (Scheme 11).

Scheme 11

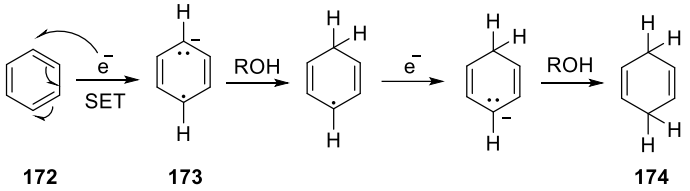

In Birch reductions, the electron withdrawing (W) groups lead to reduction at the *ipso* and *para* positions and the electron donating (D) groups lead to reduction at the *ortho* and *meta* positions (Scheme 12).

Scheme 12

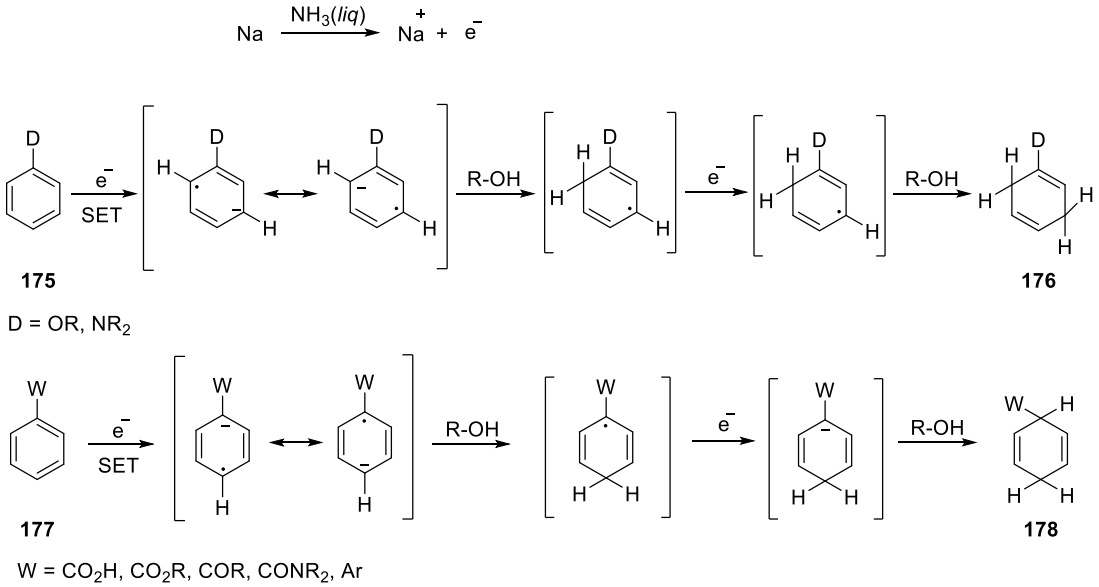

1.1.9.1 SET process in Organic Donor and Acceptor systems

Single electron transfer (SET) and polar processes are two main processes involved in charge transfer reactions in organic chemistry (Scheme 13).

Scheme 13

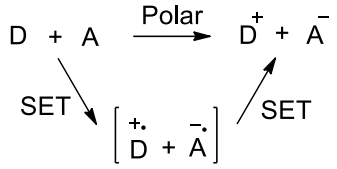

Mulliken's charge transfer theory,[43] Taube's outer-sphere/inner-sphere mechanisms[44] and Marcus's two state non adiabatic theory[45] are most important theories in electron transfer reactions in chemistry. Noncovalent interactions are interactions between molecules that stabilize the association of two or more molecules without forming ionic or covalent bonds. Aromatic systems play a major role in biological reactions through noncovalent interactions. Interactions like electrostatic, charge transfer, dispersion (Van der Walls), hydrophobic interaction contribute to noncovalent molecular interactions.

A complex between two organic molecules in which charge transfer takes place from one molecule (donor) to the other molecule (acceptor) is called charge transfer (CT) complex or electron donor acceptor-complex. The electron donor should have low ionization potential and electron acceptor should have high electron affinities. Charge transfer complexes have a neutral ground state when there is only partial electron transfer from donor to acceptor molecule.

Mulliken *et al.* reported [46] that the diffusive interaction of electron rich donor (D) with electron poor acceptor (A) gave a reversible complex [D, A] (Scheme 14).

Scheme 14

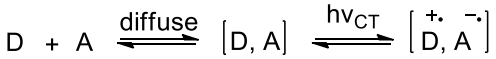

The energy levels of HOMO and LUMO play an important role in electron transfer reactions. The LUMO of the electrophilic reagents (acceptor) such as NO_2^+ and Br^+ are lower than the HOMO of aromatic molecules (Donor) and hence readily undergoes electrophilic substitution reactions. For example, benzene reacts with NO_2^+ to form nitrobenzene **180** *via* the formation of radical intermediate **179** (Scheme 15).[47]

Scheme 15

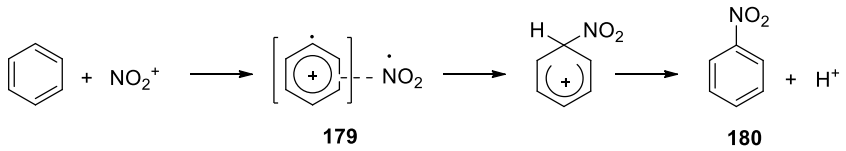

Taube proposed that both outer-sphere and inner-sphere process are involved in electron transfer reactions.Taube *et al.* reported [48] that in the reaction of chromium complex **181**with cobalt complex **182**, the electron transfer from Cr(II) to Co(III) takes place *via* a bridged intermediate **183** to give the green chromium complex **184** and cobalt complex **185** (Scheme 16). The electron transfer is accompanied by the transfer chloride ligand. This process occurs *via* inner-sphere electron transfer.

Scheme 16

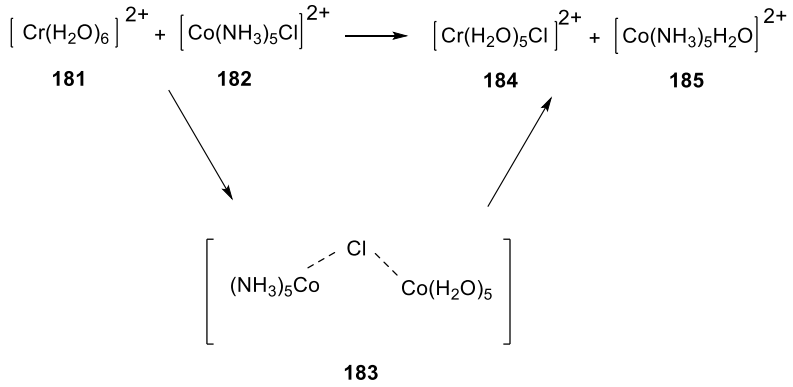

In outer-sphere electron transfer process, the organic compounds can accept or loose an electron without undergoing structural changes like bond cleavage or bond

formation. For example, nitrobenzene **180** can accept one electron to form nitrobenzene radical anion **186** without undergoing any structural change (Scheme 17).[49]

Scheme 17

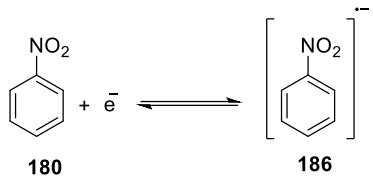

180 **186**

Marcus described that in outer-sphere mechanism, the donor (D) and acceptor (A) diffuse together to form an outer sphere precursor complex (D/A) **187** which reorganizes towards a transition state in which electron transfer takes place to form a successor complex ($D^{+\cdot}/A^{-\cdot}$) **188** that can further dissociate to give the corresponding ion pairs **189** (Scheme 18).[50]

Scheme 18

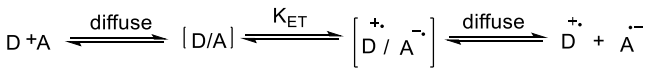

187 **188** **189**

1.1.9.2 SET and Polar Process in Quinone Chemistry

Quinone redox systems play major role in biological reactions.[51] Quinones undergo $2H^+/2e^-$ reduction in aqueous solution (or) in protic solvents.[52] The redox process of hydroquinone - quinone is a sequence of proton and electron transfer (Fig 1). In the first step, deprotonation takes place to form a phenoxide ion which is transformed into a phenoxy radical by a one-electron oxidation, then dissociation of the second OH group generates the radical anion semiquinone followed by a second one-electron oxidation to give benzoquinone. All intermediates are resonance stabilized.

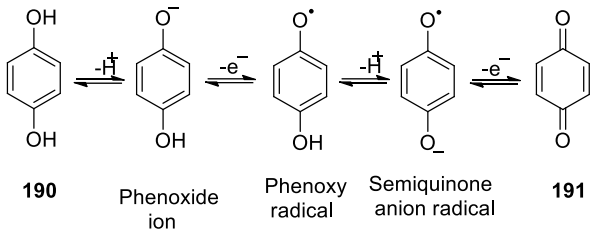

Figure 1. The redox process of hydroquinone – quinone system.

In nonaqueous (or) aprotic conditions, the quinone reduction proceeds through two consecutive single electron reductions (Fig 2).

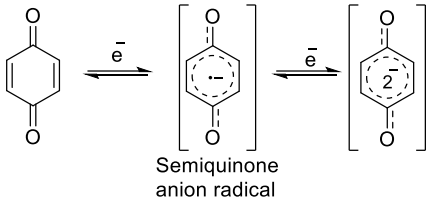

Figure 2. Quinone reduction in aprotic medium.

1.1.9.3 Addition and substitution reactions of quinone

In 1844, the first addition reaction of benzoquinone **191** with hydrogen chloride was reported by Wöhler (Scheme 19).[53]

Scheme 19

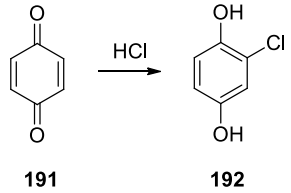

1.1.9.4 Addition and substitution reaction of quinones with amines

The reaction of various substituted anilines **193** with 1,4- benzoquinone **191** gives the addition products of 1,4- benzoquinone (Scheme 20).[54]

Scheme 20

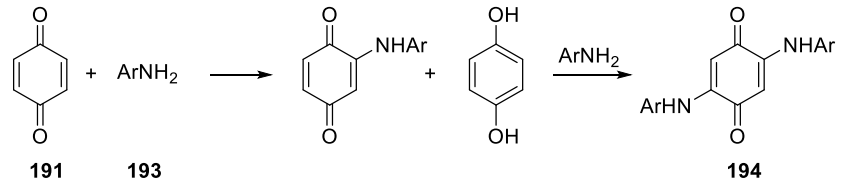

Similarly, Nagakura and coworkers reported[55] that *p*-chloranil **195** reacted with substituted aniline derivatives to form the corresponding aminoquinone products. They proposed that the outer (π)-complex **197** was formed first followed by the inner (σ)-complex **198** (Scheme 21).

Scheme 21

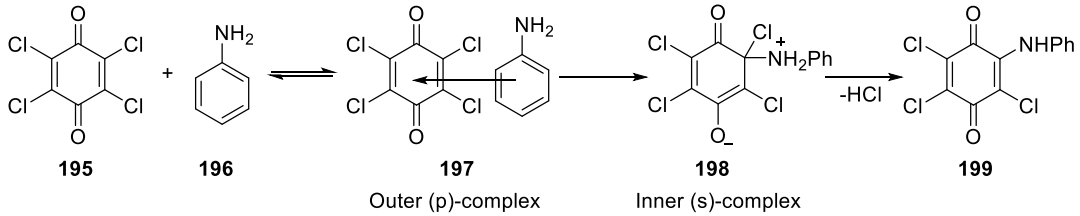

Yamaoka and Nagakura reported [56] that the reaction of *p*-chloranil **195** with n-butyl amine **200**, gave the substituted aminoquinone products. Here, the electron transfer takes place from n-butylamine **200** to *p*-chloranil **195** (Scheme 22).

Scheme 22

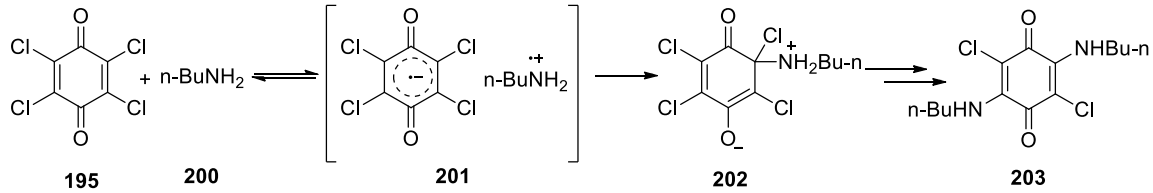

1.1.9.5 Charge Transfer and Electron Transfer Reactions of Quinones

It was reported that DABCO **204** reacted with *p*-chloranil **195** in benzene solvent to give DABCO-chloranil 1:1 complex. The reactions of *p*-chloranil or *p*-bromanil with

DABCO also gave paramagnetic species **205** in benzene and in THF solvents (Scheme 23).[57]

Scheme 23

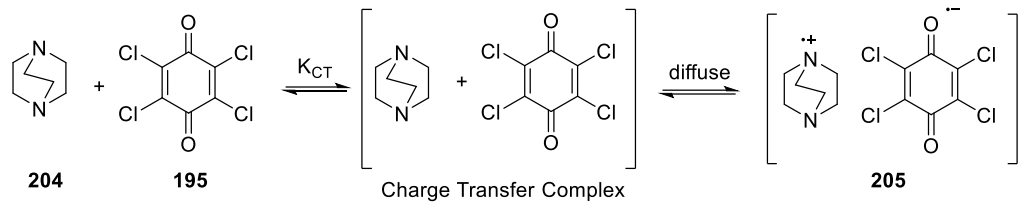

p-Chloranil **195** reacts with diclofenac **206** to form the charge transfer complex **207**. The charge transfer complex was further converted to radical ion pair **208** in methanol solvent (Scheme 24).[58]

Scheme 24

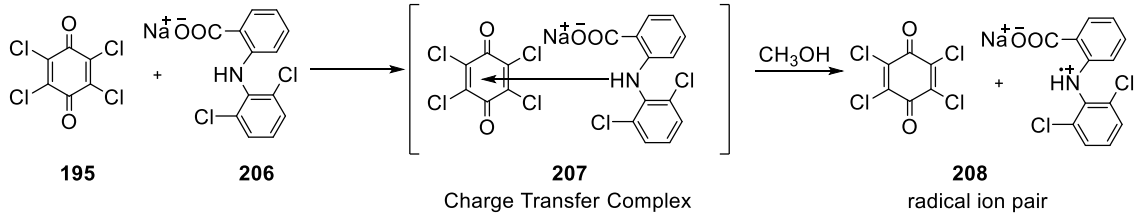

We have developed several new synthetic methods based on reaction of amine derivatives with *p*-chloranil. The results are described in Chapter 2.

1.2 References

1 (a) Hsiao, C.; Chou, I. C.; Okafor, C. D.; Bowman, J. C.; O'Neill, E. B.; Athavale, S. S.; Petrov, A. S.; Hud, N. V.; Wartell, R. M.; Harvey, S. C.; Williams, L. D. *Nature Chemistry.* **2013**, *5*, 525. (b) Bobst, A. M. *Proc. Nat. Acad. Sci. USA.* **1971**, *68*, 541. (c) Sjulstok, E.; Olsen, J. M. H.; Solov'yov, I. A. *Scientific Reports.* **2015**, *5*, 18446. (d) Grimes, C. J.; Piszkiewicz, D.; Fleischer, E. B. *Proc. Nat. Acad. Sci. USA.* **1974**, *71*, 1408.

2 (a) Kestner, N, R.; Logan, J.; Jortner, J. *J. Phys. Chem.* **1996**, *100*, 19740. (b) Penfield, K. W.; Miller, J. R.; Row, M. N. P.; Cotsaris, E.; Oliver, A. M.; Hush, N. S. *J. Am. Chem. Soc.* **1987**, *109*, 5061. (c) Meyer, T. J. *Acc. Chem. Res.* **1978**, *11*, 94. (d) Hush, N. S. Electrochemica Acta, **1968**, *13*, 1005. (e) Hopfield, J. J. *Proc. Nat. Acad. Sci. USA.* **1974**, *71*, 3640. (f) Blankenship, R. E.; Parson, W. W. *Ann. Rev. Biochem.* **1978**, *47*, 635. (g) Poole, J. S.; Hadad, C. M.; Platz, M. S.; Fredin, Z. P.; Pickard, L.; Guerrero1, E. L.; Kessler, M.; Chowdhury, G.; Kotandeniya, D.; Gates, K. S. Photochemistry and Photobiology. **2002**, *75*, 339. (h) Schuster, O. I.; Brisimitzakis, A. C. *Tetrahedron Lett*. **1982**, *23*, 4531. (i) Cossy, J.; Belotti, D. *Tetrahedron.* **2006**, *62*, 6459. (j) Hoffmann, N. *Journal of Photochemistry and Photobiology C: Photochemistry Reviews.* **2008**, *9*, 43.

3 (a) Cenas, N.; Anuservicius, Z.; Bironaite, D.; Bachmanova, G. I.; Archakov, A.; Ollinger, K. *Archives of Biochemistry and Biophysics*, **1994**, *315*, 400. (b) Hill, B. C. *J. Biol. Chem.* **1994**, *269*, 2419. (c) Grimes, C. J.; Piszkiewicz, D.; Fleischer, E. B. *Proc. Nat. Acad. Sci. USA.* **1974**, *71*, 541.

4 (a) Batie, C. J.; Kamin, H. *J. Biol. Chem.* **1984**, *259*, 11976. (b) Moreno, C. G.; Julvez, M. M; Medina, M.; Hurley, J. K.; Tollin. G. *Biochimie*, **1998**, *80*, 837.

5 Hagelueken, G.; Wiehlmann, L.; Adams, T. M.; Kolmar, H.; Heinz, D. W.; Tummler, B.; Schubert, W. D. *Proc. Nat. Acad. Sci.USA.* **2007**, *104*, 12276.

6 (a) Koval, C. A.; Howard, J. N. *Chem. Rev.* **1992**, *92*, 411. (b) Lewis, N. S. *J. Phy. Chem. B.* **1998,** *102*, 4843. (c) Corvan, J. R. C.; Whitten, D.G.; McLendon, G.L. *Chemical Physics.* **1993**, *176*, 377. (d) Tvrdy, K.; Frantsuzovc, P. A.; Kamata, P. V. *PNAS*, **2011**, *108*, 29.

7 Zhang, N.; Samanta, S. R.; Rosen, B. M.; Percec, V. *Chem. Rev.* **2014**, *114*, 5848.

8 (a) Lewis, N. S.; Nocera, D. G. *PNAS*, **2006**, *103*, 15729. (b) Gratzel, G. *Inorg. Chem.* **2005**, *44*, 6841.

9 Procter, D. J.; Flowers, R. A.; Skrydstrup, T. Organic synthesis using samarium dioxide.

10 Beeson, T. D.; Mastracchio, A.; Hong, J. B.; Ashton, K.; MacMillan, D. W. C. *Science*, **2007**, *316*, 582.

11 Mastracchio, A.; Warkentin, A. A.; Walji, A. M.; MacMillan, D. W. C. *Proc. Nat. Acad. Sci.* **2010**, *107*, 20648.

12 (a) Pham, P. V.; Ashton, K.; MacMillan, D. W. C. *Chem. Sci.*, **2011**, *2*, 1470. (b) Conrad, J. C.; Kong, J.; Laforteza, B. N.; MacMillan, D. W. C. *J. Am. Chem. Soc.* **2009**, *131*, 11640.

13 Paolobelli, A. B.; Latini, D.; Ruzziconi, R. *Tetrahedron Letters*. **1993**, *34*, 721.

14 Ashby, E. C.; DePriest, R. N.; Goel, A. B. *Tetrahedron Letters.* **1981**, *22*, 1763.

15 Kolbe, H. *Annalen der chemie und pharmacie.* **1848**, *64*, 339.

16 Stork, G.; Davies, J. E.; Meisels, A. *J. Am. Chem. Soc.* **1959**, 5516.

17 Mihelcic, J.; Moeller, K. D. *J. Am. Chem. Soc.* **2004**, *126*, 9106.

18 Hughes, C. C.; Miller, A. K.; Trauner, D. *Org. Lett.*,**2005**, *7*, 3425.

19 Morofuji, T.; Shimizu, A.; Yoshida, J. I. *J. Am. Chem. Soc.* **2014**, *136*, 4496.

20 Morofuji, T.; Shimizu, A.; Yoshida, J. I. *J. Am. Chem. Soc.* **2013**, *135*, 5000.

21 Kirste, A.; Elsler, B.; Schnakenburg, G.; Waldvogel, S. R. *J. Am. Chem. Soc.* **2012**, *134*, 3571.

22 Gallardo, I.; Guirado, G.; Marquet, J. *Chem. Eur. J.* **2001**, *7*, 1759.

23 Koch, V. R.; Miller, L. L. *J. Am. Chem. Soc.* **1973**, 8631.

24 Shono, T.; Ikeda, A. *J. Am. Chem. Soc.* **1972**, 7892.

25 Shono, T.; Mitani, M. *J. Am. Chem. Soc.* **1971**, 5284.

26 (a) Shono, T.; Kashimura, S.; Mori, Y.; Hayashi, T.; Soejima, T.; Yamaguchi, Y. *J. Org. Chem.* **1989**, *54*, 6001. (b) Shono, T. *Tetrahedron.* **1984**, *40*, 811.

27 (a) Beeson, T. D.; Mastracchio, A.; Hong, J.-B.; Ashton, K.; MacMillan, D. W. C. *Science* **2007**, *316*, 582. (b) McNally, A.; Prier, C. K.; MacMillan D. W. C. *Science* **2011**, *334*, 1114. (c) Pirnot, M. T.; Rankic, D. A.; Martin, D. B. C.; MacMillan, D. W. C. *Science* **2013**, *339*, 1593. (d) Petronijević, F. R.; Nappi, M.; MacMillan, D. W. C. *J. Am. Chem. Soc*, **2013**, *135*, 18323. (e) Prier, C. K.; Rankic, D. A.; MacMillan D. W. C. *Chem. Rev*. **2013**, *113*, 5322. (f) Zuo, Z.; MacMillan, D. W. C. *J. Am. Chem. Soc*, **2014**, *136*, 5257. (g) Terrett, J. A.; Clift, M. D.; MacMillan, D. W. C. *J. Am. Chem. Soc*, **2014**, *136*, 6858. (h) Prier, C. K.; MacMillan D. W. C. *Chem. Sci.* **2014**, *5*, 4173. (i) Chu, L.; Ohta, C.; Zuo, Z.; MacMillan, D. W. C. *J. Am. Chem. Soc*, **2014**, *136*, 10886. (j) Jeffrey, J.; Petronijević, F. R.; MacMillan, D. W. C. *J. Am. Chem. Soc,* **2015**, *137*, 8404. (k)

Cuthbertson, J. D.; MacMillan, D. W. C. *Nature* **2015**, *519*, 74. (l) Shaw, M. H.; Twilton, J.; MacMillan, D. W. C. *J. Org. Chem.* **2016**, *81*, 6898.

28 Nicewicz, D. A.; MacMillan, D. V. C. *Science*. **2008,** *322*, 77.

29 Tucker, J. W.; Nguyen, J. D.; Narayanam, J. M. R.; Krabbe, S. W.; Stephenson, C. R. J. *Chem. Commun.* **2010**, *46*, 4985.

30 Condie, A. G.; Gonzalez-Gomez, J. C.; Stephenson, C. R. J. *J. Am. Chem. Soc.* **2010**, *132*, 1464.

31 Lin, S.; Ischay, M. A.; Fry, C. G.; Yoon, T. P. *J. Am. Chem. Soc.* **2011**, *133*, 19350.

32 Ashby, E. C.; Oswald, J. *J. Org. Chem.* **1988**, *53*, 6068.

33 Blicke**,** F. F.; Powers, L. D. *J. Am. Chem. Soc.* **1929**, *51*, 3378.

34 Blomberg, **C.;** Mosher, H. S. *J. Organometal. Chem.* **1968**, *13*, 519.

35 Ashby, E. C.; Bowers, J.; Depriest, R. *Tetrahendron Letters*. **1980**, *21*, 3541.

36 Uchiyama, N.; Shirakawa, E.; Hayashi, T. *Chem. Commun*. **2013**, *49*, 364.

37 Ashby, E. C.; Argyropoulos, J. N. *J. Org. Chem.* **1986**, *51*, 472.

38 Swain, C. G.; Powell, A. L.; Sheppard, W. A.; Morgan, C. R. *J. Am. Chem. Soc.* **1979**, *101*, 3576.

39 Ashby, E. C.; Coleman, D.; Gamasa, M. *J. Org. Chem.* **1987**, *52*, 4079.

40 a) Royals, E. E. *J. Am. Chem. Soc.* **1948**, *70*, 489. b) Zook, K. D.; Mcaleer, W. J.; Horwin, L. *J. Am. Chem. Soc.* **1946**, *68*, 2404. c) Baker, R. B.; Reid, E. E. *J. Am. Chem. Soc.* **1929**, *51*, 1567. d) Soloway, S. B.; Laforge, F.B. *J. Am. Chem. Soc.* **1947**, *69*, 1244. e) Cohen, H.; Shubart, R. *J. Org. Chem.* **1973**, *38*, 4079.

41 Ashby, E. C.; Park, W. S. *Tetrahendron Letters*. **1983**, *24*, 1667.

42 (a) Birch, A. J. *J. Chem. Soc.***1944**, 430. (b) Birch, A. J. *J. Chem. Soc.* **1945**, 809.

43 a) Mulliken, R. S. *J. Chem. Phys.* **1955**, *23*, 397. b) Mulliken, R. S. *J. Am. Chem. Soc.* **1950**, *72*, 600. c) Mulliken, R. S. *J. Phys. Chem.* **1952**, *56*, 801. d) Reid, C.; Mulliken, R. S. *J. Am. Chem. Soc.* **1956**, *76*, 3869.

44 a) Taube, H. *J. Am. Chem. Soc.* **1942**, *64*, 161. b) Taube, H. *J. Am. Chem. Soc.* **1943**, *65*, 1876. c) Hochhauser, I. L.; Taube, H. *J. Am. Chem. Soc.* **1947**, *69*, 1582. d) Taube, H. *J. Am. Chem. Soc.* **1947**, *69*, 1418. e) Taube, H. *J. Am. Chem. Soc.* **1948**, *70*, 1216 f) Taube, H. *J. Am. Chem. Soc.* **1948**, *70*, 3928. g) Rich, R. L.; Taube, H. *J. Phys. Chem.* **1954**, *58*, 6. h) Rich, R. L.; Taube, H. *J. Am. Chem. Soc.* **1954**, *76*, 2608. i) Taube, H.; Myers, H.; Rich, R. L. *J. Am. Chem. Soc.* **1953**, *75*, 4118. j) Taube, H.; Myers, H. *J. Am. Chem. Soc.* **1954**, *76*, 2103. k) Saffir, P.; Taube, H. *J. Am. Chem. Soc.* **1960**, *82*, 13. l) Taube, H.; Gould, E. S. *Acc. Chem. Res.* **1969**, *2*, 321. m) Nordmeyer, F. R.; Taube, H. *J. Am. Chem. Soc.* **1968**, *90*, 1162. n) French, J. E.; Taube, H. *J. Am. Chem. Soc.* **1969**, *91*, 6951. o) Endicott, J. F.; Taube, H. *Inorg. Chem.* **1965**, *4*, 437. p) Stritar, J. A.; Taube, H. *Inorg. Chem.* **1969**, *8*, 2281. q) Hammershoi, A.; Geselowitz, D.; Taube, H. *Inorg. Chem.* **1984**, *23*, 979. r) Ford, P. C.; Rudd, D. P.; Gaunder, R.; Taube, H. *J. Am. Chem. Soc.* ***1968***, *90*, 1187.

45 a) Marcus, R. A. *J. Chem. Phys.* **1952**, *20*, 359. b) Marcus, R. A. *J. Chem. Phys.* **1957**, *26***,** 872. c) Marcus, R. A. *Can. J. Chem.* **1959**, *37***,** 155. d) Marcus, R. A. *Annu. Rev. Phys. Chem.* **1964**, *15***,** 155. e) Marcus, R. A. *J. Chem. Phys.* **1965**, *43***,** 2654. f) Marcus, R. A. *J. Chem. Phys.* **1965**, *43***,** 3477. g) R. **A.** *Electrochim. Acta* **1968**, *13***,** 995. h) Marcus, R. A. *J. Chem. Phys.* **1984**, *81***,** 5613.

46 Mulliken, R. S. *J. Am. Chem. Soc.* **1952**, *74*, 811.

47 Nagakura, S. *Mol. Cryst. Liq. Cryst.* **1985**, *126*, 9.

48 Taube, H.; Mayers, H.; Rich, R. L. *J. Am. Chem. Soc.* **1953**, *75*, 4118.

49 Wagenknecht, J. H. *J. Org. Chem.* **1977**, *42*, 1836.

50 a) Marcus, R. A. *J. Chem. Phys.* **1956**, *24*, 966. b) Marcus, R. A. *Angew. Chem. Int. Ed.* **1993**, *32*, 1111.

51 a) Efremov, R. G.; Baradaran, R.; Sazanov, L. A. *Nature,* **2010**, *465*, 441. b) Nohl, H.; Jordan, W.; Youngman, R. J. *Adv. Free. Radical. Biol.* **1986**, *2*, 211.

52 Patai, S.; Rappoport, Z.; *Eds. Electrochemistry of Quinones.* Wiley: New York, **1988**, *2*, 719.

53 Wohler, F.; *Justus Liebigs Ann. Chem*. **1844**, *51*, 145.

54 Suida, H. and Suida, W. *Justus Liebigs Ann. Chem. **1918**, 416,* 113.

55 Nogami, T.; Yoshihara, K.; Hosoya, H.; Nagakura, S. *J. Phys. Chem.* **1969**, *73*, 2670.

56 Yamaoka, T.; Nagakura, S. *Bull. Chem. Soc. Japan.* **1971**, *44*, 2971.

57 Sersen, F.; Koscal, S.; Banacky, P.; Krasnec, L. *Coll. Czech. Chem. Comm*. **1977**, *42,* 2173.

58 Ciapina, E. G.; Santini, A. O.; Weinert, P. L.; Gofardo, M. A.; Pezza, H. R.; Pezza, L. *Ecl. Quim*. **2005**, *30*, 29.

Chapter 2

Development of Organic Synthetic Methods based on Electron Transfer Reactions

2.1 Introduction

2.1.1 Aryl quinones

We have developed synthetic methods to access arylquinones and aminoquinones. Accordingly, a brief review of literature on the synthesis of these derivatives will facilitate the discussion.

Quinone derivatives are widely present in pharmacologically active natural products in plants, fungi, and bacteria. Quinones also play important role in chemistry, material science, nanotechnology, and medicines, because of its core structure possessing electron transfer properties.[1] Arylquinones are also found in nature and exhibit biological activity. For example terphenylquinone **1** has activity against human protein tyrosine kinase. The compound 2-(5-oxohexa-1,3-dienyl)-1,4-naphthaquinone **2** shows anti-malarial activity and the trimeric naphthaquinone derivative conocurvone **3** exhibits anti-HIV activity Figure 1.[2]

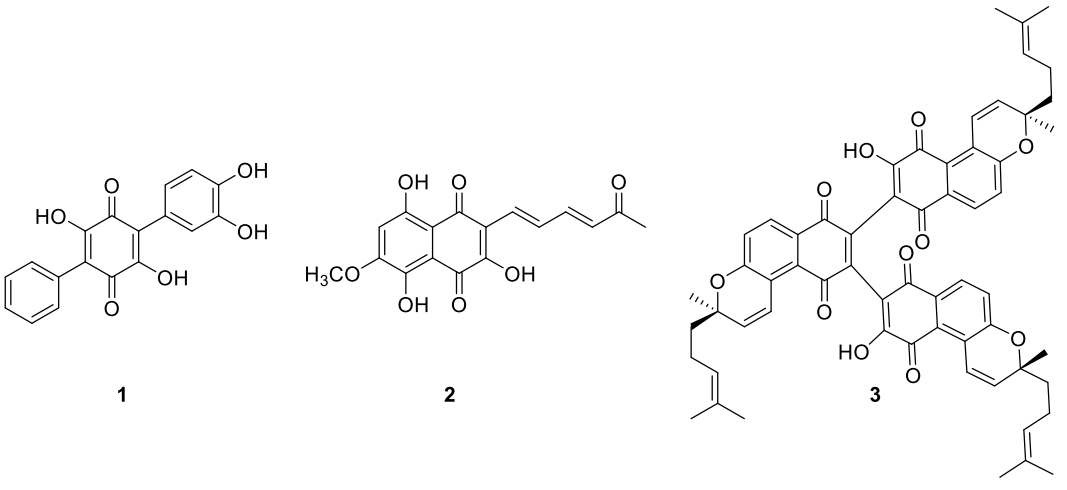

Figure 1. Pharmacologically active benzo and naphthoquinone compounds.

2.1.2 Previous reports on arylsubsubstituted 1,4-benzoquinones.

$In(OTf)_3$ catalyzed arylsubstituted 1,4-benzoquinones synthesis was reported (Scheme 1).[3]

Scheme 1

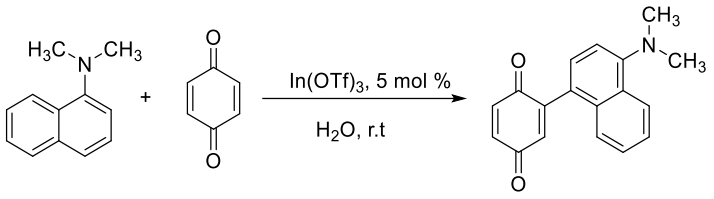

4a **5b** **6ba**

69% yield

Mathew *et al*. reported[4] that 2,5-dichloro-1,4-benzoquinone react with diazonium salt of 4-(dimethylamino) aniline to give the corresponding amino alkyl benzoquinones (Scheme 2).

Scheme 2

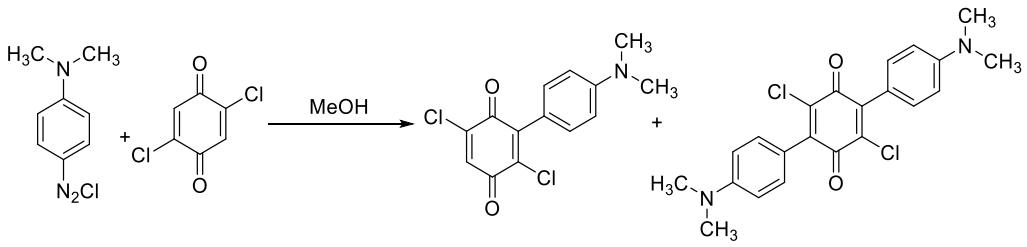

7 **8** **9** **10**

R = H, R = Br

Up to 70% yield

Errazuriz *et al*. reported [5] the oxidative cleavage of various hydroquinone dimethylethers with nitric acid- manganese dioxide, to the corresponding substituted aryl quinones in 76-95% yields (Scheme 3).

Scheme 3

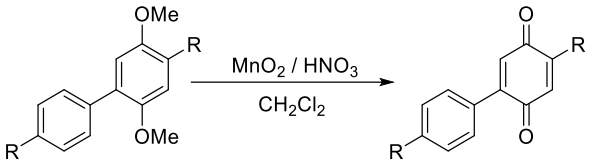

11 R = OMe, Me, Cl, H **12** up to 76-95% yield

Jiang *et al*. reported[6] the synthesis of arylnaphthoquinone derivatives using 1-naphthol in the presence of *m*-CPBA followed by triflic acid catalyzed arylation using *N,N*-dimethyl aniline (Scheme 4).

Scheme 4

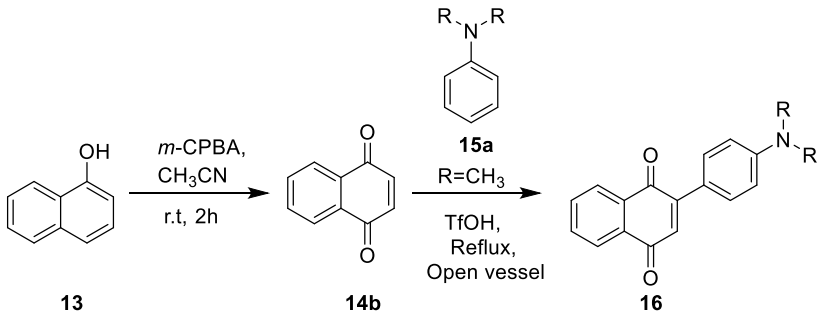

13 **14b** **16** up to 70-87% yield

2.1.3 Reaction of Primary and Secondary amino alcohols with quinone acceptors

The nitrogen-containing compounds were found to undergo Michael addition to a variety of quinones. In 1844, Wohler reported the first addition reaction of hydrogen chloride to benzoquinone resulting to give chloro hydroquinone.[7] In 1969, Nagakura *et al*. reported[8] that the reaction of *p*-chloranil with aniline gave the aminoquinone product via through single electron transfer mechanism. Aminoquinones also show electro switching properties.[9] Several of these derivatives also have medicinal,[10-12] herbicides,[13] and anti-bacterial, anti fungal, and anticancer activities. Also, some aminoquinone derivatives are involved in enzyme inhibition and DNA-cross linking processes.[14]

Delarmelina *et.al* reported[15] that 2,3-dichloro napthquinone reacted with etanolamine in the presence triethylamine to give the corresponding 1,4-addition product **18** (Scheme 5).

Scheme 5

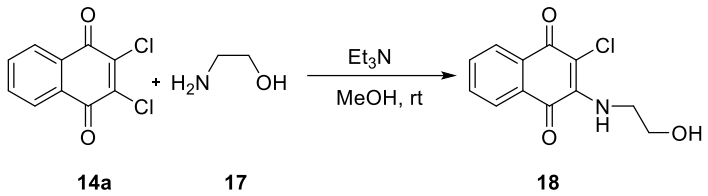

Pandurangan *et.al* reported that *p*-chloranil reacted with ethanol amine to give the corresponding 1,4-addition product **19** under reflux condition in ethanol (Scheme 6).[16]

Scheme 6

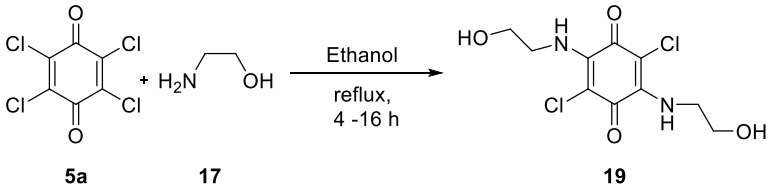

Earlier, aminoquinones were prepared in this laboratory in DCM at 25 ^{o}C (Scheme 7).[17]

Scheme 7

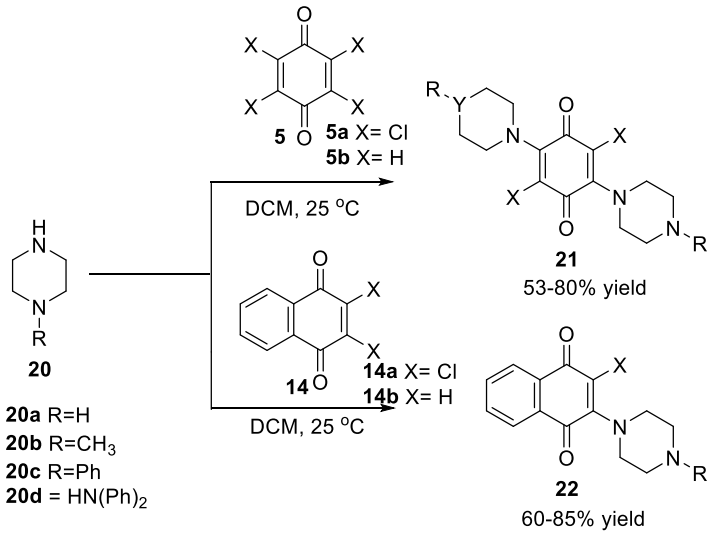

Previously, it was reported that the reaction of secondary amine with *p*-chloranil gave the aminoquinone products by polar mechanism but the SET mechanism was not considered.[18] Also, these authors did not report any epr spectral analysis of the intermediates formed in the reaction. However, it was observed in this laboratory that epr signal was observed upon mixing secondary amines with *p*-chloranil. Therefore, we have undertaken detailed studies on the reaction of arylamines and amino alcohol derivatives with *p*-chloranil. The results are described in the next section.

2.2 Results and Discussion

2.2.1 Reaction of tertiary aryl amines with quinone acceptors

Previously, it was reported in this laboratory that the reaction of *N*,*N*-diethylaniline with *p*-chloranil gave the *N*,*N*,*N*',*N*'-tetraethylbenzidine product **23** along with the formation of the corresponding hydroquinone **24** (Scheme 8).[19]

Scheme 8

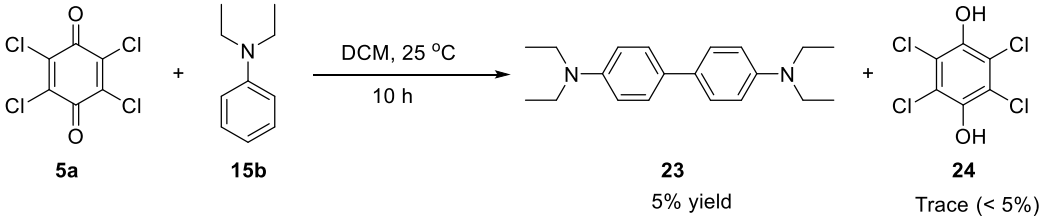

Surprisingly, the reaction of the 1-naphthylamine derivative with *p*-chloranil gave the *N*, *N*-diethylnaphthylaminoquinone product **25ab** in 62% yield (Scheme 9).

Scheme 9

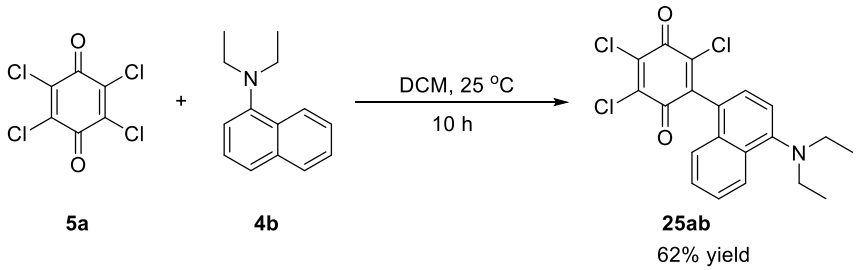

2.2.2 Electron transfer reaction of *N*,*N*-diethylnaphthylamine with quinone acceptors

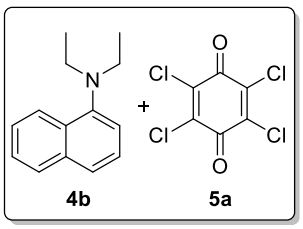

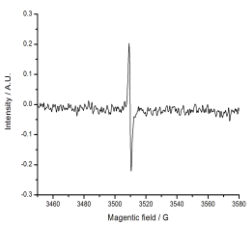

(a) 10 min

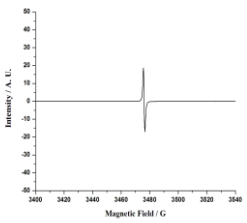

(b) 1 h

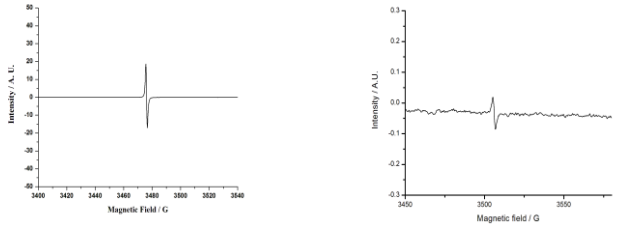

(c) 2 h (d) 6 h

Figure 2. EPR studies of *N*,*N*-diethylnaphthylamine **4b** (0.05 mmol) with quinone **5a** (0.05 mmol) in DCM solvent with various time intervals.

We have monitored the reaction of *N*, *N*-diethylnaphthylamine with *p*-chloranil in DCM by esr spectral analysis. We have observed that immediately after mixing, the esr signal was observed which disappeared after 12 h (Figure 2).

Scheme 10

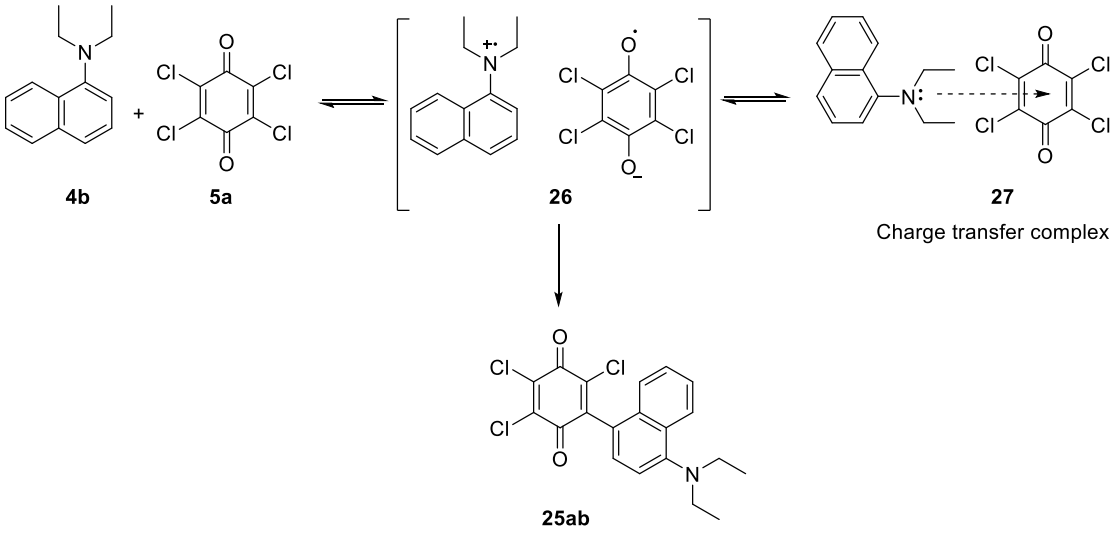

Presumably, the signal strength decreased due to formation of charge transfer complex or products from the initially formed paramagnetic intermediates **26** (Scheme 10).

We have carried out the reaction in different solvents in order to optimize the condition. We have observed that the substitution product **25ab** was obtained in 75% yield when DMF was used as solvent (Table 1, entry 4).

Table 1. Reaction of *p*-chloranil **5a** with *N*, *N*-diethyl naphthylamine **4b** [a,b]

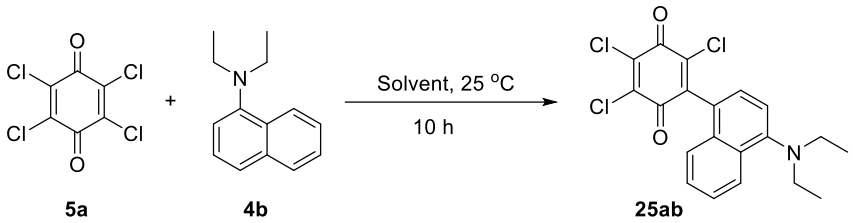

5a (2 mmol) **4b** (2 mmol) **25ab**

Entry	Solvent (5 ml)	Product **25ab** Yield (%)[b]
1	Toluene	30
2	DCM	62
3	THF	20
4	DMF	75
5	CH_3CN	72
6	NMP	70

[a]The reactions were carried out with 2 mmol of *p*-chloranil **5a** and *N*,*N*-diethyl naphthylamine **4b** at 25 °C for 10 h. [b]Isolated yield.

We have also carried out the reaction of several *N*, *N*-dialkylnaphthylamines **4** with *p*-chloranil **5a** in DMF solvent and the corresponding products **25aa-25ac** were isolated in 62-84% yield (Table 2). We have also observed that the reaction of *N*-naphthylpyrrolidine and piperidine derivatives **4d-4f** with *p*-chloranil **5a** gave the products **25ad-25af** in 45-82% yield (Table 2).

Table 2. Reaction of *p*-chloranil **5a** with *N*, *N*-dialkyl naphthylamine derivatives **4**[a,b]

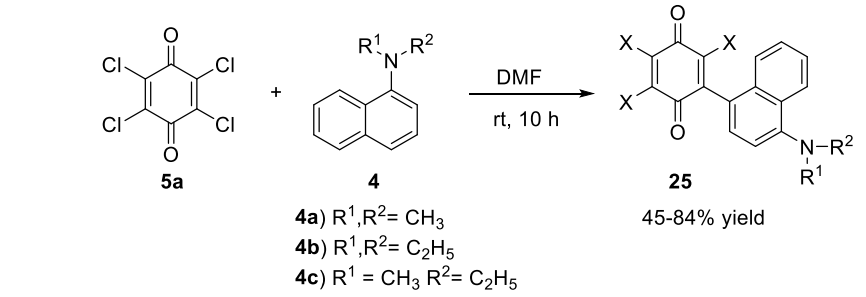

5a **4** **25**

4a) R^1,R^2= CH_3
4b) R^1,R^2= C_2H_5
4c) R^1 = CH_3 R^2= C_2H_5

45-84% yield

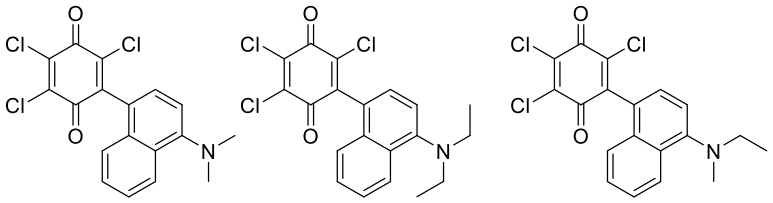

25aa 84% yield

25ab 75% yield

25ac 74% yield

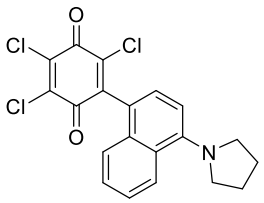

25ad 82% yield

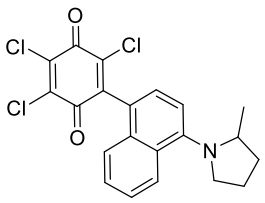

25ae 74% yield

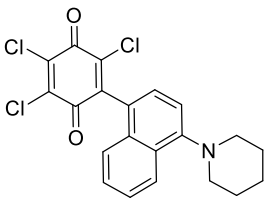

25af 62% yield

[a]The compounds **25aa-25ac** were prepared by using quinone (2 mmol) and amine (2mmol) in DMF solvent at 25 °C, and the compounds **25ad-25af** were prepared in toluene at 80 °C for 10 h.

A plausible mechanism for the formation of aromatic substitution product **25** is outlined in Scheme 11. The quinone **5** would accept an electron from the *N*, *N*-dialkylnaphthylamine **4** to give the paramagnetic intermediates of radical anion **28** and radical cation **29**. Subsequent C-C bond forming reaction would lead to the intermediate **32.** After elimination of the HX the product **25** would be formed (Scheme 11).

Scheme 11

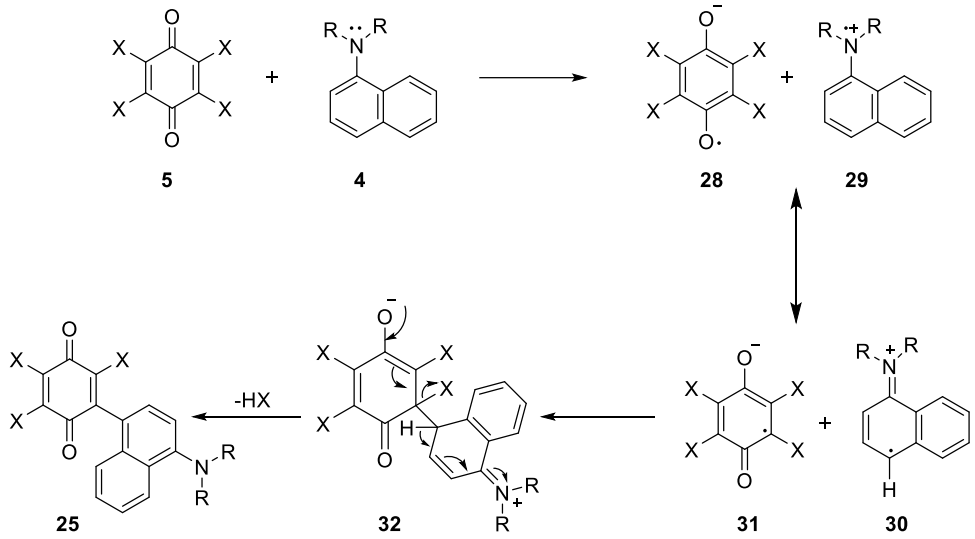

2.2.3 Reaction of *o*-chloranil with *N,N*-dialkyl naphthylamine derivatives

We have also carried out the reaction of *N*, *N*-dialkylnaphthylamines **4** with 3,4,5,6-tetrachloro-1,2-napthoquinone **33** in DMF solvent. In this case, the corresponding aryloxy product **35a** was obtained in 58-75% yield and the arylated product **34** was not formed (Scheme 12).

Scheme 12

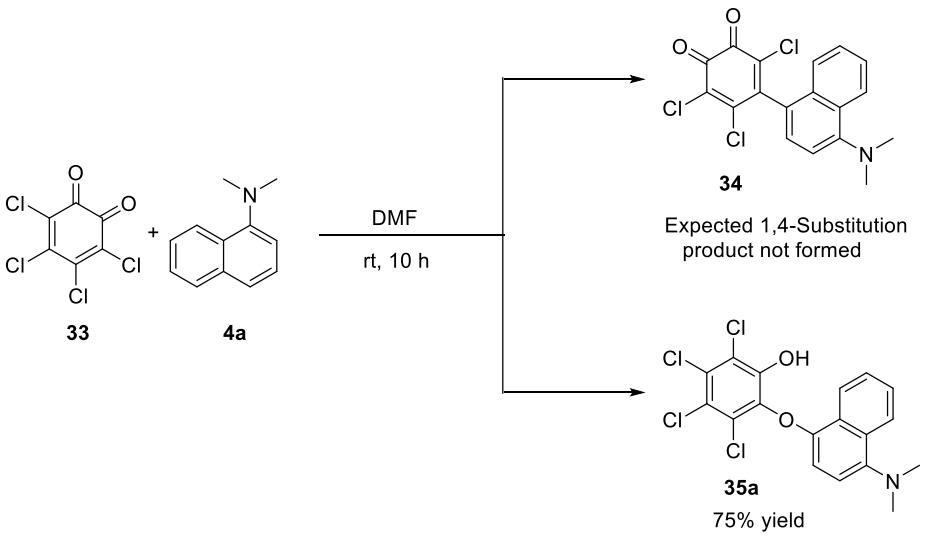

Table 3. Reaction of *o*-chloranil 33 with *N,N*-dialkyl naphthylaminederivatives 4 [a b]

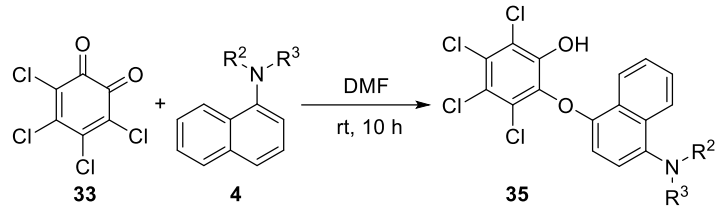

33 **4** **35**

58-75% yield

4a) R^5,R^6= CH_3
4b) R^5,R^6= C_2H_5
4c) R^5 = CH_3 R^6= C_2H_5

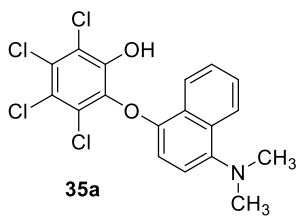

35a
75% yield

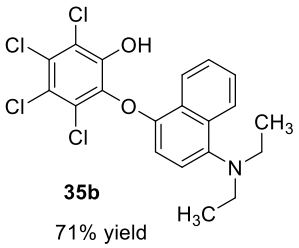

35b
71% yield

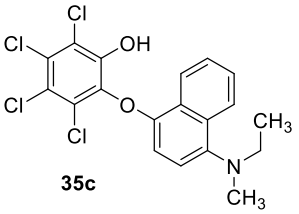

35c
69% yield

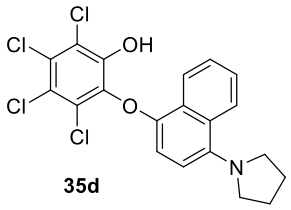

35d
67% yield

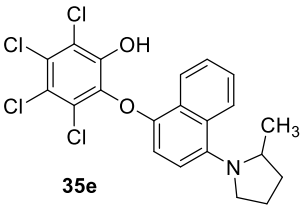

35e
63% yield

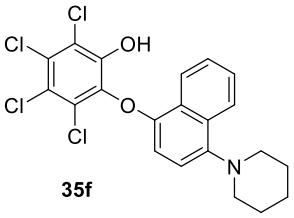

35f
58% yield

[a]The compounds **35a-35f** were prepared by using *o*-chloranil (2 mmol) and amine (2 mmol) in DMF solvent at 25 [o]C, for 10 h. [b]Isolated yield.

A tentative mechanism for the formation of aryloxy product **35** is outlined in Scheme 13. The quinone **33** would accept an electron from *N,N*-dialkylnaphthylamine **4** to give the paramagnetic radical anion **36** and radical cation **37**. Subsequent reactions of the intermediates **38** and **39** would give the intermediate **40.** After proton transfer to oxygen anion and aromatization, the product **35** would be formed (Scheme 13).

Scheme 13

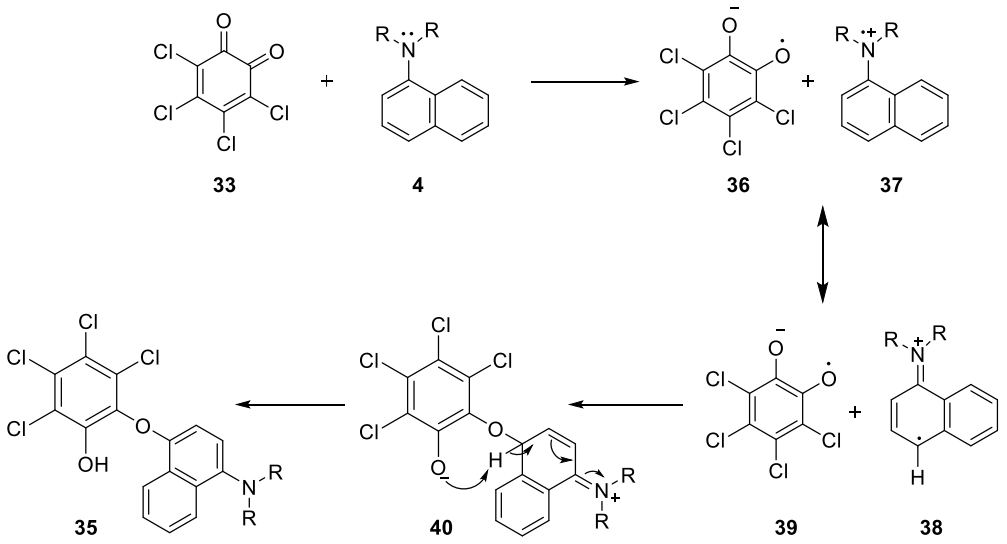

The product **35c** was characterized by X-ray- single crystal structure analysis. (Figure 3)

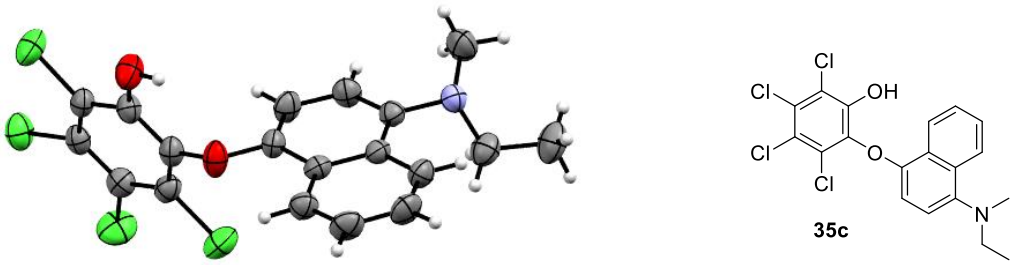

Figure 3. ORTEP representation of aryloxy product–**35c** (Thermal elipsoids were drawn with 50% probability).

Table 4. Crystal data and structure refinement for compound **35c**.

Identification code	compound **35c**	
Empirical formula	C_{19} H_{15} Cl_4 N O_2	
Formula weight	431.12	
Temperature	298(2) K	
Wavelength	0.71073 Å	
Crystal system	Triclinic	
Space group	P -1	
Unit cell dimensions	a = 8.0007(11) Å	α = 98.770(7)°.
	b = 8.9751(15) Å	β = 102.081(6)°.
	c = 13.745(2) Å	γ = 94.314(6)°.
Volume	948.0(3) $Å^3$	
Z	2	
Density (calculated)	1.510 Mg/m^3	
Absorption coefficient	0.638 mm^{-1}	
F(000)	440	
Crystal size	0.38 x 0.28 x 0.18 mm^3	
Theta range for data collection	2.545 to 27.575°.	
Index ranges	-10<=h<=10, -11<=k<=11, -17<=l<=17	
Reflections collected	28574	
Independent reflections	4367 [R(int) = 0.0716]	
Completeness to theta = 25.242°	99.9 %	
Absorption correction	None	
Refinement method	Full-matrix least-squares on F^2	
Data / restraints / parameters	4367 / 0 / 235	
Goodness-of-fit on F^2	1.063	
Final R indices [I>2sigma(I)]	R1 = 0.0448, wR2 = 0.1011	
R indices (all data)	R1 = 0.0768, wR2 = 0.1124	
Extinction coefficient	n/a	
Largest diff. peak and hole	0.285 and -0.367 e.$Å^{-3}$	

2.2.4 Reaction of aliphatic tertiary aminoalcohols with quinone acceptors

As outlined in the introductory section, ethanolamine was reported to react with chloroquinones to give only addition of amine end to the quinone (Scheme 5 and 6). It was of interest to examine the reaction of tertiary amino alcohols. Hence, we have performed the reaction of tertiary amino alcohols like *N*,*N*-dimethylaminoethanol and *N*,*N*-dimethylethylenediamine with *p*-chloranil **5a**. EPR analysis indicated that paramagnetic intermediates were formed in both the cases (Figure 4).

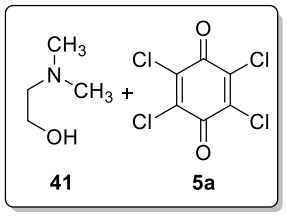

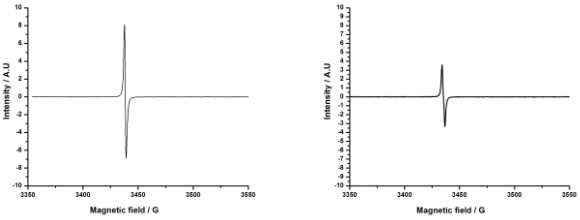

(a) 10 min (b) 1 h

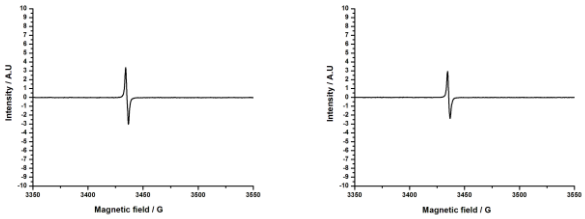

(c) 2 h (d) 6 h

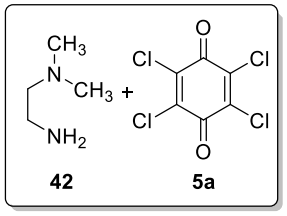

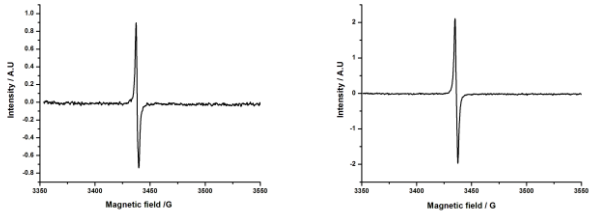

(a) 10 min (b) 1 h

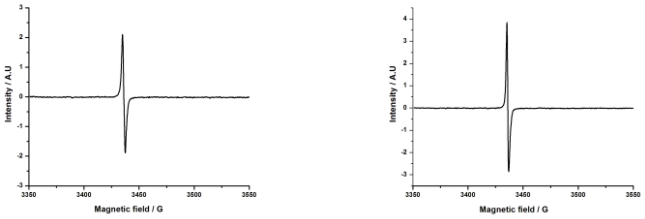

(c) 2 h (d) 6 h

Figure 4. EPR studies of *N*,*N*-dimethylaminoethanol **41** (0.05 mmol) and *N*,*N*-dimethylethylenediamine **42** (0.05 mmol) with *p*-chloranil **5a** (0.05 mmol) in DCM solvent with various time intervals.

The epr signal persisted for long time but the signal strength decreased with time. Presumably, the *N*,*N*-dimethylaminoethanol **41** reacts with *p*-chloranil to give paramagnetic intermediates which combine to give the charge transfer complex or the intermediates are slowly coupled to give the diaminoquinone product **46** (Scheme 14)

Scheme 14

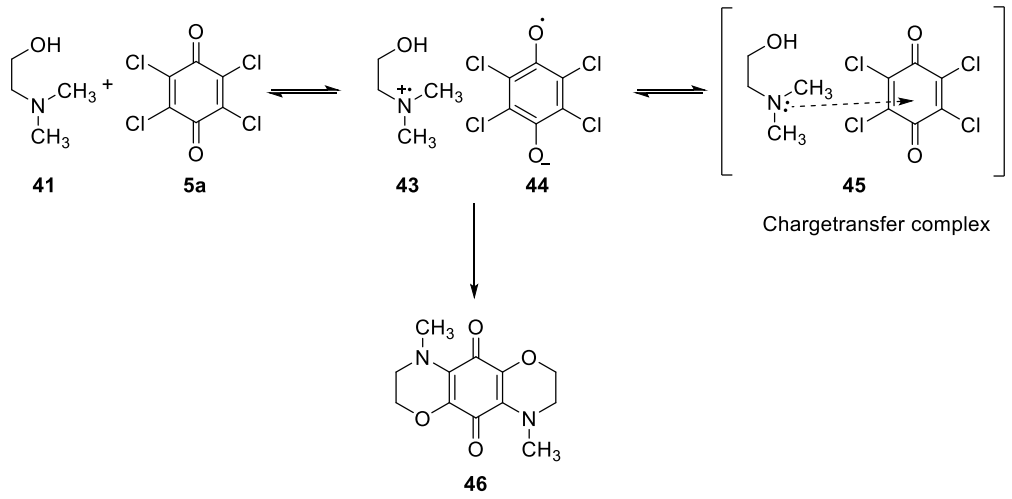

Initially, we have examined the reaction of *p*-chloranil with *N*,*N*-dimethylamino ethanol at room temperature using DCM as a solvent. We have observed that the *p*-chloranil (1 equiv.) reacts with 2-(dimethylamino)ethanol (0.5 equiv.) to afford the mono aminoquinone product **47** in 18% yield. Whereas the reaction using *p*-chloranil (2 equiv.)

and 2-(dimethylamino)ethanol (8 equiv.) in DCM solvent gave the diaminoquinone product **46** in 62% yield (Scheme 15).

Scheme 15

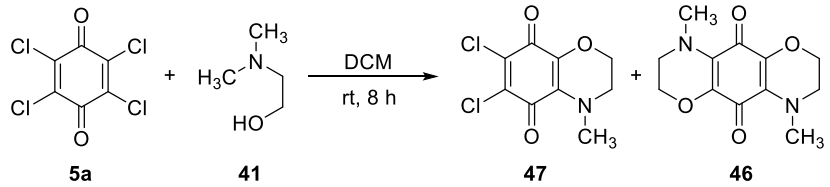

Table 5: Optimization of the reaction condition.[a]

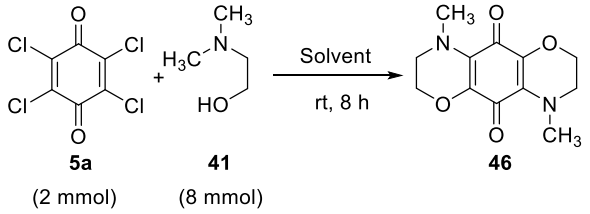

Entry	Solvent	Yield(%) **46**
1	Toluene	Trace (< 5%)
2	DCM	62
3	THF	20
4	DMF	80
5	CH_3CN	72
6	NMP	76

[a]The reactions were carried out with chloranil **5a** (2 mmol), and tertiary amino alcohol **41** (8 mmol) at rt for 8 h.[b]Isolated yield of **46**.

We have carried out this reaction under several conditions. We have found that *p*-chloranil **5a** (1 equiv.) reacts with *N*,*N*-dimethylaminoethanol **41** (4 equiv.) in toluene solvent to give the diaminoquinone product **46** only in trace amount (entry 1, Table 5). Then, we have screened different solvents, Fortunately, the reaction of *p*-chloranil (1

equiv.) with *N*,*N*-dimethylaminoethanol (4 equiv.) in DMF solvent gave the diamino quinone product **46** in 80% yield (entry 4, Table 5).

We have also carried out experiments varying the amounts of the aminoalcohol **41.**

Table 6: Effect of amino alcohol concentration.[a,b]

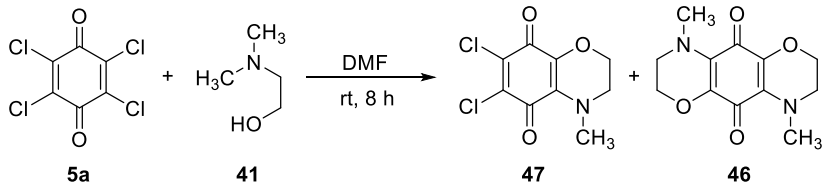

5a **41** **47** **46**

Entry	Aminoalcohol **(41)** (mmol)	Yield (%) **(47)**	Yield (%) **(46)**
1	1	30	-
2	2	15	-
3	4	Trace	trace
4	6	-	52
5	8	-	80

[a]The reactions were carried out with *p*-chloranil **5a** (2 mmol), and tertiaryamino alcohol **41** at rt for 8 h.[b]Isolated yield of **46**.

We have observed that the *p*-chloranil (1 equiv.) reacts with *N*,*N*-dimethylamino ethanol (0.5 equiv.) in DMF solvent to give the mono aminoquinone product **47** in 30% yield. The reaction of *p*-chloranil (1 equiv.) with *N*,*N*-dimethylaminoethanol (2 equiv.) in DMF solvent gave the monoaminoquinone product **47** and diaminoquinone product **46** in trace amount. Whereas the reaction using *p*-chloranil (1 equiv.) and *N*,*N*-dimethylamino ethanol (4 equiv.) in DMF solvent gave the diaminoquinone product **46** in 80% yield. We have also examined the reaction using 10 equiv. of *N*,*N*-dimethylaminoethanol but there

was no significant further change in yields of the product. The product **46** was characterized by X-ray- single crystal structure analysis (Figure 5).

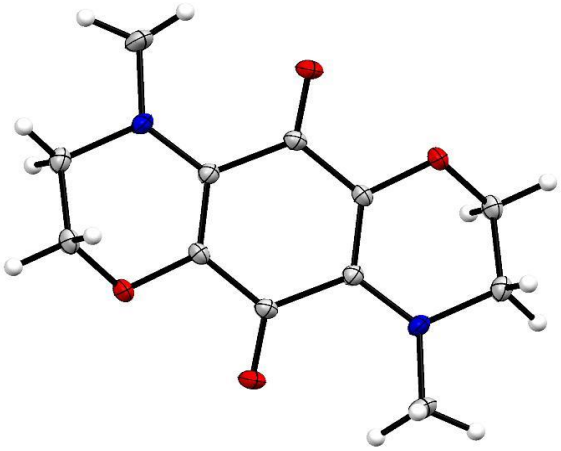

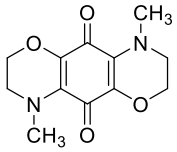

46

Figure 5. ORTEP representation of diaminoquinone product–**46** (Thermal elipsoids were drawn with 50% probability).

We have also carried out the reaction of amino alcohol **41** and the diamine **42** with *p*-chloranil and 2,3-dichloronaphthoquinone. The results are summarized in Table 8.

Table 7. Crystal data and structure refinement for compound **46**.

Identification code	compound **46**	
Empirical formula	C_{12} H_{14} N_2 O_4	
Formula weight	250.25	
Temperature	298(2) K	
Wavelength	0.71073 Å	
Crystal system	Monoclinic	
Space group	P 21/n	
Unit cell dimensions	a = 3.9451(5) Å	α = 90°.
	b = 13.2759(19) Å	β = 96.054(4)°.
	c = 10.3953(15) Å	γ = 90°.
Volume	541.41(13) $Å^3$	
Z	2	
Density (calculated)	1.535 Mg/m^3	
Absorption coefficient	0.117 mm^{-1}	
F(000)	264	
Crystal size	0.24 x 0.20 x 0.16 mm^3	
Theta range for data collection	2.497 to 27.497°.	
Index ranges	-5<=h<=5, -17<=k<=17, -13<=l<=13	
Reflections collected	8774	
Independent reflections	1220 [R(int) = 0.0554]	
Completeness to theta = 25.242°	98.7 %	
Absorption correction	None	
Refinement method	Full-matrix least-squares on F^2	
Data / restraints / parameters	1220 / 0 / 83	
Goodness-of-fit on F^2	1.225	
Final R indices [I>2sigma(I)]	R1 = 0.0811, wR2 = 0.2443	
R indices (all data)	R1 = 0.0844, wR2 = 0.2471	
Extinction coefficient	n/a	
Largest diff. peak and hole	0.467 and -0.460 $e.Å^{-3}$	

Table 8: Synthesis of fused aminoquinones

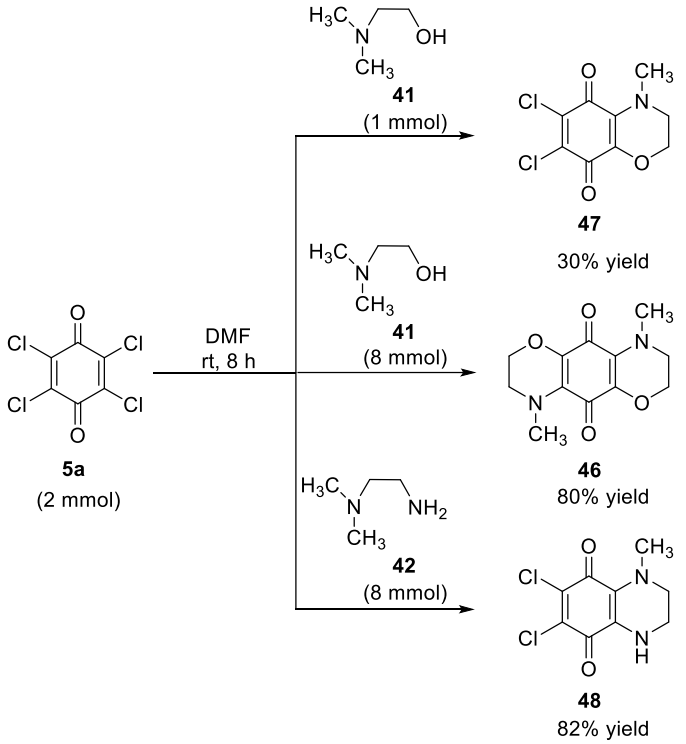

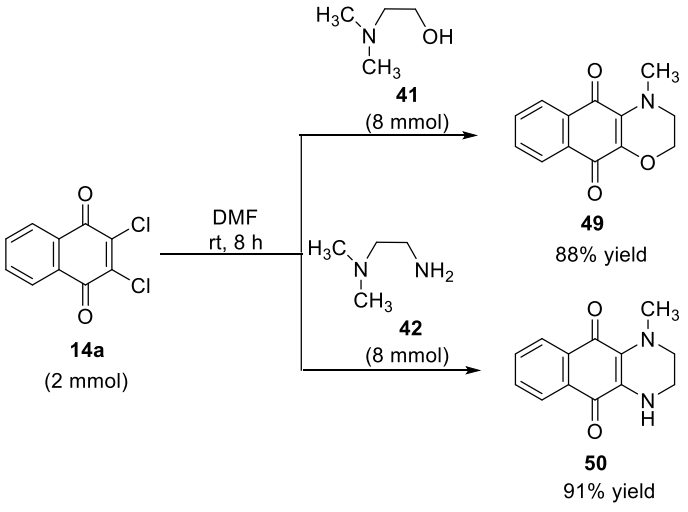

A tentative mechanisim for the formation of aminoquinone product **46** is outlined in Scheme 16. Initially, the quinone **5a** would accept an electron from *N*,*N*-dimethylaminoethanol **41** to give the paramagnetic intermediates of radical anion **44** and radical cation **51**. Then, C-N bond formation would take place followed by the elimination of HCl to give the substitution product **53.** Subsequent attack by the hydroxy end and elimination of HCl and CH_3Cl would result in the formation of the bicyclic aminoquinone product **47.** Similar further sequence of reactions would also take place resulting in the final product **46** (Scheme 16).

Scheme 16

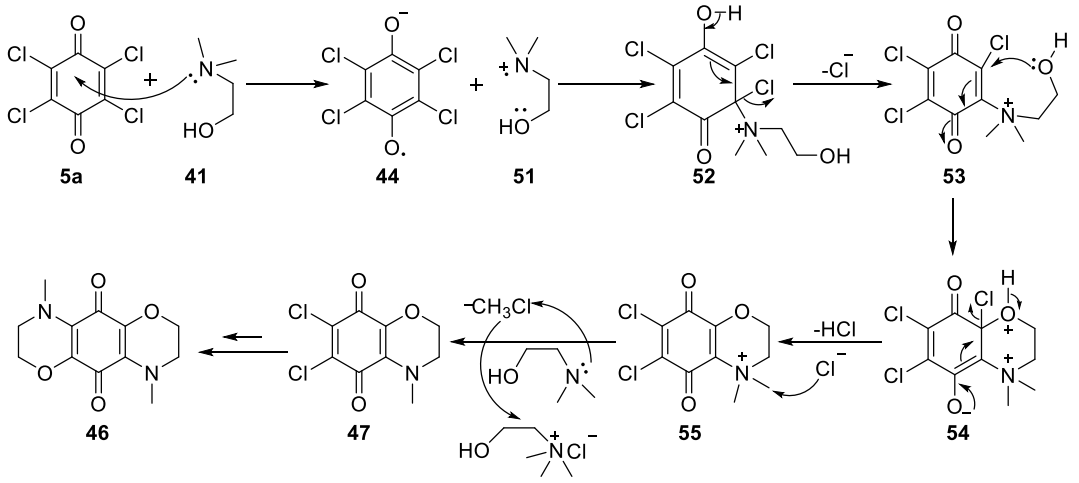

2.2.5 Reaction of cyclic tertiary amino alcohol with *p*-chloranil

Efforts were undertaken to investigate the reaction of cyclic tertiary amino alcohols with *p*-chloranil. We have observed that the reaction of cyclic tertiary amino alcohol like *N*-methyl-(*S*)-DPP **56** with *p*-chloranil **5a** gave paramagnetic intermediates as confirmed by epr spectroscopic analysis. The epr signal persisted for long time but the signal strength decreased with time (Scheme 17).

Scheme 17

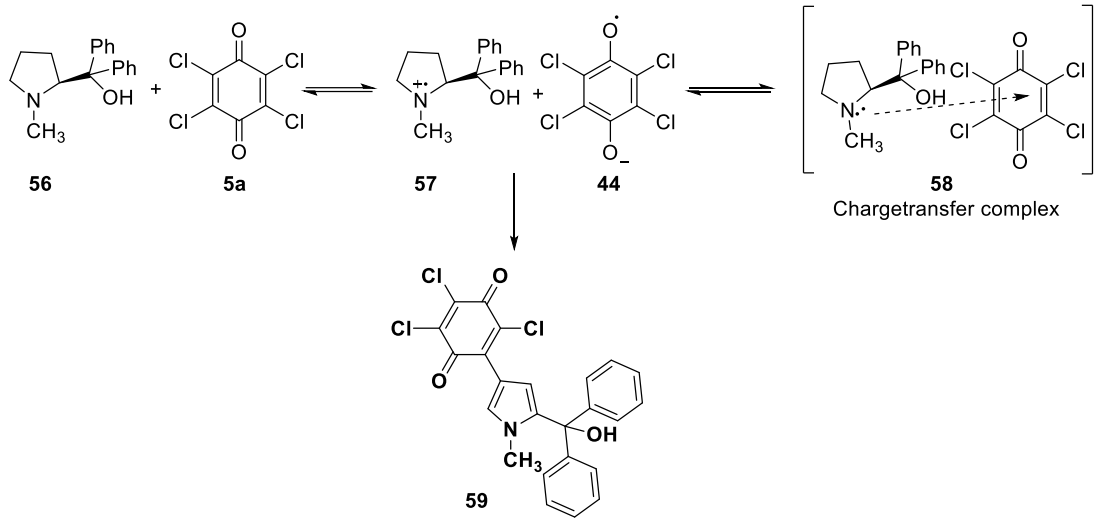

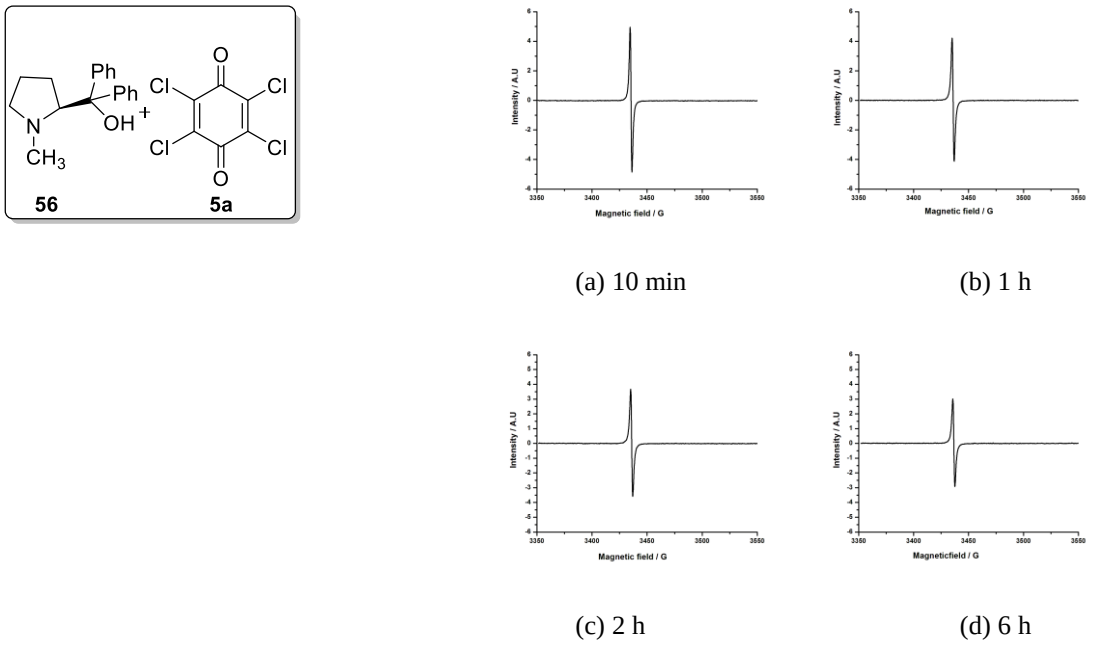

Figure 6. EPR studies of *N*-Methyl-(*S*)-DPP **56** (0.05 mmol) with quinone **5** (0.05 mmol) in DCM solvent with various time intervals.

After workup of the reaction mixture, the highly substituted pyrrole **59** was obtained in 58% yield and the expected pentacyclic product **60** was not formed (Scheme 18)

Scheme 18

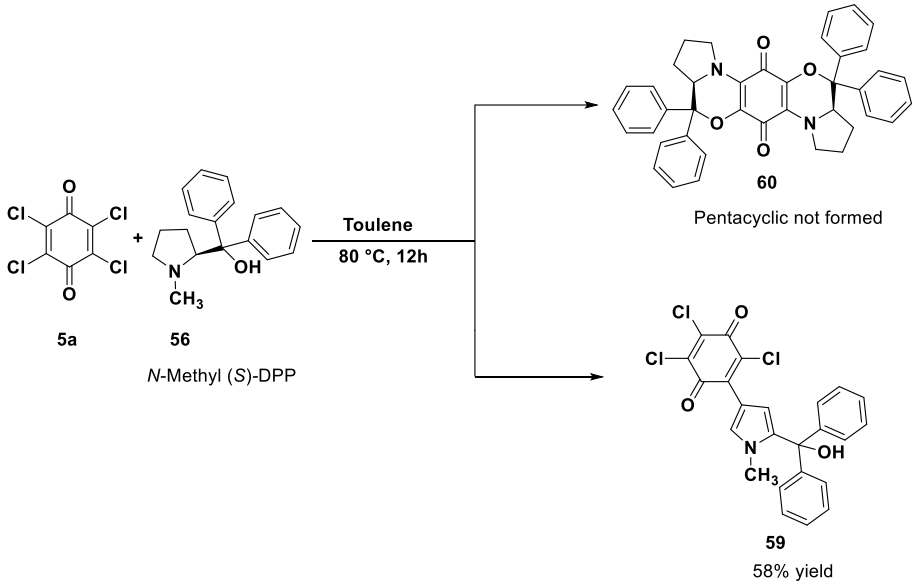

The substituted pyrrole product formation can be explained considering the reaction of the *N*-methyl-(*S*)-DPP and *p*-chloranil to give the enamine **64** *in situ* as shown in Scheme 19. Initially, the amine **56** would react with *p*-chloranil **5a** to give the amine radical cation intermediate **61**. Then, abstraction of hydrogen radical would lead to the the iminium ion **62** which after deprotonation would give the enamine intermediate **64**. that could react with chloranil **5a** to give the intermediate **67.** Subsequent reaction with *p*-chloranil **5a** would give the amine radical cation intermediate **68** that after abstraction of proton, deprotonation-oxidation sequence of reactions would give the pyrrole product **59** (Scheme 19).

Scheme 19

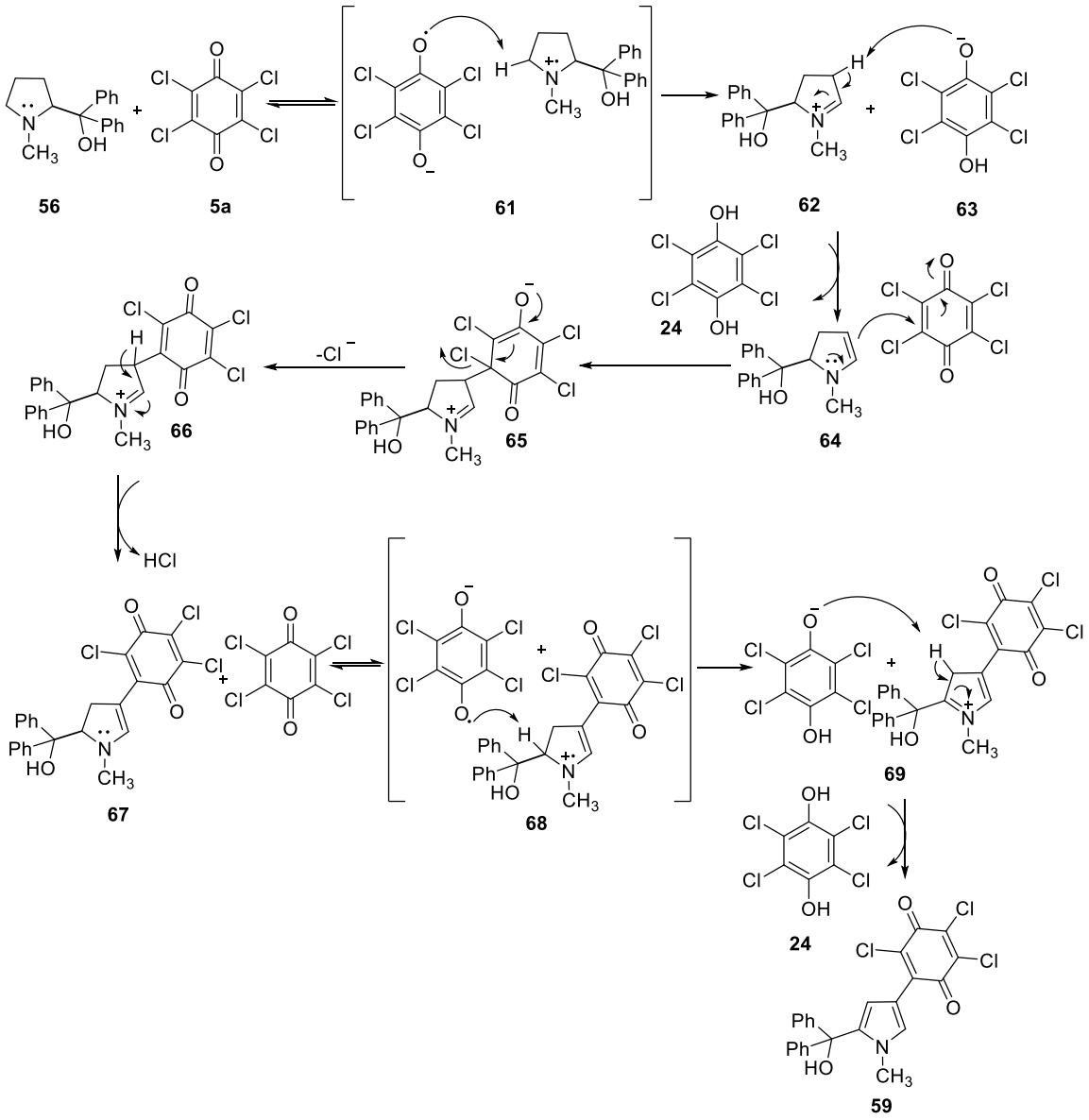

2.2.6 Reaction of cyclic secondary amino alcohol with quinone acceptors

2.2.6.1 Reaction of cyclic secondary amino alcohol with *p*-chloranil

Interestingly, when the reaction was carried out using cyclic secondary amino alcohols **70,** the tricyclic compound **72aa** with a new chiral center was formed in 55% yield and the pentacyclic compound **71** was not formed (Scheme 20).

Scheme 20

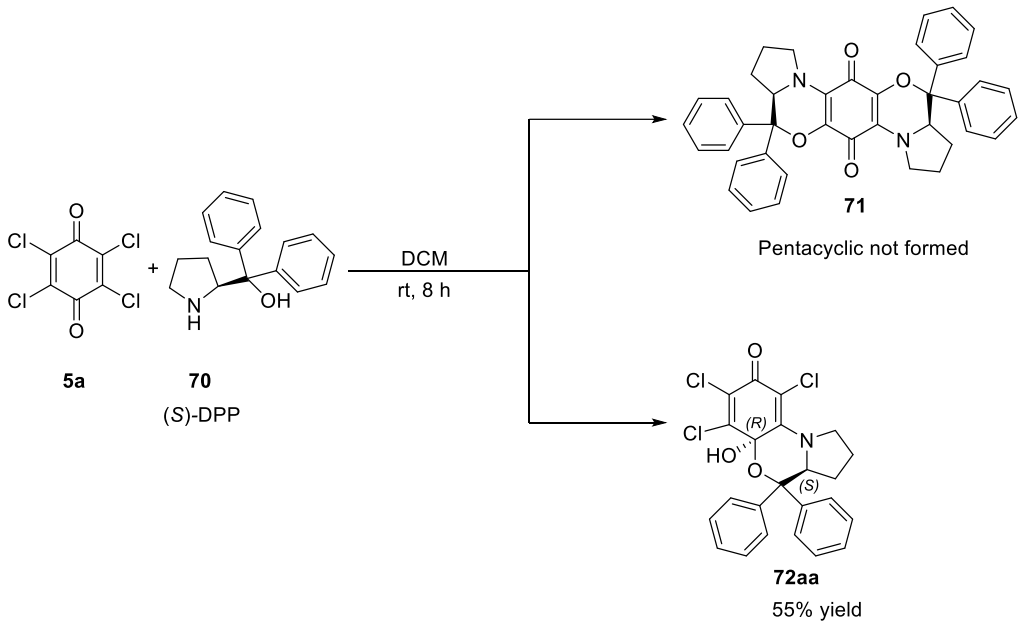

The tricyclic product **72aa** is a single diastereomer as revealed by X-ray-single crystal structure analysis (Figure 7).

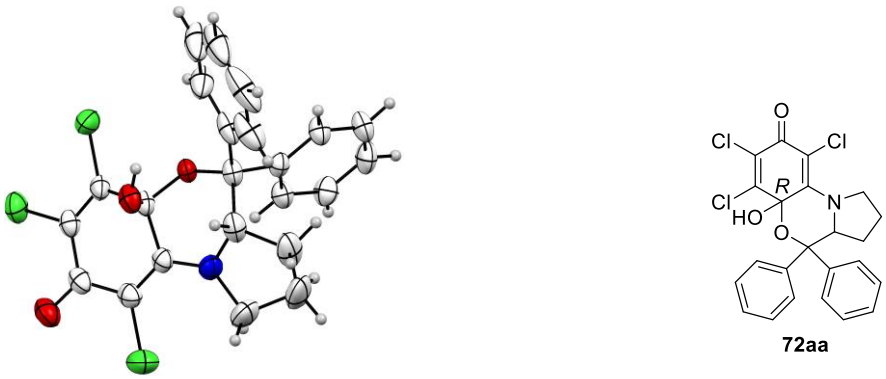

Figure 7. ORTEP representation of chiral aminoquinone–**72aa** (Thermal elipsoids were drawn with 50% probability).

Table 9. Crystal data and structure refinement for compound **72aa**.

Identification code	compound **72aa**	
Empirical formula	C_{23} H_{18} Cl_3 N O_3	
Formula weight	462.73	
Temperature	298(2) K	
Wavelength	1.54184 Å	
Crystal system	Monoclinic	
Space group	P 21	
Unit cell dimensions	a = 6.9286(2) Å	α = 90°.
	b = 12.4028(3) Å	β = 104.084(3)°.
	c = 12.4099(4) Å	γ = 90°.
Volume	1034.38(5) $Å^3$	
Z	2	
Density (calculated)	1.486 Mg/m^3	
Absorption coefficient	4.231 mm^{-1}	
F(000)	476	
Crystal size	0.18 x 0.14 x 0.10 mm^3	
Theta range for data collection	3.672 to 71.533°.	
Index ranges	-8<=h<=6, -14<=k<=9, -13<=l<=15	
Reflections collected	3946	
Independent reflections	2789 [R(int) = 0.0187]	
Completeness to theta = 67.684°	98.9 %	
Absorption correction	Semi-empirical from equivalents	
Max. and min. transmission	1.0000 and 0.36498	
Refinement method	Full-matrix least-squares on F^2	
Data / restraints / parameters	2789 / 1 / 271	
Goodness-of-fit on F^2	1.066	
Final R indices [I>2sigma(I)]	R1 = 0.0340, wR2 = 0.0926	
R indices (all data)	R1 = 0.0346, wR2 = 0.0937	
Absolute structure parameter	0.031(12)	
Extinction coefficient	n/a	
Largest diff. peak and hole	0.268 and -0.206 e.$Å^{-3}$	

Table 10. Crystal data and structure refinement for compound **72ab**.

Identification code	compound **72ab**	
Empirical formula	C_{11} H_{10} Cl_3 N O_3	
Formula weight	310.55	
Temperature	298(2) K	
Wavelength	0.71073 Å	
Crystal system	Orthorhombic	
Space group	P 21 21 21	
Unit cell dimensions	a = 7.3243(3) Å	α = 90°.
	b = 9.2129(4) Å	β = 90°.
	c = 18.0415(8) Å	γ = 90°.
Volume	1217.41(9) $Å^3$	
Z	4	
Density (calculated)	1.694 Mg/m^3	
Absorption coefficient	0.750 mm^{-1}	
F(000)	632	
Crystal size	0.28 x 0.24 x 0.20 mm^3	
Theta range for data collection	2.482 to 27.580°.	
Index ranges	-9<=h<=9, -11<=k<=12, -23<=l<=23	
Reflections collected	14562	
Independent reflections	2802 [R(int) = 0.0336]	
Completeness to theta = 25.242°	99.5 %	
Absorption correction	None	
Refinement method	Full-matrix least-squares on F^2	
Data / restraints / parameters	2802 / 0 / 163	
Goodness-of-fit on F^2	1.164	
Final R indices [I>2sigma(I)]	R1 = 0.0287, wR2 = 0.0816	
R indices (all data)	R1 = 0.0307, wR2 = 0.0829	
Absolute structure parameter	-0.002(16)	
Extinction coefficient	n/a	
Largest diff. peak and hole	0.400 and -0.543 e.$Å^{-3}$	

The reaction of *p*-chloranil with *L*-prolinol also gave the tricyclic product **72ab** as a single diastereomer as revealed by X-ray-single crystal structure analysis (Figure 8).

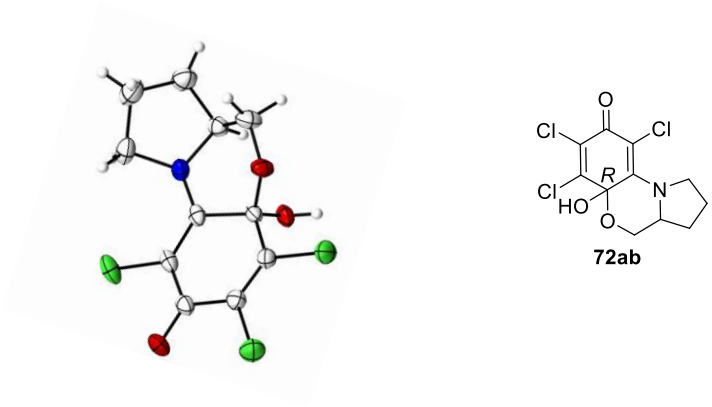

Figure 8 ORTEP representation of chiral aminoquinone-**72ab** (Thermal elipsoids were drawn with 50% probability).

The reaction of (*S*)-DPP with *p*-chloranil gave amine radical cation and *p*-chloranil radical anion and the signal strength decreases with time (Figure 9). The results are in accordance with initial formation of paramagnetic intermediates followed by formation of charge transfer complex and the tricyclic product (**72aa)**.

Scheme 21

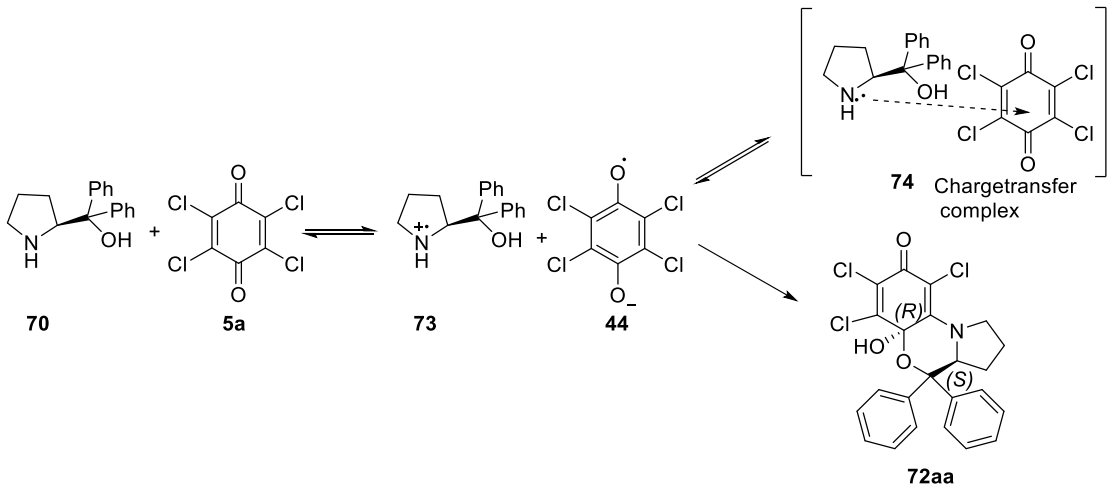

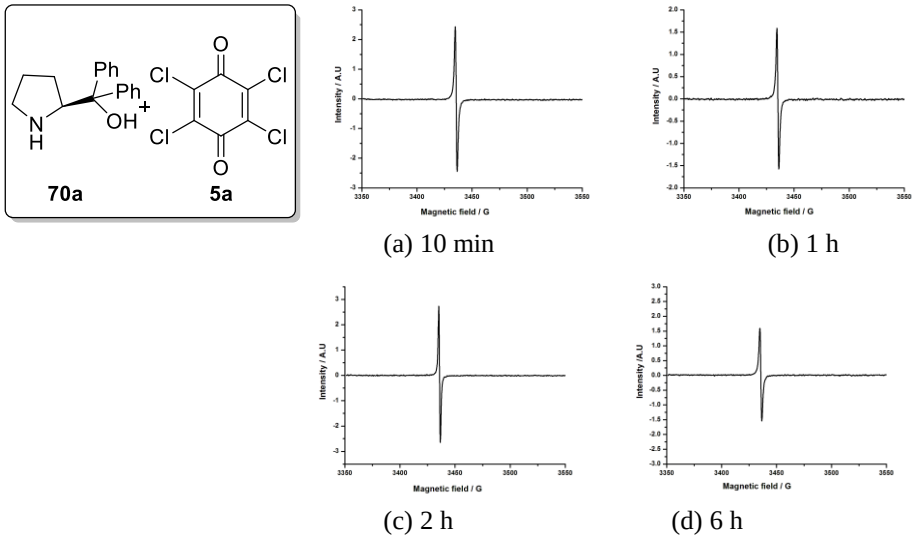

Figure 9. EPR studies of (*S*)-DPP **70a** (0.05 mmol) with *p*-chloranil **5a** (0.05 mmol) in DCM solvent with various time intervals.

2.2.6.2 Reactions of cyclic secondary amino alcohols with quinones.

The reaction of *p*-chloranil with *(S)*-DPP was carried out in various solvents. The use of DMF as solvent gave the tricyclic product **72aa** in 71% yield.

Table 11: Optimization of the reaction condition.[a,b]

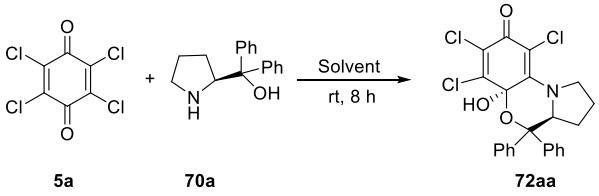

Entry	Solven (5 ml)	Yield (%)**72aa**
1	Toluene	20
2	DCM	52
3	THF	58
4	DMF	71
5	CH_3CN	53

[a]The reactions were carried out with quinone derivatives **5a** (2 mmol),and cyclic secondary amino alcohol **70a** (2 mmol) at rt for 8 h. [b]Isolated yield of **72aa**.

Therefore, we have carried out reaction of other quinone derivatives also in DMF solvent (Scheme 21a).

Scheme 21a

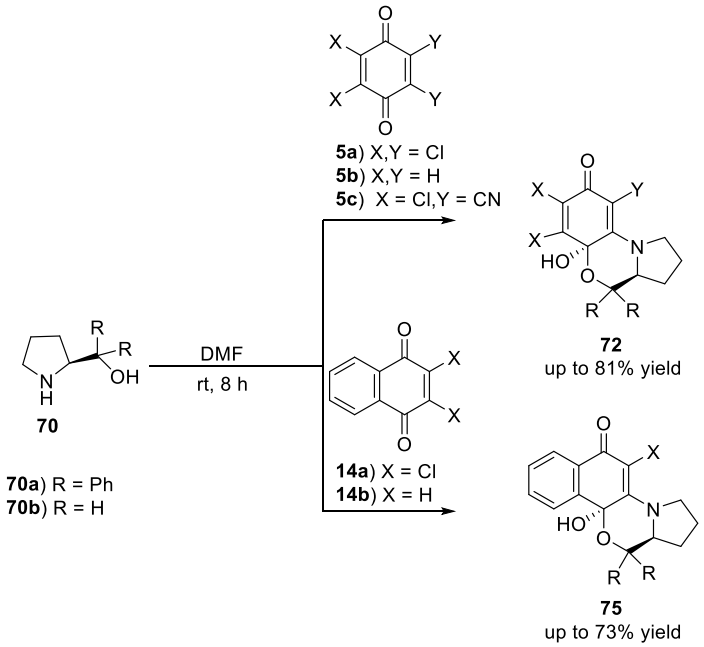

The results are summarized in Table 12.

Table 12: Synthesis of aminoquinone derivatives [a,b]

Entry	quinone	amino alcohol	Product[a]	Yield (%)[b]
1	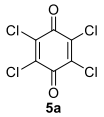 5a	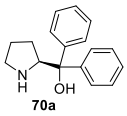 70a	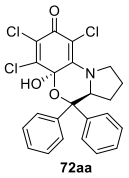 72aa	76
2	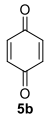 5b	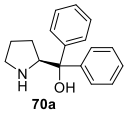 70a	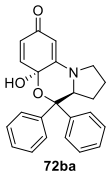 72ba	60
3	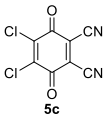 5c	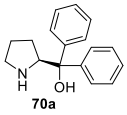 70a	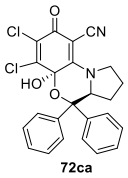 72ca	81
4	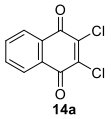 14a	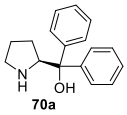 70a	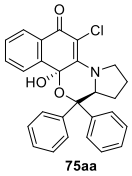 75aa	62
5	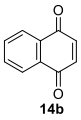 14b	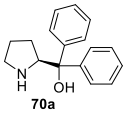 70a	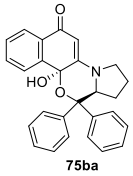 75ba	73
6	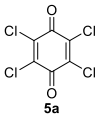 5a	 70b	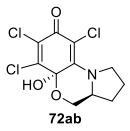 72ab	71

[a]The reactions were carried out using quinone derivatives (2 mmol), and prolinol derivatives (2 mmol) at rt for 8 h. [b]The yields are for isolated products.

A tentative mechanism for the formation of tricyclic aminoquinone product **72aa** is outlined in Scheme 22. The *p*-chloranil **5a** would accept an electron from (*S)*-DPP **70a** to give the paramagnetic radical anion **44** and radical cation **73** intermediates which would combine to give the intermediate **76.** Subsequent elimination of HCl followed by addition of alcohol moiety to the carbonyl group **77** would give the product **72aa** (Scheme 22).

Scheme 22

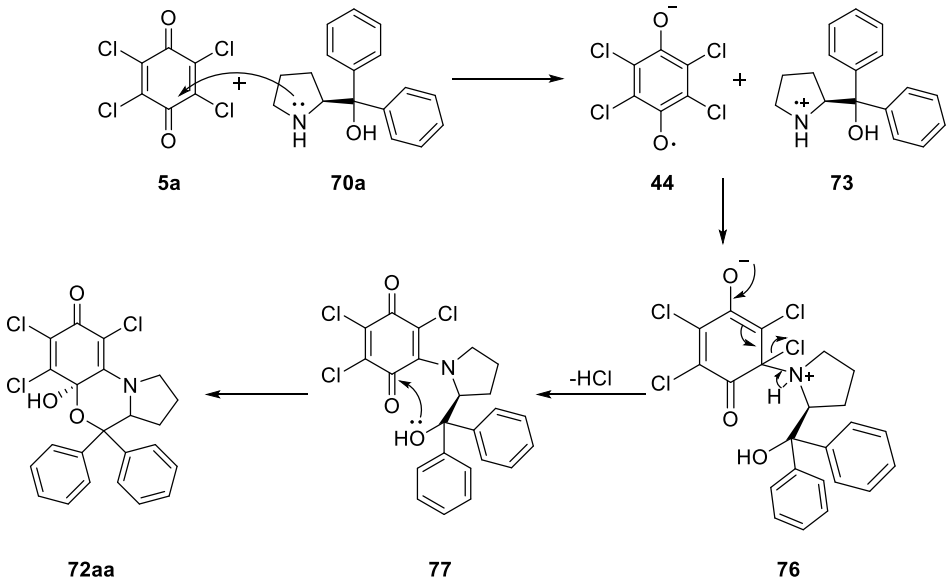

2.2.7 Synthesis of fused aminoquinol

We have observed that the tricyclic product **72ab** reacts with triflouroacetic acid **78** (TFA) to give the aromatized aminoquinol product **79** (Scheme 23).

Scheme 23

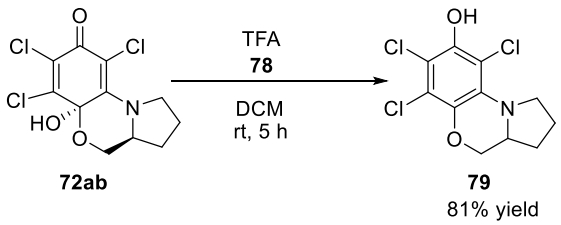

A tentative mechanism can be considered for the formation of fused aminoquinol product **79** as outlined in Scheme 24. Initially, the tricyclic aminoquinone OH group would be protonated by TFA **78.** Subsequent elimination of water molecule would lead to the carbocation intermediate **82.** Single electron transfer from triflouro acetate anion **80** to the intermediate **82** would give the aromatized intermediate **85** that may take a hydrogen from DCM to give the aminoquinol **79.** The intermediate **83** would further decompose to give carbon dioxide and hexaflouroethane[20] (Scheme 24).

Scheme 24

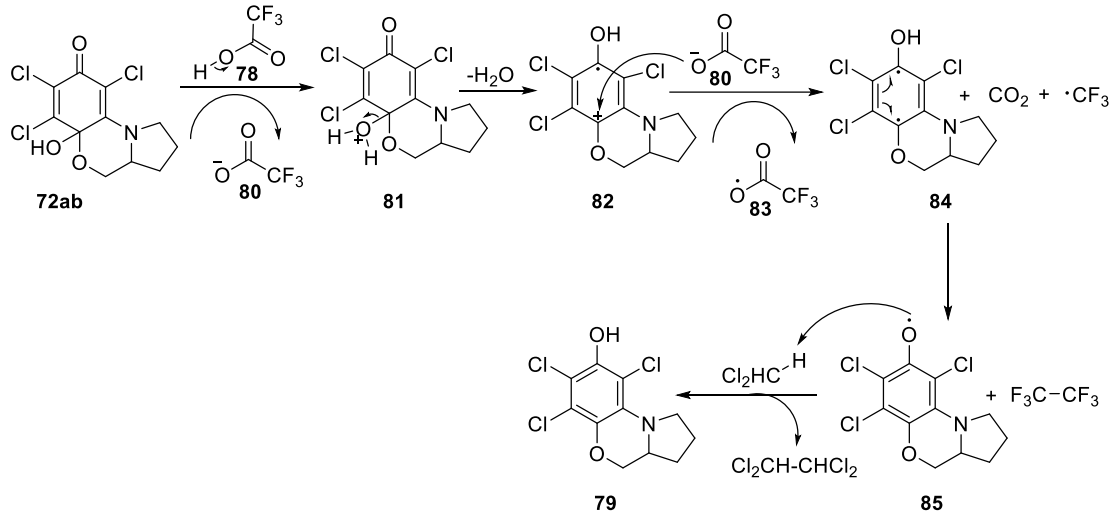

We have also carried out the TFA experiment by using 2-naphthol **86** and the chiral aminoquinone **72ab** (Scheme 25). Unfortunately, we have obtained only the racemic bi-2-naphthol **87** in 23% yield (Scheme 25).

Scheme 25

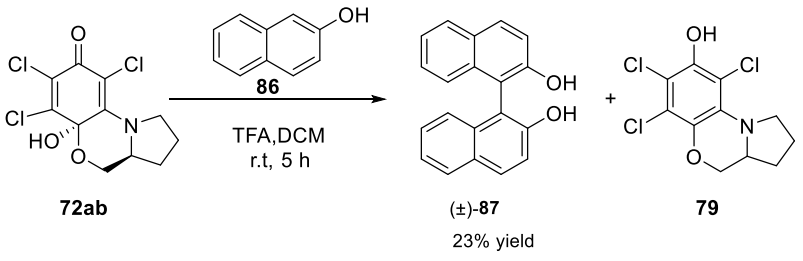

2.2.8 Synthesis of racemic bi-2-naphthol (BINOL) using *p*-chloranil, triflouroacetic acid and 2-naphthol.

We have observed that the reaction of 2-naphthol **86** with *p*-chloranil **5a** and triflouroacetic acid **78** gave the bi-2-naphthol **87** in 80% yield in DCM solvent at 25°C (Scheme 26).

Scheme 26

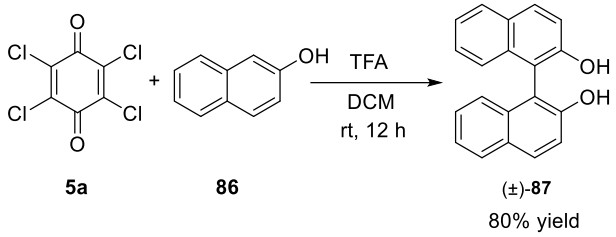

A tentative mechanism can be considered for the formation of bi-2-naphthol **87** as outlined in Scheme 27. Initially, the *p*-chloranil carbonyl groups could be protonated by TFA **78** to give the intermediates **88** and **80.** Single electron transfer from triflouro acetate anion **80** to the intermediate **89** could give the $CF_3COO^{\cdot}$**83.** Single electron transfer from 2-naphthol **86** to the intermediate **83** would generate radical cation **91** and radical **92** which after coupling and aromatization would result in the bi-2-naphthol **87** product (Scheme 27).

Scheme 27

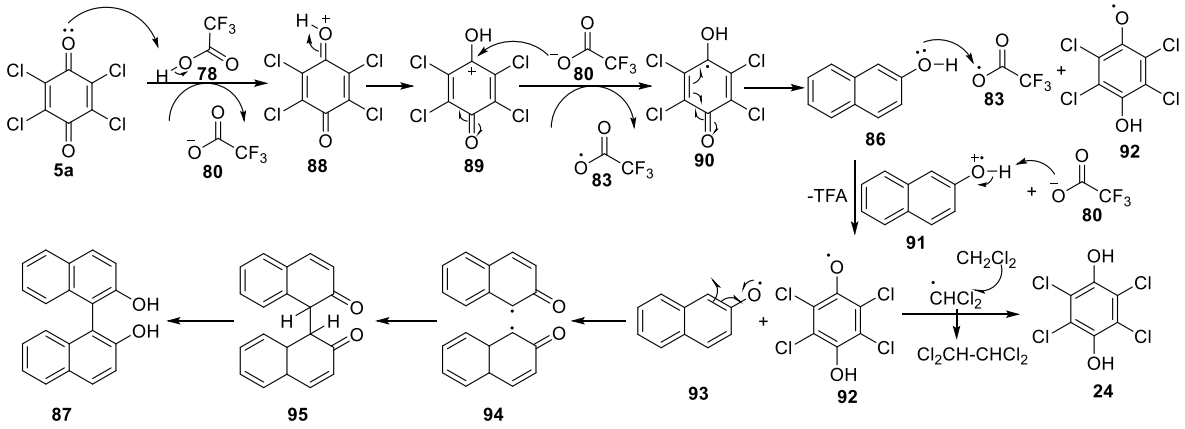

2.2.9 Synthesis of *N,N'*-Alkyl substituted meso piperazine

We have also synthesized the piperazine derivative **100** for examining its electron transfer reaction with *p*-chloranil as outlined in Scheme 28.

Scheme 28

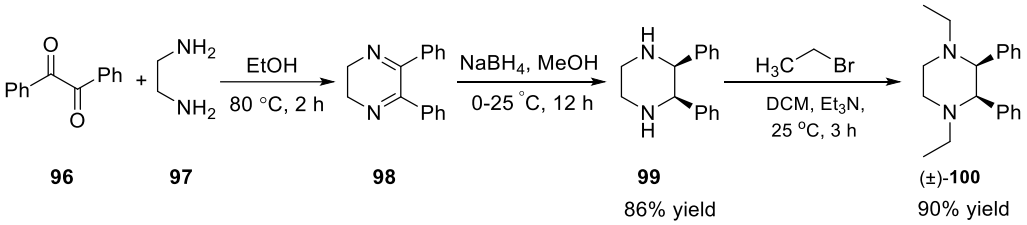

The condensation reaction between benzil **96** and ethylenediamine **97** in ethylalcohol resulted in the formation of 5,6-diphenyl-2,3-dihydropyrazine **98** which on reduction with $NaBH_4$/ MeOH gave the meso-2,3-diphenylpiperazine **99** in 86% yield. After further reaction with ethyl bromide using triethyl amine as a base in DCM solvent, the meso *N,N'*-diethyl piperazine product **100** was obtained in 90% yield.

2.2.9.1 Reaction of *N,N'*-dialkyl meso piperazine derivative with *p*-chloranil acceptor

The reaction of *N,N'*-diethylmesopiperazine with *p*-chloranil gave paramagnetic intermediates through electron transfer reaction. The strength of the epr signal decreased with time (Figure 10).

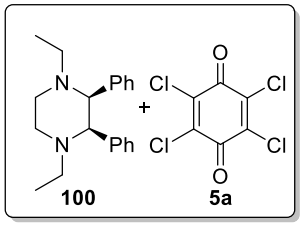

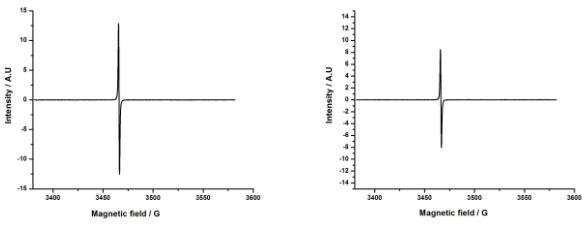

(a) 10 min (b) 1 h

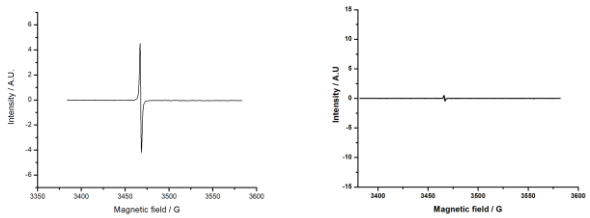

(c) 2 h (d) 6 h

Figure 10. EPR studies of *N,N'*-diethylmesopiperazine **100** (0.05 mmol) with *p*-chloranil **5a** (0.05 mmol) in DCM solvent under various time intervals.

2.2.9.2 Electron transfer reaction of *p*-chloranil and *N,N'*-diethylmesopiperazine

Scheme 29

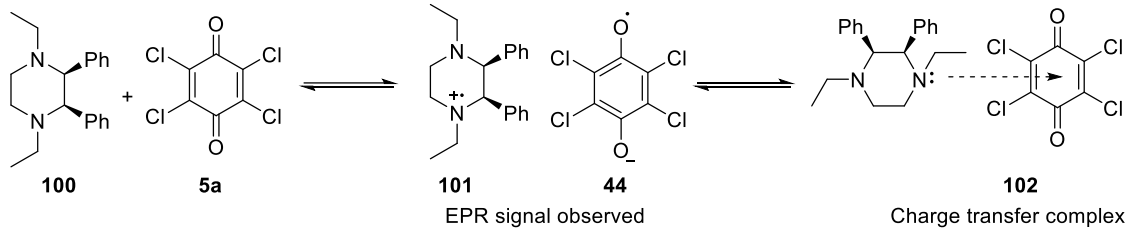

Presumably, the initially formed radical ion intermediates would give the diamagnetic charge transfer complex. There was no other organic product obtained.

Previously, electrochemical cells were constructed in this laboratory based on the reaction of simple tertiary amines like diisopropyl ethylamine, DABCO and triphenylamine with *p*-chloranil as electron acceptor and benzoquinone as electron transporter.[21] We have investigated the use of sulfones in the place of benzoquinone as electron acceptor. The results are described in the next chapter.

2.3 Conclusions

Systematic studies on the reaction of tertiary aryl amines, acyclic tertiary amino alcohols, cyclic tertiary amino alcohols, cyclic secondary amino alcohols with *p*-chloranil were carried out. The reactions gave paramagnetic intermediates but the esr signal strength decreased with time, indicating that the initially formed paramagnetic intermediates participate in further reactions. Accordingly, we have developed several new synthetic methods based on these electron transfer reactions.

We have developed a method for the synthesis of monosubstituted *N,N'*- dialkyl-1-naphthylaminoquinone derivatives using different *N,N*-dialkylnapthalene derivatives with *p*-chloranil.

Scheme 9

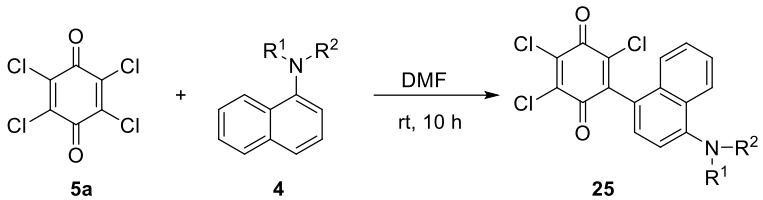

5a **4** **25**

up to 84% yield

4a) $R^1,R^2 = CH_3$
4b) $R^1,R^2 = C_2H_5$
4c) $R^1 = CH_3$ $R^2 = C_2H_5$

We have also developed a method for the synthesis of aryloxy derivatives based on electron transfer reaction of *N,N*-dialkyl naphthalene derivatives with 3,4,5,6-tetrachloro-1,2-napthoquinone.

Scheme 12

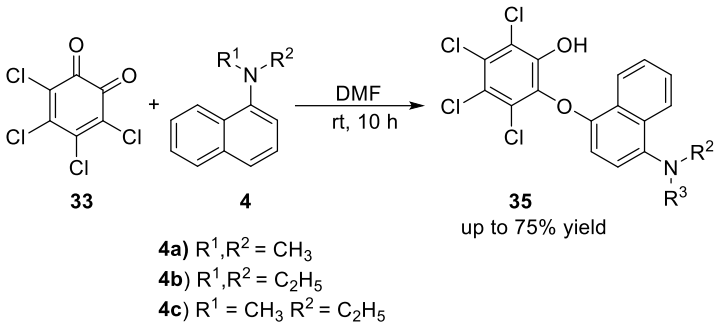

Further, a method for the synthesis of fused aminoquinone derivatives by the reaction of *p*-chloranil with *N,N*-dimethylaminoethanol was developed.

Scheme 15

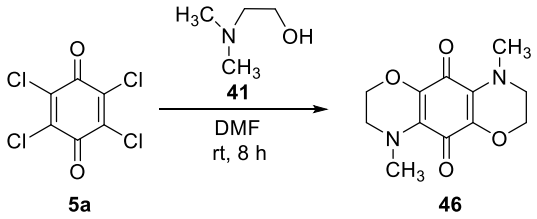

Also, a new method for the synthesis of chiral tricyclic products using quinone derivatives and different cyclic secondary amino alcohols was developed.

Scheme 4

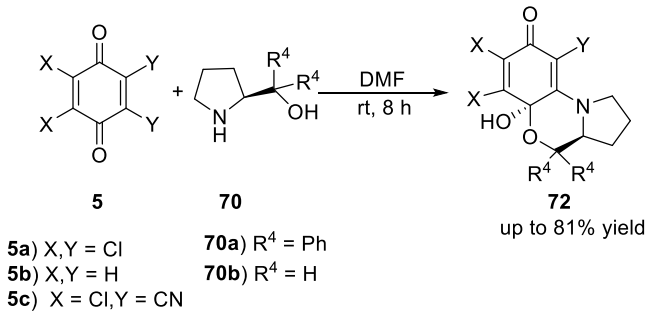

Finally, we have also developed a method for the preparation of bi-2-naphthol using *p*-chloranil, triflouroacetic acid and 2-naphthol.

Scheme 26

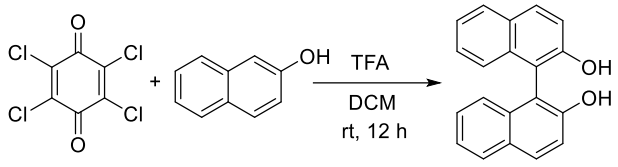

5a **86** **87**
80% yield

These methods have potential for further exploitation in organic synthesis.

2.4 Experimental Section

2.4.1 General Information

IR (KBr) and IR (neat) spectra were recorded on JASCO FT-IR spectrophotometer model-5300. The NMR spectra [^{1}H (400 MHz) and ^{13}C (100 MHz)] were recorded on Bruker-Avance-400 spectrometers chloroform-d as solvent. Chemical shifts are expressed in δ downfield with respect to the signal of internal standard tetramethylsilane (δ = 0 ppm). Coupling constants *J* are in Hz. The mass spectral analyses were carried out using Chemical Ionization (CI) or Electro Spray Ionization (ESI) techniques. EPR spectra was recorded in a spectrometer equipped with an EMX micro X source for X band measurement using Xenon 1.1b.60 software provided by the manufacturer. Analytical thin layer chromatographic tests were carried out on glass plates (3 x 10 cm) coated with 250 mμ silica gel-G and GF_{254} containing 13% calcium sulfate as binder. The spots were visualized by short exposure to iodine vapor or UV light. Column chromatography was carried out using silica gel (100-200 mesh).

All the glasswares were pre-dried at 100-120 ˚C in an air-oven for 4 h, assembled in hot condition and cooled under a stream of dry nitrogen. Unless otherwise mentioned, all the operations and transfer of reagent were carried out using standard syringe-septum technique recommended for handling air sensitive reagents and organometallic compounds.

In all experiments, a round bottom flask of appropriate size with a side arm, a side septum, a magnetic stirring bar, a condenser and a connecting tube attached to a mercury bubbler was used. The outlet of the mercury bubbler was connected to the atmosphere by a

long tube. All dry solvents and reagents used were distilled from appropriate drying agents. As a routine practice, all organic extracts were washed using saturated NaCl solution (brine) and dried over Na_2SO_4 or K_2CO_3 and concentrated on Heidolph-EL-rotary evaporator.

Toluene and THF were freshly distilled over sodium-benzophenone ketyl before use. $NaBH_4$, and NaOH were supplied by E-Merck (India) was used as received. Naphthylamine, and *N*,*N*-diethyl aniline were supplied by Avra (India) was used as received. chloranil, were purchased from Aldrich.

2.4.2 General procedure for the preparation of compounds 25aa-25af

To a reaction flask cooled under N_2, was added *N*,*N*'-dialkyl naphthylamine (2 mmol) in DMF (10 mL). To this solution chloranil (2 mmol) were added and stirred at 25 °C for 10 h. After completion of the reaction, work up with DCM, filtered on anhyd.Na_2SO_4 evaporated on rotary evaporator. The residue was subjected to chromatography on silica gel (100-200 mesh) using 20% ethyl acetate in hexane to elute the desired products.

2,3,5-Trichloro-6-(4-(dimethylamino)naphthalen-1-yl)cyclohexa-2,5-diene-1,4-dione (25aa)

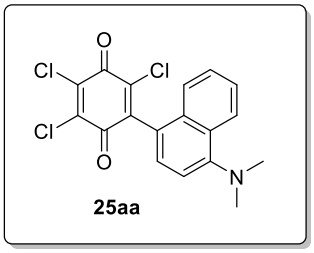

25aa

Yield : 0.638 g (84%); Violet colour solid,

mp : 118-120 ^oC;

IR (Neat) : 3049, 2936, 2827, 2781, 1680, 1562, 1510, 1458, 1386, 1329, 1252, 1210, 1102, 1040, 952, 890, 766cm^{-1}.

^{1}H NMR :(400 MHz, $CDCl_3$): 8.31-8.29 (d, J=8.08Hz, 1H), 7.54-7.37 (m, 3H), 7.23-7.21 (d, J=7.52Hz, 1H), 7.12-7.10 (d, J=7.56Hz, 1H), 2.98 (s, 6H).

^{13}C NMR **:** (100 MHz, $CDCl_3$): 175.4, 171.6, 153.1, 144.2, 142.0, 141.7, 140.5,131.5, 128.4, 127.9, 126.7, 125.3, 125.5, 125.0, 122.3, 112.7, 44.9.

HRMS : (ESI-TOF) m/z: $[M + H]^+$ Calcd for $C_{18}H_{12}Cl_3NO_2$: 380.0012; Found: 380.0016.

2,3,5-Trichloro-6-(4-(diethylamino)naphthalen-1-yl)cyclohexa-2,5-diene-1,4-dione (25ab)

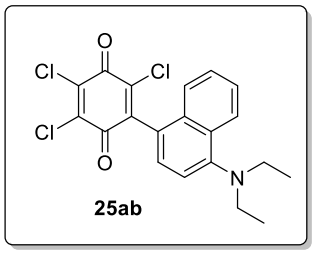

Yield : 0.612 g (75%); Violet colour solid,

mp : 135-139 ^oC;

IR (Neat) : 2972, 2928, 1684, 1568, 1508,1458, 1211, 1171, 1108, 1057, 906, 813, 766cm^{-1}.

^{1}H NMR **:** (400 MHz, $CDCl_3$): 8.38-8.36 (d, J=8.28Hz, 1H), 7.53-7.39 (m, 3H),7.25 7.23 (d, J=7.8Hz, 1H), 7.18-7.16 (d, J=7.8Hz, 1H), 3.33-3.28 (q, J=7.12Hz, 4H) 1.16-1.12 (t, J=7.12Hz, 6H).

^{13}C NMR **:** (100 MHz, $CDCl_3$):175.4, 150.6, 144.3, 142.0, 141.7, 140.5, 131.6, 130.5, 127.6, 125.4, 125.2, 124.9, 122.7, 116.4, 47.3, 12.2.

IR (Neat) : 2972, 2928, 1684, 1568, 1508, 1458, 1211, 1171, 1108, 906, 813, 766cm^{-1}.

HRMS : (ESI-TOF) m/z: $[M + H]^+$ Calcd for $C_{20}H_{16}Cl_3NO_2$: 408.0325; Found: 408.0321.

2.4.3 General procedure for the preparation of compounds 25ad-25af:

To a stirred suspension of naphthyl amines (2 mmol) in toluene (10 mL), chloranil **2** (2 mmol) was added at 25 ^oC. The contents were stirred at 80 ^oC for 10 h. Toluene was removed; water (5 mL) and DCM (15 mL) were added. The DCM layer was washed with

saturated NaCl solution, dried with Na_2SO_4 and concentrated. The residue was chromatographed on silica gel (100-200 mesh) using 20% ethyl acetate in hexane as to elute the desired products.

2,3,5-Trichloro-6-(4-(pyrrolidin-1-yl)naphthalen-1-yl)cyclohexa-2,5-diene-1,4-dione (25ad)

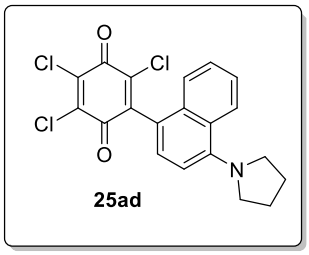

25ad

Yield : 0.665 g (82%); Violet colour solid,

mp : 168-171 ºC;

IR (Neat) : 3016, 2945, 2836, 2763, 1680, 1678, 1560, 1509, 1448, 1386, 1320, 1242, 1210, 1102, 952, 890, 756cm^{-1}.

^{1}H NMR **:** (400 MHz, $CDCl_3$): 8.31-8.28 (m, 1H), 7.45-7.41 (m, 2H), 7.39-7.34 (m, 1H), 7.21-7.19 (d, J=8.0Hz, 1H), 6.93-6.91 (d, J=8.05Hz, 1H), 3.58-3.55 (m, 4H), 2.07-2.04 (m, 4H).

^{13}C NMR **:** (125 MHz, $CDCl_3$): 175.6, 171.7, 150.1, 144.2, 141.6, 141.0, 140.5, 131.9, 128.8, 126.9, 126.5, 125.9, 125.1, 124.0, 119.5, 108.8, 52.7, 25.4.

HRMS : (ESI-TOF) m/z: $[M + H]^+$ Calcd for $C_{20}H_{14}Cl_3NO_2$: 406.0168; Found: 406.0164.

2,3,5-Trichloro-6-(4-(piperidin-1-yl)naphthalen-1-yl)cyclohexa-2,5-diene-1,4-dione (25af)

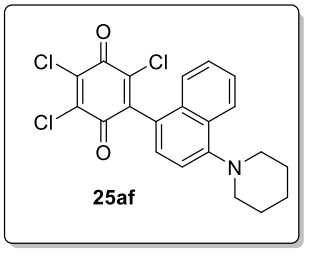

25af

Yield : 0.520 g (62%); Violet colour solid,

mp : 150-154 ºC;

IR (Neat) : 2932, 2851, 2805, 1681, 1564, 1509, 1449, 1426, 1378, 1338, 1292, 1255, 1214, 1177, 1108, 1036, 1001,905, 828, 791,765cm^{-1}.

^{1}H NMR **:** (500 MHz, $CDCl_3$): 8.28-8.26 (d, *J*=8.15 Hz, 1H), 7.53-7.50 (m, 1H), 7.47-7.44 (m, 1H), 7.39-7.38 (d, *J*=8.15 Hz, 1H), 7.23-7.22 (d, *J*=7.8 Hz, 1H), 7.12-7.10 (d, *J*=7.8 Hz, 1H), 3.14 (s, 4H), 1.91-1.86 (m, 4H), 1.71 (s, 2H).

^{13}C NMR **:** (125 MHz, $CDCl_3$): 175.6, 171.7, 153.4, 144.4, 142.1, 141.8, 140.7, 131.6, 129.1, 128.1, 126.8, 125.6, 125.1,125.0, 122.8, 113.6, 54.6, 26.6, 24.7.

HRMS : (ESI-TOF) m/z: $[M + H]^+$ Calcd for $C_{21}H_{16}Cl_3NO_2$: 420.0325; Found: 420.0364.

2.4.4 General procedure for the preparation of compounds 35a-35c:

To a reaction flask cooled under N_2, was added *N*,*N*'-dialkyl naphthylamine (2 mmol) in DMF (5 mL). To this solution *o*-chloranil (2 mmol) were added and stirred at 25 °C for 10 h. After completion of the reaction, work up with DCM, filtered on anhyd.Na_2SO_4 evaporated on rotary evaporator. The residue was subjected to chromatography on silica gel using 10% ethyl acetate in hexane to elute the desired products.

2,3,4,5-Tetrachloro-6-((4-(dimethylamino)naphthalen-1-yl)oxy)phenol (35a)

Yield : 0.625 g (75%); White solid,

mp : 165-167 ^{o}C;

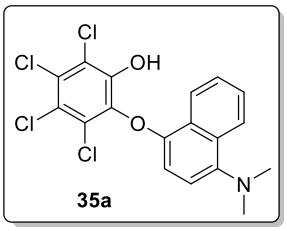

IR (KBr) : 3390, 1773, 1706, 1624, 1587, 1551, 1433,1391, 1272, 1226, 1190, 1148, 1050, 993, 952, 901, 766,823cm^{-1}.

^{1}H NMR : (400 MHz, $CDCl_3$): 11.22 (s, 1H), 8.39-8.38 (m, 1H), 8.21-8.19 (m, 1H), 7.62-7.60 (m, 2H), 6.88-6.86 (d, *J*=8.28 Hz, 1H), 6.43-6.41 (d, *J*=8.24 Hz, 1H), 2.74 (s, 6H).

^{13}C NMR : (100 MHz, $CDCl_3$): 148.7, 148.4, 146.0, 140.0, 129.7, 128.9, 127.0, 126.6, 126.1, 125.7, 124.1, 122.8, 122.0, 121.6, 114.1, 106.9, 45.5.

HRMS : (ESI-TOF) m/z: $[M + H]^+$ Calcd for $C_{18}H_{13}Cl_4NO_2$: 415.9778; Found: 415.9759.

2,3,4,5-Tetrachloro-6-((4-(diethylamino)naphthalen-1-yl)oxy)phenol (35b)

Yield : 0.631 g (71%); White solid,

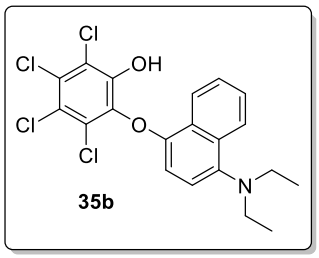

35b

mp : 130-132 ºC;

IR (KBr) : 3478, 1742, 1582, 1515, 1427, 1376, 1262, 1231, 1148, 1055, 983, 937, 802, 766, 601cm^{-1}.

^{1}H NMR : (400 MHz, $CDCl_3$): 11.23 (s, 1H), 8.35-8.26 (m, 2H), 7.61-7.58 (m, 2H), 7.02-7.00 (d, *J*=8.2 Hz, 1H), 6.48-6.46 (d, *J*=8.24 Hz, 1H), 3.09-3.04 (m, 4H), 0.95-0.92 (t, *J*=7.04 Hz, 6H).

^{13}C NMR : (100 MHz, $CDCl_3$): 148.7, 142.5, 139.9, 132.3, 128.9, 126.9, 126.6, 126.1, 125.6, 124.1, 122.6, 122.0, 121.5, 118.3, 106.9, 48.0, 12.6.

HRMS : (ESI-TOF) m/z: $[M + H]^+$ Calcd for $C_{20}H_{17}Cl_4NO_2$: 444.0091; Found: 444.0083.

2,3,4,5-Tetrachloro-6-((4-(ethyl(methyl)amino)naphthalen-1-yl)oxy)phenol 35c:

Yield : 0.594 g (69%); White solid,

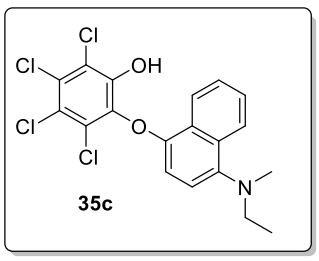

35c

mp : 124-127 ºC;

IR (KBr) : 3452, 1593, 1546, 1427, 1391, 1267, 1221,1050, 901, 808, 761, 704cm^{-1}.

^{1}H NMR : (400 MHz, $CDCl_3$): 11.22 (s, 1H), 8.40-8.38 (m, 1H), 8.22-8.19 (m, 1H), 7.61-7.59 (m, 2H), 6.90-6.88 (d, *J*=8.28 Hz, 1H), 6.44-6.42 (d, *J*=8.24 Hz, 1H), 3.00-2.95 (m, 2H), 2.70 (s, 3H),1.10-1.07 (t, *J*=6.92 Hz, 3H).

^{13}C NMR : (100 MHz, $CDCl_3$): 148.7, 148.5, 145.2, 139.9, 130.6, 128.9, 127.0, 126.6, 126.1, 125.7, 123.9, 122.8, 122.0, 121.6, 115.6, 106.9, 51.5, 41.8, 13.0.

HRMS : (ESI-TOF) m/z: $[M + H]^+$ Calcd for $C_{19}H_{15}Cl_4NO_2$: 429.9935; Found: 429.9928.

2.4.5 General procedure for the preparation of compounds (46-50)

To a reaction flask cooled under N_2, was added *N,N-dimethyl amino ethanol* (2.4 g, 8 mmol) in DMF (10 mL). To this solution quinone (2 mmol) were added and stirred at 25 °C for 8 h. After completion of the reaction, the residue was subjected to chromatography on silica gel (100-200 mesh) using 50% ethyl acetate in hexane to elute the desired products **46** to **50**.

4-Methyl-3,4-dihydro-2H-naphtho[2,3-b][1,4]oxazine-5,10-dione (49)

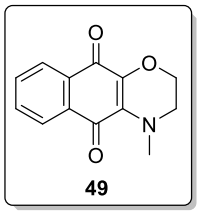

49

Yield : 0.403 g (88%); black colour solid,

mp : 145-148 °C;

IR (Neat) : 1627, 1584, 1563, 1482, 1428, 1379, 1319, 1282,1233, 1190, 1147, 1055, 1022, 952, 714 cm^{-1}.

^{1}H NMR : (400 MHz, $CDCl_3$): δ 8.05-8.04 (m, 1H), 7.98-7.96 (m, 1H), 7.67-7.59 (m, 2H), 4.28-4.26 (m, 2H), 3.35-3.33 (m, 2H),3.27 (d, *J*=1.6 Hz, 3H).

^{13}C NMR : (100 MHz, $CDCl_3$): δ 181.8, 177.0, 141.0, 134.5, 133.4, 132.7, 131.4, 130.9, 126.0, 125.6, 63.3, 50.7, 41.8.

HRMS : (ESI-TOF) m/z: $[M + H]^+$ Calcd for $C_{13}H_{11}NO_3$: 230.0812; Found: 230.0817.

6,7-Dichloro-4-methyl-3,4-dihydro-2H-benzo[b][1,4]oxazine-5,8-dione (47)

Yield : 0.418 g (30%); Black colour solid,

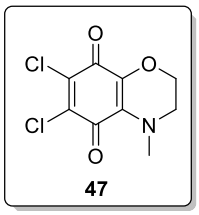

47

mp : 128-130 °C;

IR (Neat) : 1663, 1623, 1600, 1557, 1480, 1433, 1388,1322, 1246, 1201, 1162, 1112, 1017, 901, 767 cm^{-1}.

^{1}H NMR : (400 MHz, $CDCl_3$): δ 4.22-4.20 (t, *J*=3.8 Hz, 2H), 3.33-3.31 (t, *J*=3.9 Hz, 2H), 3.20 (s, 3H).

^{13}C NMR : (100 MHz, $CDCl_3$): δ 174.6, 169.9, 138.6, 138.0, 136.7, 132.1, 63.5, 50.8, 41.9.

HRMS : (ESI-TOF) m/z: $[M + H]^+$ Calcd for $C_9H_7Cl_2NO_3$: 247.9876; Found: 247.9880.

4,9-Dimethyl-3,4,8,9-tetrahydrobenzo[1,2-b:4,5-b']bis([1,4]oxazine)-5,10(2H,7H)-dione (46)

Yield : 0.4 g (80%); Black colour solid,

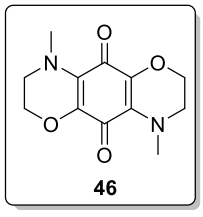

46

m.p : 190-195 °C;

IR (KBr) : 1627, 1557, 1471, 1422, 1379, 1314, 1276,1249, 1201, 1060, 974,

741 cm^{-1}.

^{1}H NMR : (400 MHz, $CDCl_3$): δ 4.1-4.08 (t, *J*=3.92 Hz, 2H), 3.18-3.16 (t, *J*=3.96 Hz, 2H), 3.09 (s, 3H).

^{13}C NMR : (100 MHz, $CDCl_3$): δ 176.4, 136.5, 129.6, 62.8, 50.8, 42.0.

HRMS : (ESI-TOF) m/z: $[M + Na]^+$ Calcd for $C_{12}H_{14}N_2O_4$: 273.0846; Found: 273.0856.

1-Methyl-1,2,3,4-tetrahydrobenzo[g]quinoxaline-5,10-dione (50)

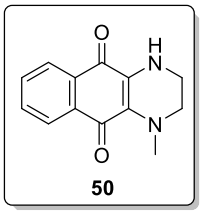

50

Yield : 0.401 g (88%); black colour solid,

mp : 124-128 °C;

IR (Neat) : 1773, 1638, 1595, 1557, 1471, 1390, 1330, 1287,1244, 1184,1152, 1055, 957, 720 cm^{-1}.

^{1}H NMR : (400 MHz, $CDCl_3$): δ 8.06-8.03 (m, 1H), 7.98-7.96 (m, 1H), 7.66-7.59 (m, 2H), 4.28-4.26 (t, *J*=4.16 Hz, 2H), 3.35-3.33 (t, *J*=4.2 Hz, 2H), 3.27 (s, 3H).

^{13}C NMR : (100 MHz, $CDCl_3$): δ 181.8, 177.0, 141.0, 134.4, 133.4, 132.7, 131.4, 130.9, 126.0, 125.6, 63.3, 50.7, 41.8.

HRMS : (ESI-TOF) m/z: $[M + H]^+$ Calcd for $C_{13}H_{12}N_2O_2$: 229.0972; Found: 229.0972.

6,7-Dichloro-1-methyl-1,2,3,4-tetrahydroquinoxaline-5,8-dione (48)

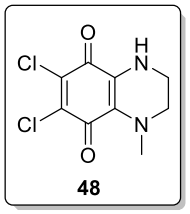

48

Yield : 0.405 g (82%); Black solid,

m.p : 127-130 °C;

IR (Neat) : 1660, 1622, 1595, 1557, 1428, 1384, 1325, 1244,1201, 1163, 1114, 1060, 1011, 909, 849, 801, 774, 725 cm^{-1}.

^{1}H NMR : (400 MHz, $CDCl_3$): δ 4.20-4.18 (m, 2H), 3.33-3.31 (m, 2H), 3.19 (s, 3H).

^{13}C NMR : (100 MHz, $CDCl_3$): δ 174.5, 169.8, 138.6, 137.9, 136.7, 132.1, 63.5, 50.8, 41.9.

HRMS : (ESI-TOF) m/z: $[M + H]^+$ Calcd for $C_9H_8Cl_2N_2O_2$: 247.0036; Found: 247.0041.

2.4.6 General procedure for the preparation of compounds 72aa-ca and 75aa-ba:

To a reaction flask cooled under N_2, was added *Prolinol derivatives* (2 mmol) in DMF (10 mL). To this solution quinone (2 mmol) were added and stirred at 25 °C for 8 h. After completion of the reaction, the residue was subjected to chromatography on silica gel (100-200 mesh) using 20-30% ethyl acetate in hexane to elute the desired products.

5-Chloro-10b-hydroxy-12,12-diphenyl-2,3,12,12a-tetrahydro-1H-naphtho[1,2-b]pyrrolo[1,2-d][1,4]oxazin-6(10bH)-one (75aa)

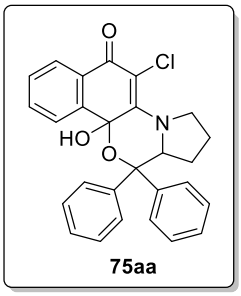

75aa

Yield : 0.54 g (62%); Yellow solid,

mp : 120-125 °C;

$[\alpha]_D^{25}$:-120.18 (*c* 0.11, $CHCl_3$);

IR (Neat) : 3227, 1594, 1534, 1479, 1446, 1293, 1276, 1106, 1024, 887, 761, 695 cm^{-1}.

^{1}H NMR : (400 MHz, $CDCl_3$): δ 7.73-7.71 (d, *J*=7.76 Hz, 1H), 7.6-7.58 (d, *J*=7.24 Hz, 3H), 7.52-7.40 (m, 4H), 7.24-7.13 (m, 4H), 6.94-6.92 (d, *J*=7.6 Hz, 2H), 5.77-5.74 (m, 1H), 5.16 (s, 1H), 4.24-4.17 (m, 1H), 4.02-3.97 (m, 1H), 2.43-2.34 (m, 1H), 1.97-1.92 (m, 1H) 1.69-1.64 (m, 1H), 0.64-0.52 (m, 1H).

^{13}C NMR : (100 MHz, $CDCl_3$): δ 177.2, 155.5, 145.5, 142.0, 139.8, 132.0, 128.8, 128.4, 128.2, 128.0, 127.8, 127.7, 127.6, 126.9, 125.7, 125.1, 101.6, 92.1, 81.4, 60.2, 52.5, 28.6, 23.0.

HRMS : (ESI-TOF) m/z: $[M + H]^+$ Calcd for $C_{27}H_{22}ClNO_3$: 444.1361; Found: 444.1371.

6,7,9-Trichloro-5a-hydroxy-4,4-diphenyl-2,3,3a,4-tetrahydro-1H-benzo[b]pyrrolo[1,2-d][1,4]oxazin-8(5aH)-one (72aa)

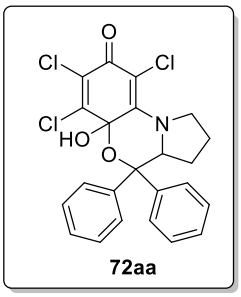

72aa

Yield : 0.70 g (76%); Yellow solid,

mp : 170-173 °C;

$[\alpha]_D^{25}$: -849.28 (*c* 0.1, $CHCl_3$);

IR (KBr) : 3287, 1627, 1545, 1452, 1408, 1347, 1287, 1221, 1150, 1052, 1013, 947, 887, 778, 756, 706, 663, 580 cm^{-1}.

^{1}H NMR : (400 MHz, $CDCl_3$): δ 7.55-7.53 (m, 2H), 7.50-7.41 (m, 3H), 7.29-7.27 (m, 3H), 6.93-6.90 (m, 2H), 5.44-5.41 (m, 1H), 4.20-4.14 (m, 1H), 3.99-3.93 (m, 1H), 3.82 (s, 1H), 2.42-2.32 (m, 1H), 1.91-1.85 (m, 1H) 1.75-1.69 (m, 1H), 0.79-0.69 (m, 1H).

^{13}C NMR : (100 MHz, $CDCl_3$): δ 170.4, 152.7, 144.7, 140.8, 140.5, 131.1, 128.6, 128.2, 127.9, 127.8, 126.6, 99.5, 92.0, 81.6, 61.2, 52.7, 29.0, 23.1.

HRMS : (ESI-TOF) m/z: $[M + H]^+$ Calcd for $C_{23}H_{18}Cl_3NO_3$: 462.0425; Found: 462.0432.

6,7,9-Trichloro-5a-hydroxy-2,3,3a,4-tetrahydro-1H-benzo[b]pyrrolo[1,2-d][1,4]oxazin-8(5aH)-one (72ab)

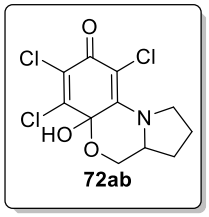

72ab

Yield : 0.44 g (71%); Yellow solid,

mp : 160-163 °C;

$[\alpha]_D^{25}$: -153.87 (*c* 0.1, $CHCl_3$);

IR (Neat) : 3319, 1617, 1541, 1465, 1444, 1298, 1255, 1190, 1038, 1017, 990, 876, 734 cm^{-1}.

^{1}H NMR : (400 MHz, $CDCl_3$): δ 8.15 (s, 1H), 4.42-4.41 (m, 1H), 4.23-4.18 (m, 2H), 4.11-4.07 (m, 1H), 2.5 (s, 1H), 2.13-2.10 (m, 1H), 2.00-1.97 (m, 1H), 1.93-1.89 (m, 1H), 1.53-1.49 (m, 1H).

^{13}C NMR : (100 MHz, $CDCl_3$): δ 169.1, 155.2, 142.8, 129.3, 98.0, 90.4, 65.7, 55.7,53.1, 28.1, 24.3.

HRMS : (ESI-TOF) m/z: $[M + H]^+$ Calcd for $C_{11}H_{10}Cl_3NO_3$: 309.9804; Found: 309.9809.

6,7-Dichloro-5a-hydroxy-8-oxo-4,4-diphenyl-2,3,3a,4,5a,8-hexahydro-1H-benzo[b]pyrrolo[1,2-d][1,4]oxazine-9-carbonitrile (72ca)

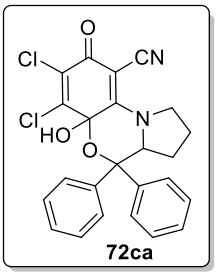

72ca

Yield : 0.73 g (81%); Light pink solid,

mp : 175-178 °C;

$[\alpha]_D^{25}$: -395.60 (*c* 0.3, $CHCl_3$);

IR (Neat) : 3276, 1610, 1556, 1495, 1441, 1358, 1304, 1106, 1046, 854, 805, 690 cm^{-1}.

^{1}H NMR : (400 MHz, $CDCl_3$): δ 8.42 (s, 1H), 7.51-7.44 (m, 4H), 7.41-7.37 (m, 1H), 7.30-7.29 (m, 3H), 6.83-6.80 (m, 2H), 5.31-5.28 (m, 1H), 4.01-3.94 (m, 1H), 3.77-3.72 (m, 1H), 3.38 (s, 1H), 1.82-1.67 (m, 2H), 0.78-0.71 (m, 1H).

^{13}C NMR : (100 MHz, $CDCl_3$): δ 172.8, 161.9, 144.6, 143.4, 141.3, 130.4, 128.7, 128.5, 128.3, 128.0, 127.0, 117.1, 90.0, 82.1, 78.9, 61.5, 51.8, 29.0, 23.1.

HRMS : (ESI-TOF) m/z: $[M + H]^+$ Calcd for $C_{24}H_{18}Cl_2N_2O_3$: 453.0767; Found: 453.0771.

5a-Hydroxy-4,4-diphenyl-2,3,3a,4-tetrahydro-1H-benzo[b]pyrrolo[1,2-d][1,4]oxazin-8(5aH)-one (72ba)

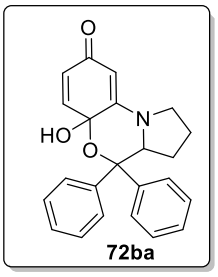

72ba

Yield : 0.43 g (60%); Light red solid,

mp : 170-175 °C;

$[\alpha]_D^{25}$: -558.17 (*c* 0.15, $CHCl_3$);

IR (Neat) : 3249, 1660, 1561, 1495, 1452, 1408, 1353, 1271, 1156, 1134, 1073, 1024, 838, 750, 695 cm^{-1}.

^{1}H NMR : (400 MHz, $CDCl_3$): δ 7.48-7.37 (m, 5H), 7.23 (s, 3H), 6.87 (s, 2H), 6.55-6.53 (d, *J*=9.0 Hz, 1H), 5.92-5.90 (d, *J*=8.9 Hz, 1H), 5.61 (s, 1H), 5.33-5.31 (d, *J*=7.6 Hz, 1H), 5.04 (s, 1H), 3.27 (s, 1H), 3.05 (s, 1H), 2.40 (s, 1H) 1.77 (s, 2H), 1.14 (s, 1H).

^{13}C NMR : (100 MHz, $CDCl_3$): δ 184.6, 158.2, 144.8, 142.0, 138.9, 128.2, 128.1, 127.8, 127.6, 127.1, 93.2, 89.4, 82.1, 59.6, 53.4, 47.6, 29.9, 22.8.

HRMS : (ESI-TOF) m/z: $[M + H]^+$ Calcd for $C_{23}H_{21}NO_3$: 360.1599; Found: 360.1606.

10b-Hydroxy-12,12-diphenyl-2,3,12,12a-tetrahydro-1H-naphtho[1,2-b]pyrrolo[1,2-d][1,4]oxazin-6(10bH)-one (75ba)

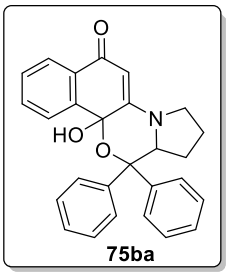

75ba

Yield : 0.59 g (73%); Light pink solid,

mp : 192-196 °C;

$[\alpha]_D^{25}$: -105.87 (*c* 0.52, $CHCl_3$);

IR (KBr) : 3121, 1603, 1546, 1494, 1453, 1386, 1298, 1164, 1009, 885, 828, 782, 704, 647, 596 cm^{-1}.

^{1}H NMR : (400 MHz, $CDCl_3$): δ 7.95-7.93 (m, 1H), 7.80-7.78 (m, 1H), 7.62-7.57 (m, 3H), 7.52-7.46 (m, 3H), 7.42-7.39 (m, 1H), 7.34 (s, 1H), 7.19-7.18 (m, 3H), 6.74-6.71 (m, 2H), 5.23-5.19 (t, *J*=7.3 Hz, 2H) 3.40-3.34 (m, 2H), 3.14-3.07 (m, 1H), 1.83-1.73 (m, 1H) 1.57-1.49 (m, 1H), 1.15-1.06 (m, 1H).

^{13}C NMR : (100 MHz, $CDCl_3$): δ 180.4, 158.5, 146.1, 143.2, 141.2, 131.7, 130.3, 128.8, 128.7, 128.1, 128.0, 127.9, 127.8, 127.2, 126.3,124.8, 93.8, 90.0, 82.6, 59.6, 47.8, 30.3, 22.9.

HRMS : (ESI-TOF) m/z: $[M + H]^+$ Calcd for $C_{27}H_{23}NO_3$: 410.1751; Found: 410.1761.

6,7,9-Trichloro-2,3,3a,4-tetrahydro-1H-benzo[b]pyrrolo[1,2-d][1,4]oxazin-8-ol (79)

Yield : 0.47 g (81%); White solid,

mp : 95-98 °C;

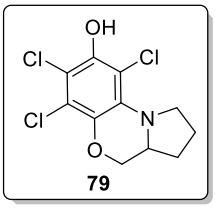

79

IR (Neat) : 3509, 1577, 1422, 1376, 1278, 1200, 1148, 1061, 1014, 859, 823 cm^{-1}.

^{1}H NMR : (400 MHz, $CDCl_3$): δ 5.68 (s, 1H), 4.25-4.20 (d, *J*=23.2 Hz, 2H), 3.47 (s, 2H), 2.95 (s, 1H), 2.30 (s, 1H), 2.01 (s, 1H) 1.91-1.88 (m, 1H), 1.76-1.72 (m, 1H).

^{13}C NMR : (100 MHz, $CDCl_3$): δ 142.9, 137.2, 132.5, 119.4, 111.8, 111.2, 65.3, 54.3, 52.7, 26.5, 22.8.

HRMS : (ESI-TOF) m/z: $[M + H]^+$ Calcd for $C_{11}H_{10}Cl_3NO_2$: 293.9850; Found: 293.9850.

2.4.7 General procedure for the preparation of racemic binol (87):

To a solution of 2-naphthol (0.288g, 2 mmol) in dry CH_2Cl_2 (10 mL) in a round bottomed flask, trifluoroacetic acid (0.3ml, 4mmol) was added slowly using a syringe after that chloranil (0.488g, 2 mmol) was added to the reaction under N_2 atmosphere and stirred at 25 °C for 5 h. The reaction quenched with premixed solid sodium bicarbonate with few pieces of ice. The product was extracted $CH2Cl_2$ (2 X 40 mL) and water (20 mL). The combined organic extract was washed with brine (20 mL), dried over anhydrous Na_2SO_4, and filtered. The solvent was evaporated and purification of residue by column chromatography on silica gel (100-200 mesh) using 20-30% ethyl acetate in hexane to elute the desired product racemic binol **87**.

1,1'-Bi-2,2'-naphthol (87)

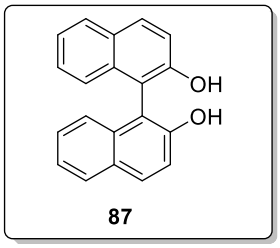

87

Yield : 0.45 g (80%); Colorless solid.

mp : 217-219 °C; (lit.[10] mp. 216-218 °C)

IR (KBr) : (cm^{-1}) 3484, 3402, 3040, 1621, 1599, 1517, 1468, 1386, 1325, 1271, 1221, 1183, 1145.

^{1}H NMR : (400 MHz, $CDCl_3$, δ ppm) 7.96 (d, *J* = 8Hz, 2H), 7.89(d, *J* = 8Hz, 2H), 7.39-7.33 (m, 4H) 7.33-7.29 (m, 2H), 7.16 (d, *J* = 8Hz, 2H), 5.09 (s, 2H).

^{13}C NMR : (100 MHz, $CDCl_3$, δ ppm) 152.6, 133.4, 131.4, 129.4, 128.4, 127.5, 124.2, 124.0, 117.7, 110.8.

2.5 References

1 Hassan, Z.; Ullah, I.; Ali, I.; Khera. R.A.; Knepper, I.; Ali, A.; Patonay, T.; Villinger, A.; Langer, P. *Tetrahedron.* **2013**, *69*, 460.

2 Ullah, I.; Khera, R. A.; Hussain, M.; Villinger, A.; Langer, P. *Tetrahedron.* **2009**, *50*, 4651.

3 Zhang, H.-B.; Liu, L.; Chen, Y.-J.; Wang, D.; Li, C.-J. *Adv. Synth.Catal.* **2006,** *348*, 229.

4 Mathew, A, E.; Robert, K.-Y.; Cheng, Z.; Cheng, C. C. *J. Med. Chem*. **1986**, *29*, 1792.

5 Errazuriz, B.; Tapia, R.; Valderrama, J. A. *Tetrahedron Letters.* **1985**, *26*, 819.

6 Jiang, J.-H.; Boominathan, S. S. K.; Hu, W.-P.; Chen, C.-Y.;Vandavasi, J. K.; Lin, Y.-T.; Wang, J.-J. *Eur. J. Org. Chem*. **2016**, 2284.

7 Wohler, F. Justus Liebigs *Ann. Chem*. **1844**, *51*, 145-163.

8 Nogami, T.; Yoshihara, K.; Hosoya, H.; Nagakura, S. *J. Phys. Chem.* **1969**, *73*, 2670.

9 Tucker, J. H. R.; Collinson, S. R. *Chem. Soc. Rev.* **2002**, *31*, 147.

10 Elslager, E. F.; Werbel, M. L.; Worth, D. F. *J. Med. Chem.* **1970**, *13*, 104.

11 Kallmayer, H. J.; Tappe, C. *Pharm. Acta Helv.* **1987**, *62*, 2.

12 Bullock, F. J.; Tweedie, J. F.; McRitchie, D. D.; Aurther, D. *J. Am. Chem. Soc.* C **1969**, 1799.

13 William, R. A.; Anja, K.-L. *Trends Biochem. Sci*. **2001**, *26*, 648.

14 Bittner, S.; Lempert, D. *Synthesis.* **1994**, 917.

15 Delarmelina, M.; Daltoe, R. D.; Cerri, M. F.; Madeira. K. P.; Rangel, L. B. A.; Junior, V. L.; Romao, W.; Taranto, A. G.; Greco, S. J. *J. Braz. Chem. Soc*. **2015**, *26*, 1804.

16 Pandurangan, K.; Murnaghan, K. D.; Walshe, A.; Muller-Bunz, H.; Paradisi, F.; Morgan, G. G. *Chem. Biol. Drug. Des.* **2011**, *78*, 787.

17 Ramusagar, M. Ph.D. Thesis **2018**, School of chemistry, University of Hyderabad.

18 Roldán, S.; Blanco, C.; Granda, M.; Menéndez, R.; Santamaría, R. *Ange. Chem.*, **2011**, *50*, 1699.

19 Anand rao, G. Ph.D. Thesis **2018**, School of chemistry, University of Hyderabad.

20 Conway, B. E.; Dzieciuch, M. *Canadian Journal of Chemistry,* **1963,** *41,* 38.

21 Shunmugaraj, M.; Ramusagar, M. Ph.D. Thesis **2018**, School of chemistry, University of Hyderabad.

Chapter 3

Construction of Electricity Harvesting Electrochemical Cell using tertiary Amines, *p*-Chloranil and Sulfones

3.1 Introduction

3.1.1 Organic solar cell

The organic photovoltaics or solar cells are flexible devices with low manufacturing cost compared to that of rigid inorganic solar cells. In organic solar cells, photo excitation of the light harvesting organic material produce coupled electron-hole pair called as exciton. The electric field splits the exciton into the charge carriers as electron-hole (positive charge) pairs. The charge carriers move to the respective electrodes. Some electron donors and acceptors used in the heterojunction solar cells are shown in Figure 1.

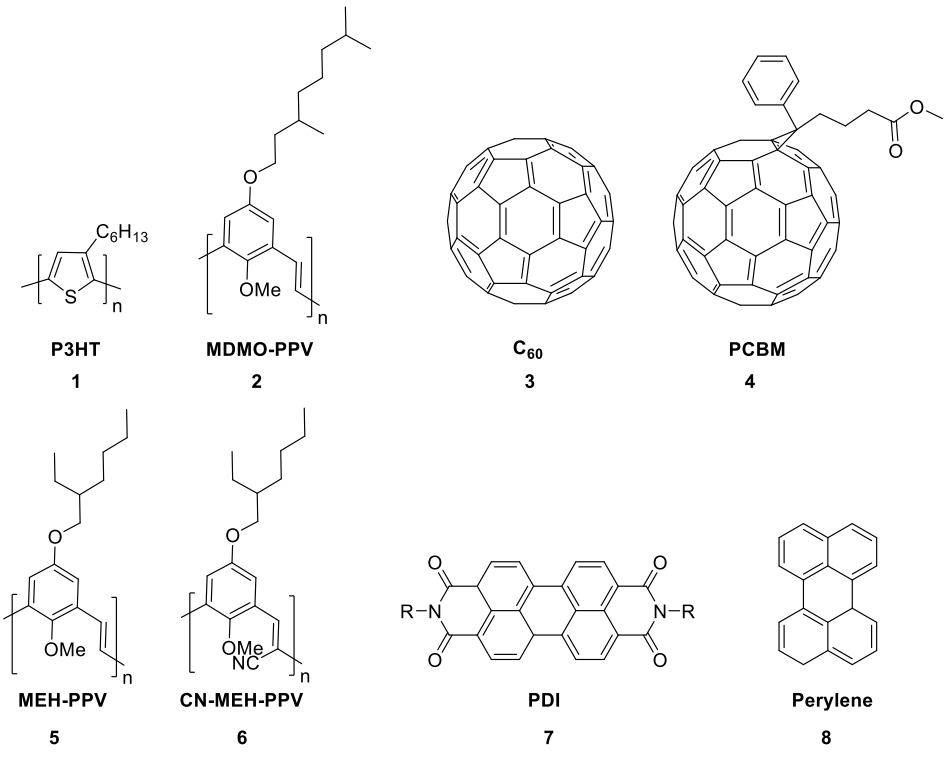

Figure 1. Major donor polymers and acceptors used in the organic solar cells.

3.1.2 Single layer organic solar cells

In organic solar cells, conductors with high work function such as indium tin oxide (ITO) are used as transparent cathode and low work function metals such as aluminum, magnesium or calcium are used as anode. The cell is made by sandwiching an organic material between the two electrodes as shown in Figure 2.

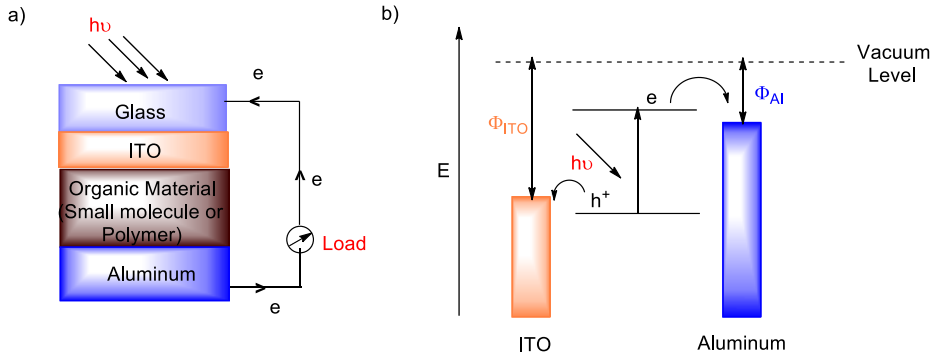

Figure 2. (a) Schematic diagram for single layer organic solar cell (b) Energy level diagram for organic solar cell.

When the organic materials are exposed to sun light, the electrons are excited to the LUMO and holes (positive charges) are produced in the HOMO. The potential created by the different work functions of the electrodes splits the electro-hole pair. Then, the electrons move to the anode and holes (positive charges) to the cathode. It was reported that magnesium phthalocyanine (MgPc) single layer solar cell (Al/MgPc/Ag) produced 0.01% efficiency.[1] Glenis and co-workers reported[2] that the single layer cell using poly-3-methyl thiophene produced 0.15% power conversion efficiency. Also, single layer cell using the conjugated polymer polyacetylene gave 0.3% conversion efficiency.[3] These types of cells produce less than 1% power conversion efficiency.

3.1.3 Bilayer or Planar donor-acceptor solar cells

The bilayer organic solar cells are constructed by sandwiching two different layers in between the two electrodes. (Figure 3 a).

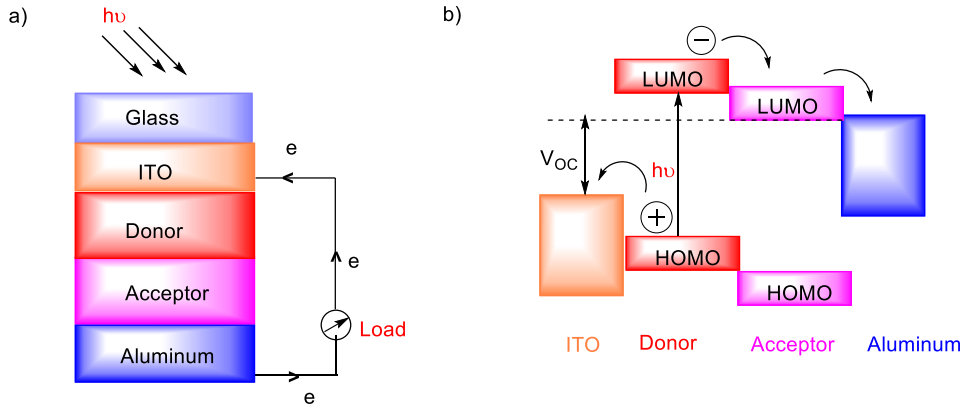

Figure 3. (a) Schematic diagram for Bilayer organic solar cell (b) Energy level diagram for bilayer organic solar cell.

The electrostatic forces are generated at the interface of layers due to the different electron affinity and ionization energy of two different layers. In this cell, the exciton splits efficiently than in the single layer cell. The layers having high electron affinity act as electron acceptor and the other layer with low ionization energy act as electron donor. Sariciftci and co-workers reported[4] 0.04% power conversion efficiency in the cell using C_{60}/MEH-PPV in double layer cell. In this cell, C_{60} works as an acceptor and poly (2-methoxy-5-(2'-ethylhexyloxy- 1,4-phenylene-vinylene), MEH-PPV as a donor. Tang *et al.* reported[5] that 1% power conversion efficiency was produced by using copper phthalocyanine (CuPc) as an electron donor and perylene tetracarboxylic derivative as an acceptor in two layer cell. It was reported that the bilayer cell using the donor polymer poly (p-phenylenevinylene) PPV and acceptor C_{60} produced around 9% power conversion efficiency. [6]

3.1.4 Bulk heterojunction solar cell

The thickness of the layer is important for effective absorption of light in organic solar cells. If the thickness of the layer is more, the exciton will recombine before reaching the electrodes. In bulk-heterojunction cell, by placing a mixture of electron donor and acceptor blend the exciton diffusion pathway is minimized. In bulk heterojunction solar cell, the donor and acceptor are mixed together and deposited over the ITO electrode (Figure 4 a).

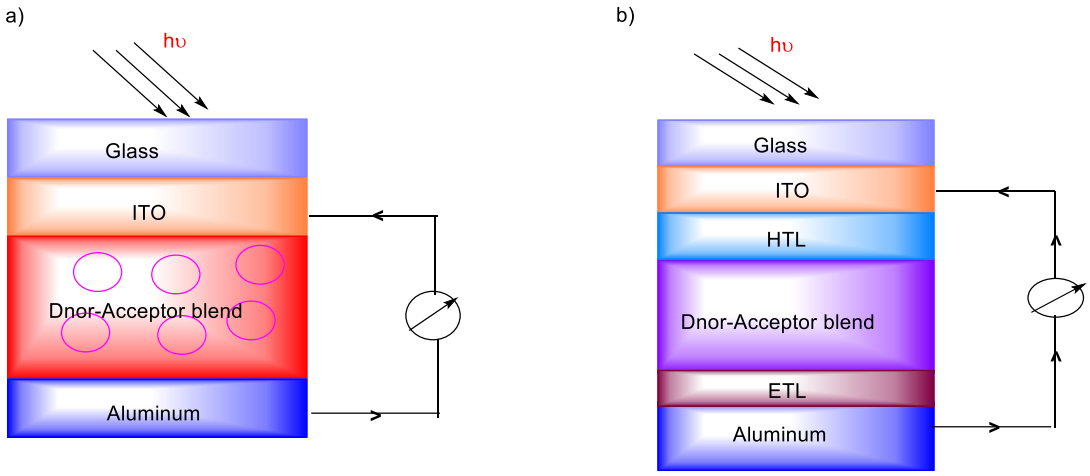

Figure 4. (a) Schematic diagram for Bulk heterojunction solar cell (b) Use of buffer HTL and ETL layers.

The efficiency of organic solar cell was improved by the introduction of fullerene based derivatives in bulk heterojunction. It was reported[7] that the cell with blend of polymer MEH-PPV donor and fullerene using Ca/MEH-PPV/PCBM/ITO gave 2.9% power conversion efficiency. Yu and co-workers[8] reported improvement by replacing MEH-PPV polymer with poly (3-octylthiophene), P3OT polymer. More recently, it was reported that by using thiophene based PTB7-Th polymer and $PC_{71}BM$ as an acceptor, the power conversion efficiency was improved to 11%.[9-12]

In 2008, mechanistic schemes involving the charge transfer complexes in equilibrium with radical cation, and anion pair and dissociated ions were proposed in donor-acceptor systems (Scheme 1).[13a] These reported reversible reactions take place at ambient conditions in the ground state of donor and acceptor. Initially, the CT complex is reported to be formed with subsequent formation of the electron transfer (ET) complex (Scheme 1). Finally, the dissociated radical ions **13**, **14** are formed by ionisation/diffusion in polar solvents. This implies that the energy barrier or activation energy for the formation of complex and radical ions is overcome by the surrounding heat (Scheme 1).

Scheme 1

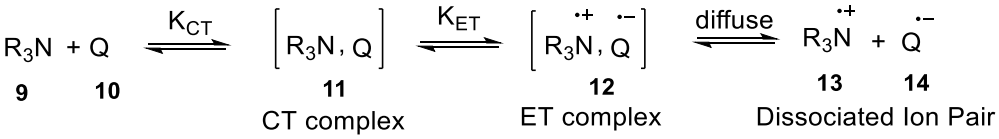

As described in Chapter 2, amines readily undergo electron transfer reactions to give the corresponding radical cations and anions in dipolar aprotic solvent like PC (propylene carbonate) which then lead to the corresponding charge transfer complexes in equilibrium with the radical ions (Scheme 2).

Scheme 2

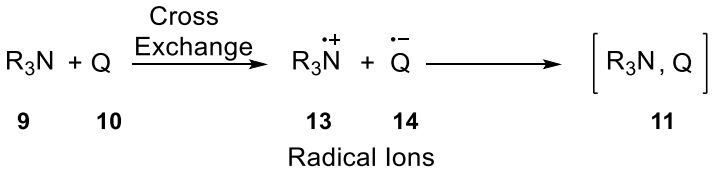

An interesting possibility is the development of an electrochemical cell device based on transport of charges in these radical cation and anion pair species to the electrodes to complete the circuit and regenerating the donor and acceptor. If the electron transfer from the amine donor to the quionone acceptor could again happen, then the

device would be useful in converting the heat around it to electricity continuously (Figure5).

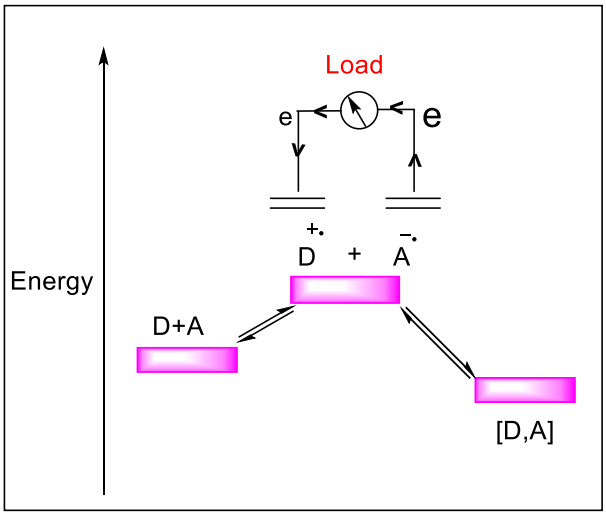

Figure 5. Ground state electron transfer between organic electron donor (D) and acceptor (A) - Construction of an electricity harvesting cell.

We have envisaged the construction of an electrochemical cell so as to transport the charge carriers (i.e. electron in $\mathbf{Q}^{-\cdot}$ and the hole in $R_3N^{+\cdot}$) formed in such reactions under ambient temperature conditions to produce electricity (Fig. 5). The difference between ground state electron transfer process in such cells and the electron transfer involved in donor/acceptor photovoltaic or solar cells is that in the later case the electron transfer from a donor to an acceptor takes place after photoexcitation of the electron in the ground state to excited state.

We have decided to use sulfone as electron acceptor or transporter in the ground state electricity harvesting cells. Accordingly, a brief review of the reports on the sulfones as electron acceptor will be useful for the discussion.

3.1.5 Application of sulfones as electron acceptors

Sulfone containing material is attractive for use as a phosphorescent host material because sulfone group possesses a strong electron accepting nature.[13b-d,14] For example, 5',5""-sulfonyl-di-1,1':3',1"-terphenyl **15** (BTPS estimated electron affinity EA = 2.9 eV) is useful as a host material for high efficiency blue and green phosphorescent OLEDs.[15]

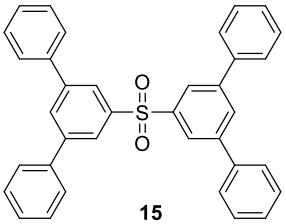

15
BTPS

Figure 6. Structure for the electron acceptor host material

Bissulfone **16** (estimated electron affinity EA = 2.28 eV) was used as high triplet energy electron acceptor in blue phosphorescent light emitting devices.[16a] The main reason for insertion of sulfone groups in host compounds[17] is that the acceptor group influences a strong inductive electron withdrawing effect which lowers both HOMO and LUMO energies of the triplet synthon and improves electron injection. The bissulfone **17** is also useful as electron acceptor but its electron affinity was estimated to be low (EA = 1.04 eV).[16b]

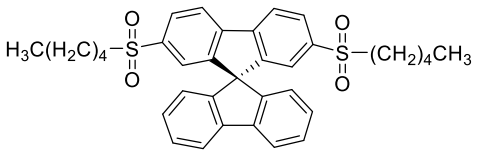

16

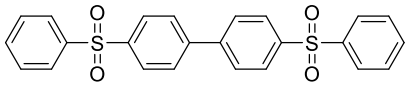

17

Figure 7. Chemical structures of the electron acceptor host compounds

Fluorinated sulfones are useful as electrolytes in high energy Li-ion batteries. The fluorination lowers the HOMO and LUMO energy levels and raises the oxidation potentials of the sulfone molecules.[18]

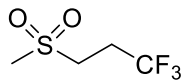

18

FPMS

Figure 8. Schematic diagram for Fluorinated sulfone used in Li ion batteries

Schoenebeck *et. al* reported[19] that reductive cleavage of sulfones and sulfonamides by a neutral organic super electron donor (SED) compound **20**. In these reactions, electron transfer from super electron donor (SED) to the arenesulfonyl group leads to the formation of radical-anion and radical cation intermediates (Scheme 3).[19]

Scheme 3

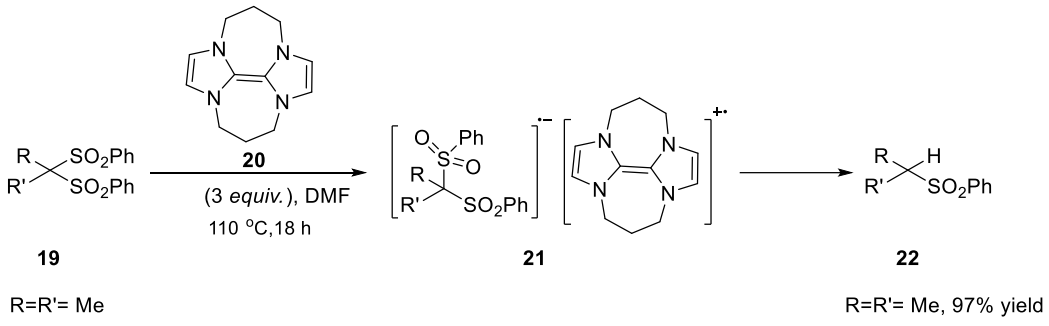

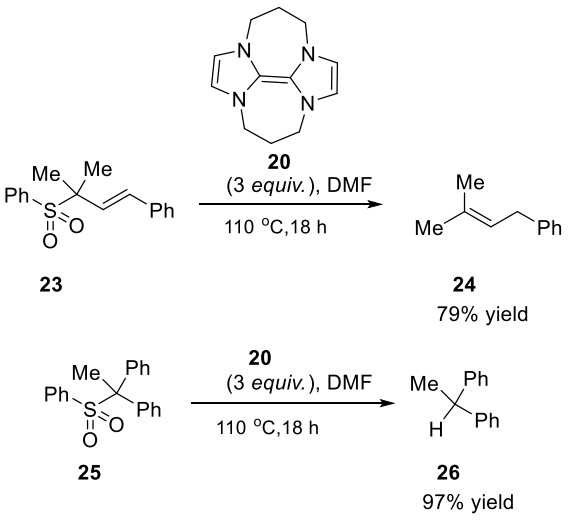

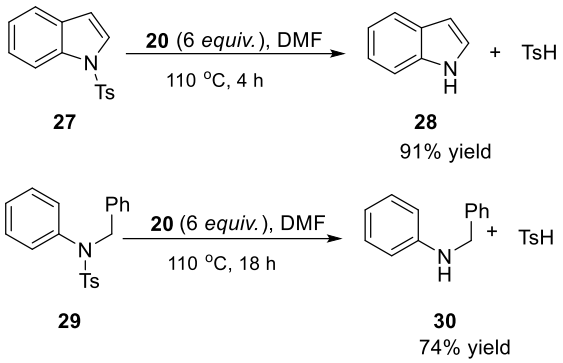

Sullivan, *et al* reported [20] that reductive cleavage of sulfonamides by a photoactivated neutral organic super electron donor (Scheme 4).

Scheme 4

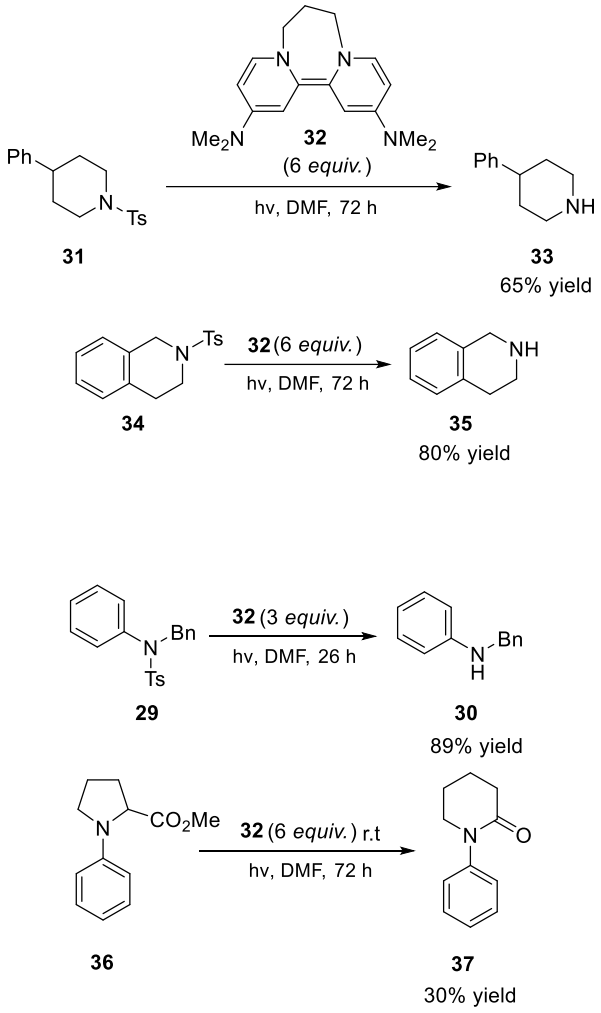

Merchant *et al* reported [21] that fluoro alkylated products are obtained by the nickel-catalyzed cross coupling reaction of alkyl sulfones with aryl zinc reagent (Scheme 5).

Scheme 5

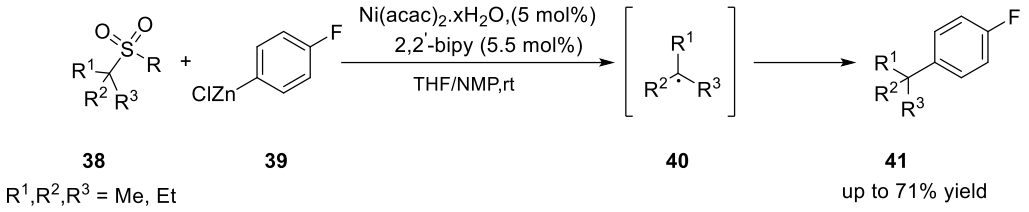

Delaunay *et* al reported[22] that heteroarylalkylsulfones undergo cathodic cleavage reaction to give radical anion intermediates, resulting in alkanesulfinate anion in high yield along with the corresponding hydrocarbon (Scheme 6).

Scheme 6

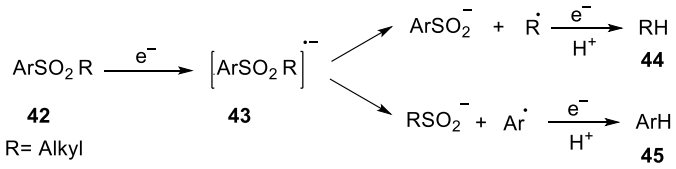

Vasilieva *et al* reported[23] that the electrochemical reduction of 2-methylthioxanthen-9-one sulfoxide and sulfone give radical anions (Scheme 7).

Scheme 7

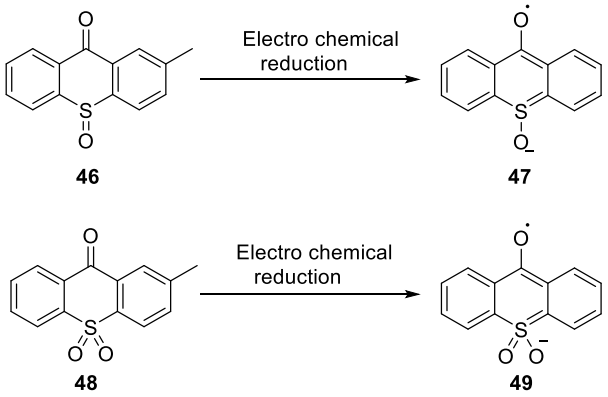

Kaiser *et al* reported[24] that thiaxanthone-5-dioxide, thianthrene-5,10-tetroxide and 2,7-dimethyl thianthrene-5,10-tetroxide on reduction with metals like potassium give radical anions. Here, the sulfonyl group accepts electron from potassium (K) (Scheme 8).

Scheme 8

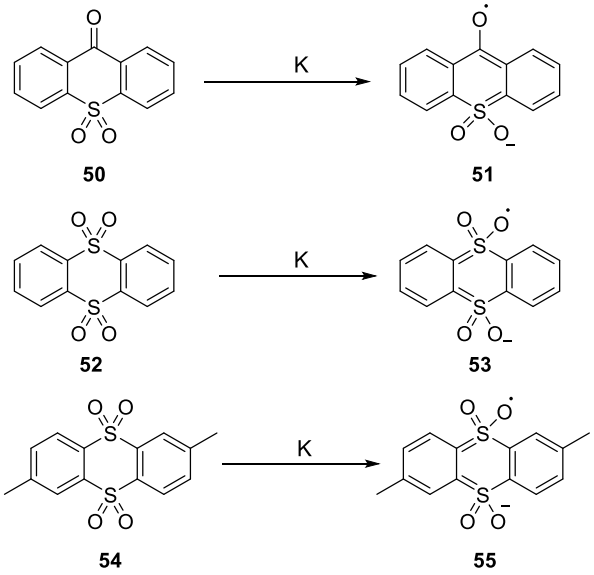

Fehnel *et al* reported[25] that thiaxanthone-5-dioxide on treatment with Zn dust gives intense blue color due to the formation of sulfone anion (Scheme 9).

Scheme 9

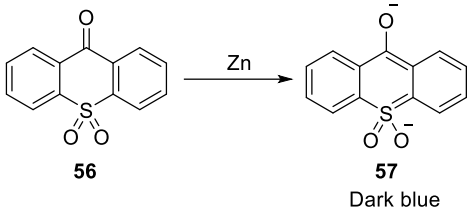

We have investigated the application of sulfones as electron acceptor in electricity harvesting electrochemical cells. The results are described in the next section.

3.2 Results and Discussion

3.2.1 Organic electrochemical cells using sulfones as electron transporters

We have undertaken efforts to construct electricity harvesting electrochemical cells based on ground state electron transfer reactions. We have selected the highly electron deficient *p*-chloranil **63** (Cl_4BQ) as acceptor and benzoquinone (BQ) **64**, dimethylsulfone **65** and sulfolane **66** as electron transporter. Also, the amines and *N*,*N'*-tetramethyl-1,4-phenylenediamine (TMPDA) **58**, triphenylamine (TPA) **59**, 1,4-diazabicyclo[2.2.2]octane (DABCO) **60**, *N*, *N*-diisopropylethylamine (DIPEA) **61** and *N*,*N*-diisopropylbenzamide (DiPrBA) **62** were selected as electron donors for the construction of the electrochemical cell.

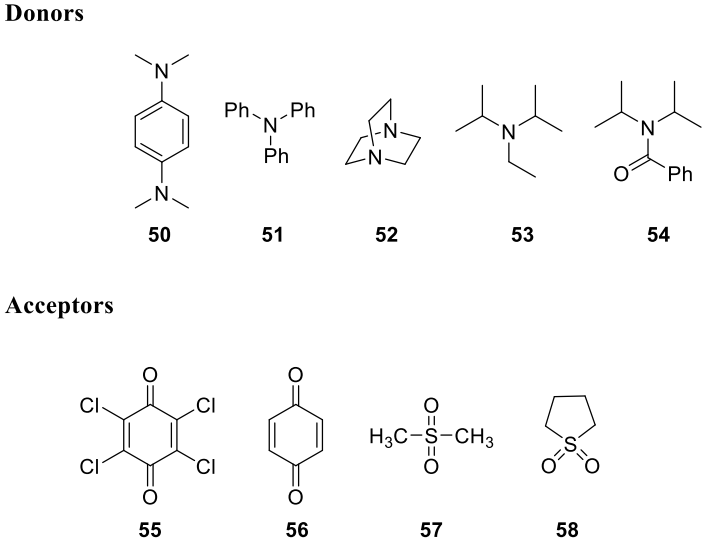

Figure 9: Eelectron donors and acceptors for use in electrochemical cells.

Recently, electrochemical cells were constructed in this laboratory based on ground state electron transfer reactions using various donor amines and *p*-chloranil acceptor with TiO_2 as solid support in PC solvent under different configurations.[26]

3.2.2 Two layer cell configuration

Previously, it was observed in this laboratory that the cells can be easily constructed by making donor and acceptor pastes using TiO_2, polyethylene oxide (PEO) and propylene carbonate (PC) and coating on commercially available Al (0.2mm x 5cm x 5cm) and SS (SS 304, 0.05mm x 5cm x 5cm) foils or graphite sheet (0.4mm x 5cm x 5cm). The configuaration of two layer cell was constructed as shown in Figure 10.

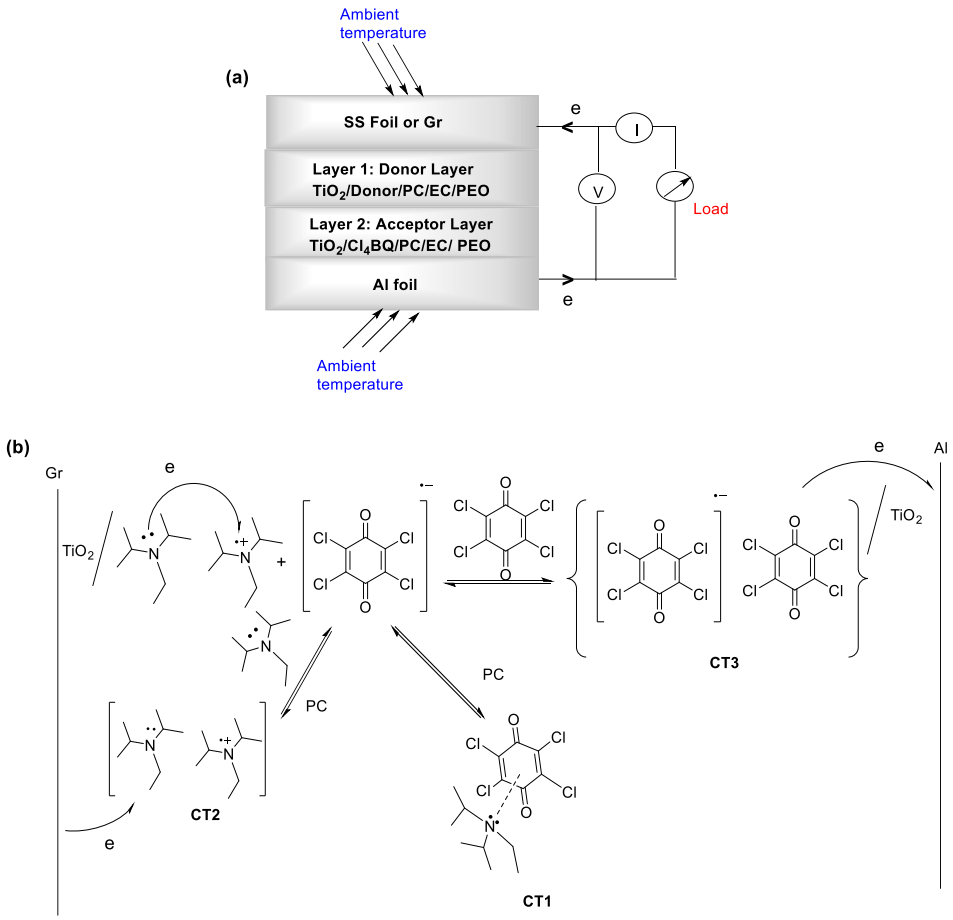

Figure 10. (a) Schematic diagram of cell with two layer configuration (b) Tentative mechanism for electron transport via $D/D^{\cdot+}$ and $A^{\cdot-}/A$ exchange reactions.

The acceptor layer was coated on Al foil and the donor layer was coated on SS foil or Graphite sheet. The foils were then sandwiched to construct the electrochemical cell. However, visible holes were formed on SS foils indicating corrosion and hence later

graphite sheets were used. It was observed that the two layer cells conducted in this way (Figure 10) did not produce power after 24 h. Hence, multilayer cells gave better results (Figure 11) .

3.2.3 Multilayer Cell Configuration

(a)

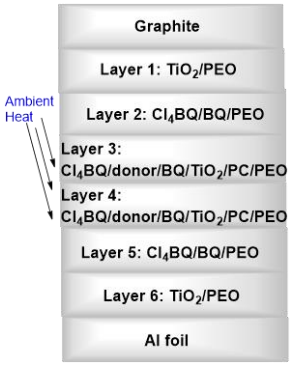

(b)

	1 h after packing	48 h after packing
Donor	**Pmax(mW)/FF(40 °C)**	**Pmax(mW)/FF(40 °C)**
TMPDA	1.614/0.282	1.299/0.263
TPA	0.939/0.219	0.728/0.219
DABCO	4.806/0.432	3.776/0.434
DIPEA	11.74/0.296	8.338/0.394

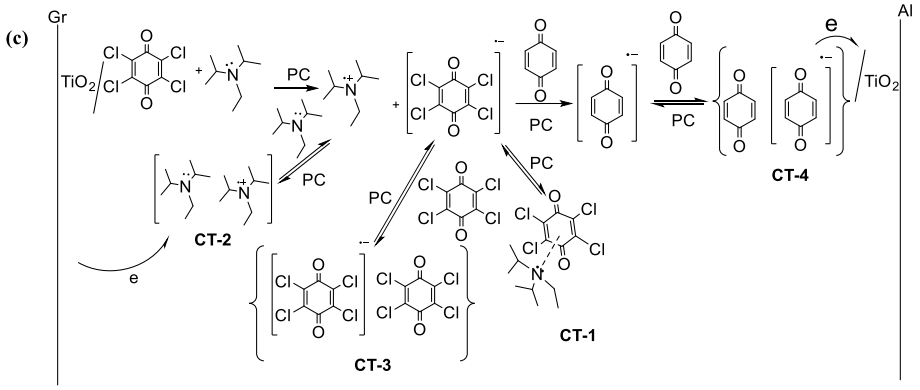

Figure 11. (a) Schematic diagrams of multi-layer cell using BQ along with *p*-chloranil without TiO_2 in PC layer (c) Tentative mechanism for electron transport to the electrodes via D/D.+ and A-/A exchange reactions.

The IV-data were recorded at 1 h and 48 h after packing. The higher power outputs (Pmax) were observed 1 h after packing compared to that observed after 48 h. Presumably, the power output becomes less as the initially formed amine radical cations and *p*-chloranil anions might be converted to the corresponding charge transfer complex (CT 1) in accordance with decrease in epr signal strength observed earlier (Figure 11c). The

complexes CT 2 and CT 3 may also contribute to the conduction. The results indicate that increase in the temperature of the cell (from 28 °C to 40 °C) increases the power output due to increase in the rate of electron transfer between the donor-acceptor and also dissociation of the formed charge transfer complexes into radical ions. Also, the increase in temperature would help in crossing the activation energy barrier for transport of ions to the electrodes and hence would also improve the conductance.

The epr studies indicated that the initially formed radical ions are transformed to charge transfer complexes with time as discussed in chapter 2. This could account for the reduction of current and Pmax values with time as the concentration of radical ions would be lesser with time. It was reported that radical anions of compounds with lesser electron affinity are stabilized to more extent in polar solvents. Since, benzoquinone (BQ) has lesser electron affinity (EA 1.91 eV) compared to *p*-chloranil (EA 2.78 ev), the BQ could accept electron from *p*-chloranil radical anion and hence the *p*-chloranil will be available for reversible electron transfer from the amines. Indeed, the Pmax values were higher in reactions using BQ for electron transport.[27,28]

It was of interest to us to develop electrochemical cells using different donors and *p*-chloranil along with sulfolane and dimethylsulfone as electron transporter. Accordingly, we have constructed the cell using the different donors and the sulfolane as transporter using Cl_4BQ and tertiary amines (Figure 12). The electron affinity (EA) values of sulfolane and dimethylsulfone were not reported but expected to be less than the EA (2.28 eV) of bissulfone **8**[16a] and bissulfone **9** (EA=1.04 eV)[16b] compared to that of benzoquinone (EA=1.91 eV) and *p*-chloranil (EA=2.78 eV). We have constructed the cell in 5 layer configuration using sulfolane (Figure 12). In this configuration, the solvent PC (propylene

carbonate) was used for dissolving the donor, acceptor and sulfolane to facilitate the electron transport from the *p*-chloranil radical anion (Figure 12).

Figure 12: Five layer cell with sulfolane in two layers

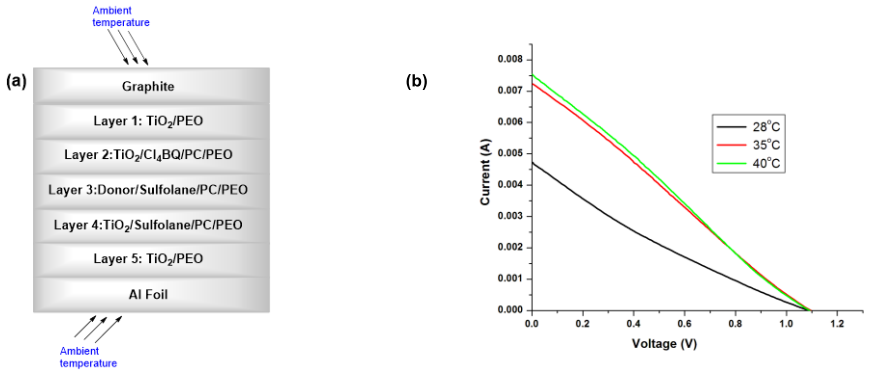

1 h after packing

Donor	**Pmax/mW/FF(28 °C)**	**Pmax/mW/FF(35 °C)**	**Pmax/mW/FF(40 °C)**
TMPDA	3.62/0.240	4.782/0.242	5.159/0.241
TPA	2.091/0.269	2.249/0.271	2.391/0.273
DABCO	3.516/0.273	5.788/0.271	8.543/0.291
DIPEA	3.315/0.280	4.956/0.281	6.071/0.29
DiPrBA	3.649/0.263	3.693/0.268	3.948/0.27

48 h after packing

Donor	**Pmax/mW/FF(28 °C)**	**Pmax/mW/FF(35 °C)**	**Pmax/mW/FF(40 °C)**
TMPDA	0.318/0.259	0.426/0.27	0.434/0.268
TPA	0.659/0.251	0.777/0.256	0.993/0.266
DABCO	1.055/0.205	2.017/0.255	2.102/0.256
DIPEA	1.168/0.255	1.591/0.289	1.929/0.321
DiPrBA	0.694/0.279	0.877/0.299	0.896/0.298

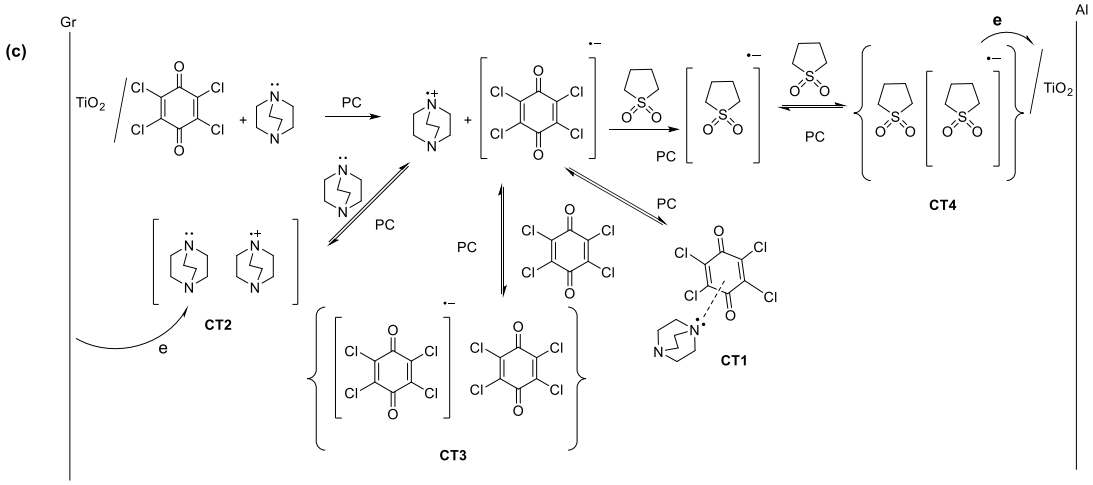

Figure 12. (a) Schematic diagram of multi-layer with Cl_4BQ/Sulfolane/Donor/PC/TiO_2/PEO configuration. (b) Representative IV for the cell (Table ES 1, entry 3, DABCO donor). (c) Tentative mechanism for electron transport to the electrodes via D/D.+ and A-/A exchange reactions.

We have recorded the IV-data at 1 h and 48 h after packing the cell as outlined in Figure 12. The power output (Pmax) values at 1h are high compared the values at 48 h, as initially more number of radical ions will be present leading to better conduction. The power output becomes less with time indicating that the amine radical cations and *p*-chloranil anions may converted to charge transfer complexes (CT1, CT2 and CT3). The conduction is expected to decrease with formation of CT complexes, especially with the formation of CT1 complex, if this complex precipitates out of the solution.

Among various donors TMPDA, TPA, DABCO, DIPEA and DiPrBA, the donor DABCO gave better results at 28 ^{o}C, 35 ^{o}C, and 40 ^{o}C (Figure 3). While increasing temperature, the Pmax and FF values increased and highest values are obtained at 40 ^{o}C. This may be due to the increase in rate of electron transport and also dissociation of charge transfer complexes (CT1, CT2 and CT3) to the radical ions at higher temperature. The increase in the temperature may also induce the ions to cross the activation energy barrier for conduction. The electron affinity (EA) of dimethylsulfone is expected to be less than that of the bissulfone **8**[16a] (EA=2.28 eV) and bissulfone **9** (EA=1.04 eV)[16b] compared to that of benzoquinone (EA=1.91 eV) and *p*-chloranil (EA=2.78 eV). However, we have constructed the cell using dimethylsulfone in 2 layers with different donors using PC as solvent (Figure 13).

Figure 13: Five layer cell with Dimethylsulfone in two layers

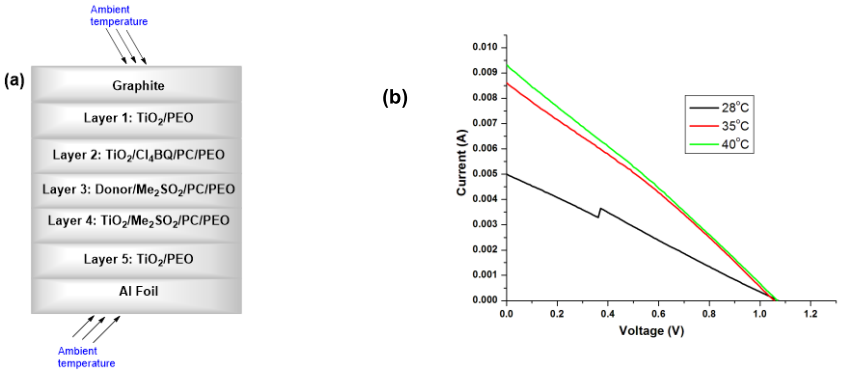

1 h after packing

Donor	**Pmax/mW/FF(28 °C)**	**Pmax/mW/FF(35 °C)**	**Pmax/mW/FF(40 °C)**
TMPDA	3.998/0.231	4.361/0.243	4.84/0.283
TPA	2.151/0.265	2.206/0.268	2.308/0.273
DABCO	3.152/0.226	6.549/0.273	6.925/0.269
DIPEA	2.647/0.279	3.168/0.290	3.624/0.294
DiPrBA	2.847/0.271	2.86/0.270	3.354/0.278

48 h after packing

Donor	**Pmax/mW/FF(28 °C)**	**Pmax/mW/FF(35 °C)**	**Pmax/mW/FF(40 °C)**
TMPDA	0.507/0.261	0.553/0.263	0.779/0.258
TPA	1.027/0.242	1.238/0.26	1.279/0.254
DABCO	1.467/0.274	2.575/0.283	2.692/0.271
DIPEA	0.717/0.275	1.07/0.295	1.165/0.298
DiPrBA	1.314/0.277	1.703/0.317	1.774/0.305

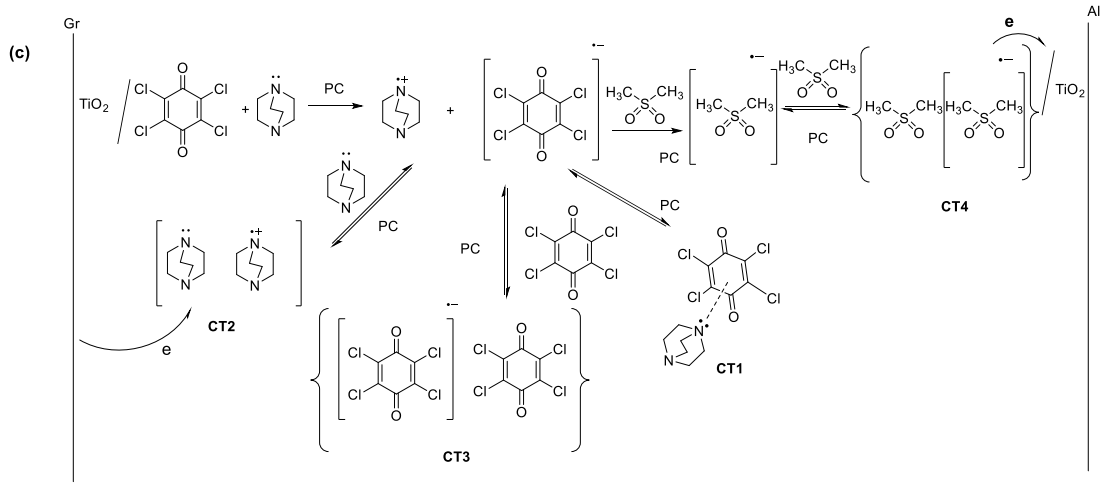

Figure 13. (a) Schematic diagram of multi-layer with Cl_4BQ/Dimethylsulfone/Donor/PC/TiO_2/PEO configuration. (b) Representative IV for the cell (Table ES 2, entry 9, DABCO donor). (c) Tentative mechanism for electron transport to the electrodes via D/D.+ and A-/A exchange reactions.

We have recorded IV-data at 1 h and 48 h after packing the cell. Among various donors, the donor DABCO gave better results at 28 ^{o}C, 35 ^{o}C, and 40 ^{o}C (Figure 13). The recorded IV data of cell 1 h after packing the cell the power maximum (Pmax) and fill factor (FF) values for DABCO are Pmax 6.925 mW, with FF 0.269 at 40 ^{o}C (Table ES2 entry 9) but decreased to Pmax 2.692 mW with FF 0.271 after 48h.

We have then constructed the 6 layer cell using donor in two PC layers and *p*-chloranil (Cl_4BQ) in one layer with dimethyl sulfone as electron transporter (Figure 14).

Figure 14: Six layer cell using Me_2SO_2 in one layer(end layer)

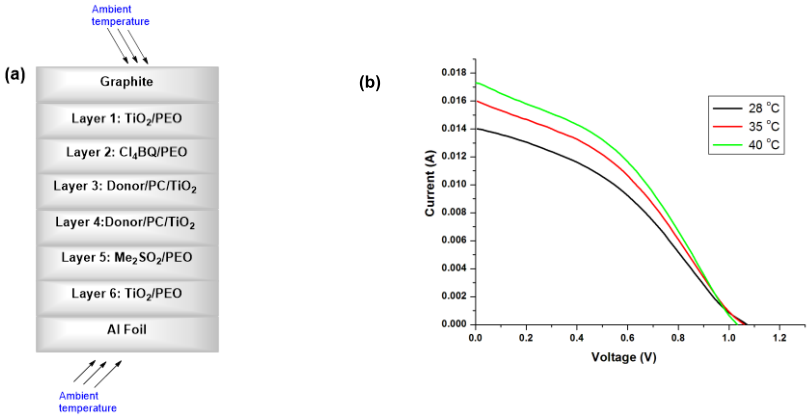

1 h after packing

Donor	**Pmax/mW/FF(28 °C)**	**Pmax/mW/FF(35 °C)**	**Pmax/mW/FF(40 °C)**
DIPEA	6.24/0.277	7.650/0.283	12.02/0.318
NMP	3.413/0.182	4.623/0.190	5.986/0.200
DABCO	3.368/0.249	5.154/0.252	5.336/0.232

48 h after packing

Donor	**Pmax/mW/FF(28 °C)**	**Pmax/mW/FF(35 °C)**	**Pmax/mW/FF(40 °C)**
DIPEA	5.534/0.369	6.397/0.378	6.991/0.392
NMP	1.804/0.186	2.589/0.197	3.026/0.210
DABCO	1.535/0.215	2.027/0.205	2.25/0.207

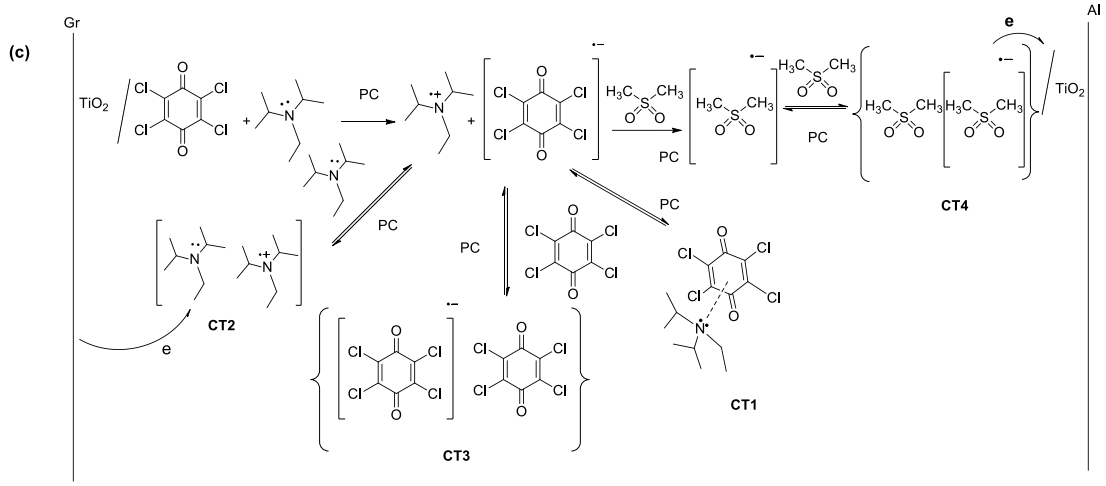

Figure 14. (a) Schematic diagram of multi-layer with Cl_4BQ/DimethylSulfone /Donor/PC/TiO_2/PEO configuration. (b) Representative IV for the cell (Table ES 2, entry 11, DIPEA donor). (c) Tentative mechanism for electron transport to the electrodes via D/D.+ and A-/A exchange reactions.

We have recorded IV-data at 1 h and 48 h after packing the cell as outlined in Figure 14. Interestingly, in this configuration higher output (Pmax) was obtained for all donors. Among various donors, DIPEA gave better results at 28 ºC, 35 ºC, and 40 ºC (Figure 14). However, the value at 40 ºC Pmax 12.02 mW at 1h with FF 0.318 decreased to Pmax 6.991 mW with FF 0.392 after 48h.

We have then constructed the 6 layer cell using *p*-chloranil (Cl_4BQ) in three layers and dimethyl sulfone electron transporter in two layers as shown in Figure 15.

Figure 15: Six layer cell using Me_2SO_2 in two layer(end layer) TiO_2 in PC layer

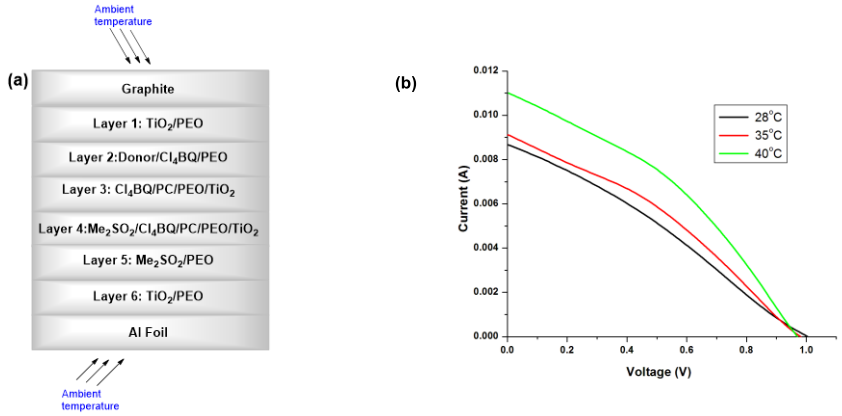

1 h after packing

Donor	**Pmax/mW/FF(28 °C)**	**Pmax/mW/FF(35 °C)**	**Pmax/mW/FF(40 °C)**
TMPDA	0.308/0.255	0.602/0.293	1.524/0.332
TPA	2.076/0.236	2.901/0.269	3.80/0.279
DABCO	7.299/0.236	10.41/0.287	10.99/0.321
DIPEA	6.380/0.250	8.373/0.291	12.42/0.351
DiPrBA	2.394/0.226	2.523/0.250	4.04/0.267

48 h after packing

Donor	**Pmax/mW/FF(28 °C)**	**Pmax/mW/FF(35 °C)**	**Pmax/mW/FF(40 °C)**
TMPDA	0.669/0.210	1.078/0.263	1.216/0.288
TPA	2.853/0.3	3.11/0.322	3.756/0.337
DABCO	3.554/0.304	4.932/0.384	5.501/0.414
DIPEA	2.572/0.295	2.96/0.331	3.874/0.363
DiPrBA	1.83/0.254	2.111/0.281	2.405/0.289

Figure 15 (continued)

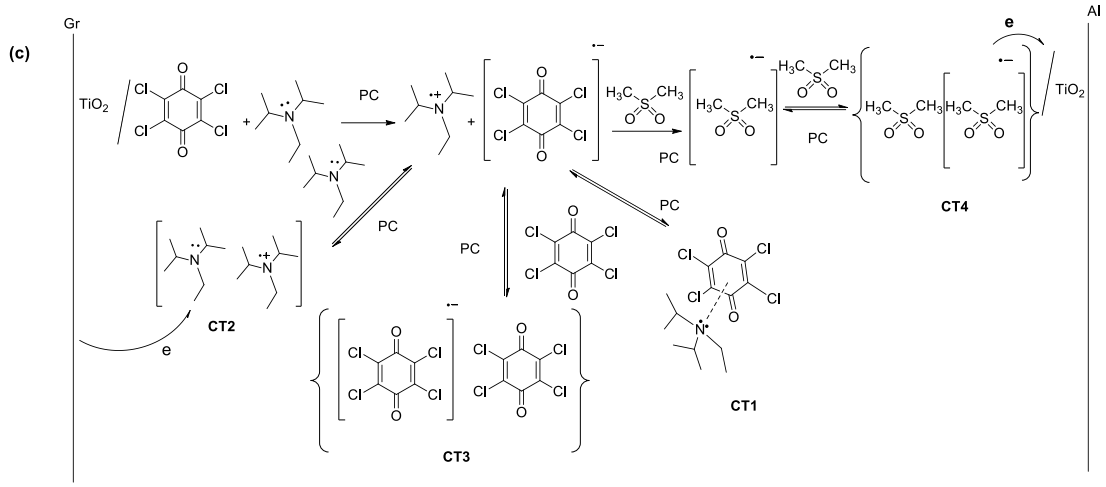

Figure 15. (a) Schematic diagram of multi-layer with Cl_4BQ/Dimethylsulfone/Donor/PC/TiO_2/PEO configuration. (b) Representative IV for the cell (Table ES 3, entry 14, DIPEA donor). (c) Tentative mechanism for electron transport to the electrodes via D/D.+ and A-/A exchange reactions.

We have recorded IV-data at 1 h and 48 h after packing as outlined in Figure 15. Among various donors TMPDA, TPA, DABCO, DIPEA and DiPrBA, the donor DIPEA gave better results at 28 ^{o}C, 35 ^{o}C, and 40 ^{o}C (Figure 15). However, the power output (Pmax) decreased to more extent in this configuration. For example, the Pmax value of DIPEA was Pmax 12.42 mW at 1h but it decreased to Pmax 3.874 mW after 48h.

We have then constructed the 6 layer cell using *p*-chloranil (Cl_4BQ) in four layers and dimethyl sulfone in four layers (Figure 16).

Figure 16: Six layer cell using Me_2SO_2 in four layer(end layer) TiO_2 in PC layer

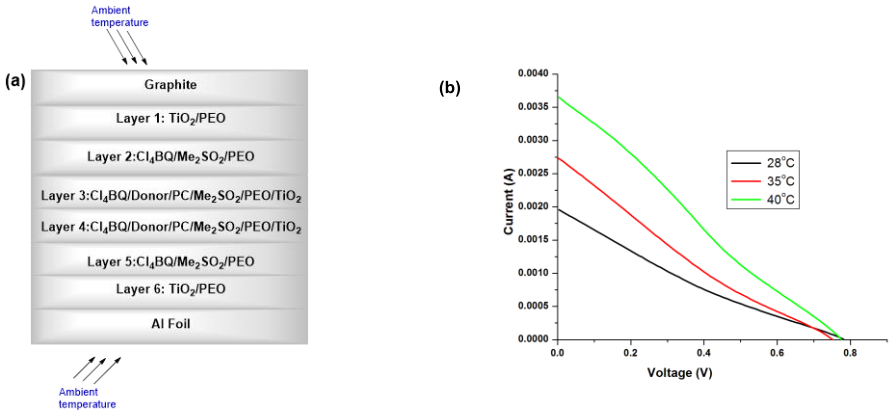

Figure 16 (continued)

1 h after packing

Donor	**Pmax/mW/FF(28 °C)**	**Pmax/mW/FF(35 °C)**	**Pmax/mW/FF(40 °C)**
TMPDA	1.077/0.186	1.635/0.204	1.863/0.232
TPA	1.182/0.255	1.348/0.259	1.412/0.257
DABCO	2.642/0.191	3.324/0.182	4.051/0.201
DIPEA	4.314/0.349	6.39/0.327	8.392/0.379
DiPrBA	3.5/0.268	4.167/0.275	4.248/0.277

48 h after packing

Donor	**Pmax/mW/FF(28 °C)**	**Pmax/mW/FF(35 °C)**	**Pmax/mW/FF(40 °C)**
TMPDA	0.294/0.221	0.317/0.228	0.448/0.238
TPA	0.667/0.261	0.783/0.258	0.847/0.271
DABCO	0.731/0.161	1.225/0.169	2.427/0.195
DIPEA	0.312/0.204	0.430/0.209	0.688/0.243
DiPrBA	1.385/0.31	1.573/0.311	1.584/0.34

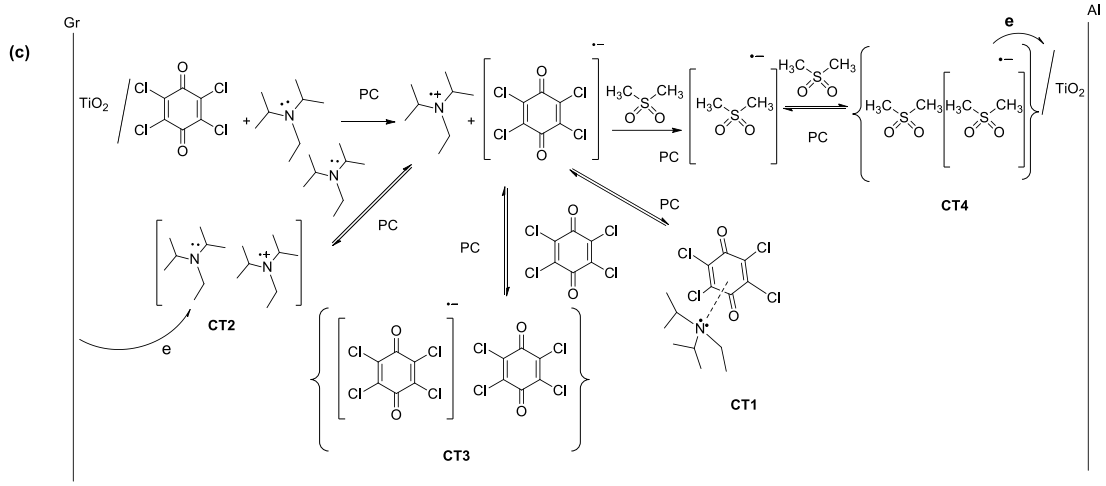

Figure 16. (a) Schematic diagram of multi-layer with Cl_4BQ/Me_2SO_2/Donor/PC/TiO_2/PEO configuration. (b) Representative IV for the cell (Table ES 3, entry 19, DIPEA donor). (c) Tentative mechanism for electron transport to the electrodes via D/D.+ and A-/A exchange reactions.

We have recorded IV-data at 1 h and 48 h after packing as outlined in Figure 16. Again, the donor DIPEA gave better results at 1h (Figure 16). However, only very poor Pmax and FF values were obtained at 40 ^{o}C in this configuration.

Comparison of BQ and Me_2SO_2 as electron transporters

Figure 17: Six layer cell using Me_2SO_2 or BQ in two layers

We have also constructed cells in similar configurations using BQ and Me_2SO_2 as electron transporters using *p*-chloranil (Cl_4BQ) as electron acceptor.

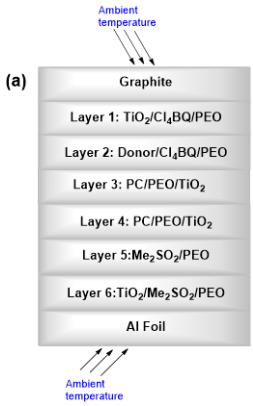

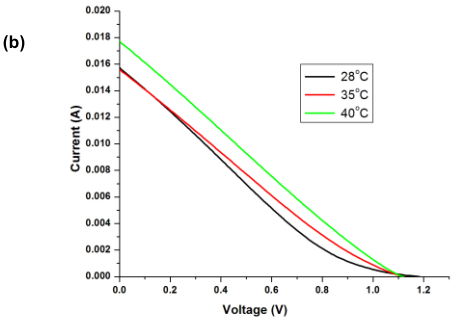

1 h after packing		48 h after packing
Donor	**Pmax/mW/FF(40 °C)**	**Pmax/mW/FF(40 °C)**
TMPDA	2.814/0.274	1.307/0.272
TPA	1.693/0.203	1.87/0.218
DABCO	2.865/0.282	1.524/0.271
DIPEA	5.525/0.226	4.649/0.235
DiPrBA	1.115/0.225	0.997/0.246

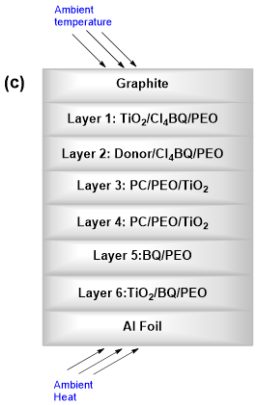

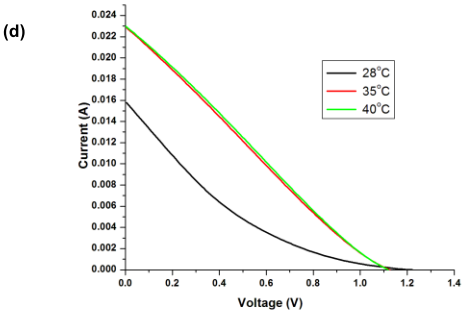

Figure 17 (continued)

1 h after packing		48 h after packing
Donor	**Pmax/mW/FF(40 °C)**	**Pmax/mW/FF(40 °C)**
TMPDA	2.772/0.241	0.669/0.241
TPA	1.117/0.214	1.045/0.228
DABCO	1.633/0.249	1.15/0.237
DIPEA	5.286/0.196	6.253/0.243
DiPrBA	1.246/0.215	0.495/0.214

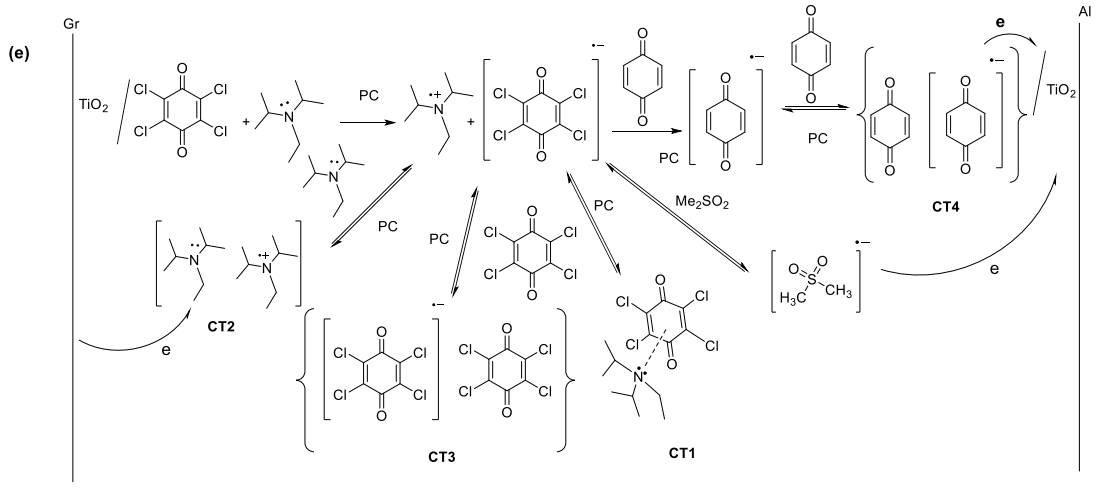

Figure 17. (a) Schematic diagram of multi-layer with Cl_4BQ/Me_2SO_2/Donor/PC/TiO_2/PEO configuration. (b) Schematic diagram of multi-layer with Cl_4BQ/ Donor/PC/BQ/TiO_2/PEO configuration. (c) Representative IV for the cell (Table ES 4, entry 31, DIPEA donor). (d) Representative IV for the cell (Table ES 4, entry 26, DIPEA donor). (e) Tentative mechanism for electron transport to the electrodes via D/D.+ and A-/A exchange reactions.

Among various donors TMPDA, TPA, DABCO, DIPEA and DiPrBA, the donor DIPEA gave better results compared to other donors (Figure 17). The Pmax and FF values at 40 ^oC for TMPDA, TPA, DABCO, after 48h (using BQ as electron transporter) were less compared to the Pmax and FF values at 40 ^oC for TMPDA, TPA, DABCO, realized using Me_2SO_2 (Figure 17). Clearly, the conduction was better with Me_2SO_2 compared to BQ as electron transporter in PC solvent. However, in the case of DIPEA the Pmax and FF values increased at 48h using BQ as electron transporter.

Comparison of BQ and Me_2SO_2 in PC solvent

Figure 18: Six layer cell using Me_2SO_2 or BQ in three layers.

We have also constructed cells in 6 layers configuration using Me_2SO_2 or BQ in three layers as shown in Figure 18.

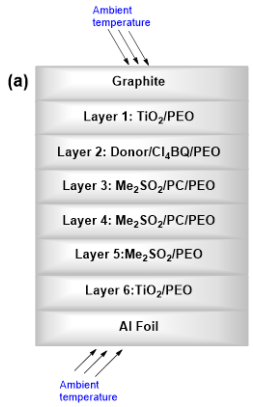

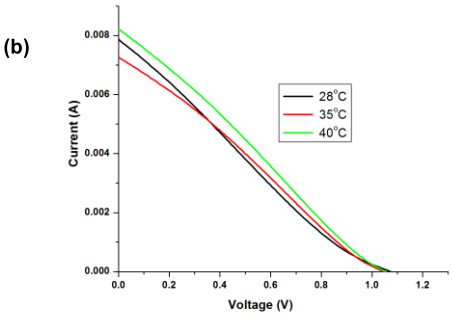

1 h after packing		48 h after packing
Donor	**Pmax/mW/FF(40 °C)**	**Pmax/mW/FF(40 °C)**
TPA	2.607/0.264	1.932/0.258
DABCO	8.497/0.255	5.691/0.268
DIPEA	12.83/0.238	2.24/0.258

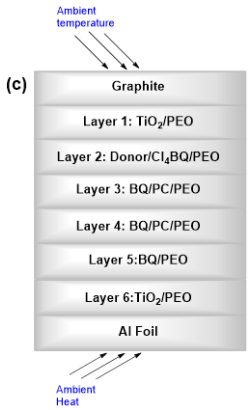

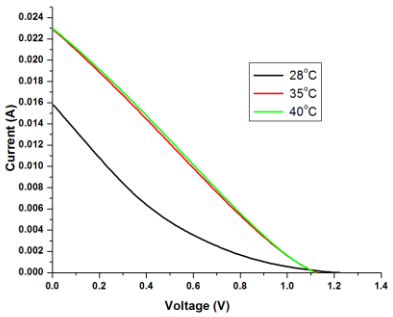

1 h after packing		48 h after packing
Donor	**Pmax/mW/FF(40 °C)**	**Pmax/mW/FF(40 °C)**
TPA	2.015/0.236	1.384/0.222
DABCO	6.302/0.23	4.093/0.248
DIPEA	14.79/0.202	2.347/0.239

Interestingly, the Pmax and FF values at 40 ^{o}C for TPA, DABCO, DIPEA were higher at 48h using Me_2SO_2 as electron transporter compared to the Pmax and FF values at 40 ^{o}C for TPA, DABCO, DIPEA using BQ as electron transporter. Clearly, the conduction seems to be better with Me_2SO_2 compared to BQ as electron transporter.

Although, further studies may be required for the understanding the effect of different electron transporters on the functioning of the organic electrochemical cells, the results will be useful in planning future research efforts in this area.

3.3 Conclusions

We have developed a simple electrochemical cell device based on electron transfer reactions in ground state with readily available amine or amide as donors and *p*-chloranil as electron acceptor and dimethyl sulfone as transporter at ambient temperatures. In these electrochemical cell devices, the donors react with acceptors to give radical ions and produce electricity in the ground state. The use of the simple dimethyl sulfone gives similar or better results compared to using benzoquinone as electron transporter. Further systematic studies on the prevention of the formation of charge transfer complexes (CT1) by finding a better electron transporter would lead to more fruitful results.

3.4 Experimental Section

3.4.1 General Information

P-Chloranil, N, N-diisopropylethylamine (DIPEA), 1,4-diazabicyclo[2.2.2]octane (DABCO) dimethylsulfone (Me_2SO_2) and TiO_2 were purchased from Avra chemicals (India). *p*-benzoquinone (BQ), triphenylamine (TPA), N,N'-tetramethyl-1,4-phenylenediamine (TMPDA), propylene carbonate (PC), ethylene carbonate (EC) and polyethylene oxide (PEO) were purchased from Sigma Aldrich. Netural alumina (Al_2O_3) was purchased from SRL chemicals, India. Zinc oxide (ZnO) was purchased from E-Merck, India. The metal oxides were heated at 150 °C in a vacuum oven for 2 h before use. PC and EC were always kept under molecular sieves. N, N-diisopropylbenzamide was prepared from the literature procedure. Graphite sheet (0.4mm thickness, 5cm x 5cm, Resistivity, $\rho = 2x10^{-4}\Omega.m$) was purchased from Falcon Graphite Industries, Hyderabad, India. Aluminium Foil (0.2mm thickness, 5cm x 5cm, Resistivity, $\rho = 2x10^{-5}\Omega.m$) and Stainless steel (0.4mm thickness, 5cm x 5cm, Resistivity, $\rho = 5x10^{-4}\Omega.m$) were purchased from Aluminium Enterprises and Rasik Metals, Hyderabad, India. EPR spectra was recorded on a Bruker-ER073 instrument equipped with an EMX micro X source for X band measurement using Xenon 1.1b.60 software provided by the manufacturer. Electrical measurements were carried out by ZAHNER instrument using CIMPS software. The current-voltage curve was drawn using Origin software.

3.4.2 Procedure for IV measurement for electrochemical cell

The voltage and current of the fabricated cell was initially measured using an multimeter. The IV characteristics were measured by ZAHNER instrument using CIMPS software. The IV characteristics of the cell were done under dark condition without illumination of light. The cell was recorded at scan rate of 1mV/S to get maximum power (Pmax) and fill factor (FF). The cell potentiostat should be open circuit voltage (Voc) before the measurement.

3.4.3 Preparation of Electrochemical Cells

Simple solution processing and casting techniques were followed for the construction of the cell device.

Configuration 1 (Figure 12, Table ES1)

The PEO (0.05 g) was dissolved in dichloromethane and mixed with TiO_2 (0.5 g) powder. DCM was removed to obtain a paste for coating on Al and Graphite foils. After 1 h, TiO_2 (0.5 g) /Sulfolane (0.24 g)/PC (0.5 g)/PEO (0.05 g) in DCM was coated on TiO_2/PEO/Al and dried. TiO_2 (0.5 g) /Cl_4BQ (0.25 g)/PC (0.5 g)/ PEO (0.05 g) in DCM was coated on TiO_2/PEO/Gr and dried in air at room temperature overnight. Donor (1 mmol)/ Sulfolane (0.120 g)/ PC (0.5 g)/PEO (0.1 g) was heat coat before packing on dried coated Al foil. The cell was prepared by sandwiching the coated Al/Gr layers. The rim of the cell prepared in this way was sealed all around using TiO_2/PEO paste, then with commercial adhesive Bondfix (India) and covered with cellophane tape.

Configuration 2 (Figure 13, Table ES2)

The PEO (0.05 g) was dissolved in dichloromethane and mixed with TiO_2 (0.5 g) powder. DCM was removed to obtain a paste for coating on Al and Graphite foils. After 1 h, TiO_2 (0.5 g) /Me_2SO_2 (0.188 g)/PC (0.5 g)/PEO (0.05 g) in DCM was coated on TiO_2/PEO/Al and dried. TiO_2 (0.5 g) /Cl_4BQ (0.25 g)/PC (0.5 g)/ PEO (0.05 g) in DCM was coated on TiO_2/PEO/Gr and dried in air at room temperature overnight. Donor (1 mmol)/ Me_2SO_2 (0.094 g)/ PC (0.5 g)/PEO (0.1 g) was heat coat before packing on dried coated Al foil. The cell was prepared by sandwiching the coated Al/Gr layers. The rim of the cell prepared in this way was sealed all around using TiO_2/PEO paste, then with commercial adhesive Bondfix (India) and covered with cellophane tape.

Configuration 3 (Figure 14, Table ES2)

The PEO (0.05 g) was dissolved in dichloromethane and mixed with TiO_2 (0.5 g) powder. DCM was removed to obtain a paste for coating on Al and Graphite foils. After 1 h, Me_2SO_2 (0.376 g)/PEO (0.05 g) in DCM was coated on TiO_2/PEO/Al and dried. Cl_4BQ (0.25 g)/PEO (0.05 g) in DCM was coated on TiO_2/PEO/Gr and dried. Donor (2 mmol)/ PC (0.5 g)/ TiO_2 (0.25 g) slurry was prepared and casted above the coated layer on Al and Graphite and dried in air at room temperature overnight. The cell was prepared by sandwiching the coated Al/Gr layers. The rim of the cell prepared in this way was sealed all around using TiO_2/PEO paste, then with commercial adhesive Bondfix (India) and covered with cellophane tape. After packing the cell was connected immediately to charge a Ni-Cd battery through a Zener diode.It was disconnected while carry out the IV-curve measurement.

Configuration 4 (Figure 15, Table ES3)

The PEO (0.05 g) was dissolved in dichloromethane and mixed with TiO_2 (0.5 g) powder. DCM was removed to obtain a paste for coating on Al and Graphite foils. After 1 h, Me_2SO_2 (0.376 g)/PEO (0.05 g) in DCM was coated on TiO_2/PEO/Al and dried. Donor (1 mmol)/Cl_4BQ (0.25 g)/PEO (0.05 g) in DCM was coated on TiO_2/PEO/Gr and dried. Me_2SO_2 (0.188 g) /Cl_4BQ (0.025 g)/ PC (0.5 g) /PEO (0.05 g) /TiO_2 (0.25 g) was coated on coated Al. and Cl_4BQ (0.025 g)/ PC (0.5 g) /PEO (0.05 g) /TiO_2 (0.25 g) was coated on coated Graphite and dried in air at room temperature overnight. The cell was prepared by sandwiching the coated Al/Gr layers. The rim of the cell prepared in this way was sealed all around using TiO_2/PEO paste, then with commercial adhesive Bondfix (India) and covered with cellophane tape.

Configuration 5 (Figure 16, Table ES3)

The PEO (0.1 g) was dissolved in dichloromethane and mixed with TiO_2 (0.5 g) powder. DCM was removed to obtain a paste for coating on Al, The PEO (0.05 g) was dissolved in dichloromethane and mixed with TiO_2 (0.5 g) powder. DCM was removed to obtain a paste for coating on Graphite foils. After 1 h, Cl_4BQ (0.1 g)/Me_2SO_2 (0.094 g)/PEO (0.05 g) in DCM was coated on TiO_2/PEO/Al and TiO_2/PEO/Gr and dried. Cl_4BQ (0.025 g)/Donor (1 mmol) /PC (0.5 g) /Me_2SO_2 (0.094 g) / TiO_2 (0.25 g)/ PEO (0.05 g) in DCM slurry was prepared and casted above the coated layer on Al and Graphite and dried in air at room temperature overnight. The cell was prepared by sandwiching the coated Al/Gr layers. The rim of the cell prepared in this way was sealed all around using TiO_2/PEO paste, then with commercial adhesive Bondfix (India) and covered with cellophane tape.

Configuration 6 (Figure 17, Table ES4)

TiO_2 (0.5 g)/Me_2SO_2 (0.188 g)/PEO (0.05 g) in DCM slurry was prepared coated layer on Al and TiO_2 (0.5 g)/ Cl_4BQ (0.25 g)/PEO (0.05 g) in DCM slurry was prepared coated layer on Graphite and dried. After 1 h, Me_2SO_2 (0.188 g)/PEO (0.05 g) in DCM was coated on coated Al. Cl_4BQ (0.25 g)/Donor (1 mmol)/ PEO (0.05 g) in DCM slurry was prepared coated layer on coated Graphite and dried. PC (0.5 g) / PEO (0.05 g) / TiO_2 (0.25 g) in DCM slurry was prepared and casted above the coated layer on Al and Graphite and dried in air at room temperature overnight. The cell was prepared by sandwiching the coated Al/Gr layers. The rim of the cell prepared in this way was sealed all around using TiO_2/PEO paste, then with commercial adhesive Bondfix (India) and covered with cellophane tape.

Configuration 7 (Figure 17, Table ES4)

TiO_2 (0.5 g)/BQ (0.22 g)/PEO (0.05 g) in DCM slurry was prepared coated layer on Al and TiO_2 (0.5 g)/ Cl_4BQ (0.25 g)/PEO (0.05 g) in DCM slurry was prepared coated layer on Graphite and dried. After 1 h, BQ (0.22 g)/PEO (0.05 g) in DCM was coated on coated Al. Cl_4BQ (0.25 g)/Donor (1 mmol)/ PEO (0.05 g) in DCM slurry was prepared coated layer on coated Graphite and dried. PC (0.5 g) / PEO (0.05 g) / TiO_2 (0.25 g) in DCM slurry was prepared and casted above the coated layer on Al and Graphite and dried in air at room temperature overnight. The cell was prepared by sandwiching the coated Al/Gr layers. The rim of the cell prepared in this way was sealed all around using TiO_2/PEO paste, then with commercial adhesive Bondfix (India) and covered with cellophane tape.

Configuration 8 (Figure 18, Table ES5)

The PEO (0.05 g) was dissolved in dichloromethane and mixed with TiO_2 (0.5 g) powder. DCM was removed to obtain a paste for coating on Al and Graphite foils. After 1 h, Me_2SO_2 (0.188 g)/PEO (0.05 g) in DCM was coated on TiO_2/PEO/Al, Cl_4BQ (0.5 g)/Donor (2 mmol)/ PEO (0.05 g) in DCM was coated on TiO_2/PEO/Gr and dried in air at room temperature overnight. Me_2SO_2 (0.094 g)/PC (0.75 g) / PEO (0.05 g) was disolved and mixed with TiO_2 (0.5 g) powder heat coat before packing on dried coated layer on Al and Graphite The cell was prepared by sandwiching the coated Al/Gr layers. The rim of the cell prepared in this way was sealed all around using TiO_2/PEO paste, then with commercial adhesive Bondfix (India) and covered with cellophane tape.

Configuration 9 (Figure 18, Table ES5)

The PEO (0.05 g) was dissolved in dichloromethane and mixed with TiO_2 (0.5 g) powder. DCM was removed to obtain a paste for coating on Al and Graphite foils. After 1 h, BQ (0.22 g)/PEO (0.05 g) in DCM was coated on TiO_2/PEO/Al, Cl_4BQ (0.5 g)/Donor (2 mmol)/ PEO (0.05 g) in DCM was coated on TiO_2/PEO/Gr and dried in air at room temperature overnight. BQ (0.11 g)/PC (0.75 g) / PEO (0.05 g) was disolved and mixed with TiO_2 (0.5 g) powder heat coat before packing on dried coated layer on Al and Graphite The cell was prepared by sandwiching the coated Al/Gr layers. The rim of the cell prepared in this way was sealed all around using TiO_2/PEO paste, then with commercial adhesive Bondfix (India) and covered with cellophane tape.

Table ES1. TiO_2 in edge layer, Sulfolane in 2 layers donor in PC as solvent.

Cell Configuration 1 (Figure 12)

(Sulfolane in 2 layers)

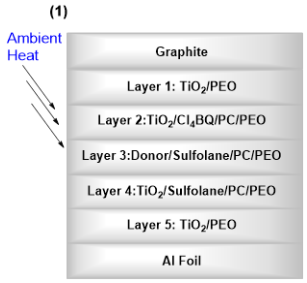

(Entries 1-5)

Entry	Cell Configuration	Time after packing	T °C[c]	Voc (V)	Isc (mA)	Vmax (V)	Imax (mA)	Pmax (mW)	Fill Factor
1	Gr---------- Layer1:TiO_2(0.5g) + PEO(0.05g) Layer2: TiO_2(0.5g) + Cl_4BQ(0.25g) + PC (0.5g) + PEO(0.05g) Layer3: TMPDA(0.164g)+Sulfolane(0.120g) +PC (0.5g) PEO(0.1g) Layer4: TiO_2(0.5g) + Sulfolane(0.24g) + PC (0.5g) + PEO(0.05g) Layer5: TiO_2(0.5g) + PEO(0.05g) Al----------	1 h	28 °C	0.928	16.26	0.453	7.987	3.62	0.24
			35 °C	0.963	20.5	0.465	10.28	4.782	0.242
			40 °C	0.99	21.59	0.472	10.94	5.159	0.241
		48 h	28 °C	0.972	1.27	0.528	0.603	0.318	0.259
			35 °C	0.975	1.615	0.568	0.750	0.426	0.27
			40 °C	0.976	1.661	0.518	0.838	0.434	0.268
		96 h	40 °C	0.958	1.266	0.53	0.591	0.313	0.258
2	Gr---------- Layer1:TiO_2(0.5g) + PEO(0.05g) Layer2: TiO_2(0.5g) + Cl_4BQ(0.25g) + PC (0.5g) + PEO(0.05g) Layer3: TPA(0.245g)+Sulfolane(0.120g) +PC (0.5g) PEO(0.1g) Layer4: TiO_2(0.5g) + Sulfolane(0.24g) + PC (0.5g) + PEO(0.05g) Layer5: TiO_2(0.5g) + PEO(0.05g) Al----------	1 h	28 °C	1.026	7.573	0.53	3.95	2.091	0.269
			35 °C	1.028	8.087	0.526	4.28	2.249	0.271
			40 °C	1.046	8.384	0.545	4.387	2.391	0.273
		48 h	28 °C	1.008	2.611	0.493	1.338	0.659	0.251
			35 °C	0.992	3.057	0.493	1.578	0.777	0.256
			40 °C	0.996	3.753	0.5	1.989	0.993	0.266
		96 h	40 °C	1.009	1.897	0.449	0.988	0.443	0.232
3	Gr---------- Layer1:TiO_2(0.5g) + PEO(0.05g) Layer2: TiO_2(0.5g) + Cl_4BQ(0.25g) + PC (0.5g) + PEO(0.05g) Layer3: DABCO(0.112g)+Sulfolane(0.120g) +PC (0.5g) PEO(0.1g) Layer4: TiO_2(0.5g) + Sulfolane(0.24g) + PC (0.5g) + PEO(0.05g) Layer5: TiO_2(0.5g) + PEO(0.05g) Al----------	1 h	28 °C	1.053	12.24	0.501	7.022	3.516	0.273
			35 °C	1.045	20.41	0.517	11.21	5.788	0.271
			40 °C	1.059	27.71	0.536	15.95	8.543	0.291
		48 h	28 °C	1.088	4.725	0.499	2.117	1.055	0.205
			35 °C	1.095	7.231	0.523	3.857	2.017	0.255
			40 °C	1.091	7.531	0.517	4.065	2.102	0.256
		96 h	40 °C	1.065	3.063	0.499	1.446	0.721	0.221
4	Gr---------- Layer1:TiO_2(0.5g) + PEO(0.05g) Layer2: TiO_2(0.5g) + Cl_4BQ(0.25g) + PC (0.5g) + PEO(0.05g) Layer3: DIPEA(0.13g)+Sulfolane(0.120g) +PC (0.5g)	1 h	28 °C	1.031	11.48	0.527	6.295	3.315	0.28
			35 °C	1.039	16.96	0.518	9.571	4.956	0.281
			40 °C	1.052	19.9	0.524	11.59	6.071	0.29

	PEO(0.1g) Layer4: TiO_2(0.5g) + Sulfolane(0.24g) + PC (0.5g) + PEO(0.05g) Layer5: TiO_2(0.5g) + PEO(0.05g) Al----------	48 h	28 ºC 35 ºC 40 ºC	1.1 1.078 1.08	4.163 5.098 5.562	0.549 0.567 0.598	2.129 2.804 3.226	1.168 1.591 1.929	0.255 0.289 0.321
		96 h	40 ºC	0.988	1.805	0.541	0.985	0.532	0.299
5	Gr---------- Layer1:TiO_2(0.5g) + PEO(0.05g) Layer2: TiO_2(0.5g) + Cl_4BQ(0.25g) + PC (0.5g) + PEO(0.05g) Layer3: DiPrBA(0.205g)+Sulfolane(0.120g) +PC (0.5g) PEO(0.1g) Layer4: TiO_2(0.5g) + Sulfolane(0.24g) + PC (0.5g) + PEO(0.05g) Layer5: TiO_2(0.5g) + PEO(0.05g) Al----------	1 h	28 ºC 35 ºC 40 ºC	1.043 1.048 1.063	13.32 13.16 13.78	0.508 0.541 0.559	7.19 6.833 7.06	3.649 3.693 3.948	0.263 0.268 0.27
		48 h	28 ºC 35 ºC 40 ºC	0.962 0.943 0.954	2.586 3.112 3.149	0.482 0.497 0.499	1.442 1.765 1.798	0.694 0.877 0.896	0.279 0.299 0.298
		96 h	40 ºC	0.928	1.551	0.502	0.874	0.438	0.305

Table ES2 TiO_2 in edge layer, Dimethylsulfone in 2 layers, donor in PC as solvent.

Cell Configuration 2 (Figure 13)

(Dimethylsulfone in 2 layers)

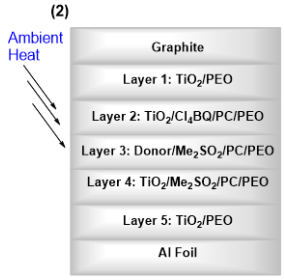

(Entries 6-10)

Cell Configuration 3 (Figure 14)

(Dimethylsulfone in 1 layer)

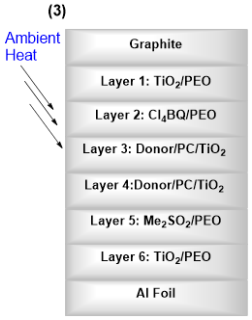

(Entries 11-13)

Entry	Cell Configuration	Time after packing	T °C[c]	Voc (V)	Isc (mA)	Vmax (V)	Imax (mA)	Pmax (mW)	Fill Factor
6	Gr---------- Layer1: TiO_2(0.5g) + PEO (0.05g) Layer2: TiO_2(0.5g) + Cl_4BQ(0.25g) + PC (0.5g) + PEO (0.05g) Layer3: DIPEA(0.13g) + Me2SO2(0.094g) + PC (0.5g) + PEO (0.1g) Layer4: TiO_2(0.5g) + Me2SO2(0.188g) + PC (0.5g) + PEO (0.05g) Layer5: TiO_2(0.5g) + PEO (0.05g) Al----------	1 h	28 °C	0.993	9.56	0.529	5.006	2.647	0.279
			35 °C	0.997	10.97	0.539	5.875	3.168	0.29
			40 °C	1.018	12.11	0.543	6.671	3.624	0.294
		48 h	28 °C	0.942	2.771	0.451	1.59	0.717	0.275
			35 °C	0.928	3.908	0.484	2.21	1.07	0.295
			40 °C	0.918	4.26	0.487	2.394	1.165	0.298
		96 h	40 °C	0.863	2.146	0.445	1.134	0.504	0.273
7	Gr---------- Layer1: TiO_2(0.5g) + PEO (0.05g) Layer2: TiO_2(0.5g) + Cl_4BQ(0.25g) + PC (0.5g) + PEO (0.05g) Layer3: TMPDA(0.164g) + Me2SO2(0.094g) + PC (0.5g) + PEO (0.1g) Layer4: TiO_2(0.5g) + Me2SO2(0.188g) + PC (0.5g) + PEO (0.05g) Layer5: TiO_2(0.5g) + PEO (0.05g) Al----------	1 h	28 °C	0.995	17.41	0.474	8.443	3.998	0.231
			35 °C	1.026	17.46	0.486	8.983	4.361	0.243
			40 °C	1.049	16.29	0.53	9.133	4.84	0.283
		48 h	28 °C	0.993	1.96	0.52	0.976	0.507	0.261
			35 °C	0.987	2.137	0.515	1.076	0.553	0.263
			40 °C	0.979	3.081	0.502	1.554	0.779	0.258
		96 h	40 °C	0.939	1.996	0.478	0.954	0.456	0.243
8	Gr---------- Layer1: TiO_2(0.5g) + PEO (0.05g) Layer2: TiO_2(0.5g) + Cl_4BQ(0.25g) + PC (0.5g) + PEO (0.05g) Layer3: TPA(0.245g) + Me2SO2(0.094g) + PC (0.5g) + PEO (0.1g) Layer4: TiO_2(0.5g) + Me2SO2(0.188g) + PC (0.5g) + PEO (0.05g) Layer5: TiO_2(0.5g) + PEO (0.05g) Al----------	1 h	28 °C	1.085	7.492	0.541	3.977	2.151	0.265
			35 °C	1.092	7.531	0.552	3.999	2.206	0.268
			40 °C	1.077	7.865	0.547	4.223	2.308	0.273
		48 h	28 °C	1.016	4.171	0.465	2.211	1.027	0.242
			35 °C	0.966	4.931	0.47	2.637	1.238	0.26
			40 °C	0.993	5.07	0.479	2.671	1.279	0.254
		96 h	40 °C	0.942	2.518	0.445	1.362	0.605	0.255
9	Gr---------- Layer1: TiO_2(0.5g) + PEO (0.05g) Layer2: TiO_2(0.5g) + Cl_4BQ(0.25g) + PC (0.5g) + PEO (0.05g) Layer3: DABCO(0.112g) + Me2SO2(0.094g) + PC (0.5g) +	1 h	28 °C	1.066	13.07	0.519	6.077	3.152	0.226
			35 °C	1.082	22.16	0.501	13.06	6.549	0.273
			40 °C	1.078	23.9	0.5	13.86	6.925	0.269

	PEO (0.1g) Layer4: TiO_2(0.5g) + Me2SO2(0.188g) + PC (0.5g) + PEO (0.05g) Layer5: TiO_2(0.5g) + PEO (0.05g) Al----------	48 h	28 ºC 35 ºC 40 ºC	1.073 1.056 1.068	4.987 8.606 9.302	0.521 0.588 0.582	2.187 4.384 4.629	1.467 2.575 2.692	0.274 0.283 0.271
		96 h	40 ºC	1.023	4.235	0.496	1.91	0.947	0.219
10	Gr---------- Layer1: TiO_2(0.5g) + PEO (0.05g) Layer2: TiO_2(0.5g) + Cl_4BQ(0.25g) + PC (0.5g) + PEO (0.05g) Layer3: DiPrBA(0.205g) + Me2SO2(0.094g) + PC (0.5g) + PEO (0.1g) Layer4: TiO_2(0.5g) + Me2SO2(0.188g) + PC (0.5g) + PEO (0.05g) Layer5: TiO_2(0.5g) + PEO (0.05g) Al----------	1 h	28 ºC 35 ºC 40 ºC	1.101 1.098 1.106	9.534 9.591 10.9	0.548 0.542 0.548	5.196 5.276 6.118	2.847 2.86 3.354	0.271 0.272 0.278
		48 h	28 ºC 35 ºC 40 ºC	1.001 0.955 0.985	4.744 5.63 5.911	0.485 0.493 0.499	2.711 3.455 3.558	1.314 1.703 1.774	0.277 0.317 0.305
		96 h	40 ºC	0.924	2.062	0.528	1.497	0.789	0.415
11	Gr---------- Layer1: TiO_2(0.5g) + PEO (0.05g) Layer2: Cl_4BQ(0.25g) + PEO (0.05g) Layer3: DIPEA(0.26g) + PC (0.5g) + TiO2 (0.25g) Layer4: DIPEA(0.26g) + PC (0.5g) + TiO2 (0.25g) Layer5: Me2SO2(0.376g) + PEO (0.05g) Layer6: TiO_2(0.5g) + PEO (0.05g) Al----------	1 h	28 ºC 35 ºC 40 ºC	1.076 1.037 1.117	20.92 26.06 33.85	0.544 0.539 0.569	11.47 14.20 21.11	6.24 7.650 12.02	0.277 0.283 0.318
		48 h	28 ºC 35 ºC 40 ºC	1.072 1.059 1.032	14.01 15.98 17.29	0.605 0.584 0.594	9.151 10.95 11.77	5.534 6.397 6.991	0.369 0.378 0.392
		96 h	40 ºC	0.974	7.976	0.581	4.796	2.786	0.359
12	Gr---------- Layer1: TiO_2(0.5g) + PEO (0.05g) Layer2: Cl_4BQ(0.25g) + PEO (0.05g) Layer3: NMP(0.198g) + PC (0.5g) + TiO2 (0.25g) Layer4: NMP(0.198g) + PC (0.5g) + TiO2 (0.25g) Layer5: Me2SO2(0.376g) + PEO (0.05g) Layer6: TiO_2(0.5g) + PEO (0.05g) Al----------	1 h	28 ºC 35 ºC 40 ºC	0.967 0.943 1.008	19.45 25.81 29.73	0.354 0.349 0.388	9.642 13.26 15.42	3.413 4.623 5.986	0.182 0.190 0.200
		48 h	28 ºC 35 ºC 40 ºC	1.041 1.045 1.04	9.3 12.59 13.85	0.431 0.432 0.42	4.185 5.996 7.201	1.804 2.589 3.026	0.186 0.197 0.21
		96 h	40 ºC	1.042	17.46	0.406	7.952	3.231	0.178
13	Gr---------- Layer1: TiO_2(0.5g) + PEO (0.05g) Layer2: Cl_4BQ(0.25g) + PEO (0.05g) Layer3: DABCO(0.224g) + PC (0.5g) + TiO2 (0.25g) Layer4: DABCO(0.224g) + PC (0.5g) + TiO2 (0.25g) Layer5: Me2SO2(0.376g) + PEO (0.05g) Layer6: TiO_2(0.5g) + PEO (0.05g) Al----------	1 h	28 ºC 35 ºC 40 ºC	0.953 0.938 0.978	14.20 21.78 23.52	0.483 0.465 0.503	6.972 11.09 10.60	3.368 5.154 5.336	0.249 0.252 0.232
		48 h	28 ºC 35 ºC 40 ºC	0.883 0.875 0.862	8.071 11.3 12.64	0.419 0.425 0.399	3.667 4.771 5.647	1.535 2.027 2.25	0.215 0.205 0.207
		96 h	40 ºC	0.889	5.947	0.393	2.767	1.087	0.206

Table ES3 TiO_2 in edge layer, Cl_4BQ in PC layers, Sulfolane in 2&4 layers PC as solvent.

Cell Configuration 4 (Figure 15)

(Sulfolane in 2 layers)

(4)

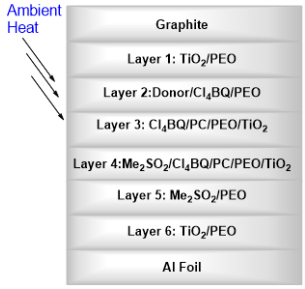

(Entries 14-18)

Cell Configuration 5 (Figure 16)

(Sulfolane in 4 layers)

(5)

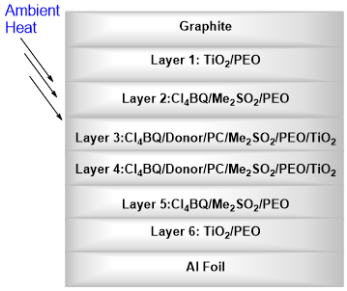

(Entries 19-23)

Entry	Cell Configuration	Time after packing	T °C[c]	Voc (V)	Isc (mA)	Vmax (V)	Imax (mA)	Pmax (mW)	Fill Factor
14	Gr---------- Layer1:TiO_2(0.5g) + PEO(0.05g) Layer2: Cl_4BQ(0.25g) +DIPEA (0.17ml) + PEO(0.05g) Layer3: Cl_4BQ (0.025g) + PC (0.5g) + TiO_2 (0.25g) + PEO(0.05g) Layer4: Me_2SO_2 (0.188g) + Cl_4BQ (0.025g) + PC (0.5g) + TiO_2 (0.25g) + PEO(0.05g) Layer5: Me_2SO_2 (0.376g) + PEO (0.05g) Layer6: TiO_2(0.5g) + PEO(0.05g) Al----------	1 h	28 °C	1.098	23.26	0.556	11.48	6.38	0.25
			35 °C	1.07	26.86	0.566	14.81	8.373	0.291
			40 °C	1.084	32.61	0.608	20.42	12.42	0.351
		48 h	28 °C	1.005	8.667	0.516	4.981	2.572	0.295
			35 °C	0.982	9.118	0.546	5.418	2.96	0.331
			40 °C	0.971	11.0	0.572	6.769	3.874	0.363
		96 h	40 °C	0.957	4.54	0.504	2.843	1.432	0.33
15	Gr---------- Layer1:TiO_2(0.5g) + PEO(0.05g) Layer2: Cl_4BQ(0.25g) + N,N-Diisopropyl benzamide (0.205g) + PEO(0.05g) Layer3: Cl_4BQ (0.025g) + PC (0.5g) + TiO_2 (0.25g) + PEO(0.05g) Layer4: Me_2SO_2 (0.188g) + Cl_4BQ (0.025g) + PC (0.5g) + TiO_2 (0.25g) + PEO(0.05g) Layer5: Me_2SO_2 (0.376g) + PEO (0.05g) Layer6: TiO_2(0.5g) + PEO(0.05g) Al----------	1 h	28 °C	1.116	9.493	0.512	4.67	2.394	0.226
			35 °C	1.086	9.485	0.516	4.989	2.523	0.25
			40 °C	1.102	13.75	0.532	7.594	4.04	0.267
		48 h	28 °C	1.127	6.386	0.534	3.429	1.83	0.254
			35 °C	1.086	6.927	0.558	3.781	2.111	0.281
			40 °C	1.068	7.787	0.543	4.428	2.405	0.289
		96 h	40 °C	1.077	4.256	0.504	2.265	1.141	0.249
16	Gr---------- Layer1:TiO_2(0.5g) + PEO(0.05g) Layer2: Cl_4BQ(0.25g) + TPA(0.245g) + PEO(0.05g) Layer3: Cl_4BQ (0.025g) + PC (0.5g) + TiO_2 (0.25g) + PEO(0.05g) Layer4: Me_2SO_2 (0.188g) + Cl_4BQ (0.025g) + PC (0.5g) + TiO_2 (0.25g) + PEO(0.05g) Layer5: Me_2SO_2 (0.376g) + PEO (0.05g) Layer6: TiO_2(0.5g) + PEO(0.05g) Al----------	1 h	28 °C	0.939	9.372	0.443	4.693	2.076	0.236
			35 °C	0.94	11.5	0.443	6.552	2.901	0.269
			40 °C	0.972	14.04	0.463	8.216	3.8	0.279
		48 h	28 °C	1.049	9.079	0.509	5.601	2.853	0.3
			35 °C	0.984	9.818	0.523	5.947	3.11	0.322
			40 °C	0.982	11.36	0.52	7.23	3.756	0.337
		96 h	40 °C	1.031	5.82	0.517	3.537	1.828	0.305
17	Gr---------- Layer1:TiO_2(0.5g) + PEO(0.05g) Layer2: Cl_4BQ(0.25g) + TMPDA(0.116g) + PEO(0.05g) Layer3: Cl_4BQ (0.025g) + PC (0.5g) + TiO_2 (0.25g) + PEO(0.05g)	1 h	28 °C	0.219	5.525	0.197	1.57	0.308	0.255
			35 °C	0.468	4.404	0.269	2.242	0.602	0.293
			40 °C	0.715	6.415	0.364	4.193	1.524	0.332

	Layer4: Me_2SO_2 (0.188g) + Cl_4BQ (0.025g) + PC (0.5g) + TiO_2 (0.25g) + PEO(0.05g) Layer5: Me_2SO_2 (0.376g) + PEO (0.05g) Layer6: TiO_2(0.5g) + PEO(0.05g) Al----------	48 h	28 ºC	0.853	3.736	0.409	1.637	0.669	0.21
			35 ºC	0.821	4.995	0.346	3.12	1.078	0.263
			40 ºC	0.798	5.298	0.354	3.431	1.216	0.288
		96 h	40 ºC	0.791	0.768	0.238	0.520	0.123	0.204
18	Gr---------- Layer1:TiO_2(0.5g) + PEO(0.05g) Layer2: Cl_4BQ(0.25g) + DABCO(0.112g) + PEO(0.05g) Layer3: Cl_4BQ (0.025g) + PC (0.5g) + TiO_2 (0.25g) + PEO(0.05g) Layer4: Me_2SO_2 (0.188g) + Cl_4BQ (0.025g) + PC (0.5g) + TiO_2 (0.25g) + PEO(0.05g) Layer5: Me_2SO_2 (0.376g) + PEO (0.05g) Layer6: TiO_2(0.5g) + PEO(0.05g) Al----------	1 h	28 ºC	0.986	31.34	0.561	13.01	7.299	0.236
			35 ºC	0.98	37.02	0.625	16.66	10.41	0.287
			40 ºC	0.992	34.5	0.621	17.7	10.99	0.321
		48 h	28 ºC	1.018	11.49	0.504	7.054	3.554	0.304
			35 ºC	1.009	12.71	0.579	8.525	4.932	0.384
			40 ºC	1.007	13.2	0.596	9.23	5.501	0.414
		96 h	40 ºC	0.981	8.165	0.487	5.353	2.608	0.326
19	Gr---------- Layer1:TiO_2(0.5g) + PEO(0.05g) Layer2: Cl_4BQ(0.1g) + Me_2SO_2 (0.094g) + PEO(0.05g) Layer3: Cl_4BQ (0.025g) + DIPEA(0.112g)+PC (0.5g) + Me_2SO_2 (0.094g) + PEO(0.05g) +TiO_2 (0.25g) Layer4: Cl_4BQ (0.025g) + DIPEA(0.112g)+PC (0.5g) + Me_2SO_2 (0.094g) + PEO(0.05g) +TiO_2 (0.25g) Layer5: Cl_4BQ(0.1g) + Me_2SO_2 (0.094g) + PEO(0.05g) Layer6: TiO_2(0.5g) + PEO(0.1g) Al----------	1 h	28 ºC	1.059	11.68	0.615	7.012	4.314	0.349
			35 ºC	1.015	19.25	0.669	9.555	6.39	0.327
			40 ºC	1.003	22.07	0.658	12.75	8.392	0.379
		48 h	28 ºC	0.783	1.956	0.332	0.940	0.312	0.204
			35 ºC	0.752	2.735	0.307	1.403	0.430	0.209
			40 ºC	0.776	3.649	0.334	2.063	0.688	0.243
		96 h	40 ºC	0.819	3.955	0.375	1.918	0.718	0.222
20	Gr---------- Layer1:TiO_2(0.5g) + PEO(0.05g) Layer2: Cl_4BQ(0.1g) + Me_2SO_2 (0.094g) + PEO(0.05g) Layer3: Cl_4BQ (0.025g) + DABCO(0.112g)+PC (0.5g) + Me_2SO_2 (0.094g) + PEO(0.05g) +TiO_2 (0.25g) Layer4: Cl_4BQ (0.025g) + DABCO(0.112g)+PC (0.5g) + Me_2SO_2 (0.094g) + PEO(0.05g) +TiO_2 (0.25g) Layer5: Cl_4BQ(0.1g) + Me_2SO_2 (0.094g) + PEO(0.05g) Layer6: TiO_2(0.5g) + PEO(0.1g) Al----------	1 h	28 ºC	0.965	14.33	0.558	4.733	2.642	0.191
			35 ºC	0.947	19.33	0.37	8.984	3.324	0.182
			40 ºC	0.941	21.39	0.371	10.92	4.051	0.201
		48 h	28 ºC	0.9	5.066	0.379	1.931	0.731	0.161
			35 ºC	0.892	8.105	0.356	3.446	1.225	0.169
			40 ºC	0.896	13.87	0.353	6.876	2.427	0.195
		96 h	40 ºC	0.854	5.543	0.361	2.421	0.874	0.185
21	Gr---------- Layer1:TiO_2(0.5g) + PEO(0.05g) Layer2: Cl_4BQ(0.1g) + Me_2SO_2 (0.094g) + PEO(0.05g) Layer3: Cl_4BQ (0.025g) + TMPDA(0.164g)+PC (0.5g) + Me_2SO_2 (0.094g) + PEO(0.05g) +TiO_2 (0.25g) Layer4: Cl_4BQ (0.025g) + TMPDA(0.164g)+PC (0.5g) + Me_2SO_2 (0.094g) + PEO(0.05g) +TiO_2 (0.25g) Layer5: Cl_4BQ(0.1g) + Me_2SO_2 (0.094g) + PEO(0.05g) Layer6: TiO_2(0.5g) + PEO(0.1g) Al----------	1 h	28 ºC	0.706	8.211	0.281	3.832	1.077	0.186
			35 ºC	0.696	11.51	0.28	5.84	1.635	0.204
			40 ºC	0.694	11.59	0.292	6.391	1.863	0.232
		48 h	28 ºC	0.647	2.063	0.315	0.935	0.294	0.221
			35 ºC	0.635	2.194	0.303	1.046	0.317	0.228
			40 ºC	0.646	2.912	0.326	1.376	0.448	0.238
		96 h	40 ºC	0.612	2.193	0.294	1.104	0.324	0.242
22	Gr---------- Layer1:TiO_2(0.5g) + PEO(0.05g) Layer2: Cl_4BQ(0.1g) + Me_2SO_2 (0.094g) + PEO(0.05g) Layer3: Cl_4BQ (0.025g) + DiPrBA(0.205g)+PC (0.5g) + Me_2SO_2 (0.094g) + PEO(0.05g) +TiO_2 (0.25g) Layer4: Cl_4BQ (0.025g) + DiPrBA(0.205g)+PC (0.5g) + Me_2SO_2 (0.094g) + PEO(0.05g) +TiO_2 (0.25g) Layer5: Cl_4BQ(0.1g) + Me_2SO_2 (0.094g) + PEO(0.05g) Layer6: TiO_2(0.5g) + PEO(0.1g) Al----------	1 h	28 ºC	1.057	12.37	0.524	6.683	3.5	0.268
			35 ºC	1.082	14.0	0.514	8.111	4.167	0.275
			40 ºC	1.029	14.91	0.516	8.24	4.248	0.277
		48 h	28 ºC	1.036	4.313	0.53	2.612	1.385	0.31
			35 ºC	1.02	4.954	0.526	2.989	1.573	0.311
			40 ºC	0.998	4.669	0.537	2.951	1.584	0.34

		96 h	40 °C	0.957	3.16	0.508	1.936	0.983	0.325
23	Gr---------- Layer1:TiO_2(0.5g) + PEO(0.05g) Layer2: Cl_4BQ(0.1g) + Me_2SO_2 (0.094g) + PEO(0.05g) Layer3: Cl_4BQ (0.025g) + TPA(0.245g)+PC (0.5g) + Me_2SO_2 (0.094g) + PEO(0.05g) +TiO_2 (0.25g) Layer4: Cl_4BQ (0.025g) + TPA(0.245g)+PC (0.5g) + Me_2SO_2 (0.094g) + PEO(0.05g) +TiO_2 (0.25g) Layer5: Cl_4BQ(0.1g) + Me_2SO_2 (0.094g) + PEO(0.05g) Layer6: TiO_2(0.5g) + PEO(0.1g) Al----------	1 h	28 °C	1.037	4.479	0.513	2.304	1.182	0.255
			35 °C	1.018	5.122	0.505	2.673	1.348	0.259
			40 °C	1.04	5.285	0.506	2.794	1.412	0.257
		48 h	28 °C	1.071	2.386	0.535	1.249	0.667	0.261
			35 °C	1.053	2.884	0.511	1.534	0.783	0.258
			40 °C	1.043	2.994	0.514	1.649	0.847	0.271
		96 h	40 °C	1.055	2.234	0.502	1.169	0.586	0.249

Comparision of BQ and Me_2SO_2Using in PC solvent

Table ES4 TiO_2 in PC layer, Dimethylsulfone (or) BQ in 2 layers PC as solvent.

Cell Configuration 6 (Figure 17)

(Dimethylsulfone in 2 layers)

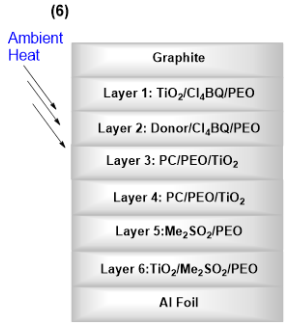

(Entries 24-28)

Cell Configuration 7 (Figure 17)

(BQ in 2 layers)

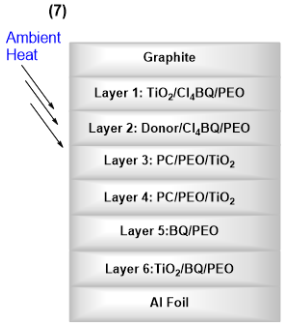

(Entries 29-33)

Entry	Cell Configuration	Time after packing	T °C[c]	Voc (V)	Isc (mA)	Vmax (V)	Imax (mA)	Pmax (mW)	Fill Factor
24	Gr---------- Layer1: TiO_2(0.5g) + Cl_4BQ(0.25g) + PEO (0.05g) Layer2: DABCO(0.112g)+Cl_4BQ(0.25g) + PEO (0.05g) Layer3: PC (0.5g) + PEO (0.05g) +TiO2 (0.25g) Layer4: PC (0.5g) + PEO (0.05g) +TiO2 (0.25g) Layer5: Me2SO2(0.188g) + PEO (0.05g) Layer6: TiO_2(0.5g) + Me2SO2(0.188g) + PEO (0.05g) Al----------	1 h	28 °C	1.093	6.205	0.522	2.962	1.545	0.228
			35 °C	1.106	10.26	0.491	5.534	2.717	0.239
			40 °C	1.065	9.556	0.549	5.223	2.865	0.282
		48 h	28 °C	1.112	3.477	0.533	1.348	0.717	0.186
			35 °C	1.124	4.016	0.584	1.936	1.131	0.251
			40 °C	1.12	5.021	0.59	2.584	1.524	0.271
		96 h	40 °C	1.114	4.555	0.479	1.878	0.898	0.177
25	Gr---------- Layer1: TiO_2(0.5g) + Cl_4BQ(0.25g) + PEO (0.05g) Layer2: TPA(0.245g)+Cl_4BQ(0.25g) + PEO (0.05g) Layer3: PC (0.5g) + PEO (0.05g) +TiO2 (0.25g) Layer4: PC (0.5g) + PEO (0.05g) +TiO2 (0.25g)	1 h	28 °C	1.099	6.225	0.408	2.953	1.205	0.176
			35 °C	1.109	6.717	0.445	3.329	1.481	0.199
			40 °C	1.121	7.437	0.459	3.69	1.693	0.203

	Layer5: Me2SO2(0.188g) + PEO (0.05g) Layer6: TiO_2(0.5g) + Me2SO2(0.188g) + PEO (0.05g) Al----------	48 h	28 ºC	1.176	5.377	0.449	2.372	1.065	0.168
			35 ºC	1.046	6.716	0.504	3.376	1.702	0.242
			40 ºC	1.116	7.668	0.488	3.831	1.87	0.218
		96 h	40 ºC	1.198	4.858	0.491	2.17	1.065	0.183
26	Gr---------- Layer1: TiO_2(0.5g) + Cl_4BQ(0.25g) + PEO (0.05g) Layer2: DIPEA(0.13g)+Cl_4BQ(0.25g) + PEO (0.05g) Layer3: PC (0.5g) + PEO (0.05g) +TiO2 (0.25g) Layer4: PC (0.5g) + PEO (0.05g) +TiO2 (0.25g) Layer5: Me2SO2(0.188g) + PEO (0.05g) Layer6: TiO_2(0.5g) + Me2SO2(0.188g) + PEO (0.05g) Al----------	1 h	28 ºC	1.129	20.63	0.493	10.43	5.138	0.221
			35 ºC	1.133	21.5	0.484	10.9	5.271	0.216
			40 ºC	1.143	21.4	0.495	11.16	5.525	0.226
		48 h	28 ºC	1.184	15.72	0.446	7.966	3.549	0.191
			35 ºC	1.121	15.57	0.491	7.866	3.858	0.221
			40 ºC	1.12	17.7	0.517	8.991	4.649	0.235
		96 h	40 ºC	1.186	14.16	0.481	7.108	3.416	0.203
27	Gr---------- Layer1: TiO_2(0.5g) + Cl_4BQ(0.25g) + PEO (0.05g) Layer2: TMPDA(0.166g)+Cl_4BQ(0.25g) + PEO (0.05g) Layer3: PC (0.5g) + PEO (0.05g) +TiO2 (0.25g) Layer4: PC (0.5g) + PEO (0.05g) +TiO2 (0.25g) Layer5: Me2SO2(0.188g) + PEO (0.05g) Layer6: TiO_2(0.5g) + Me2SO2(0.188g) + PEO (0.05g) Al----------	1 h	28 ºC	1.131	7.96	0.579	4.313	2.495	0.277
			35 ºC	1.149	9.197	0.555	4.936	2.737	0.259
			40 ºC	1.143	8.996	0.594	4.739	2.814	0.274
		48 h	28 ºC	1.025	4.616	0.515	2.197	1.131	0.239
			35 ºC	1.015	4.671	0.568	2.212	1.256	0.265
			40 ºC	1.005	4.789	0.566	2.31	1.307	0.272
		96 h	40 ºC	0.982	2.031	0.445	0.977	0.434	0.218
28	Gr---------- Layer1: TiO_2(0.5g) + Cl_4BQ(0.25g) + PEO (0.05g) Layer2: DiPrBA(0.205g)+Cl_4BQ(0.25g) + PEO (0.05g) Layer3: PC (0.5g) + PEO (0.05g) +TiO2 (0.25g) Layer4: PC (0.5g) + PEO (0.05g) +TiO2 (0.25g) Layer5: Me2SO2(0.188g) + PEO (0.05g) Layer6: TiO_2(0.5g) + Me2SO2(0.188g) + PEO (0.05g) Al----------	1 h	28 ºC	1.099	3.689	0.531	1.849	0.982	0.242
			35 ºC	1.103	4.225	0.526	2.087	1.097	0.235
			40 ºC	1.135	4.366	0.513	2.172	1.115	0.225
		48 h	28 ºC	1.15	3.654	0.537	1.839	0.987	0.235
			35 ºC	1.13	3.495	0.552	1.798	0.991	0.251
			40 ºC	1.134	3.571	0.544	1.833	0.997	0.246
		96 h	40 ºC	1.092	2.529	0.486	1.316	0.639	0.232
29	Gr---------- Layer1: TiO_2(0.5g) + Cl_4BQ(0.25g) + PEO (0.05g) Layer2: DABCO(0.112g)+Cl_4BQ(0.25g) + PEO (0.05g) Layer3: PC (0.5g) + PEO (0.05g) +TiO2 (0.25g) Layer4: PC (0.5g) + PEO (0.05g) +TiO2 (0.25g) Layer5: BQ(0.22g) + PEO (0.05g) Layer6: TiO_2(0.5g) + BQ(0.22g)+ PEO (0.05g) Al----------	1 h	28 ºC	1.118	4.096	0.604	1.666	1.007	0.22
			35 ºC	1.13	4.9	0.581	2.337	1.358	0.245
			40 ºC	1.14	5.758	0.563	2.903	1.633	0.249
		48 h	28 ºC	1.192	2.943	0.437	1.409	0.615	0.176
			35 ºC	1.202	3.591	0.53	1.808	0.957	0.222
			40 ºC	1.209	4.007	0.558	2.059	1.15	0.237
		96 h	40 ºC	1.207	2.976	0.467	1.486	0.694	0.193
30	Gr---------- Layer1: TiO_2(0.5g) + Cl_4BQ(0.25g) + PEO (0.05g) Layer2: TPA(0.245g)+Cl_4BQ(0.25g) + PEO (0.05g) Layer3: PC (0.5g) + PEO (0.05g) +TiO2 (0.25g) Layer4: PC (0.5g) + PEO (0.05g) +TiO2 (0.25g) Layer5: BQ(0.22g) + PEO (0.05g) Layer6: TiO_2(0.5g) + BQ(0.22g) + PEO (0.05g) Al----------	1 h	28 ºC	1.14	3.231	0.481	1.434	0.689	0.187
			35 ºC	1.153	3.92	0.511	1.823	0.931	0.206
			40 ºC	1.164	4.477	0.517	2.16	1.117	0.214
		48 h	28 ºC	1.196	2.964	0.52	1.448	0.752	0.212
			35 ºC	1.152	3.537	0.531	1.74	0.923	0.227

			40 ºC	1.153	3.976	0.535	1.954	1.045	0.228
		96 h	40 ºC	1.208	3.157	0.538	1.527	0.821	0.215
31	Gr---------- Layer1: TiO_2(0.5g) + Cl_4BQ(0.25g) + PEO (0.05g) Layer2: DIPEA(0.13g)+Cl_4BQ(0.25g) + PEO (0.05g) Layer3: PC (0.5g) + PEO (0.05g) +TiO2 (0.25g) Layer4: PC (0.5g) + PEO (0.05g) +TiO2 (0.25g) Layer5: BQ(0.22g) + PEO (0.05g) Layer6: TiO_2(0.5g) + BQ(0.22g) + PEO (0.05g) Al----------	1 h	28 ºC	1.166	17.98	0.378	8.302	3.14	0.15
			35 ºC	1.174	18.85	0.461	9.067	4.182	0.189
			40 ºC	1.187	22.72	0.479	11.05	5.286	0.196
		48 h	28 ºC	1.223	15.77	0.364	7.077	2.578	0.134
			35 ºC	1.126	22.91	0.511	11.9	6.077	0.236
			40 ºC	1.12	22.99	0.508	12.32	6.253	0.243
		96 h	40 ºC	1.222	16.23	0.402	7.348	2.956	0.149
32	Gr---------- Layer1: TiO_2(0.5g) + Cl_4BQ(0.25g) + PEO (0.05g) Layer2: TMPDA(0.166g)+Cl_4BQ(0.25g) + PEO (0.05g) Layer3: PC (0.5g) + PEO (0.05g) +TiO2 (0.25g) Layer4: PC (0.5g) + PEO (0.05g) +TiO2 (0.25g) Layer5: BQ(0.22g) + PEO (0.05g) Layer6: TiO_2(0.5g) + BQ(0.22g) + PEO (0.05g) Al----------	1 h	28 ºC	1.233	8.982	0.551	4.524	2.492	0.225
			35 ºC	1.233	8.741	0.614	4.386	2.692	0.25
			40 ºC	1.234	9.34	0.573	4.835	2.772	0.241
		48 h	28 ºC	1.134	2.036	0.505	1.001	0.505	0.219
			35 ºC	1.135	2.267	0.518	1.17	0.605	0.235
			40 ºC	1.133	2.451	0.53	1.264	0.669	0.241
		96 h	40 ºC	1.044	1.364	0.47	0.647	0.304	0.214
33	Gr---------- Layer1: TiO_2(0.5g) + Cl_4BQ(0.25g) + PEO (0.05g) Layer2: DiPrBA(0.205g)+Cl_4BQ(0.25g) + PEO (0.05g) Layer3: PC (0.5g) + PEO (0.05g) +TiO2 (0.25g) Layer4: PC (0.5g) + PEO (0.05g) +TiO2 (0.25g) Layer5: BQ(0.22g) + PEO (0.05g) Layer6: TiO_2(0.5g) + BQ(0.22g) + PEO (0.05g) Al----------	1 h	28 ºC	1.158	5.325	0.498	2.394	1.191	0.193
			35 ºC	1.15	4.615	0.552	2.213	1.222	0.23
			40 ºC	1.146	5.055	0.518	2.406	1.246	0.215
		48 h	28 ºC	1.202	1.171	0.544	0.525	0.285	0.203
			35 ºC	1.196	1.54	0.558	0.703	0.392	0.213
			40 ºC	1.193	1.94	0.545	0.907	0.495	0.214
		96 h	40 ºC	1.202	0.623	0.573	0.287	0.164	0.22

Comparision of BQ and Me_2SO_2Using PC solvent

Table ES5 Dimethylsulfone (or) BQ in 3 layers PC as solvent.

Cell Configuration 8 (Figure 18)

(Dimethylsulfone in 4 layers)

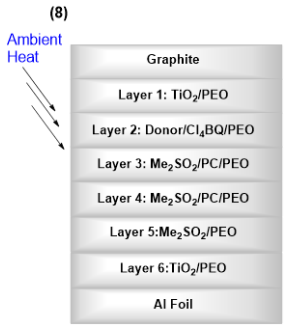

(Entries 34-36)

Cell Configuration 9 (Figure 18)

(BQ in 4 layers)

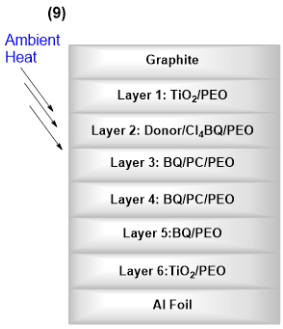

(Entries 37-39)

Entry	Cell Configuration	Time after packing	T °C[c]	Voc (V)	Isc (mA)	Vmax (V)	Imax (mA)	Pmax (mW)	Fill Factor
34	Gr---------- Layer1: TiO_2(0.5g) + PEO (0.05g) Layer2: DIPEA(0.26g)+Cl_4BQ(0.5g) + PEO (0.05g) Layer3: Me2SO2(0.094g) + PC (0.75g) + PEO (0.05g) Layer4: Me2SO2(0.094g) + PC (0.75g) + PEO (0.05g) Layer5: Me2SO2(0.188g) + PEO (0.05g) Layer6: TiO_2(0.5g) + PEO (0.05g) Al----------	1 h	28 °C	1.07	29.32	0.524	15.58	8.155	0.26
			35 °C	1.078	35.95	0.556	19.66	10.93	0.282
			40 °C	1.087	49.63	0.522	24.59	12.83	0.238
		48 h	28 °C	1.074	7.862	0.457	4.203	1.921	0.228
			35 °C	1.047	7.264	0.507	3.953	2.002	0.263
			40 °C	1.055	8.226	0.526	4.261	2.24	0.258
		96 h	40 °C	1.006	10.03	0.509	5.628	2.863	0.284
35	Gr---------- Layer1: TiO_2(0.5g) + PEO (0.05g) Layer2: DABCO(0.224g)+Cl_4BQ(0.5g) + PEO (0.05g) Layer3: Me2SO2(0.094g) + PC (0.75g) + PEO (0.05g) Layer4: Me2SO2(0.094g) + PC (0.75g) + PEO (0.05g) Layer5: Me2SO2(0.188g) + PEO (0.05g) Layer6: TiO_2(0.5g) + PEO (0.05g) Al----------	1 h	28 °C	1.068	22.42	0.469	12.74	5.977	0.25
			35 °C	1.08	27.94	0.502	15.5	7.783	0.258
			40 °C	1.093	30.49	0.518	16.4	8.497	0.255
		48 h	28 °C	1.092	15.78	0.488	8.137	3.967	0.23
			35 °C	1.094	19.02	0.533	10.11	5.389	0.259
			40 °C	1.098	19.31	0.546	10.43	5.691	0.268
		96 h	40 °C	1.08	5.27	0.515	2.71	1.395	0.245
36	Gr---------- Layer1: TiO_2(0.5g) + PEO (0.05g) Layer2: TPA(0.490g)+Cl_4BQ(0.5g) + PEO (0.05g) Layer3: Me2SO2(0.094g) + PC (0.75g) + PEO (0.05g) Layer4: Me2SO2(0.094g) + PC (0.75g) + PEO (0.05g) Layer5: Me2SO2(0.188g) + PEO (0.05g) Layer6: TiO_2(0.5g) + PEO (0.05g) Al----------	1 h	28 °C	1.071	7.722	0.512	3.905	2.001	0.242
			35 °C	1.023	8.001	0.527	4.069	2.142	0.262
			40 °C	1.046	9.455	0.527	4.949	2.607	0.264
		48 h	28 °C	1.157	5.652	0.517	2.94	1.521	0.233
			35 °C	1.114	6.745	0.524	3.554	1.863	0.248
			40 °C	1.106	6.772	0.548	3.527	1.932	0.258
		96 h	40 °C	1.161	3.944	0.536	1.976	1.06	0.231

37	Gr---------- Layer1: TiO_2(0.5g) + PEO (0.05g) Layer2: DIPEA(0.26g)+Cl_4BQ(0.5g) + PEO (0.05g) Layer3: BQ(0.11g) + PC (0.75g) + PEO (0.05g) Layer4: BQ(0.11g) + PC (0.75g) + PEO (0.05g) Layer5: BQ(0.22g) + PEO (0.05g) Layer6: TiO_2(0.5g) + PEO (0.05g) Al----------	1 h	28 °C	1.173	28.51	0.54	13.22	7.141	0.214
			35 °C	1.165	30.94	0.541	13.25	7.173	0.199
			40 °C	1.175	62.46	0.508	29.13	14.79	0.202
		48 h	28 °C	1.102	8.742	0.486	4.49	2.182	0.226
			35 °C	1.087	8.966	0.483	4.727	2.284	0.235
			40 °C	1.086	9.051	0.515	4.555	2.347	0.239
		96 h	40 °C	1.005	3.803	0.404	1.815	0.732	0.192
38	Gr---------- Layer1: TiO_2(0.5g) + PEO (0.05g) Layer2: DABCO(0.224g)+Cl_4BQ(0.5g) + PEO (0.05g) Layer3: BQ(0.11g) + PC (0.75g) + PEO (0.05g) Layer4: BQ(0.11g) + PC (0.75g) + PEO (0.05g) Layer5: BQ(0.22g) + PEO (0.05g) Layer6: TiO_2(0.5g) + PEO (0.05g) Al----------	1 h	28 °C	1.159	23.83	0.547	11.31	6.19	0.224
			35 °C	1.15	27.18	0.486	12.91	6.27	0.201
			40 °C	1.166	23.52	0.554	11.37	6.302	0.23
		48 h	28 °C	1.173	13.54	0.476	7.768	3.696	0.233
			35 °C	1.169	13.49	0.542	7.367	3.995	0.253
			40 °C	1.17	14.12	0.524	7.808	4.093	0.248
		96 h	40 °C	1.175	10.05	0.451	5.632	2.539	0.215
39	Gr---------- Layer1: TiO_2(0.5g) + PEO (0.05g) Layer2: TPA(0.490g)+Cl_4BQ(0.5g) + PEO (0.05g) Layer3: BQ(0.11g) + PC (0.75g) + PEO (0.05g) Layer4: BQ(0.11g) + PC (0.75g) + PEO (0.05g) Layer5: BQ(0.22g) + PEO (0.05g) Layer6: TiO_2(0.5g) + PEO (0.05g) Al----------	1 h	28 °C	1.168	6.538	0.522	3.215	1.677	0.22
			35 °C	1.148	6.78	0.536	3.351	1.795	0.231
			40 °C	1.152	7.418	0.541	3.726	2.015	0.236
		48 h	28 °C	1.223	4.037	0.537	1.893	1.017	0.206
			35 °C	1.201	5.048	0.531	2.421	1.286	0.212
			40 °C	1.189	5.244	0.551	2.512	1.384	0.222
		96 h	40 °C	1.185	3.962	0.507	1.905	0.966	0.206

3.5 References

1 Ghosh, A. K.; Morel, D. L.; Feng, T.; Shaw, R. F.; Rowe Jr, C. A. *Journal of Applied Physics.* **1974,** *45,* 230.

2 Gelenis, S.; Tourillon, G.; Granier, F. *Thin Solid Films.* 1986, 139, 221.

3 Weinberger, B. R.; Akhtar, M.; Gau, S. C. *Synthetic Metals*. 1982, 4, 187.

4 Sariciftci, N. S.; Braun, D.; Zhang, C.; Srdanov, V. I.; Heeger, A. J.; Stucky, G.; Wudl, F. *Appt. Phys. Lett.* **1993**, *62*, 585.

5 Tang, C. W. Appl. Phy. Lett.,**1986**, *48*, 183.

6 Halls, J. J. M.; Pichler, K.; Friend, R. H.; Moratti, S. C.; Holmes, A. B. *Appt. Phys. Lett.* **1996**, *68*, 3120.

7 Yu, G.; Gao, J.; Hummelen, J. C.; Wudl, F.; Heeger, A. J. *Science.* **1995**, *270*, 1789.

8 Yu, G.; Wang, J.; McElvain, J.; Heeger, A. J. *Adv. Mater.* **1998**, *10,* 1431.

9 He, Z.; Xiao, B.; Liu, F.; Wu, H.; Yang, Y.; Xiao, S.; Wang, C.; Russell, T. P.; Cao, Y. *Nature Photonics.* **2015,** *9,* 174.

10 Halls, J. J. M.; Walsh, C. A.; Greenham, N. C.; Marseglia, E. A.; Friend, R. H.; Moratti, S. C.; Holmes, A. B. *Nature.* **1995,** *376,* 498.

11 a) Gebeyehu, D.; Maennig, B.; Drechsel, J.; Leo, K.; Pfeiffer, M. *Solar Energy Materials & Solar Cells.* **2003,** *79,* 81. b) Spanggaard, H.; Krebs, F. C.; *Solar Energy Materials & Solar Cells.* **2004,** *83,* 81. c) Gunes, S.; Neugebauer, H.; Sariciftci, N. S. *Chem. Rev.* **2007,** *107,* 1324.

12 a) Hoppe, H.; Sariciftci, N. S. *J. Mater. Res.* 2004, 19, 1924. b) Yang, L.; Cappel, U. B.; Unger, E. L.; Karlsson, M.; Karlsson, K. M.; Gabrielsson, E.; Sun, L.;

Boschloo, G.; Hagfeldt, A.; Johansson, E. M. J. *Phys. Chem. Chem. Phys.* **2012,** *14*, 779. c) Jeon, N. J.; Lee, H. G.; Kim, Y. C.; Seo, J.; Noh, J. H.; Lee, J.; Seok, S. *J. Am. Chem. Soc.* **2014,** *136,* 7837.

13 (a) Rosokha S. V.; Kochi, J. K. *Acc. Chem. Res.*, **2008**, *41,* 641. (b) Huang, T. H.; Whang, W. T.; Shen, J. Y.; Wen, Y.S.; Lin, J. T.; Ke, T. H.; Chen, L. Y.; Wu, C. C. *Adv*. *Funct*. *Mater*. **2006**, *16*, 1449. (c) Yang, F.; Sun, K.; Cao, Z. J.; Li, Z. H.; Wong, M. S. *Synth*. *Met.* **2008**, *158*, 391. (d) Moss, K. C.; Bourdakos, K. N.; Bhalla, V.; Kamtekar, K. T.; Bryce, M. R.; Fox, M. A.; Vaughan, H. L.; Dias, F. B.; Monkman, A.P. *J. Org. Chem.* **2010**, *75*, 6771.

14 Huang, T. H.; Lin, J. T.; Chen, L. Y.; Lin, Y. T.; Wu, C. C. *Adv*. *Mater*. **2006**, *18*, 602.

15 Sasabe, H.; Seino, Y.; Kimura, M.; Kido, J. *Chem. Mater.* **2012**, *24*, 1404.

16 (a) Ertl, C. D.; Bolink, H. J.; Housecroft, C. E.; Constable, E. C.; Orti, E.; Junquera-Hernandez, J. M.; Neuburger, M.; Shavaleev, N. M.; Nazeeruddin, M. K.; Vonlanthen, D. *Eur. J. Org. Chem.* **2016**, 2037. (b) Kim, S-J.; Leroy, J.;Zuniga, C.; Zhang, Y.; Zhu, L.; Sears, J. S.; Barlow, S.; Bredas, J-L.; Marder, S. R.; Kippelen, B. *Organic. Electronics*. **2011**, *12*, 1314.

17 (a) Yang, X.; Zhou, G.; Wong, W. Y.; *Chem. Soc. Rev.* **2015**, *44*, 8484. (b) Gaj, M. P.; Fuentes-Hernandez, C.; Zhang, Y.; Marder, S. R.; Kippelen, B. *Org. Electron.* **2015**, *16*, 109. (c) Romain, M.; Tondelier, D.; Geffroy, B.; Shirinskaya, A.; Jeannin, O.; Rault-Berthelot, J.; Poriel, C. *Chem. Commun*. **2015**, *51*, 1313. (d) Jeon, S. O.; Earmme, T.; Jenekhe, S. A.; *J. Mater. Chem. C.* **2014,** *2*, 10129. (e) Jeon, Y. P.; Kim, K. S.; Lee, K. K.; Moon, I. K.; Choo, D.C.; Lee, J. Y.; Kim, T.W.; *J. Mater. Chem. C.* **2015,** *3*, 6192. (f) Li, Y.; Li, X.-L.; Cai, X.; Chen, D.;

Liu, X.; Xie, G.; Wang, Z.; Wu, Y.-C.; Lo, C.-C.; Lien, A.; Peng, J.; Cao, Y.; Sun. S.-J. *J. Mater. Chem. C.* **2015,** *3*, 6986. (g) Li, Y.; Wang, Z.; Li, X.; Xie, G.; Chen, D.; Wang, Y.-F.; Lo, C.-C.; Lien, A.; Peng, J.; Cao, Y.; Su, S.-J. *J. Mater. Chem.* **2015,** *27*, 1100. (h) Chan, C.-Y.; Wong, Y.-C.; Chan, M.-Y.; Cheung, S.-H.; So, S.-K.; Yam, V. W.-W. *Chem Mater.* **2014,** *26*, 6585. (i) Song, W.; Lee, I.; Lee, J. Y. *Adv. Mater.* **2015,** *27*, 4358.

18 Su, C.-C.; He, M.; Redfern, P. C.; Curtiss, L. A.; Shkrob, l. A.; Zhang, Z. C. *Energy. Environ. Sci*. **2017**, *10*, 900.

19 Schoenebeck, F.; Murphy, J. A.; Zhou, S.-z.; Uenoyama, Y.; Miclo, Y.; Tuttle, T. *J. Am. Chem. Soc.* **2007**, *129*, 13368.

20 Sullivan, S. O.; Doni, E.; Tuttle, T.; Murphy, J. A. *Angew. Chem. Int. Ed*. 2014, *53*, 474.

21 Merchant, R. R.; Edwards, J. T.; Qin, T.; Kruszyk, M. M.; Cheng Bi, ; Guanda Che,;Bao, D.-H.; Qiao, W.; Sun, L.; Collins, M. R.;Fadeyi, O. O.; Gallego, G. M.; Mousseau, J.J.; Nuhant, P.; Baran, P.S. *Science*. **2018,** *360*, 75.

22 Delaunay, J.; Mabon, G.;Badre, M. C.;Orliac, A.; Simonet, J. *Tetrahedron Letters*. **1992**, *33*, 2149.

23 Vasilieva, N. V.; Irtegova, I. G.; Loskutov, V. A.; Shundrin, L. *Mendeleev. Commun.* **2013**, *23*, 334.

24 Kaiser, E. T.; Eargle, D. H. *J. Am. Chem. Soc.* **1963**, *85*, 1821.

25 Fehnel, E. A. *J. Am. Chem. Soc.* **1949**, *71*, 1063.

26 Shanmugaraja, M. Ph.D. Thesis **2018**, School of chemistry, University of hyderabad.

27 Shalev, H.; Evans, D, H. *J. Am. Chem. Soc.* **1989**, *111*, 2667.

28 Kebarle, P.; Chowdhury, S. *Chem. Rev*. **1987**, *87*, 513.

Chapter-4

Electricity Harvesting Cell based on Electron Transfer Reaction of *p*-Chloranil with DMSO.

4.1 Introduction

4.1.1 Application of Dimethyl Sulfoxide as Reagent in Organic Synthesis:-

DMSO is widely used as solvent in organic chemistry. However, it can also participate in several reactions as a reagent. In this chapter, we have used DMSO as a donor in the construction of electrochemical cells as it was reported that DMSO gives paramagnetic intermediates on reaction with *p*-chloranil. Accordingly, a brief review on the reaction of DMSO with different organic substrates will be helpful.

4.1.2 DMSO as a –Me- source

Alkylation of isoquinoline *N*-oxides using DMSO as a methyl source in the presence of palladium catalyzed compounds was reported (Scheme 1).[1]

Scheme 1

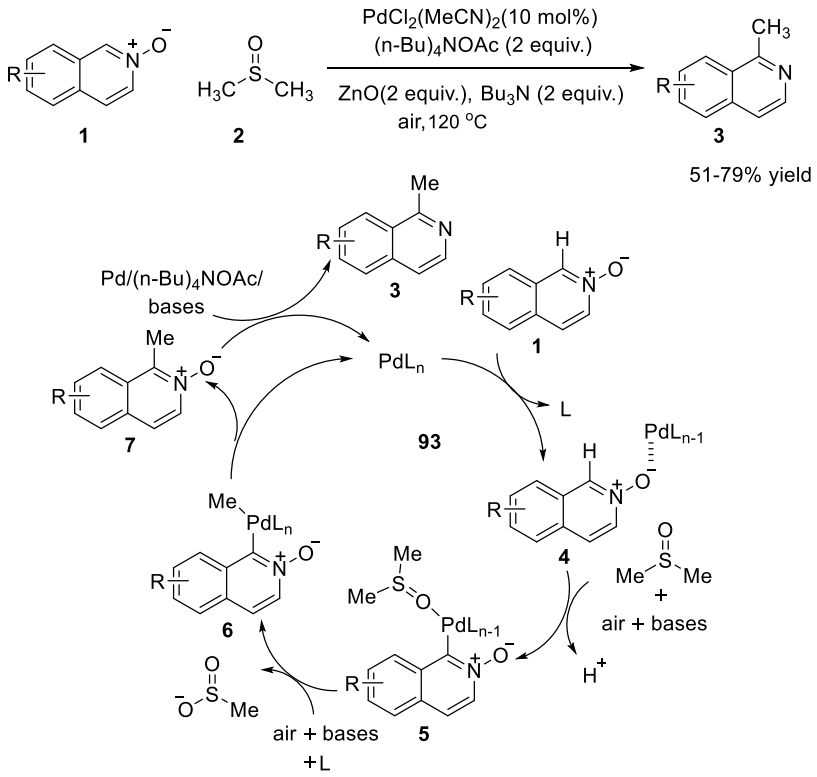

A simple method for iron catalyzed methylation of aromatic nitro compounds with DMSO in the presence of formic acid and triethylamine was reported (Scheme 2).[2]

Scheme 2

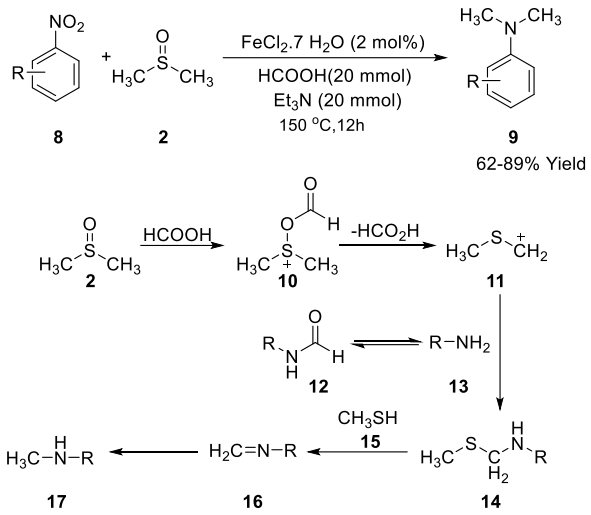

4.1.3 DMSO as a –CH_2- source

Oxidative C-S bond cleavage by the reaction of DMSO with various acetylarenes and heteroarenes selectively transformed gave the corresponding β-amino ketones, followed by C-C and C-N bond formation.[3,4] In this reaction, DMSO acts as one carbon bridge (Scheme 3).

Scheme 3

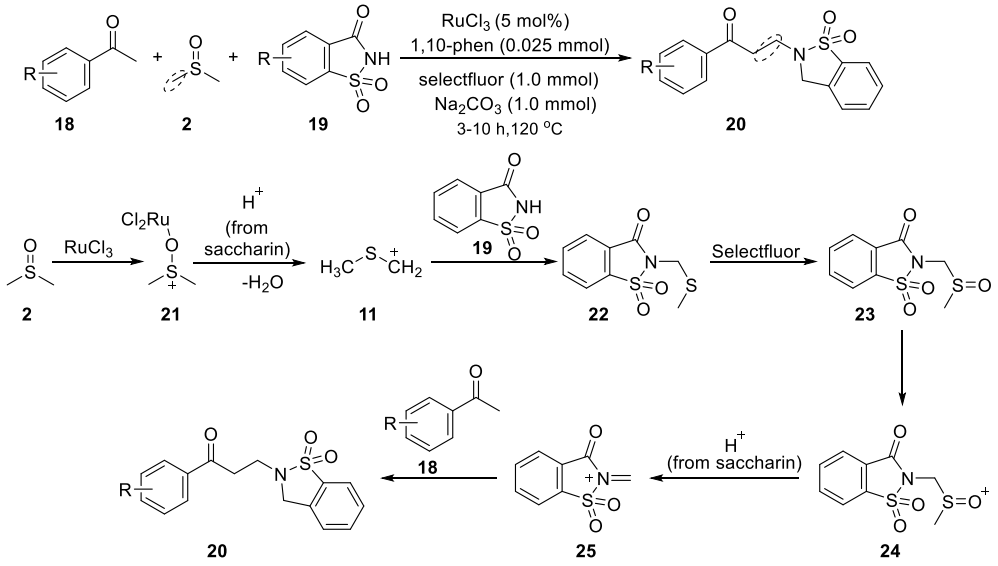

Oxazolidines are obtained by the reaction of certain 1,2-amino alcohols with phosphorus pentoxide in DMSO solvent (Scheme 4).[5]

Scheme 4

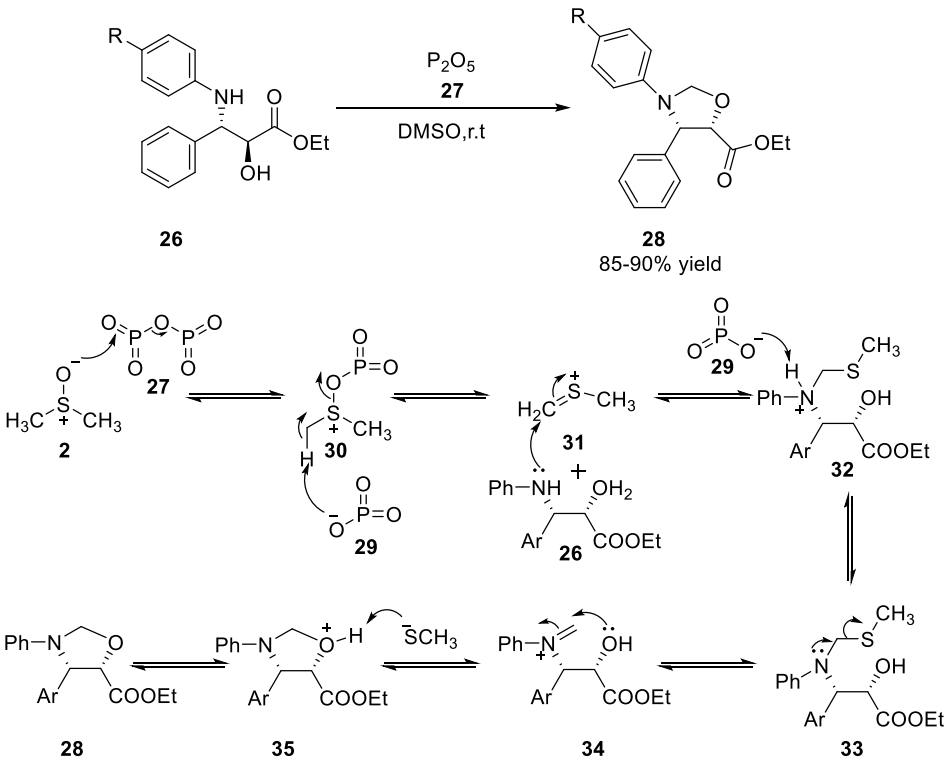

Condensation of benzamides gives methylene bisamides using ammonium persulfate in DMSO solvent (Scheme 5).[6]

Scheme 5

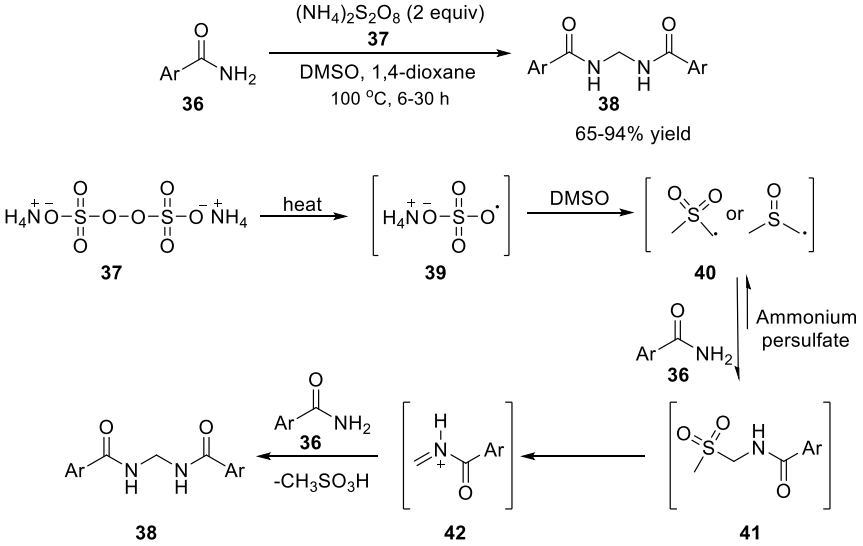

Quinazolines and dihydroquinazolines were prepared from amidines on treatment using $Cu(OTf)_2$ catalyst and excess Selectfluor in DMSO solvent (Scheme 6).[7]

Scheme 6

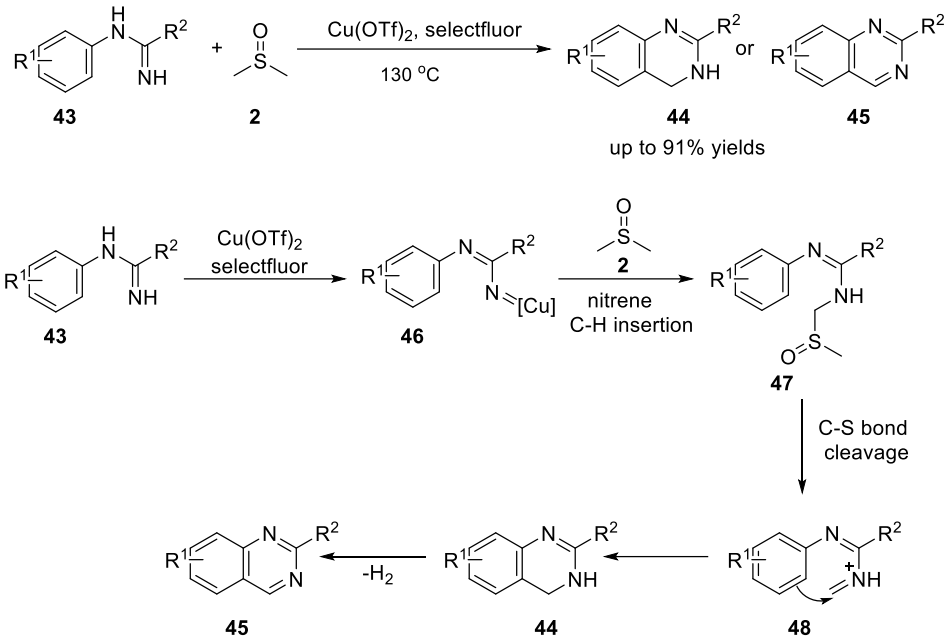

4.1.4 DMSO based annulation or aromatization source:-

Pyridine derivatives were prepared through ammonium iodide promoted cyclization reaction using methyl ketone and ammonium acetate in DMSO solvent (Scheme 7).[8]

Scheme 7

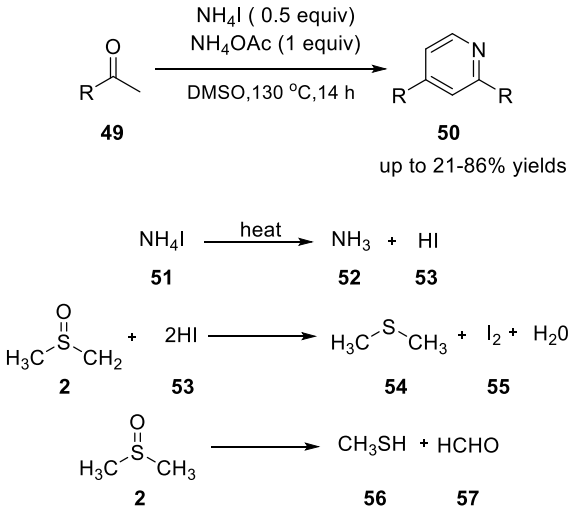

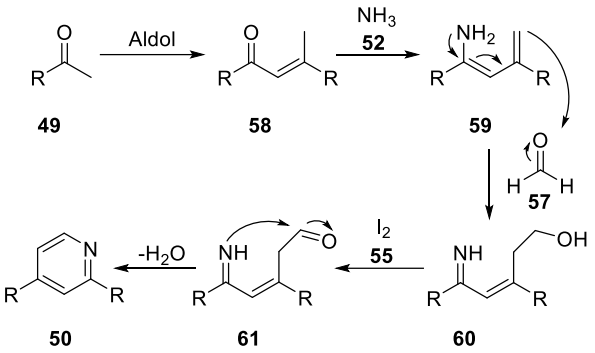

Synthesis of 1,3,5-triarylbenzenes from chalcones using sodium tert-butoxide in DMSO solvent was reported (Scheme 8).[9]

Scheme 8:

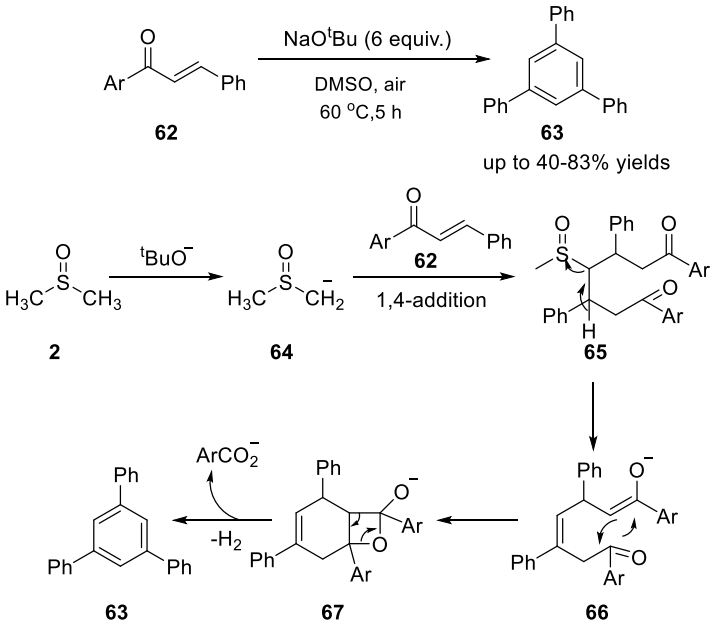

4.1.5 DMSO as a –CHO- source:-

Ammonium acetate promoted formylation of indoles using DMSO as solvent was reported (Scheme 9).[10]

Scheme 9

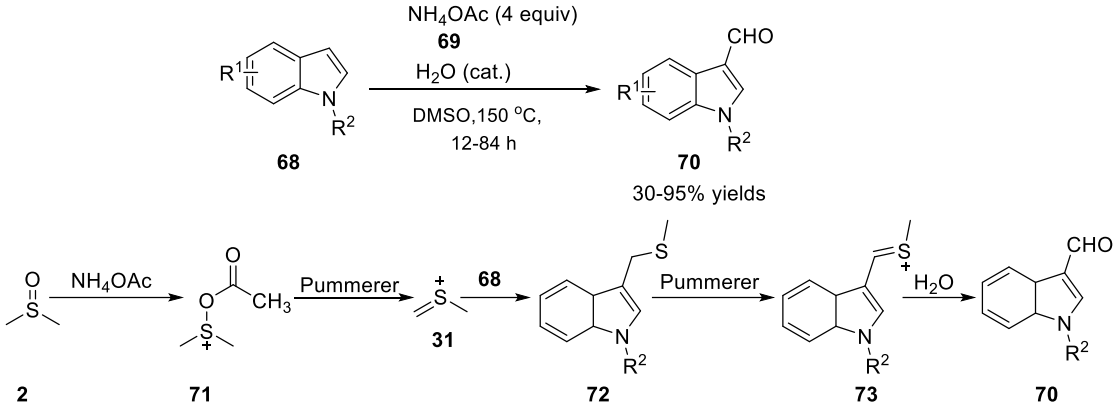

Copper catalyzed formylation reaction of 1H-pyrroles gave the corresponding α-formylated substituted pyrrole derivatives in moderate to good yields (Scheme 10).[11]

Scheme 10

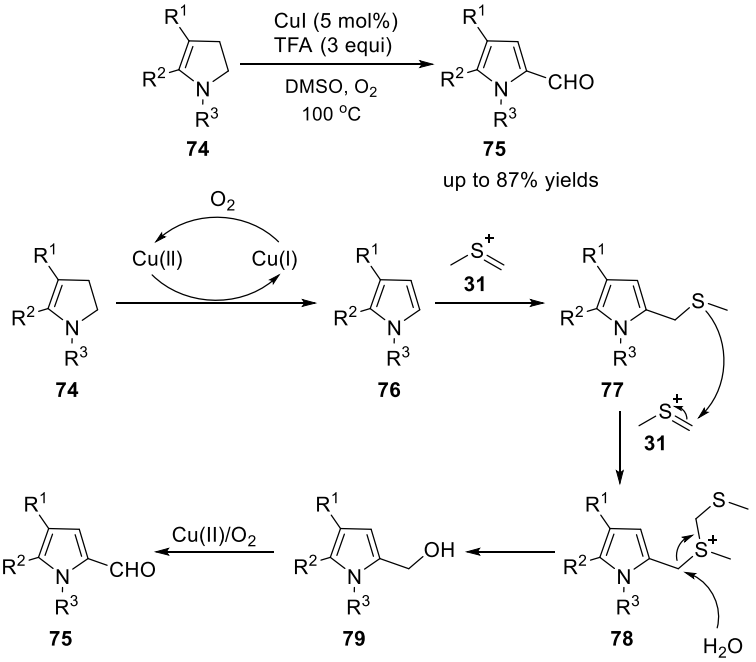

A Cu-catalyzed method for formylation of imidazo[1,2-a]pyridines with DMSO by using O_2 as the oxidant was reported (Scheme 11).[12]

Scheme 11

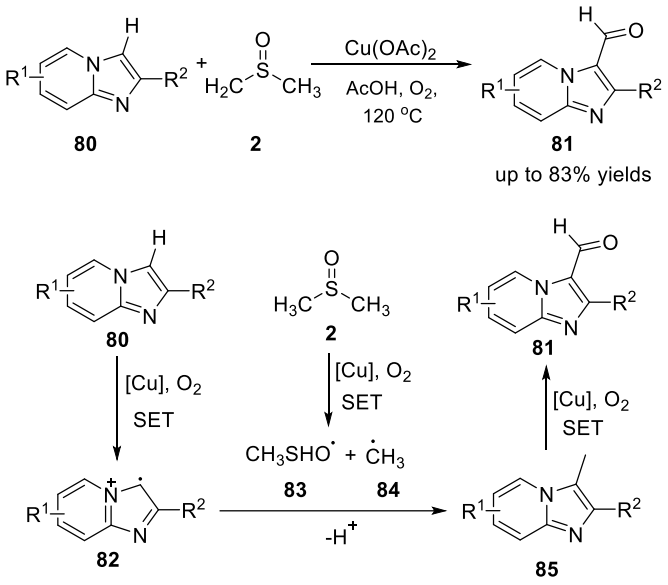

4.1.6 DMSO as a –SMe- source:-

Methylthiolation of aryl C-H bonds in the presence of Cu(II)-mediated under oxidative conditions using DMSO as the methylthio source was reported (Scheme 12).[13]

Scheme 12

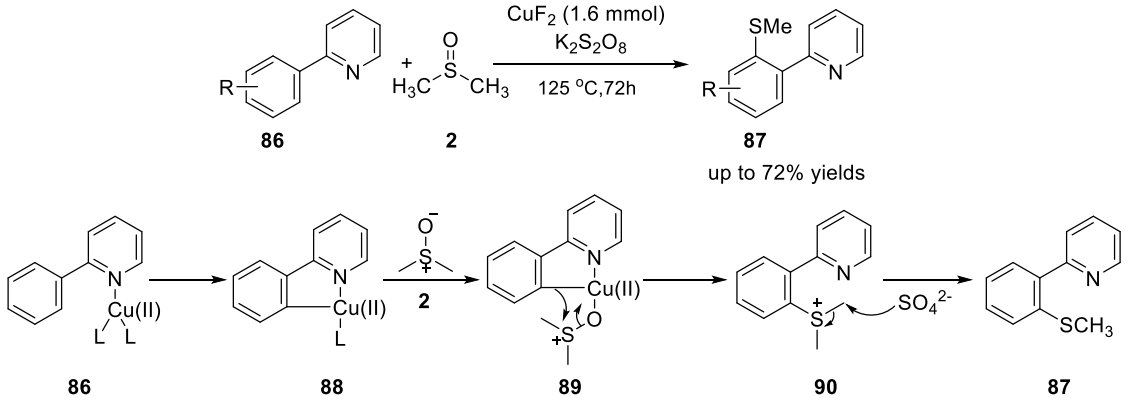

Highly regioselective para-methylthiolation of arylamines by using DMSO as the methylthio source was reported (Scheme 13).[14]

Scheme 13

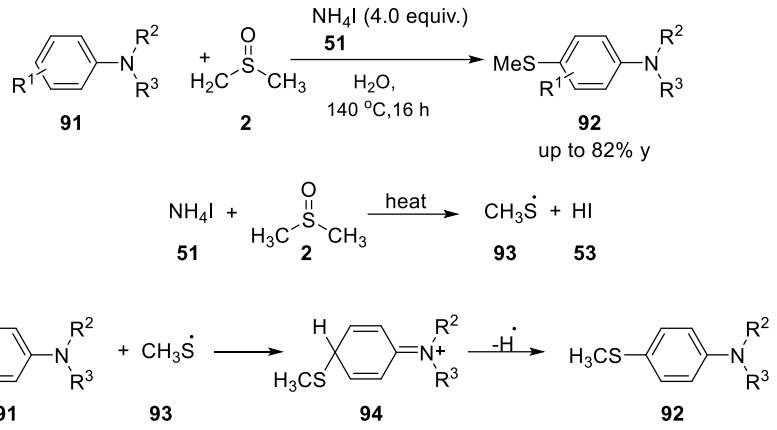

Thiomethylation products were obtained by the reaction of three-component coupling of *o*-(trimethylsilyl) phenyl triflate, DMSO and α-bromo carbonyl compounds on reaction with potassium fluoride (Scheme 14).[15]

Scheme 14

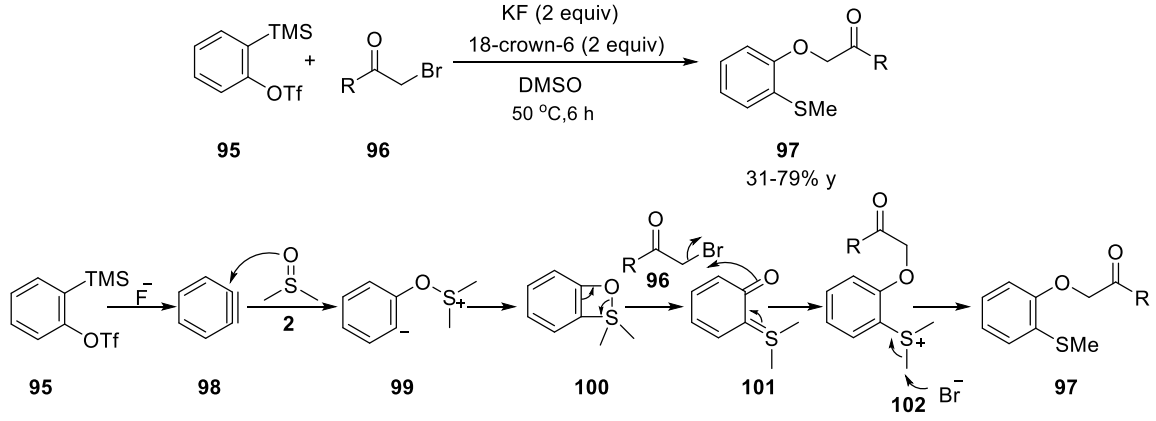

4.1.7 DMSO as –SO_2Me source:

Methyl sulfone was prepared by the reaction of halobenzenes using DMSO in the presence of potassium tert-butoxide under Cu_2O catalyzed aerobic oxidative methyl sulfonylation (Scheme 15).[16]

Scheme 15

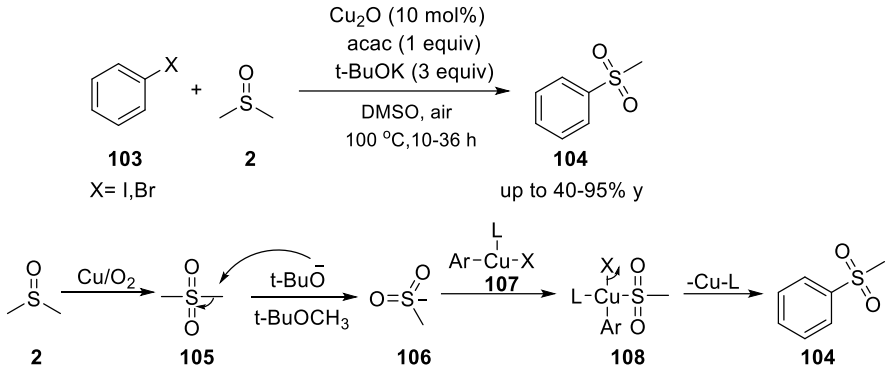

Conversion of styrenes into β-keto methyl sulfones by reaction with catalytic CuBr and diethyl phosphite in DMSO under oxygen atmosphere was reported (Scheme 16).[17]

Scheme 16

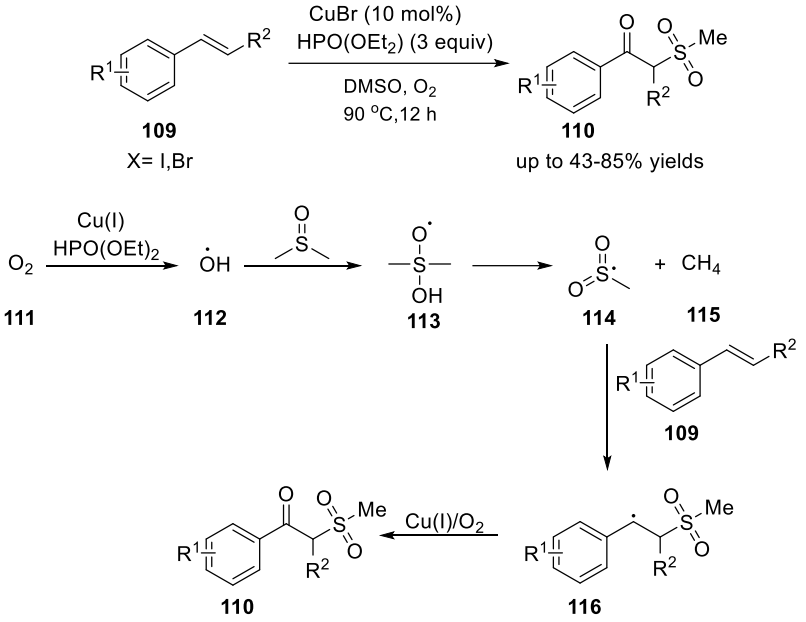

4.1.8 DMSO based cyanation (-CN):-

Palladium catalyzed 3-cyanation of indoles using DMSO as source of the cyano group was reported (Scheme 17).[18]

Scheme 17

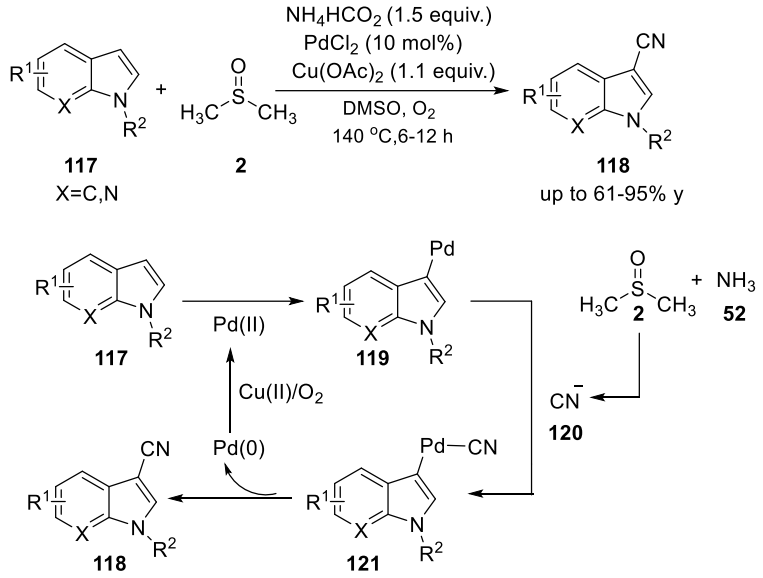

4.1.9 DMSO as a –CH_2SMe source

Synthesis of *N*-methylthiomethyl triazoles from alkynes, diphenyl phosphoryl azide (DPPA) and DMSO under copper catalysis was reported (Scheme 18).[19]

Scheme 18

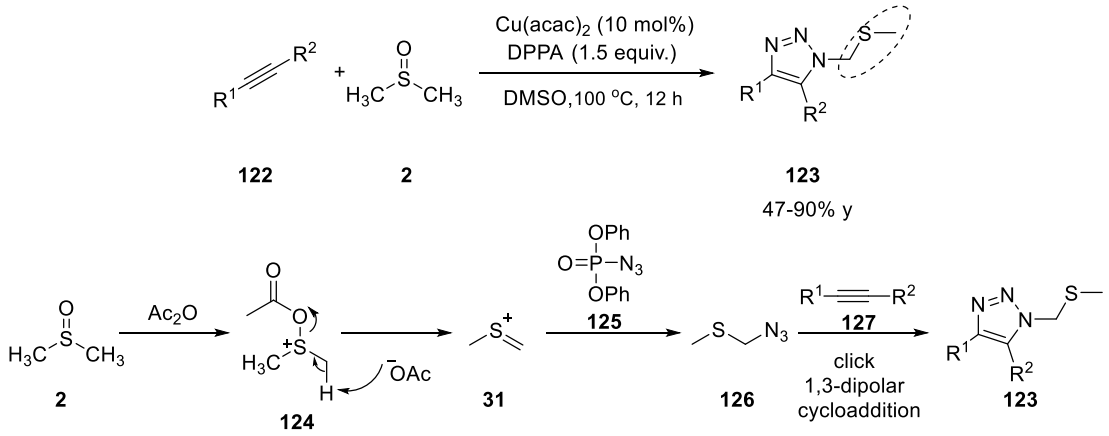

4.1.9.1 Electron Transfer Reactions using DMSO

The DMSO radical cations was obtained from methyl carboxymethylsulfoxide by electron impact induced fragmentation (Scheme 19).[20]

Scheme 19

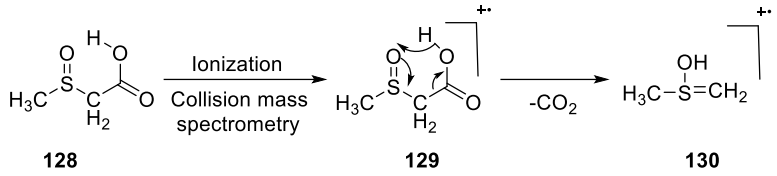

It was reported that the *p*-chloranil reacted with DMSO in chloroform to give the corresponding charge transfer complex followed by the formation of the corresponding radical ions. (Scheme 20).[21]

Scheme 20

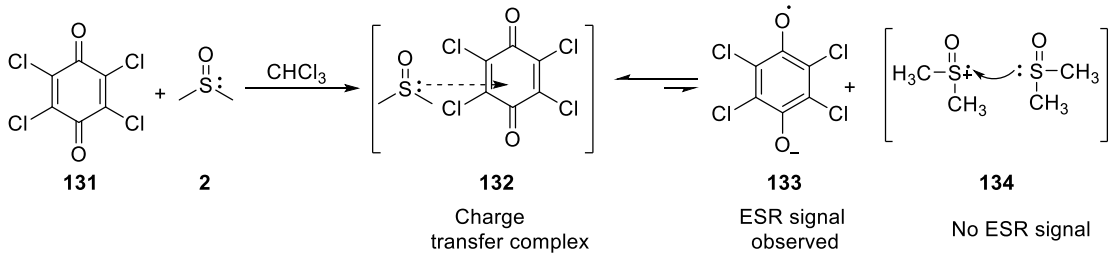

Since DMSO is a polar solvent like PC, and also functions as an electron donor, we have undertaken efforts to construct the electricity harvesting electrochemical cell using DMSO as solvent. We have also constructed the cell using DMSO as a donor with PC as a solvent. The results are described in the next section.

4.2 Results and Discussion

4.2.1 Organic Electrochemical cells using DMSO solvent

We have constructed electrochemical cells based on ground state electron transfer reactions using various aminedonors and *p*-chloranil acceptor under different configurations using PC as solvent, sulfones as electron transporter and TiO_2 as solid support.[22] In continuation of these studies, we have decided to investigate the use of DMSO in the construction of the electrochemical cell.

We have selected the highly electron deficient *p*-chloranil **131** (Cl_4BQ) as acceptor. and the benzoquinone **(135)** and dimethylsulfone **136** as electron transporters for our studies. Also, we have selected the donors *N*,*N*-diethylaniline ($PhNEt_2$) **137**, *N*,*N'*-tetramethyl-1,4-phenylenediamine(TMPDA) **138**, triphenylamine (TPA) **139**, 1,4-diazabicyclo[2.2.2]octane (DABCO) **140**, *N*, *N*-diisopropylethylamine (DIPEA) **141** and *N*,*N*-diisopropylbenzamide (DiPrBA) **142** along with DMSO or DMSO **143** and PC mixture for the construction of the organic electrochemical cell.

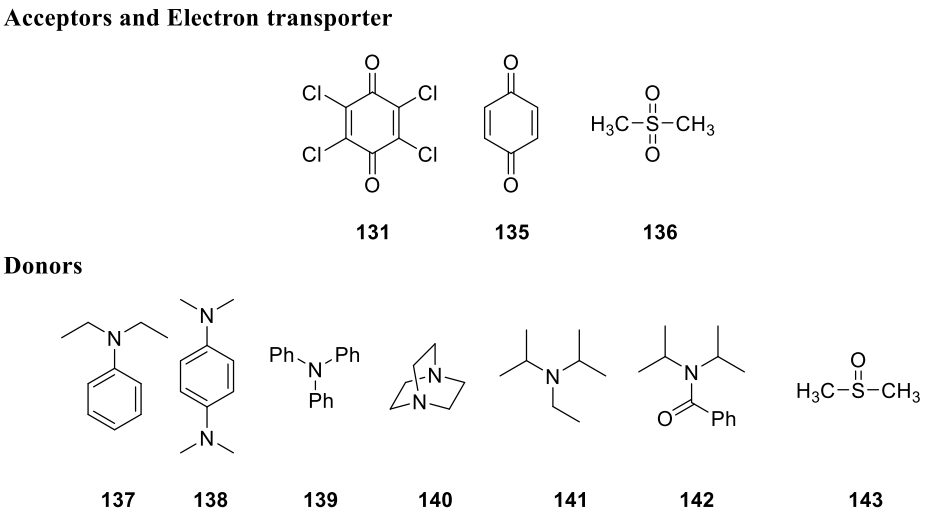

Figure 1: Eelectron acceptors and donors for use in electrochemical cells.

The results are discussed in the next sections.

4.2.2 Construction of Electrochemical cells in 4 layer configuration using DMSO as solvent

We have first constructed the 4 layer cell using Cl_4BQ in two layers and the amine or amide donors in middle layers using DMSO as solvent (Figure 2).

Figure 2: Four layers cell with Cl_4BQ in two layers without using TiO_2

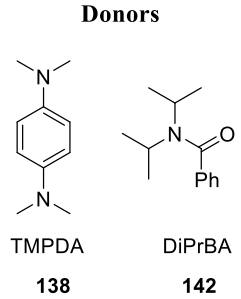

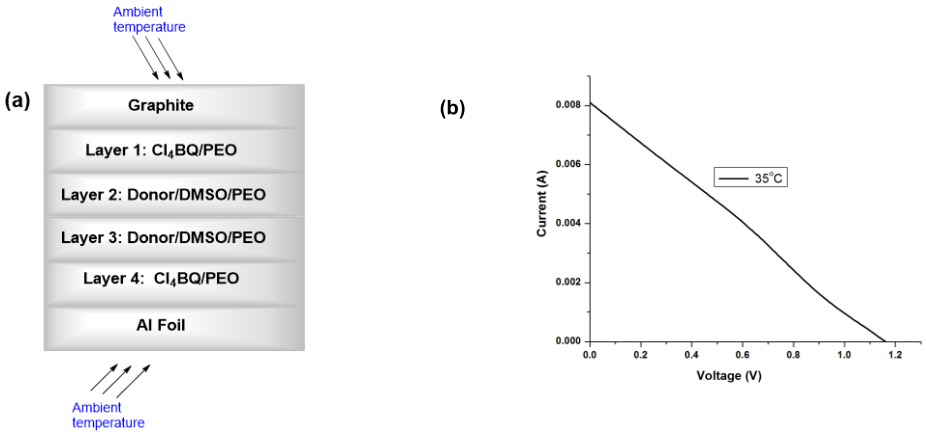

	1 h after packing		48 h after packing
Donor	**Pmax/mW/FF(28 °C)**	**Pmax/mW/FF(35 °C)**	**Pmax/mW/FF(35 °C)**
TMPDA	7.033/0.236	10.72/0.25	2.43/0.258
DiPrBA	1.47/0.219	6.333/0.221	1.57/0.204

Figure 2 (continued)

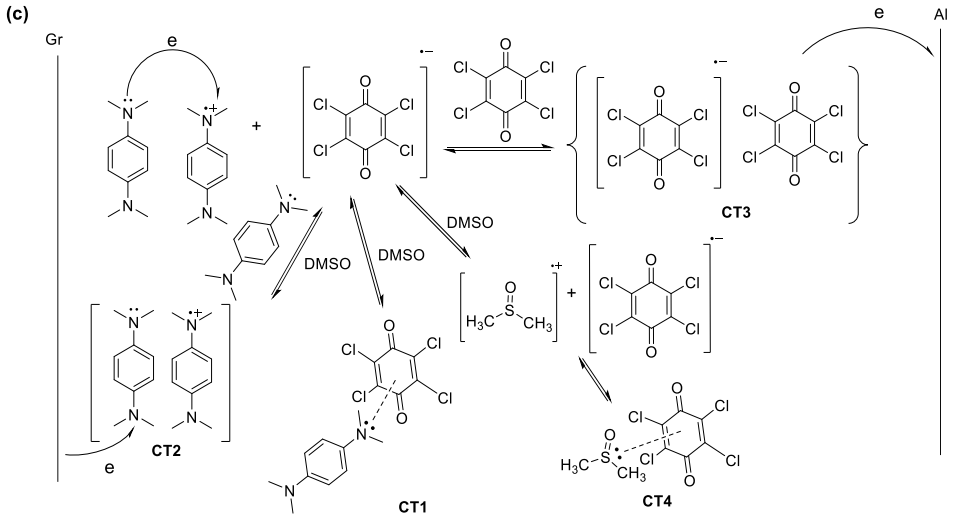

Figure 2. (a) Schematic diagram of multi-layer with Cl_4BQ/Donor/DMSO/PEO configuration. (b) Representative IV for the cell (Table ES 1, entry 2, TMPDA donor). (c) Tentative mechanism for electron transport to the electrodes via D/D.+ and A-/A exchange reactions.

We have recorded IV-data at 1 h and 48 h after packing as outlined in Figure 2. In this configuration, the initial power output was high Pmax 10.72 mW at 1h after packing, but it decreased very much to Pmax 2.43 mW at 48h.

We have then constructed the 4 layer cell using Cl_4BQ in two layers along with TiO_2 and amine or amide donors in middle layers using DMSO as solvent (Figure 3).

Figure 3: Four layers cell with Cl_4BQ and TiO_2 in two layers

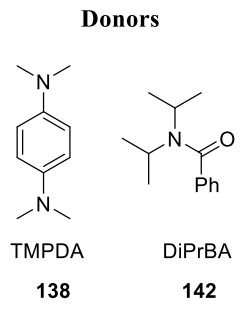

Figure 3 (continued)

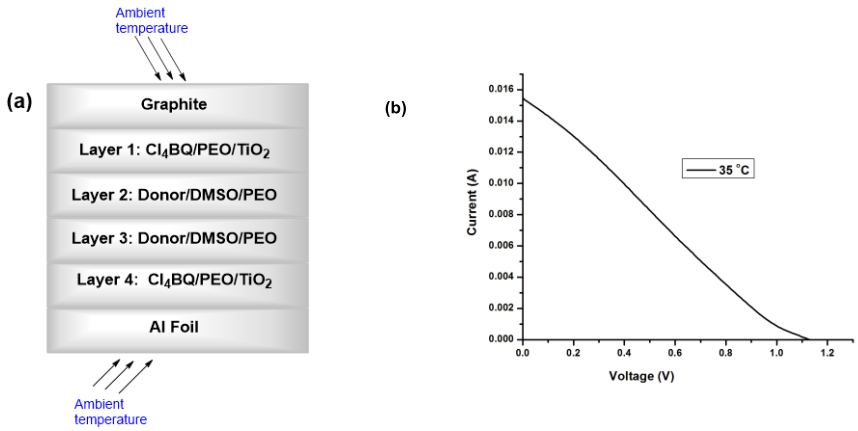

1 h after packing			**48 h after packing**
Donor	**Pmax/mW/FF(28 °C)**	**Pmax/mW/FF(35 °C)**	**Pmax/mW/FF(35 °C)**
TMPDA	2.138/0.221	4.385/0.294	2.85/0.338
DiPrBA	4.905/0.269	7.971/0.287	4.139/0.237

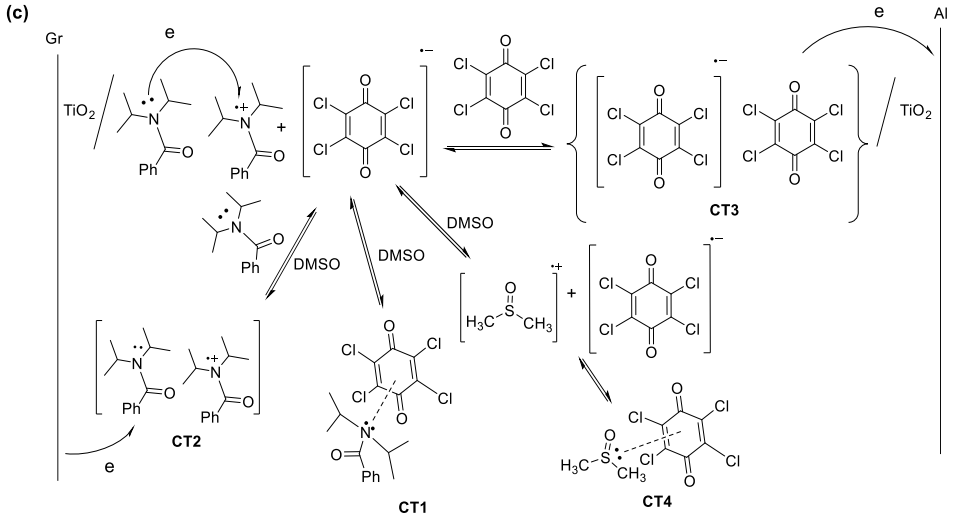

Figure 3. (a) Schematic diagram of multi-layer with Cl_4BQ/Donor/DMSO/TiO_2/PEO configuration. (b) Representative IV for the cell (Table ES 1, entry 3, DiPrBA donor). (c) Tentative mechanism for electron transport to the electrodes via D/D.+ and A-/A exchange reactions.

In this configuration, the power output decreased at 1h compared to previous configuration (Figure 2) but the Pmax values at 48h was higher. We have then constructed the 4 layers cell using TiO_2 in edge layers with Cl_4BQ and donor in middle layers using DMSO as solvent.

Figure 4: Four layer cell with Cl_4BQ in two layers using *N,N*-dialkyl benzamides

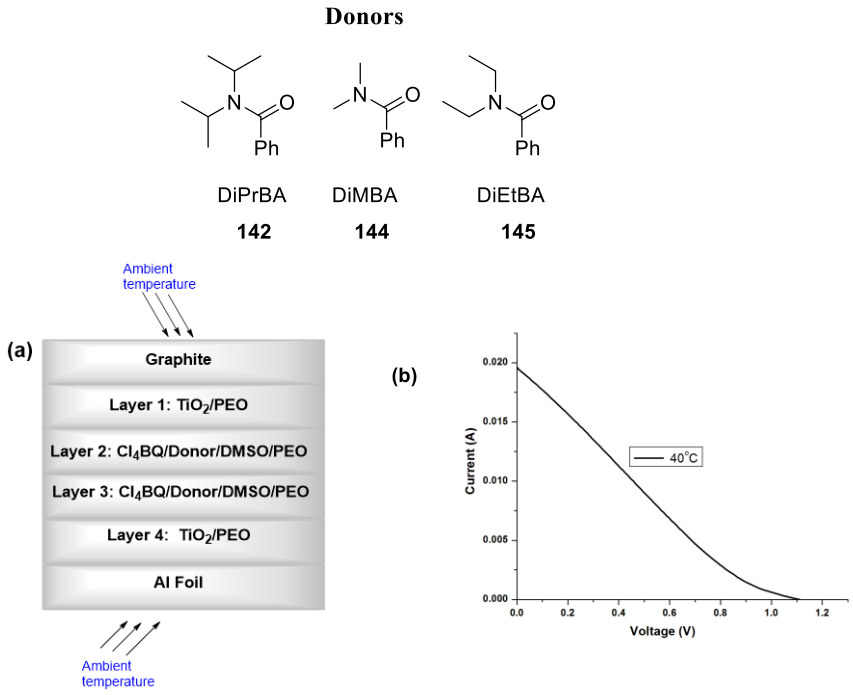

1 h after packing **48 h after packing**

Donor	**Pmax/mW/FF(28 °C)**	**Pmax/mW/FF(35 °C)**	**Pmax/mW/FF(40 °C)**	**Pmax/mW/FF(40 °C)**
DiMBA	2.762/0.164	3.75/0.178	4.363/0.16	2.954/0.126
DiEtBA	5.118/0.204	5.411/0.202	6.292/0.202	2.296/0.168
DiPrBA	4.42/0.185	6.24/0.213	6.666/0.217	4.568/0.21

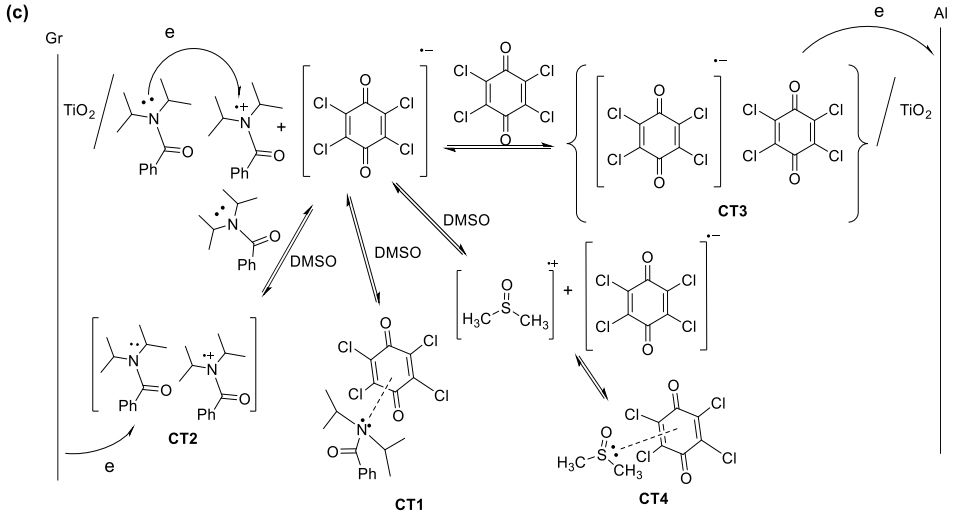

Figure 4. (a) Schematic diagram of multi-layer with Cl_4BQ/DMSO/Donor/TiO_2/PEO configuration. (b) Representative IV for the cell (Table ES 1, entry 7, DiPrBA donor). (c) Tentative mechanism for electron transport to the electrodes via D/D.+ and A-/A exchange reactions.

In this configuration, among the substituents methyl, ethyl and isopropyl in the benzamides, the power output was high in diisopropyl benzamide. This is in accordance with higher steric hinderance to form CT complex with Cl_4BQ and hence the radical ions are expected to form to more extent (Figure 4).

We have then constructed the 6 layers cell using Cl_4BQ in four layers and donor along with Cl_4BQ in layer 2 and TiO_2 in the edge layers 1 and 6 (Figure 5).

Figure 5: Six layer cell with Cl_4BQ in four layers and donor in layer 2

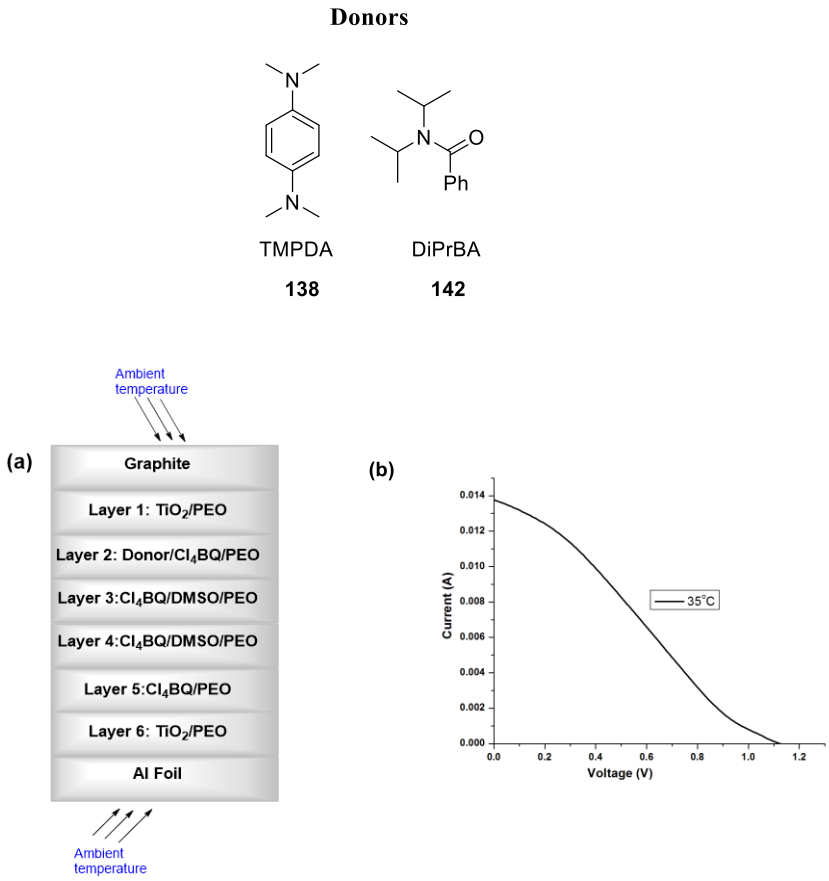

1 h after packing			48 h after packing
Donor	**Pmax/mW/FF(28 °C)**	**Pmax/mW/FF(35 °C)**	**Pmax/mW/FF(35 °C)**
TMPDA	2.437/0.229	7.236/0.306	4.13/0.267
DiPrBA	3.976/0.198	6.9/0.234	3.514/0.219

Figure 5 (continued)

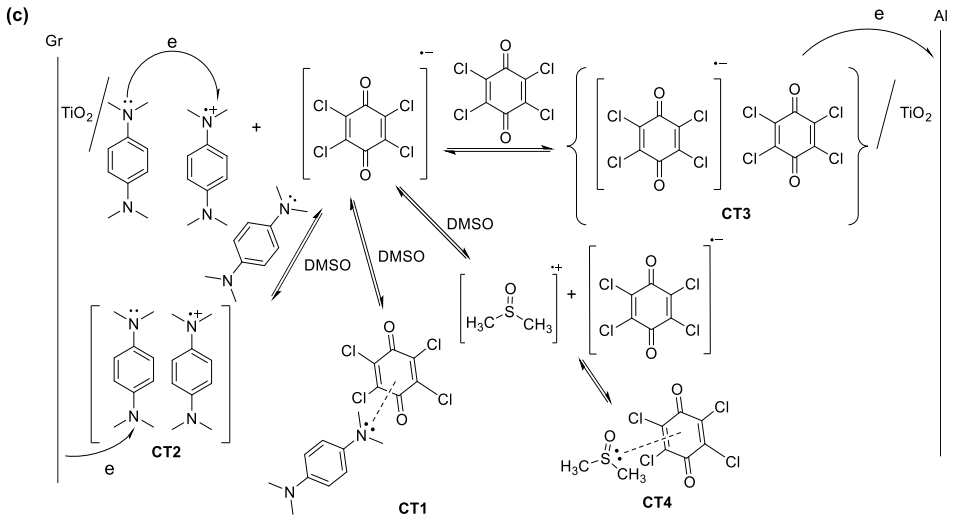

Figure 5. (a) Schematic diagram of multi-layer with Cl_4BQ/DMSO/Donor/TiO_2/PEO configuration. (b) Representative IV for the cell (Table ES 2, entry 11, TMPDA donor). (c) Tentative mechanism for electron transport to the electrodes via D/D.+ and A-/A exchange reactions.

In this configuration, the amine or amide donor in layer 2 is closer to Gr and the power output with TMPDA donor gave better results at 1h but the power decreased after 48h. We have then constructed the 6 layers cell using Cl_4BQ in one layer,TiO_2 in edge layers and the donor in layer 2.

Figure 6: Six layers cell with Cl_4BQ in layer 5 and Donor in layer 2 and DMSO in middle layers

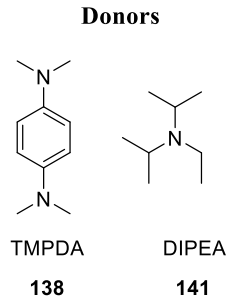

Figure 6 (continued)

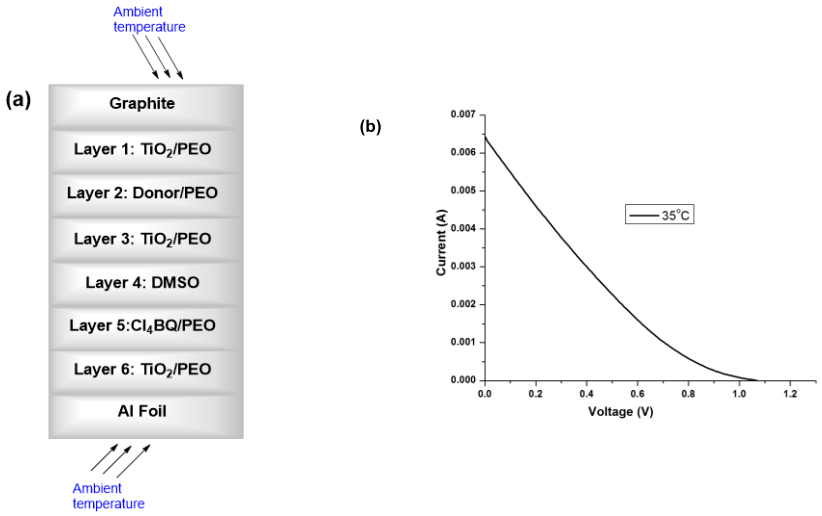

1 h after packing			48 h after packing
Donor	**Pmax/mW/FF(28 °C)**	**Pmax/mW/FF(35 °C)**	**Pmax/mW/FF(35 °C)**
DIPEA,	1.384/0.14	2.502/0.203	1.199/0.174
TMPDA	1.239/0.248	2.267/0.278	1.343/0.193

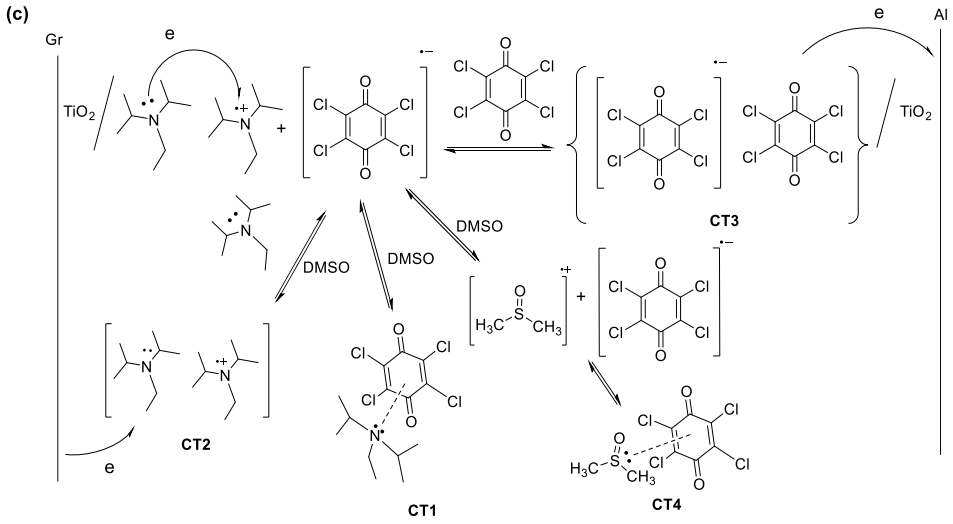

Figure 6. (a) Schematic diagram of multi-layer with Cl_4BQ/DMSO/Donor/TiO_2/PEO configuration. (b) Representative IV for the cell (Table ES 2, entry 13, DIPEA donor). (c) Tentative mechanism for electron transport to the electrodes via D/D.+ and A-/A exchange reactions.

In this configuration, the power output was very low. Presumably, there is very little interaction between the Cl_4BQ and the donor. We have then constructed the 6 layers cell using Cl_4BQ in four layers TiO_2 in edge layers amine or amide donor in middle layers.

Figure 7: Six layer cell with Cl_4BQ in four layers and donor in middle DMSO layers

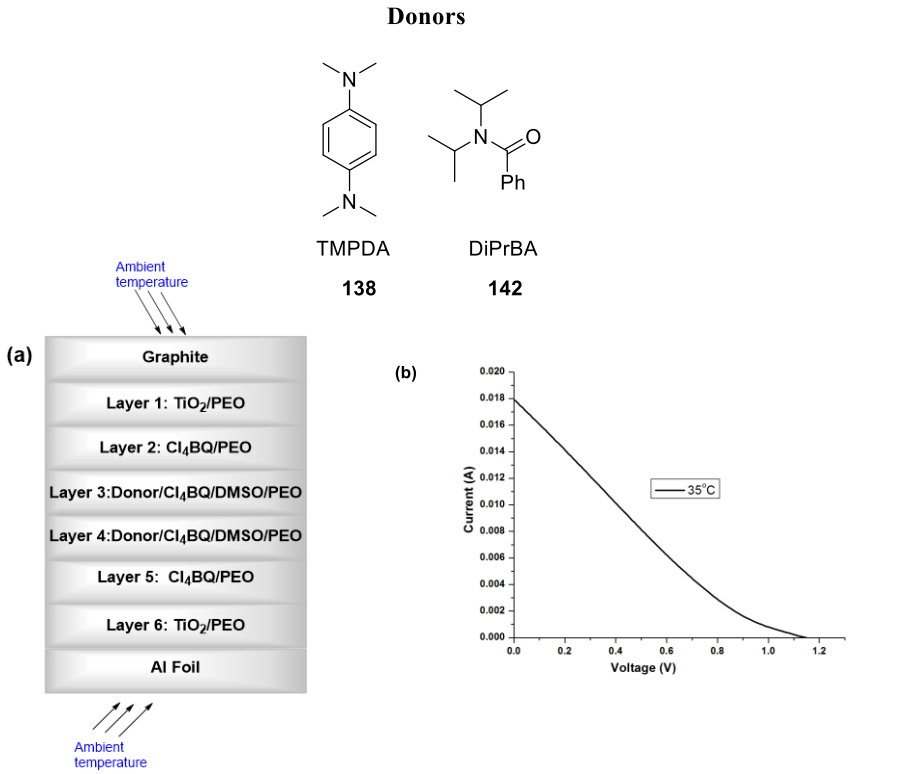

1 h after packing			48 h after packing
Donor	**Pmax/mW/FF(28 °C)**	**Pmax/mW/FF(35 °C)**	**Pmax/mW/FF(35 °C)**
TMPDA,	2.443/0.26	4.515/0.301	1.501/0.206
DiPrBA	4.618/0.21	6.77/0.231	4.112/0.2

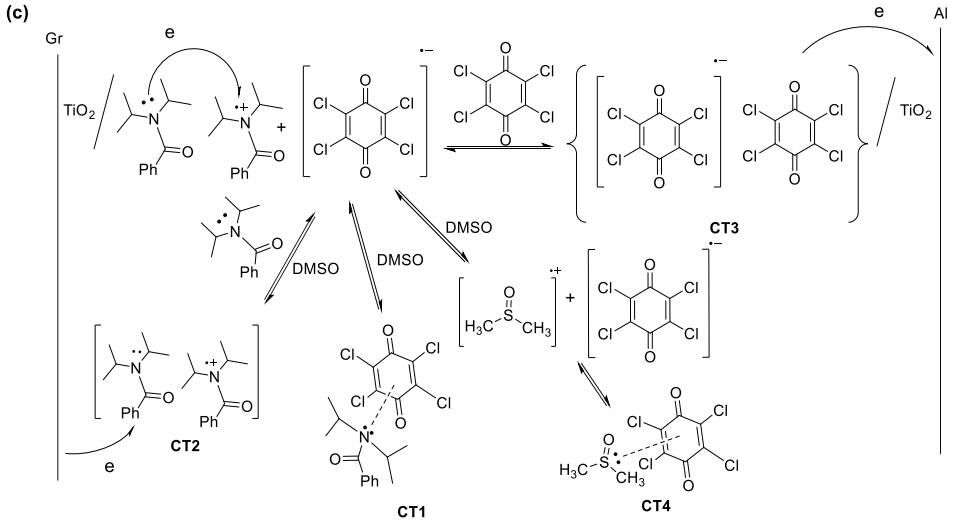

Figure 7. (a) Schematic diagram of multi-layer with Cl_4BQ/DMSO/Donor/TiO_2/PEO configuration. (b) Representative IV for the cell (Table ES 3, entry 15, DiPrBA donor). (c) Tentative mechanism for electron transport to the electrodes via D/D.+ and A-/A exchange reactions.

In this configuration (Figure 7), the power output decreased at 1h and 48h compared to previous configuration (Figure 5). We have then constructed the 6 layers cell using Cl_4BQ in four layers, DiPrBA in layer 4 and another donor in layer 3.

Figure 8: Six layer cell with Cl_4BQ in four layers and two different donors in middle layers

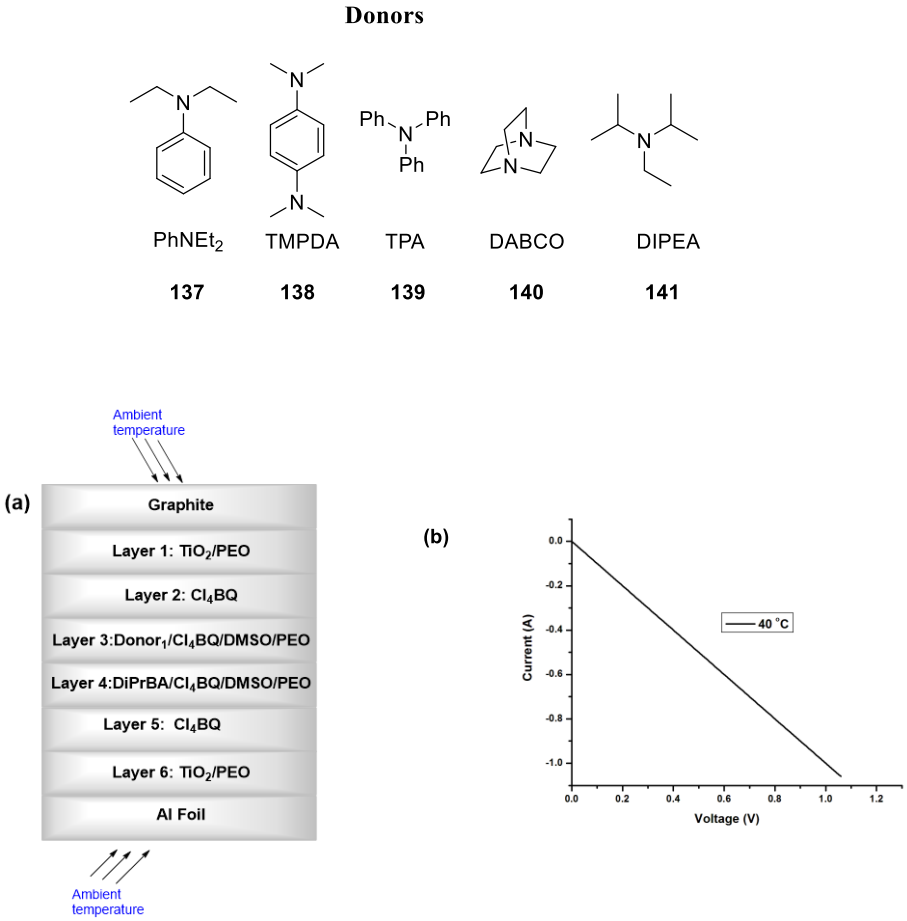

1 h after packing			48 h after packing
Donor	**Pmax/mW/FF(28 °C)**	**Pmax/mW/FF(35 °C)**	**Pmax/mW/FF(40 °C)**	**Pmax/mW/FF(40 °C)**
TMPDA	4.172/0.282	5.758/0.307	6.37/0.323	8.603/0.399
TPA	1.457/0.261	2.036/0.295	2.535/0.34	2.342/0.291
DABCO	8.026/0.208	8.544/0.259	9.699/0.244	3.664/0.25
DIPEA	6.758/0.218	7.554/0.253	7.933/0.261	3.084/0.228
PhNEt2	5.357/0.243	6.403/0.229	7.144/0.248	6.304/0.274

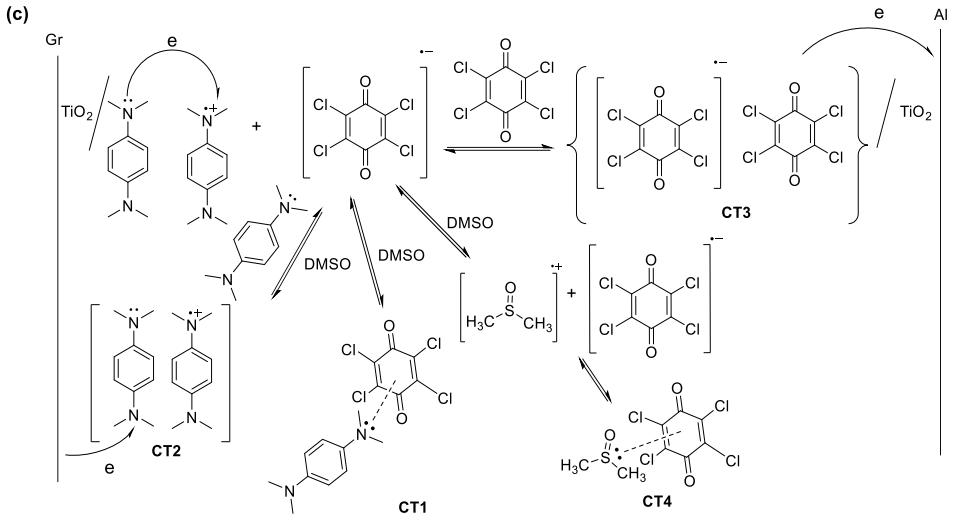

Figure 8. (a) Schematic diagram of multi-layer with Cl_4BQ/DMSO/Donor/TiO_2/PEO, Cl_4BQ/DMSO/DiPrBA/TiO_2/PEO configuration. (b) Representative IV for the cell (Table ES 3, entry 21, TMPDA donor). (c) Tentative mechanism for electron transport to the electrodes via D/D.+ and A-/A exchange reactions.

Surprisingly, in this configuration (Figure 8), the donor DABCO gave better results at 28 ºC, 35 ºC, and 40 ºC (Figure 8) at 1h. The Pmax and FF values for DABCO were high (9.699 mW/0.244) at 40 ºC but decreased to Pmax 3.664 mW, with FF 0.25 after 48h. The Pmax and FF values for TMPDA were 6.37 mW/0.323 at 40 ºC at 1h but increased to Pmax 8.603 mW, with FF 0.399 after 48h. We have then constructed the 6 layers cell using Cl_4BQ in four layers amide donor in middle layers using DMSO as solvent (Figure 9).

Figure 9: Six layer cell with Cl_4BQ in four layers with amide donors in middle layer

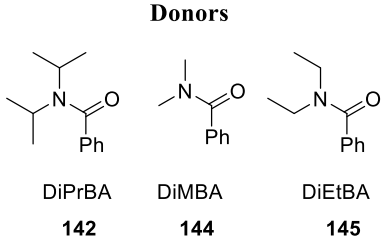

Figure 9 (continued)

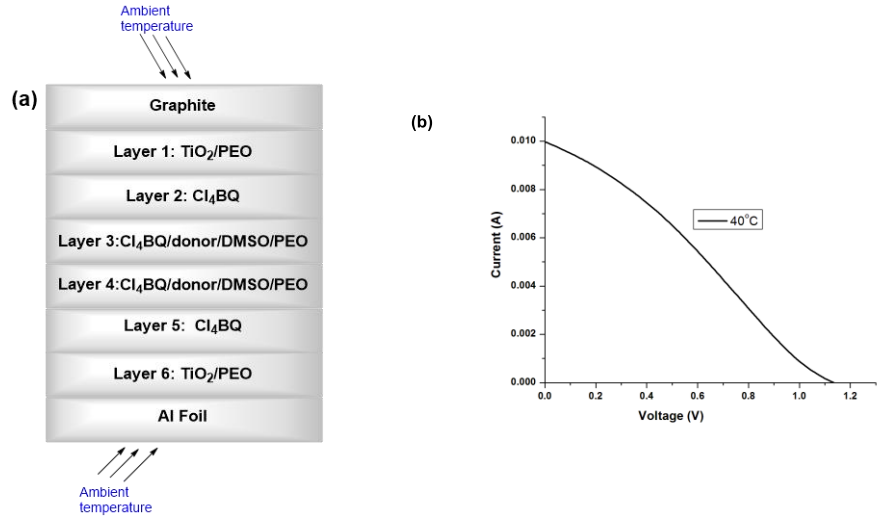

	1 h after packing		**48 h after packing**	
Donor	**Pmax/mW/FF(28 °C)**	**Pmax/mW/FF(35 °C)**	**Pmax/mW/FF(40 °C)**	**Pmax/mW/FF(40 °C)**
DiMBA	1.641/0.192	2.529/0.219	2.896/0.242	1.712/0.199
DiEtBA	3.045/0.208	4.018/0.234	4.60/0.253	2.631/0.265
DiPrBA	3.768/0.241	4.754/0.283	5.009/0.304	3.292/0.29

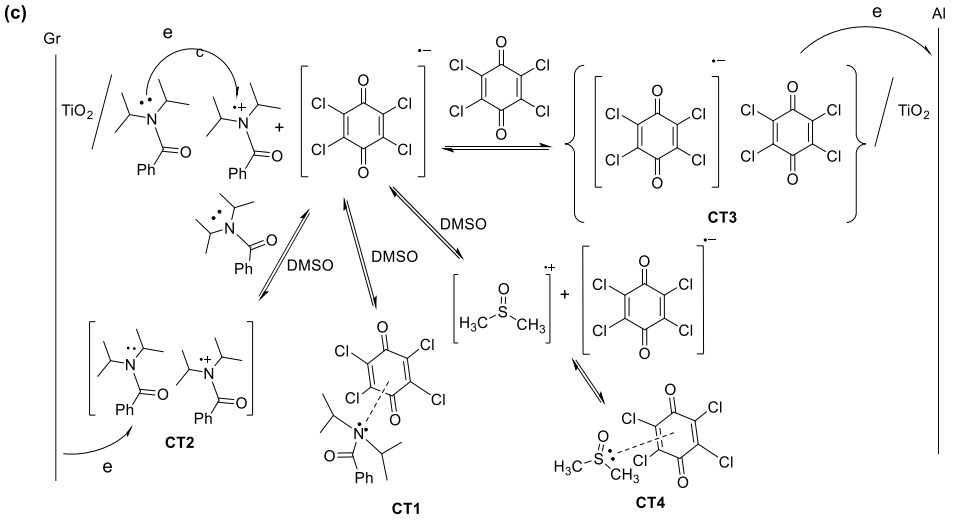

Figure 9. (a) Schematic diagram of multi-layer with Cl_4BQ/DMSO/Donor/TiO_2/PEO configuration. (b) Representative IV for the cell (Table ES 3, entry 23, DiPrBA donor). (c) Tentative mechanism for electron transport to the electrodes via D/D.+ and A-/A exchange reactions.

Interestingly, this 6 layers configuration (Figure 9) gave less power compared to previous 4 layers configuration (Figure 4).

4.2.3 Construction of Electrochemical cell using PC as solvent and DMSO as donor

The dielectric constant (Ɛ) of PC (Ɛ= 65.5)[23] is higher than that of DMSO (Ɛ= 48.4)[24]. The DMSO was reported to react to transfer electron to *p*-chloranil. Accordingly, we have constructed cells using PC as solvent and DMSO as donor. We have constructed the 6 layers cell using Cl_4BQ in four layers TiO_2 in PC layers and TiO_2 in edge layers and DMSO as donor (Figure 10).

Figure 10: Six layer cell with Cl_4BQ in four layers and DMSO donor with PC solvent in middle layers

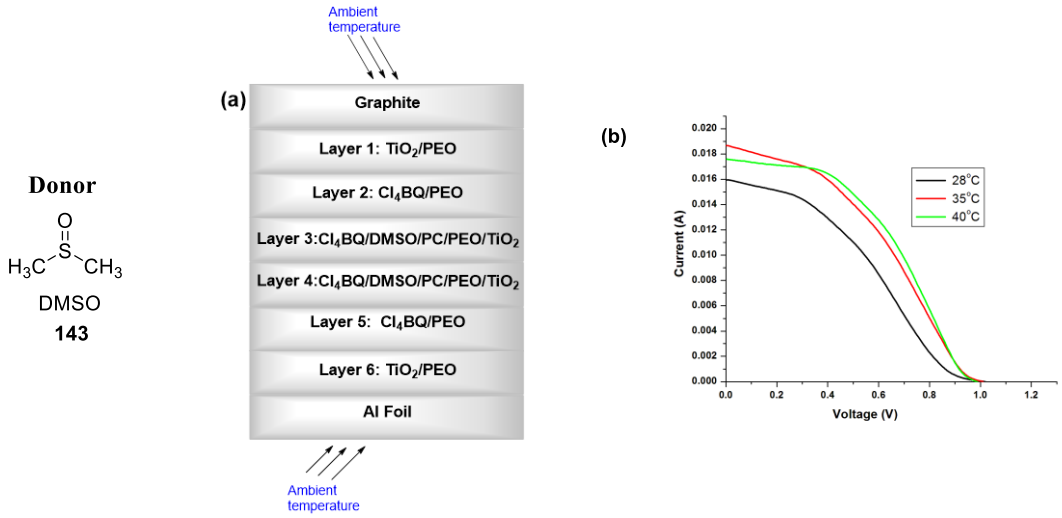

1 h after packing

Donor	**Pmax/mW/FF(28 °C)**	**Pmax/mW/FF(35 °C)**	**Pmax/mW/FF(40 °C)**
DMSO	6.135/0.276	6.833/0.315	7.318/0.366

48 h after packing

Donor	**Pmax/mW/FF(28 °C)**	**Pmax/mW/FF(35 °C)**	**Pmax/mW/FF(40 °C)**
DMSO	5.511/0.339	7.159/0.38	7.669/0.441

Figure 10 (continued)

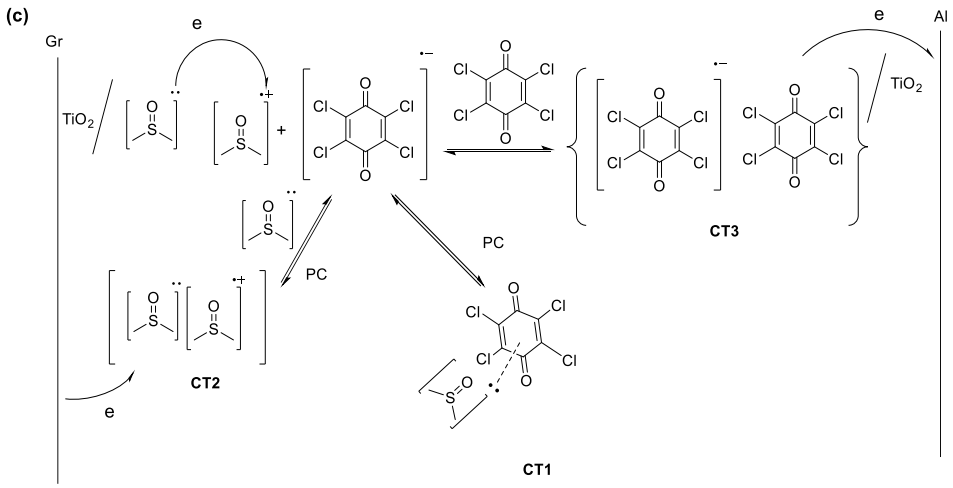

Figure 10. (a) Schematic diagram of multi-layer with Cl_4BQ/DMSO/PC/TiO_2/PEO configuration. (b) Representative IV for the cell (Table ES 4, entry 25, DMSO donor). (c) Tentative mechanism for electron transport to the electrodes via D/D.+ and A-/A exchange reactions.

In this case, the donor DMSO gave high power (Pmax 7.318 mW) at 40 ^oC after 1h packing but the power output was increased to (Pmax 7.669 mW) at 40 ^oC after 48h packing. The shape of the IV curve was also good at 40 ^oC. The Pmax also remained in the higher range for a long time but after three weeks the power output was reduced to (Pmax 1.713mW). We have also constructed the 6 layers cell using Cl_4BQ in layer 1 and BQ in 3 layers and TiO_2 in edge layers (Figure 11).

Figure 11: Six layer cell with Cl_4BQ in layer 2 and BQ in three layers and TiO_2 in edge layers

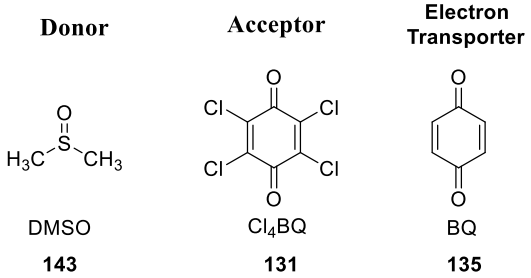

Figure 11 (continued)

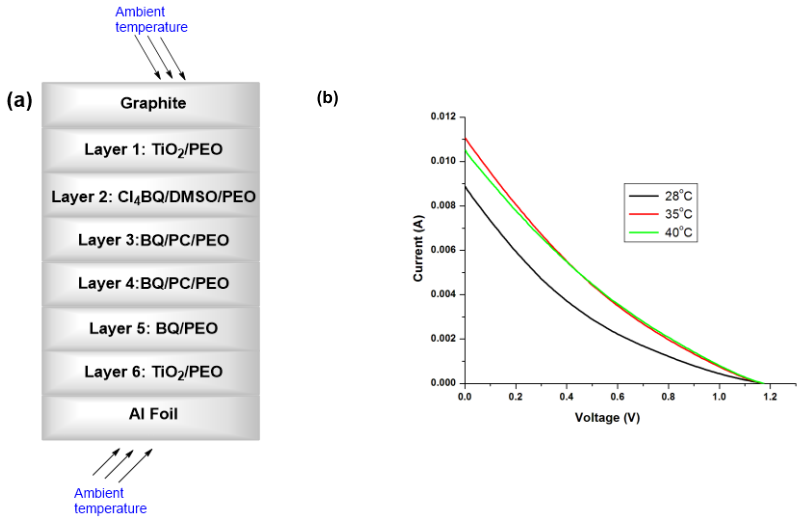

1 h after packing

Donor	**Pmax/mW/FF(28 °C)**	**Pmax/mW/FF(35 °C)**	**Pmax/mW/FF(40 °C)**
DMSO	2.462/0.159	3.04/0.183	3.488/0.2

48 h after packing

Donor	**Pmax/mW/FF(28 °C)**	**Pmax/mW/FF(35 °C)**	**Pmax/mW/FF(40 °C)**
DMSO	1.491/0.143	2.231/0.173	2.241/0.182

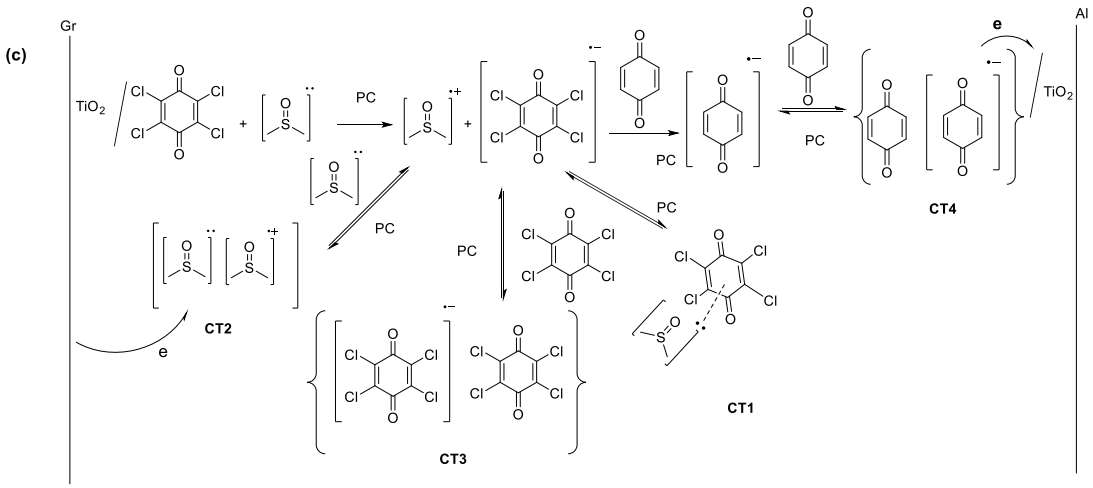

Figure 11. (a) Schematic diagram of multi-layer with Cl_4BQ/DMSO/PC/BQ/TiO_2/PEO configuration and (b) Representative IV for the cell (Table ES 4, entry 26, DMSO donor). (c) Tentative mechanism for electron transport to the electrodes *via* D/D.+ and A-/A exchange reactions.

In this configuration (Figure 11) the power output was low compared to previous configuration (Figure 10). Presumably, the presence of Cl_4BQ in only one layer leads to poorer results. Next, we turned towards the construction of 6 layers cell using Cl_4BQ in

four layers and BQ as electron transporter, TiO_2 in PC layers and edge layers using DMSO as donor (Figure 12).

Figure 12: Six layer cell with Cl_4BQ and BQ in four layers and DMSO in middle layers

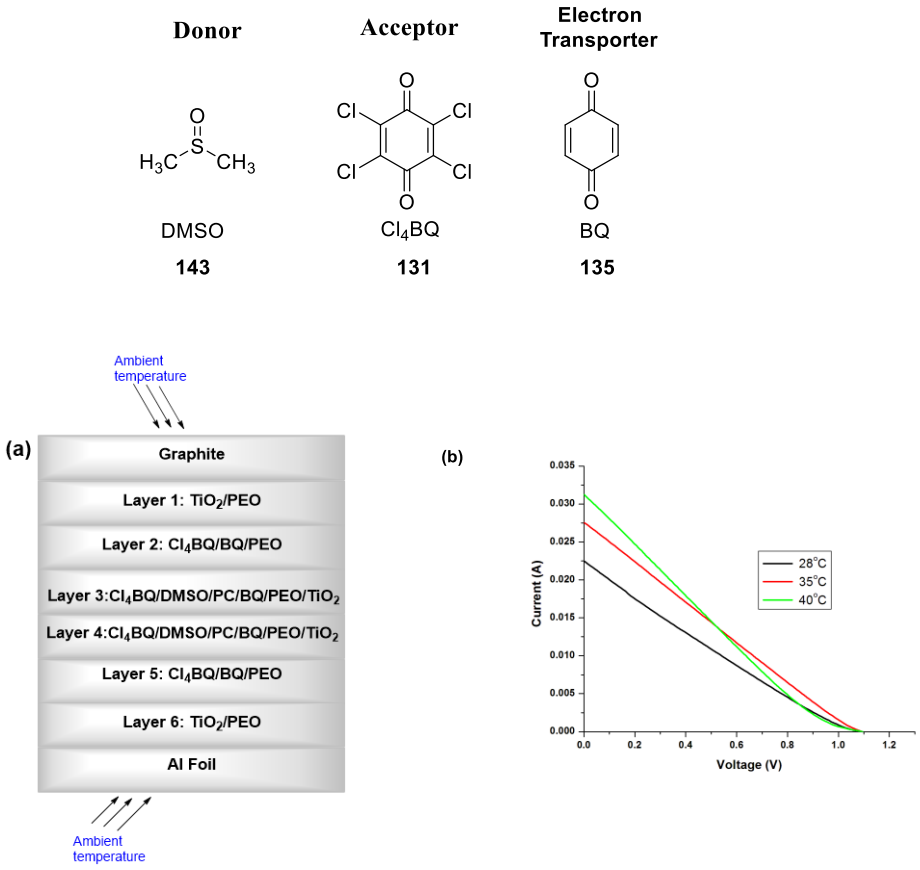

1 h after packing

Donor	**Pmax/mW/FF(28 °C)**	**Pmax/mW/FF(35 °C)**	**Pmax/mW/FF(40 °C)**
DMSO	3.867/0.179	4.28/0.158	5.109/0.191

48 h after packing

Donor	**Pmax/mW/FF(28 °C)**	**Pmax/mW/FF(35 °C)**	**Pmax/mW/FF(40 °C)**
DMSO	5.439/0.224	7.223/0.24	7.312/0.214

Figure 12 (continued)

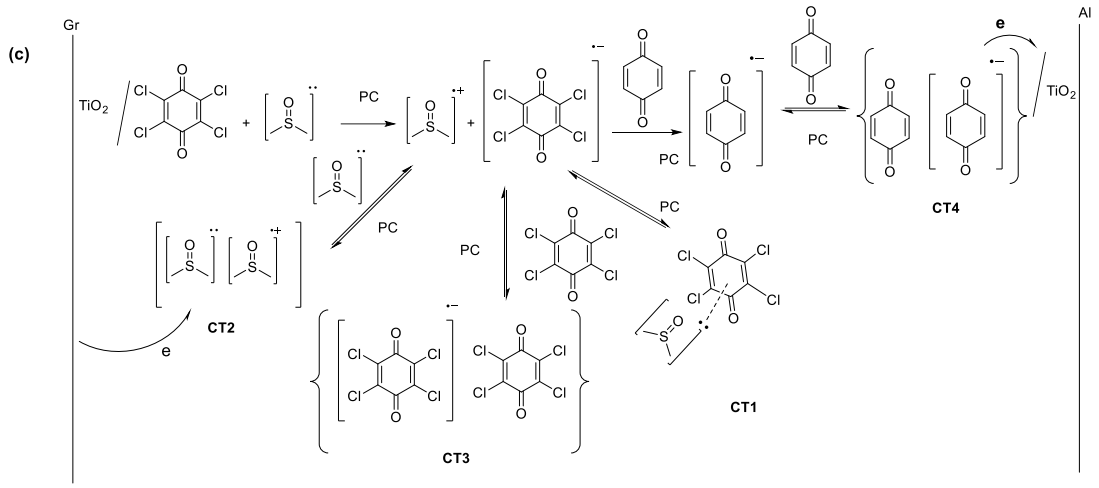

Figure 12. (a) Schematic diagram of multi-layer with Cl_4BQ/DMSO/PC/BQ/TiO_2/PEO configuration and (b) Representative IV for the cell (Table ES 4, entry 27, DMSO donor). (c) Tentative mechanism for electron transport to the electrodes *via* D/D.+ and A-/A exchange reactions.

We have recorded IV-data at 1h and 48h after packing. The 48 h IV-data values are high compared to 1h. The donor DMSO gave high power (Pmax 5.109 mW) at 40 ^oC after 1h packing and the power output increased to Pmax 7.312 mW at 40 ^oC after 48h packing as outlined in Figure 12. This configuration gave higher power up to four weeks, but after four weeks, the power output was reduced to Pmax 2.513mW. Presumably, the transporter BQ accepts electron from *p*-chloranil radical anion and hence the *p*-chloranil will be available for reversible electron transfer from the amines. Indeed, the Pmax values were higher in reactions using BQ for electron transport.

We have then constructed the 6 layers cell using Cl_4BQ in four layers and BQ in four layers TiO_2 in PC layers and TiO_2(1g) in edge layers using DMSO as donor (Figure 13).

Figure 13: Six layer cell with Cl_4BQ and BQ in four layers and more TiO_2 (1 g) in layer 1 and 6

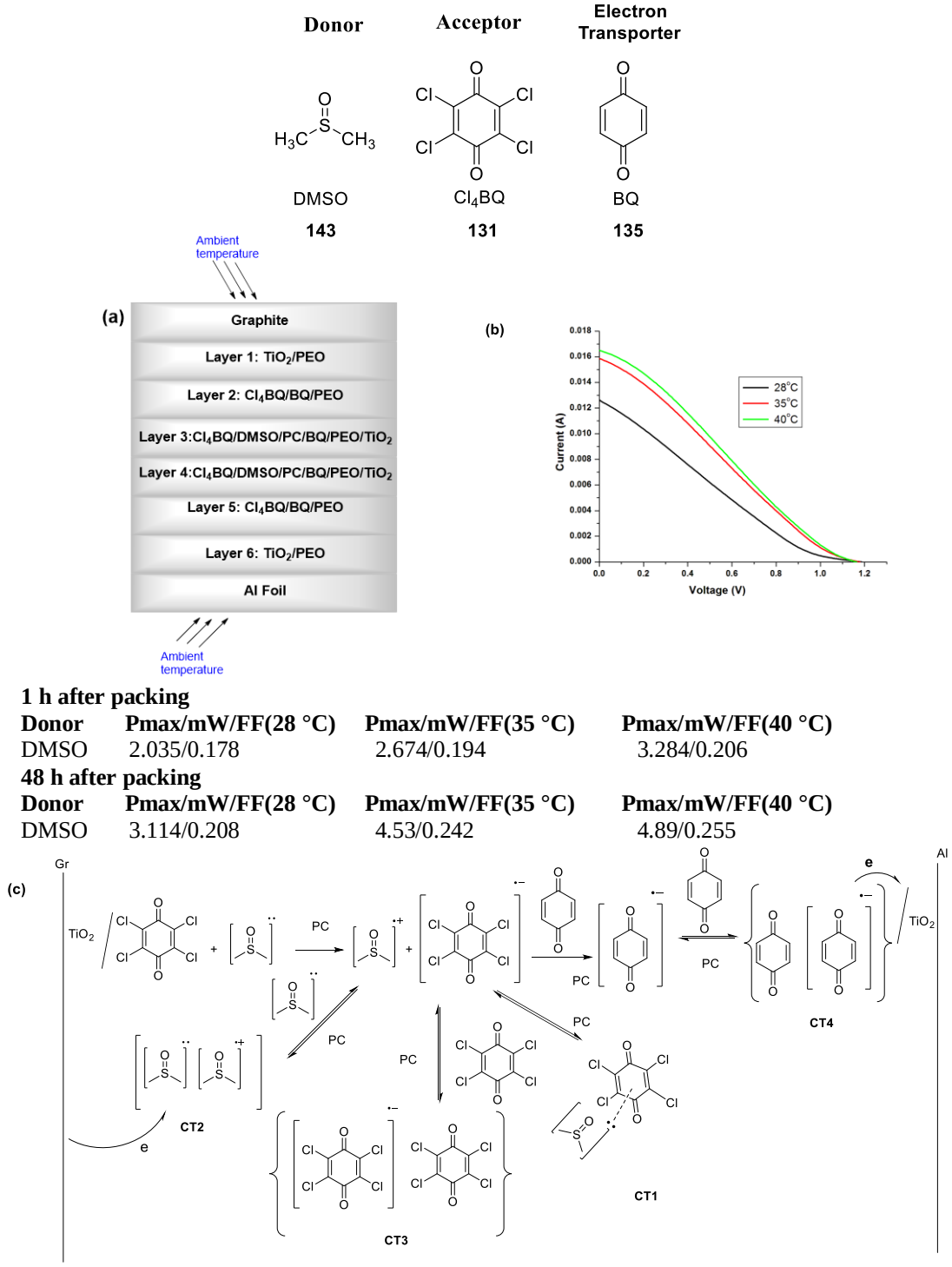

1 h after packing

Donor	**Pmax/mW/FF(28 °C)**	**Pmax/mW/FF(35 °C)**	**Pmax/mW/FF(40 °C)**
DMSO	2.035/0.178	2.674/0.194	3.284/0.206

48 h after packing

Donor	**Pmax/mW/FF(28 °C)**	**Pmax/mW/FF(35 °C)**	**Pmax/mW/FF(40 °C)**
DMSO	3.114/0.208	4.53/0.242	4.89/0.255

Figure 13. (a) Schematic diagram of multi-layer with Cl_4BQ/DMSO/PC/BQ/TiO_2/PEO configuration and (b) Representative IV for the cell (Table ES 5, entry 28, DMSO donor). (c) Tentative mechanism for electron transport to the electrodes *via* D/D.+ and A-/A exchange reactions.

In this configuration high power (Pmax 3.284 mW) was obtained for four weeks but it reduced to Pmax 1.669mW after 4 weeks. However, the use of TiO_2 (1g) would have also reduced the power output.

We have then constructed the 6 layers cell using Cl_4BQ in four layers and TiO_2 (0.75g) in edge layers and using DMSO as donor (Figure 14).

Figure 14: Six layer cell with Cl_4BQ in four layers and TiO_2 in edge layers

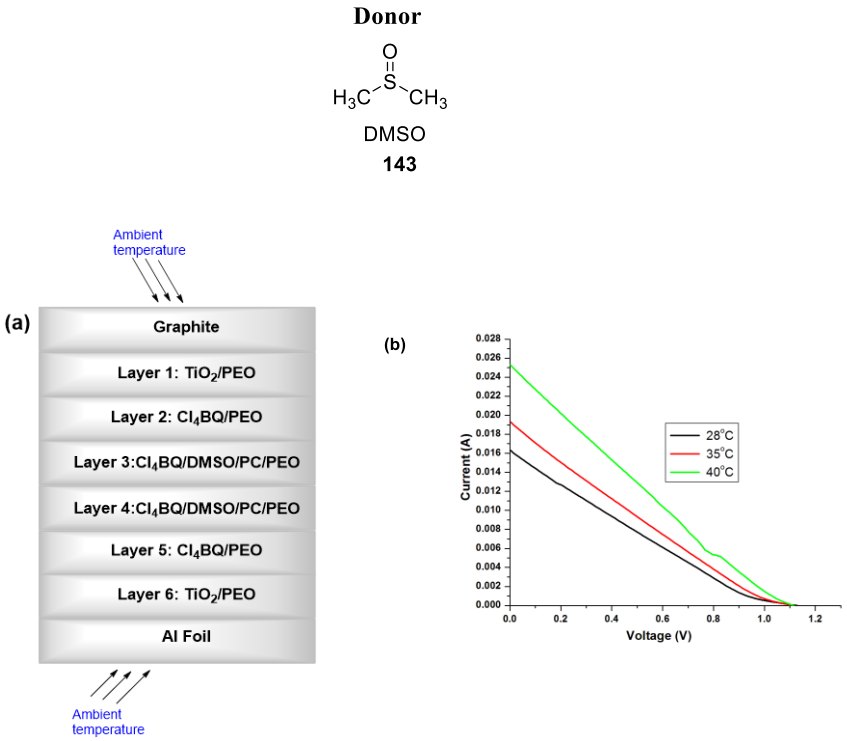

1 h after packing

Donor	**Pmax/mW/FF(28 °C)**	**Pmax/mW/FF(35 °C)**	**Pmax/mW/FF(40 °C)**
DMSO	4.244/0.197	5.245/0.208	7.015/0.217

48 h after packing

Donor	**Pmax/mW/FF(28 °C)**	**Pmax/mW/FF(35 °C)**	**Pmax/mW/FF(40 °C)**
DMSO	3.869/0.211	4.679/0.218	6.463/0.229

Figure 14 (continued)

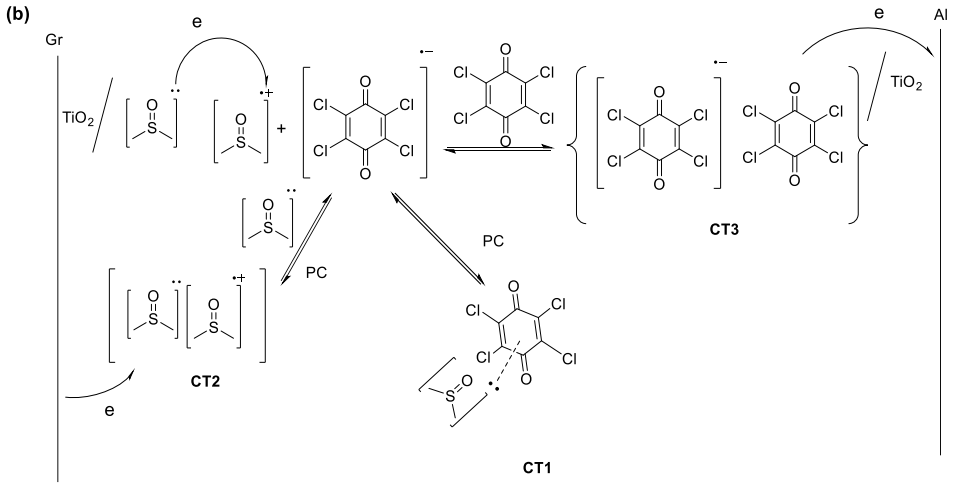

Figure 14. (a) Schematic diagram of multi-layer with Cl_4BQ/DMSO/PC/TiO_2/PEO configuration. (b) Representative IV for the cell (Table ES 5, entry 29, DMSO donor). (c) Tentative mechanism for electron transport to the electrodes via D/D.+ and A-/A exchange reactions.

In this configuration, the initial power output was high Pmax 7.015mW at 1h after packing but it decreased to Pmax 6.463mW after 48h. This configuration was stable up to three weeks. After three weeks, the power output was reduced to Pmax 1.139mW .

We have then constructed the 6 layers cell using Cl_4BQ in four layers and TiO_2 in edge layers amine or amide donor in middle layers along with DMSO donor (Figure 15).

Figure 15: Six layer cell with Cl_4BQ in four layers and TiO_2 in edge layers with DMSO and another Donor in PC

Donors

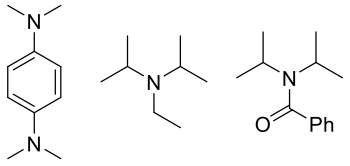

138 **141** **142**

Figure 15 (continued)

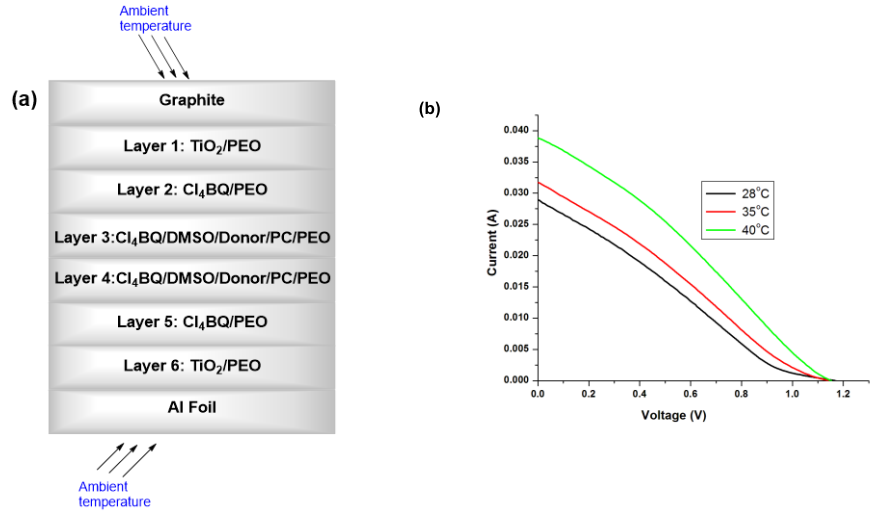

1 h after packing

Donor	**Pmax/mW/FF(28 °C)**	**Pmax/mW/FF(35 °C)**	**Pmax/mW/FF(40 °C)**
TMPDA	11.31/0.302	12.35/0.326	12.81/0.345
DIPEA	8.998/0.207	14.53/0.247	16.63/0.265
DiPrBA	5.509/0.18	7.131/0.185	8.341/0.196

48 h after packing

Donor	**Pmax/mW/FF(28 °C)**	**Pmax/mW/FF(35 °C)**	**Pmax/mW/FF(40 °C)**
TMPDA	2.869/0.247	3.228/0.253	4.082/0.275
DIPEA	7.97/0.236	9.428/0.259	12.99/0.29
DiPrBA	4.935/0.195	6.254/0.223	9.673/0.25

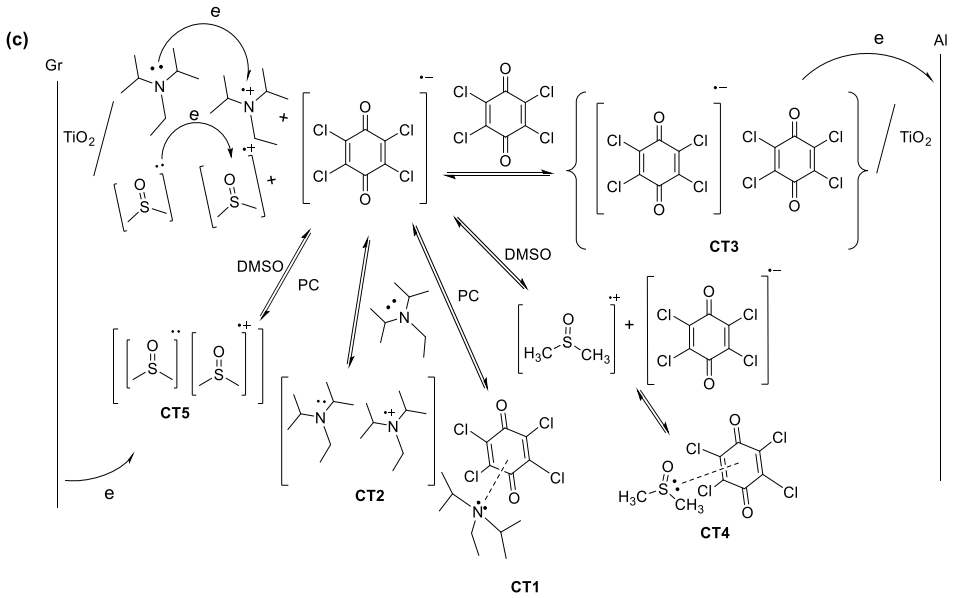

Figure 15. (a) Schematic diagram of multi-layer with Cl_4BQ/DMSO/Donor/PC/TiO_2/PEO configuration. (b) Representative IV for the cell (Table ES 5, entry 30, DIPEA donor). (c) Tentative mechanism for electron transport to the electrodes via D/D.+ and A-/A exchange reactions.

Among various donors, the donor DIPEA gave better results at 28 ^{o}C, 35 ^{o}C, and 40 ^{o}C (Figure 15). The recorded IV data of cell (after 1 h packing) the power maximum (Pmax) and fill factor (FF) values for DIPEA are Pmax 16.63 mW, with FF 0.265 at 40 ^{o}C but decreased to Pmax 12.99 mW, with FF 0.29 after 48h. The power produced was high in this configuration but after three weeks the power output was reduced to Pmax 1.201mW.

We have then constructed the 6 layers cell using Cl_4BQ in two layers and TiO_2 in PC layers and edge layers with donor in middle layers along with DMSO donor (Figure 16).

Figure 16: Six layer cell with Cl_4BQ in two layer and another donor along with DMSO in PC

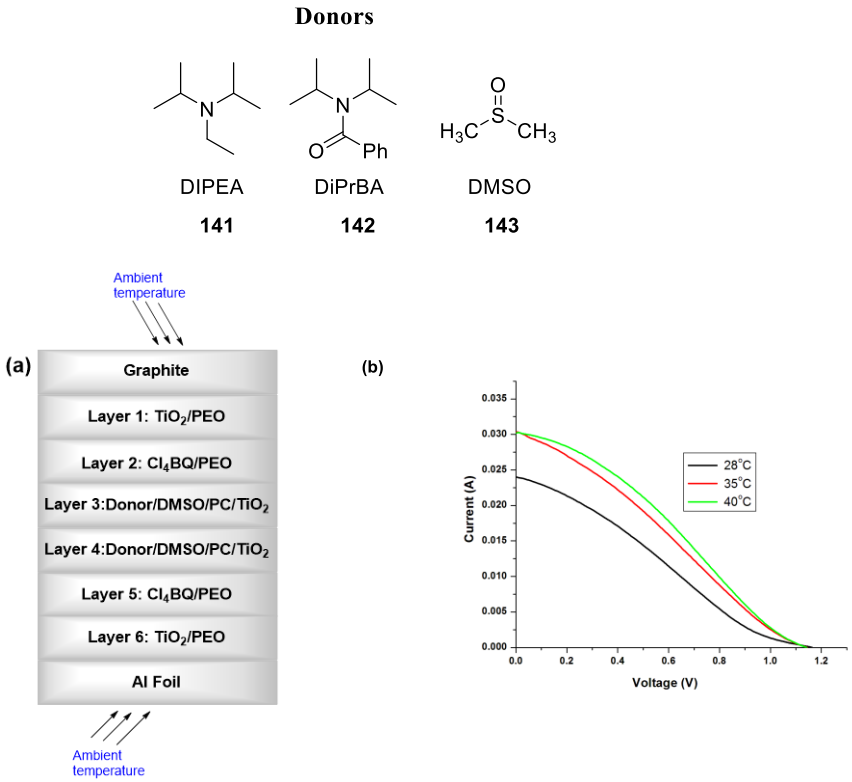

Figure 16 (continued)

1 h after packing

Donor	Pmax/mW/FF(28 °C)	Pmax/mW/FF(35 °C)	Pmax/mW/FF(40 °C)
DIPEA	7.181/0.235	9.45/0.261	10.7/0.297
DiPrBA	4.794/0.204	6.03/0.216	6.005/0.23

48 h after packing

Donor	Pmax/mW/FF(28 °C)	Pmax/mW/FF(35 °C)	Pmax/mW/FF(40 °C)
DIPEA	7.202/0.258	9.67/0.278	10.75/0.312
DiPrBA	4.395/0.227	6.271/0.239	6.271/0.248

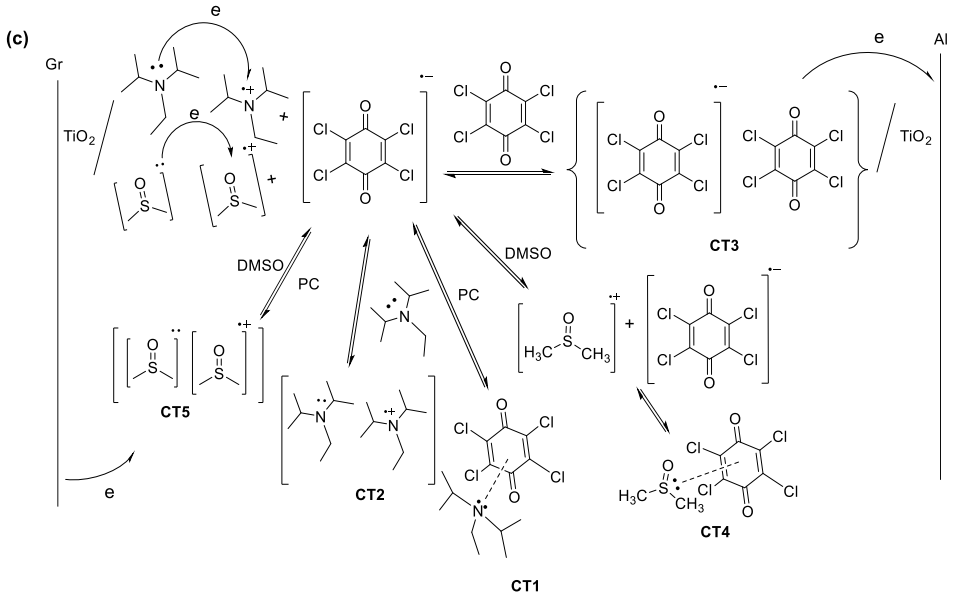

Figure 16. (a) Schematic diagram of multi-layer with Cl_4BQ/DMSO/Donor/PC/TiO_2/PEO configuration. (b) Representative IV for the cell (Table ES 6, entry 33, DIPEA donor). (c) Tentative mechanism for electron transport to the electrodes via D/D.+ and A-/A exchange reactions.

In this case, the power output 40 ℃ remained approximately the same for 48h. This configuration is also stable up to one week. The higher power (DIPEA, Pmax 10.7 mW) was reduced to Pmax 5.083mW after one week.

Comparison of DMSO and other donors

We have also constructed the 6 layers cell using Cl_4BQ in one layer and donor in middle layers TiO_2 in PC (Figure 17).

Figure 17: Six layer cell with Cl_4BQ in layer 2 donor in middle layers and TiO_2 in edge layers

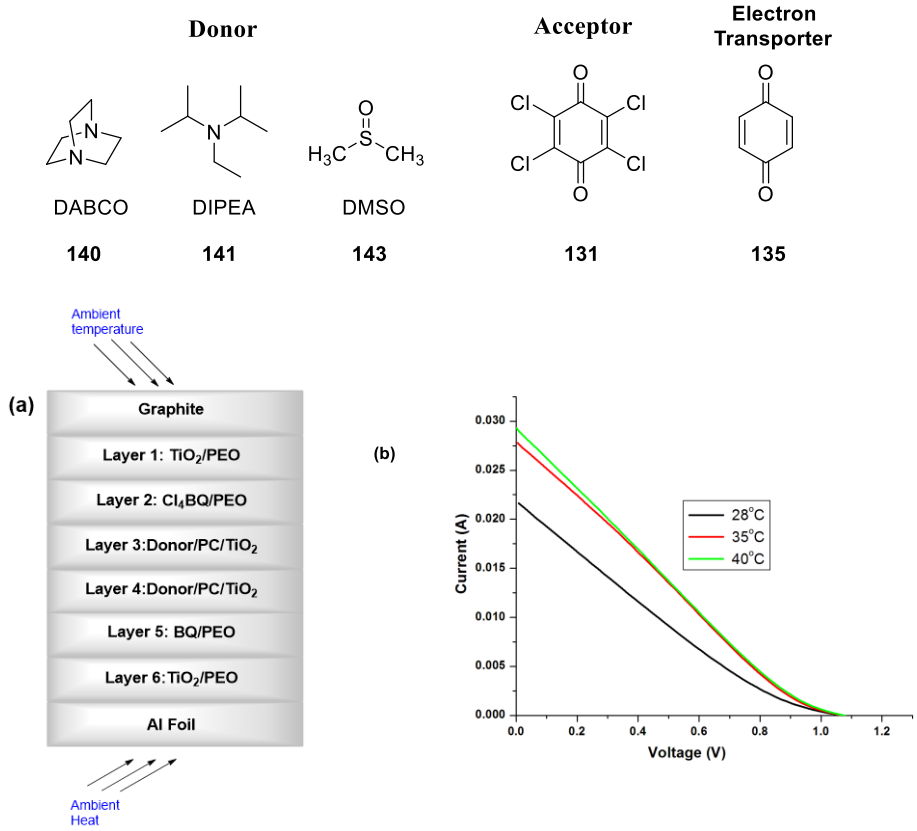

1 h after packing

Donor	Pmax/mW/FF(28 °C)	Pmax/mW/FF(35 °C)	Pmax/mW/FF(40 °C)
DMSO	3.7/0.149	5.641/0.172	6.156/0.159
DABCO	0.766/0.154	1.297/0.186	1.434/0.224
DIPEA	3.012/0.298	3.656/0.277	3.983/0.29

48 h after packing

Donor	Pmax/mW/FF(28 °C)	Pmax/mW/FF(35 °C)	Pmax/mW/FF(40 °C)
DMSO	4.668/0.201	6.805/0.229	6.899/0.218
DABCO	0.685/0.215	0.808/0.143	0.967/0.208
DIPEA	1.166/0.245	1.375/0.248	1.412/0.243

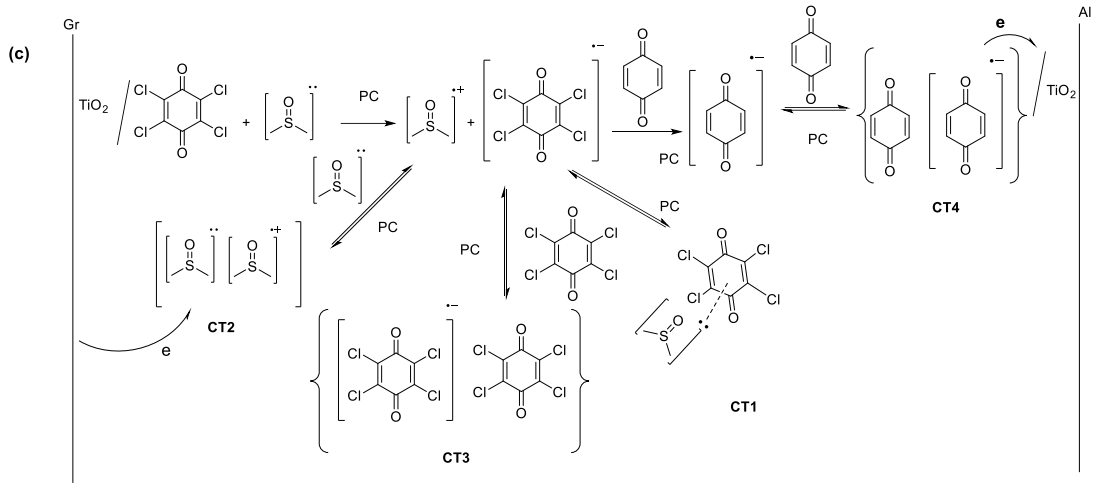

Figure 17. (a) Schematic diagram of multi-layer with Cl_4BQ/DMSO/PC/BQ/TiO_2/PEO configuration and (b) Representative IV for the cell (Table ES 6, entry 36, DMSO donor). (c) Tentative mechanism for electron transport to the electrodes *via* D/D.+ and A-/A exchange reactions.

In this configuration, the donor DMSO gave better results compared to other donors. The power output was (DMSO, Pmax 6.156 mW) at 40 ^oC at 1h after packing but the power output was increased to Pmax 6.899 mW at 40 ^oC after 48h.

Clearly, the DMSO as donor in PC gave higher power output compared to other donors

Some configurations with higher Pmax values are summarized below.

Cell Configuration (C C)

C C 10 (Figure 11)

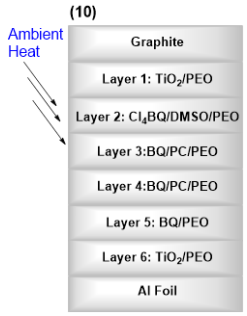

C C11 (Figure 12)

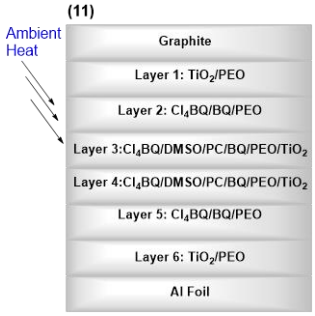

C C 12 (Figure 13)

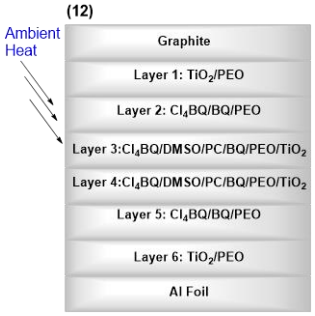

48 h after packing

Donor	**Pmax/mW/FF(40 °C)**	**Donor**	**Pmax/mW/FF(40 °C)**	**Donor**	**Pmax/mW/FF(40 °C)**
DMSO	2.241/0.182	DMSO	7.312/0.214	DMSO	4.89/0.255

C C 13 (Figure 14)

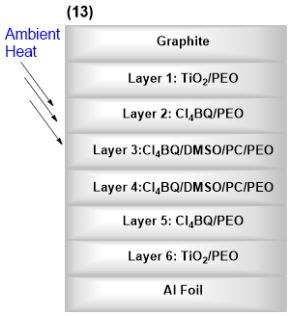

C C 9 (Figure 10)

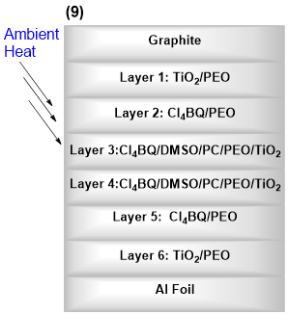

C C14 (Figure 15)

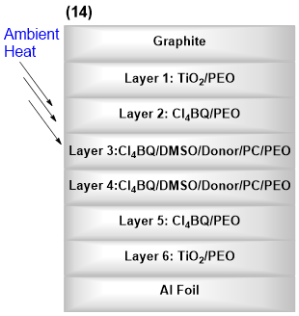

48 h after packing

Donor	**Pmax/mW/FF(40 °C)**	**Donor**	**Pmax/mW/FF(40 °C)**	**Donor**	**Pmax/mW/FF(40 °C)**
DMSO	6.463/0.229	DMSO	7.669/0.441	DMSO, DIPEA	16.63/0.265

Methods are available for storing solar heat in simple chemicals like aq. NaOH and $CaCl_2$ for regenerating heat (40 ^oC to 60 ^oC) when required.[45] Therefore, the ambient heat harvesting device reported here has the potential for developing devices that could produce electricity 24x7, day and night, rainy or cloudy atmospheric conditions. These low/ambient heat harvesting electricity producing cells can be readily stacked, thus

suitable for putting up units for large-scale applications. However, long term performance of these cell devices remains to be established. Since, these cells utilize readily accessible inexpensible materials, there is plenty of scope for further research and development to improve the performance of the devices.

4.3 Conclusions

The DMSO was used as solvent in the construction of electrochemical cells along with other donors and *p*-chloranil to produce Pmax of 4.568mW to 8.603mW in different cell configurations at 48h and 40 ^{o}C. The DMSO as donor using PC solvent gave higher power output at 48h, (Pmax 7.669mW to 10.75mW) for the cells constructed at various configurations at 48h and 40 ^{o}C.

The devices utilize inexpensive materials already manufactured in large scale and hence it will be suitable in bulk-scale power generation units. Further systematic investigations on the development of these electrochemical cells have potential to come up with devices for practical applications for the generation of electricity for household, grid and automobile applications.

4.4 Experimental Section

4.4.1 General Information

P-Chloranil, N, N-diisopropylethylamine (DIPEA), 1,4-diazabicyclo[2.2.2]octane (DABCO) and TiO_2 were purchased from Avra chemicals (India). *p*-benzoquinone (BQ), triphenylamine (TPA), N,N'-tetramethyl-1,4-phenylenediamine (TMPDA), propylene carbonate (PC), ethylene carbonate (EC) and polyethylene oxide (PEO) were purchased from Sigma Aldrich. Netural alumina (Al_2O_3) and dimethylsulfoxide (DMSO) was purchased from SRL chemicals, India. Zinc oxide (ZnO) was purchased from E-Merck, India. The metal oxides were heated at 150 °C in a vacuum oven for 2 h before use. PC and EC were always kept under molecular sieves. N, N-diisopropylbenzamide was prepared from the literature procedure. Graphite sheet (0.4mm thickness, 5cm x 5cm, Resistivity, $\rho = 2x10^{-4}\Omega.m$) was purchased from Falcon Graphite Industries, Hyderabad, India. Aluminium Foil (0.2mm thickness, 5cm x 5cm, Resistivity, $\rho = 2x10^{-5}\Omega.m$) and Stainless steel (0.4mm thickness, 5cm x 5cm, Resistivity, $\rho = 5x10^{-4}\Omega.m$) were purchased from Aluminium Enterprises and Rasik Metals, Hyderabad, India. EPR spectra was recorded on a Bruker-ER073 instrument equipped with an EMX micro X source for X band measurement using Xenon 1.1b.60 software provided by the manufacturer. Electrical measurements were carried out by ZAHNER instrument using CIMPS software. The current-voltage curve was drawn using Origin software.

4.4.2 Procedure for IV measurement for electrochemical cell

The voltage and current of the fabricated cell was initially measured using an multimeter. The IV characteristics were measured by ZAHNER instrument using CIMPS software. The IV characteristics of the cell were done under dark condition without illumination of light. The cell was recorded at scan rate of 1mV/S to get maximum power (Pmax) and fill factor (FF). The cell potentiostat should be open circuit voltage (Voc) before the measurement.

4.4.3 Preparation of Electrochemical Cells

Configuration 1 (Figure 2, Table ES1)

Cl_4BQ (0.75 g)/PEO (0.05 g) in DCM slurry was prepared coated layer on Al and Graphite foils. and dried in air at room temperature overnight. Donor (0.1 g)/DMSO (0.5 ml)/PEO (0.05 g) was heat coat before packing on dried coated Al and Graphite foils. The cell was prepared by sandwiching the coated Al/Gr layers. The rim of the cell prepared in this way was sealed all around using TiO_2/PEO paste, then with commercial adhesive Bondfix (India) and covered with cellophane tape.

Configuration 2 (Figure 3, Table ES1)

Cl_4BQ (0.25 g)/TiO_2(0.5 g)/PEO (0.05 g) in DCM slurry was prepared coated layer on Al and Graphite foils. and dried in air at room temperature overnight. Donor (0.2 g)/DMSO (0.5 ml)/PEO (0.05 g) was heat coat before packing on dried coated Al and Graphite foils. The cell was prepared by sandwiching the coated Al/Gr layers. The rim of the cell prepared in this way was sealed all around using TiO_2/PEO paste, then with commercial adhesive Bondfix (India) and covered with cellophane tape

Configuration 3 (Figure 4, Table ES1)

The PEO (0.05 g) was dissolved in dichloromethane and mixed with TiO_2 (0.75 g) powder. DCM was removed to obtain a paste for coating on Al and Graphite foils. Cl_4BQ (0.15 g) and Donor (0.1 g) stirred in DCM for three hours DCM was removed to this DMSO (0.5 ml)/PEO (0.05 g) was added heated at 50 ^{o} C for 30 minutes in oven coat before packing on dried coated Al and Graphite foils. The cell was prepared by sandwiching the coated Al/Gr layers. The rim of the cell prepared in this way was sealed all around using TiO_2/PEO paste, then with commercial adhesive Bondfix (India) and covered with cellophane tape

Configuration 4 (Figure 5, Table ES2)

The PEO (0.05 g) was dissolved in dichloromethane and mixed with TiO_2 (0.5 g) powder. DCM was removed to obtain a paste for coating on Al and Graphite foils. Cl_4BQ (0.25 g)/PEO (0.05 g) stirred for one hour in DCM was coated on TiO_2/PEO/Al, Cl_4BQ (0.25 g)/Donor (0.05 g)/PEO (0.05 g) stirred for one hour in DCM was coated on TiO_2/PEO/Gr. After each coat keep at 50 ^{o} C for 10 minutes in oven, and dried in air at room temperature overnight. Cl_4BQ (0.05 g) /DMSO (0.5 ml)/PEO (0.05 g) was heated at 50 ^{o} C for 10 minutes in oven coat before packing on dried coated Al and Graphite foils. The cell was prepared by sandwiching the coated Al/Gr layers. The rim of the cell prepared in this way was sealed all around using TiO_2/PEO paste, then with commercial adhesive Bondfix (India) and covered with cellophane tape.

Configuration 5 (Figure 6, Table ES2)

The PEO (0.05 g) was dissolved in dichloromethane and mixed with TiO_2 (0.5 g) powder. DCM was removed to obtain a paste for coating on Al and Graphite foils. Cl_4BQ (0.25 g)/PEO (0.05 g) was drop coat on TiO_2/PEO/Al, Donor (0.2 g)/PEO (0.05 g) was drop coat on TiO_2/PEO/Gr. TiO_2 (0.5 g)/PEO (0.05 g) was drop coat on coated Graphite, After each coat keep at 50 ^{o}C for 10 minutes in oven, and dried in air at room temperature overnight. DMSO (1ml) was drop coat on before packing on dried coated Al and Graphite foils. The cell was prepared by sandwiching the coated Al/Gr layers. The rim of the cell prepared in this way was sealed all around using TiO_2/PEO paste, then with commercial adhesive Bondfix (India) and covered with cellophane tape.

Configuration 6 (Figure 7, Table ES3)

The PEO (0.05 g) was dissolved in dichloromethane and mixed with TiO_2 (0.5 g) powder. was drop coat on Al and Graphite foils. Cl_4BQ (0.25 g)/PEO (0.05 g) in DCM slurry was prepared drop coat on coated Al and Graphite. After each coat keep at 50 ^{o}C for 10 minutes in oven, and dried in air at room temperature overnight.Cl_4BQ (0.025 g)/Donor (0.1 g)/DMSO (0.5 ml)/PEO (0.05 g) was heated at 50 ^{o}C for 10 minutes in oven coat before packing on dried coated Al and Graphite foils. The cell was prepared by sandwiching the coated Al/Gr layers. The rim of the cell prepared in this way was sealed all around using TiO_2/PEO paste, then with commercial adhesive Bondfix (India) and covered with cellophane tape.

Configuration 7 (Figure 8, Table ES3)

The PEO (0.05 g) was dissolved in dichloromethane and mixed with TiO_2 (0.75 g) powder. DCM was removed to obtain a paste for coating on Al and Graphite foils. After 1 h, Cl_4BQ (0.12 g) in DCM slurry was prepared coat on coated Al and Graphite and dried in air at room temperature overnight. Cl_4BQ (0.12 g)/Donor 2 (0.1 g) stirred for three hours in DCM

at 40 ^{o} C DCM was removed to this DMSO (0.7 ml)/PEO (0.05 g) was added heated at 50 ^{o}C for 30 minutes in oven coat before packing on dried coated Al and Cl_4BQ (0.12 g)/Donor 1 (0.1 g) stirred for three hours in DCM at 40 ^{o} C DCM was removed to this DMSO (0.7 ml)/PEO (0.05 g) was added heated at 50 ^{o}C for 30 minutes in oven coat before packing on dried coated Graphite foils. The cell was prepared by sandwiching the coated Al/Gr layers. The rim of the cell prepared in this way was sealed all around using TiO_2/PEO paste, then with commercial adhesive Bondfix (India) and covered with cellophane tape.

Configuration 8 (Figure 9, Table ES3)

The PEO (0.05 g) was dissolved in dichloromethane and mixed with TiO_2 (0.75 g) powder. DCM was removed to obtain a paste for coating on Al and Graphite foils. After 1 h, Cl_4BQ (0.12 g) in DCM slurry was prepared coat on coated Al and Graphite and dried in air at room temperature overnight. Cl_4BQ (0.12 g)/Donor (0.1 g) stirred for three hours in DCM at 40 ^{o} C DCM was removed to this DMSO (0.7 ml)/PEO (0.05 g) was added heated at 50 ^{o} C for 30 minutes in oven coat before packing on dried coated Al and Graphite foils. The cell was prepared by sandwiching the coated Al/Gr layers. The rim of the cell prepared in this way was sealed all around using TiO_2/PEO paste, then with commercial adhesive Bondfix (India) and covered with cellophane tape.

Configuration 9 (Figure 10, Table ES4)

The PEO (0.05 g) was dissolved in dichloromethane and mixed with TiO_2 (0.5 g) powder. DCM was removed to obtain a paste for coating on Al and Graphite foils. After 1 h, Cl_4BQ (0.1 g)/PEO (0.05 g) in DCM was coated on TiO_2/PEO/Al, and TiO_2/PEO/Gr dried

DMSO (0.078 g)/ Cl_4BQ (0.025 g)/PC (0.5 g) / PEO (0.05 g)/TiO_2(0.25 g) slurry was prepared and casted above the coated layer on Al and Graphite and dried in air at room temperature overnight. The cell was prepared by sandwiching the coated Al/Gr layers. The rim of the cell prepared in this way was sealed all around using TiO_2/PEO paste, then with commercial adhesive Bondfix (India) and covered with cellophane tape.

Configuration 10 (Figure 11, Table ES4)

The PEO (0.05 g) was dissolved in dichloromethane and mixed with TiO_2 (0.5 g) powder. DCM was removed to obtain a paste for coating on Al and Graphite foils. After 1 h, BQ (0.22 g)/PEO (0.05 g) in DCM was coated on TiO_2/PEO/Al, and DMSO(0.156 g)/Cl_4BQ (0.5 g)/PEO (0.05 g) in DCM was coated on TiO_2/PEO/Gr dried. BQ (0.11 g)/PC (0.75 g) /PEO (0.05 g) was heated to dissolve the compound and mixed with TiO_2 (0.5 g) powder coated on coated Al and Graphite foils. dried in air at room temperature overnight. The cell was prepared by sandwiching the coated Al/Gr layers. The rim of the cell prepared in this way was sealed all around using TiO_2/PEO paste, then with commercial adhesive Bondfix (India) and covered with cellophane tape.

Configuration 11 (Figure 12, Table ES4)

The PEO (0.05 g) was dissolved in dichloromethane and mixed with TiO_2 (0.5 g) powder. DCM was removed to obtain a paste for coating on Al and Graphite foils. After 1 h, Cl_4BQ (0.1 g)/BQ(0.1 g)/PEO (0.05 g) in DCM was coated on TiO_2/PEO/Al, and TiO_2/PEO/Gr dried. DMSO (0.078 g)/ Cl_4BQ (0.025 g)/PC (0.5 g) /BQ(0.1 g)/ PEO (0.05 g)/TiO_2(0.25 g) slurry was prepared and casted above the coated layer on Al and Graphite and dried in air at room temperature overnight. The cell was prepared by sandwiching the coated Al/Gr layers. The rim of the cell prepared in this way was sealed all around using TiO_2/PEO paste, then with commercial adhesive Bondfix (India) and covered with cellophane tape.

Configuration 12 (Figure 13, Table ES5)

The PEO (0.1 g) was dissolved in dichloromethane and mixed with TiO_2 (1.0 g) powder. DCM was removed to obtain a paste for coating on Al and Graphite foils. After 1 h, Cl_4BQ (0.1 g)/BQ(0.1 g)/PEO (0.05 g) in DCM was coated on TiO_2/PEO/Al, and TiO_2/PEO/Gr dried. DMSO (0.078 g)/ Cl_4BQ (0.025 g)/PC (0.5 g) /BQ(0.1 g)/ PEO (0.05 g)/TiO_2(0.25 g) slurry was prepared and casted above the coated layer on Al and Graphite and dried in air at room temperature overnight. The cell was prepared by sandwiching the coated Al/Gr layers. The rim of the cell prepared in this way was sealed all around using TiO_2/PEO paste, then with commercial adhesive Bondfix (India) and covered with cellophane tape.

Configuration 13 (Figure 14, Table ES5)

The PEO (0.05 g) was dissolved in dichloromethane and mixed with TiO_2 (0.75 g) powder. DCM was removed to obtain a paste for coating on Al and the PEO (0.025 g) was dissolved in dichloromethane and mixed with TiO_2 (0.75 g) powder. DCM was removed to obtain a paste for coating on Graphite foils. After 1 h, Cl_4BQ (0.25 g)/PEO (0.025 g) in DCM was coated on TiO_2/PEO/Al, and TiO_2/PEO/Gr dried. DMSO (0.1 ml)/ Cl_4BQ (0.05 g)/PC (0.5 g) /PEO (0.05 g) was heated at 50 ^{o}C for 1 hour in oven coat before packing on dried coated Al and Graphite foils. dried in air at room temperature overnight. The cell was prepared by sandwiching the coated Al/Gr layers. The rim of the cell prepared in this way was sealed all around using TiO_2/PEO paste, then with commercial adhesive Bondfix (India) and covered with cellophane tape.

Configuration 14 (Figure 15, Table ES5)

The PEO (0.05 g) was dissolved in dichloromethane and mixed with TiO_2 (0.75 g) powder. DCM was removed to obtain a paste for coating on Al and Graphite foils. After 1 h, Cl_4BQ (0.25 g)/PEO (0.025 g) in DCM was coated on TiO_2/PEO/Al, and TiO_2/PEO/Gr dried. DMSO (0.1 ml)/ Cl_4BQ (0.1 g)/Donor(0.1 g)/PC (0.5 g) /PEO (0.05 g) was heated at 50 ^{o}C for 1 hour in oven coat before packing on dried coated Al and Graphite foils. dried in air at room temperature overnight. The cell was prepared by sandwiching the coated Al/Gr layers. The rim of the cell prepared in this way was sealed all around using TiO_2/PEO paste, then with commercial adhesive Bondfix (India) and covered with cellophane tape.

Configuration 15 (Figure 16, Table ES6)

The PEO (0.05 g) was dissolved in dichloromethane and mixed with TiO_2 (0.5 g) powder. DCM was removed to obtain a paste for coating on Al and Graphite foils. After 1 h, Cl_4BQ (0.25 g)/PEO (0.05 g) in DCM was coated on TiO_2/PEO/Al, and TiO_2/PEO/Gr dried. DMSO(0.188 g)/Donor (1 mmol) /PC (0.5 g) / TiO_2 (0.25 g) was coated on coated Al and Graphite foils. dried in air at room temperature overnight. The cell was prepared by sandwiching the coated Al/Gr layers. The rim of the cell prepared in this way was sealed all around using TiO_2/PEO paste, then with commercial adhesive Bondfix (India) and covered with cellophane tape.

Configuration 16 (Figure 17, Table ES6)

The PEO (0.05 g) was dissolved in dichloromethane and mixed with TiO_2 (0.5 g) powder. DCM was removed to obtain a paste for coating on Al and Graphite foils. After 1 h, BQ(0.44 g)/PEO (0.05 g) in DCM was coated on TiO_2/PEO/Al, and Cl_4BQ(0.25 g)/PEO (0.05 g) in DCM was coated on TiO_2/PEO/Gr and dried. Donor(2 mmol)/PC (0.5 g)/ TiO_2(0.25 g) slurry was prepared and casted above the coated layer on Al and Graphite and dried in air at room temperature overnight. The cell was prepared by sandwiching the coated Al/Gr layers. The rim of the cell prepared in this way was sealed all around using TiO_2/PEO paste, then with commercial adhesive Bondfix (India) and covered with cellophane tape. After packing the cell was connected immediately to charge a Ni-Cd battery through a Zener diode.It was disconnected while carry out the IV-curve measurement.

Table ES1 Cl_4BQ in edge layer, DMSO used as solvent.

Cell Configuration 1 (Figure 2) (Cl_4BQ in 2 layers)

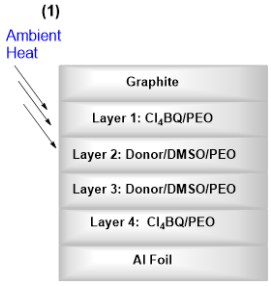

(Entries 1-2)

Cell Configuration 2 (Figure 3) (Cl_4BQ in 2 layers)

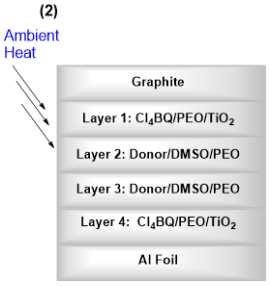

(Entries 3-4)

Cell Configuration 3 (Figure 4) (Cl_4BQ in 2 layers)

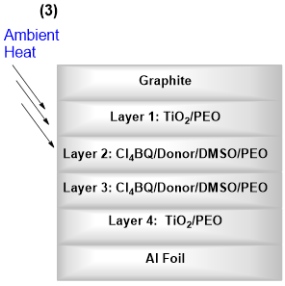

(Entries 5-8)

Entry	Cell Configuration	Time after packing	T °C[c]	Voc (V)	Isc (mA)	Vmax (V)	Imax (mA)	Pmax (mW)	Fill Factor
1	Gr---------- Layer1: Cl_4BQ(0.75g) + PEO(0.05g) Layer2: DMSO (0.5ml) + DiPrBA (0.1g) Layer3: DMSO (0.5ml) + DiPrBA (0.1g) Layer4: Cl_4BQ(0.75g) + PEO(0.05g) Al----------	1 h	28 °C 35 °C	1.049 1.062	6.399 26.96	0.461 0.478	3.193 13.25	1.47 6.333	0.219 0.221
		48 h	35 °C	1.079	7.121	0.442	3.556	1.57	0.204
		96 h	35 °C	1.099	1.035	0.497	0.500	0.248	0.219
2	Gr---------- Layer1: Cl_4BQ(0.75g) + PEO(0.05g) Layer2: DMSO (0.5ml) + TMPDA (0.1g) Layer3: DMSO (0.5ml) + TMPDA (0.1g) Layer4: Cl_4BQ(0.75g) + PEO(0.05g) Al----------	1 h	28 °C 35 °C	1.067 1.09	27.94 39.29	0.479 0.533	14.68 20.13	7.033 10.72	0.236 0.25
		48 h	35 °C	1.163	8.093	0.58	4.193	2.43	0.258
		96 h	35 °C	1.13	5.554	0.585	2.676	1.566	0.25
3	Gr---------- Layer1: Cl_4BQ(0.25g) + TiO_2(0.5g) + PEO(0.05g) Layer2: DiPrBA (0.2g)+ DMSO (0.5ml) + PEO(0.05g) Layer3: DiPrBA (0.2g)+ DMSO (0.5ml) + PEO(0.05g) Layer4: Cl_4BQ(0.25g) + TiO_2(0.5g) + PEO(0.05g) Al----------	1 h	28 °C 35 °C	1.096 1.101	16.65 25.18	0.498 0.53	9.848 15.05	4.905 7.971	0.269 0.287
		48 h	35 °C	1.13	15.43	0.488	8.478	4.139	0.237
		96 h	35 °C	1.136	9.282	0.53	4.88	2.584	0.245
4	Gr---------- Layer1: Cl_4BQ(0.25g) + TiO_2(0.5g) + PEO(0.05g) Layer2: TMPDA (0.2g)+ DMSO (0.5ml) + PEO(0.05g) Layer3: TMPDA (0.2g)+ DMSO (0.5ml) + PEO(0.05g) Layer4: Cl_4BQ(0.25g) + TiO_2(0.5g) + PEO(0.05g) Al----------	1 h	28 °C 35 °C	0.898 0.876	10.76 17.05	0.344 0.378	6.226 11.62	2.138 4.385	0.221 0.294
		48 h	35 °C	0.786	10.73	0.385	7.402	2.85	0.338
		96 h	35 °C	0.747	5.516	0.329	3.527	1.159	0.282
5	Gr---------- Layer1:TiO_2(0.75g) + PEO(0.05g) Layer2: Cl_4BQ(0.15g) + N,N-Diethyl benzamide (0.1g)+ DMSO (0.5ml) + PEO(0.05g) Layer3: Cl_4BQ(0.15g) + N,N-Diethyl benzamide (0.1g)+	1 h	28 °C 35 °C 40 °C	0.993 1.018 1.082	25.32 26.34 28.82	0.389 0.417 0.44	13.17 12.99 14.29	5.118 5.411 6.292	0.204 0.202 0.202

	DMSO (0.5ml) + PEO(0.05g) Layer4: TiO_2(0.75g) + PEO(0.05g) Al----------	48 h	40 ºC	1.084	12.57	0.401	5.722	2.296	0.168
		96 h	40 ºC	1.049	5.059	0.372	2.361	0.878	0.166
6	Gr---------- Layer1:TiO_2(0.75g) + PEO(0.05g) Layer2: Cl_4BQ(0.15g) + N,N-DiMethyl benzamide (0.1g)+ DMSO (0.5ml) + PEO(0.05g) Layer3: Cl_4BQ(0.15g) + N,N-DiMethyl benzamide (0.1g)+ DMSO (0.5ml) + PEO(0.05g) Layer4: TiO_2(0.75g) + PEO(0.05g) Al----------	1 h	28 ºC	0.997	9.569	0.362	4.685	1.696	0.178
			35 ºC	1.057	15.18	0.335	7.539	2.522	0.157
			40 ºC	1.018	15.69	0.36	7.801	2.804	0.176
		48 h	40 ºC	1.101	11.8	0.398	5.096	2.028	0.156
		96 h	40 ºC	1.096	4.378	0.406	2.122	0.862	0.18
7	Gr---------- Layer1:TiO_2(0.75g) + PEO(0.05g) Layer2: Cl_4BQ(0.25g)+ DiPrBA (0.2g)+ DMSO (1ml) + PEO(0.05g) Layer3: Cl_4BQ(0.25g)+ DiPrBA (0.2g)+ DMSO (1ml) + PEO(0.05g) Layer4: TiO_2(0.75g) + PEO(0.05g) Al----------	1 h	28 ºC	1.005	23.78	0.395	11.19	4.42	0.185
			35 ºC	1.066	27.46	0.453	13.77	6.24	0.213
			40 ºC	0.984	31.21	0.44	15.17	6.666	0.217
		48 h	40 ºC	1.112	19.58	0.457	9.995	4.568	0.21
		96 h	40 ºC	1.058	14.47	0.483	8.605	4.154	0.271
8	Gr---------- Layer1:TiO_2(0.75g) + PEO(0.05g) Layer2: Cl_4BQ(0.3g)+ N,N-Dimethyl benzamide (0.2g)+ DMSO (1ml) + PEO(0.05g) Layer3: Cl_4BQ(0.3g)+ N,N-Dimethyl benzamide (0.2g)+ DMSO (1ml) + PEO(0.05g) Layer4: TiO_2(0.75g) + PEO(0.05g) Al----------	1 h	28 ºC	0.984	17.09	0.334	8.27	2.762	0.164
			35 ºC	0.964	21.83	0.343	10.94	3.75	0.178
			40 ºC	1.063	25.71	0.342	12.76	4.363	0.16
		48 h	40 ºC	1.09	21.47	0.309	9.551	2.954	0.126
		96 h	40 ºC	1.09	13.4	0.396	5.919	2.341	0.16

Table ES2 TiO_2 in edge layer,Cl_4BQ in middle layers, DMSO used as solvent.

Cell Configuration 4 (Figure 5) (Cl_4BQ in 4 layers)

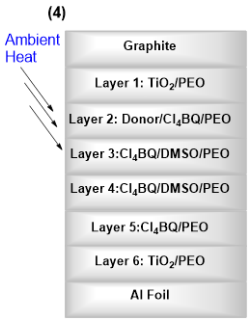

(Entries 11-12)

Cell Configuration 5 (Figure 6) (Cl_4BQ in 1 layer)

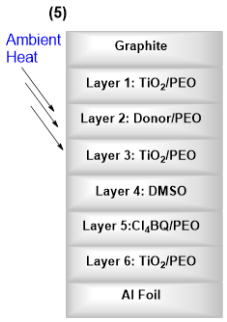

(Entries 13-14)

Entry	Cell Configuration	Time after packing	T °C[c]	Voc (V)	Isc (mA)	Vmax (V)	Imax (mA)	Pmax (mW)	Fill Factor
11	Gr---------- Layer1: TiO_2(0.5g) + PEO (0.05g) Layer2: Cl_4BQ(0.25g) + PEO (0.05g) Layer3: Cl_4BQ(0.05g) +DMSO(0.5ml) + PEO (0.05g) Layer4: Cl_4BQ(0.05g) +DMSO(0.5ml) + PEO (0.05g) Layer5: TMPDA(0.05g) + Cl_4BQ(0.25g) + PEO (0.05g) Layer6: TiO_2(0.5g) + PEO (0.05g) Al----------	1 h	28 °C 35 °C	1.105 1.126	9.631 21.03	0.464 0.525	5.252 13.8	2.437 7.236	0.229 0.306
		48 h	35 °C	1.126	13.76	0.502	8.235	4.13	0.267
		96 h	35 °C	1.08	3.978	0.416	1.93	0.802	0.187
12	Gr---------- Layer1:TiO_2(0.5g) + PEO(0.05g) Layer2: Cl_4BQ(0.25g) + N,N-Diisopropylbenzamide (0.05g)+ PEO(0.05g) Layer3: Cl_4BQ (0.05g) + DMSO (0.5ml) + PEO(0.05g) Layer4: Cl_4BQ (0.05g) + DMSO (0.5ml) + PEO(0.05g) Layer5: DiPrBA(0.05g) + Cl_4BQ(0.25g) + PEO(0.05g) Layer6: TiO_2(0.5g) + PEO(0.05g) Al----------	1 h	28 °C 35 °C	1.06 1.08	18.96 27.29	0.429 0.496	9.263 13.91	3.976 6.9	0.198 0.234
		48 h	35 °C	1.129	14.24	0.477	7.37	3.514	0.219
		96 h	35 °C	1.132	8.139	0.494	4.298	2.121	0.23
13	Gr---------- Layer1:TiO_2(0.5g) + PEO(0.05g) Layer2: DIPEA (0.2ml)+ PEO(0.05g) Layer3: TiO_2(0.5g) + PEO(0.05g) Layer4: DMSO (1ml) Layer5: Cl_4BQ(0.25g) + PEO(0.05g) Layer6: TiO_2(0.5g) + PEO(0.05g) Al----------	1 h	28 °C 35 °C	0.975 0.994	10.13 12.39	0.253 0.312	5.476 8.033	1.384 2.502	0.14 0.203
		48 h	35 °C	1.072	6.412	0.398	3.015	1.199	0.174
		96 h	35 °C	1.074	5.682	0.396	2.818	1.115	0.183
14	Gr---------- Layer1:TiO_2(0.5g) + PEO(0.05g) Layer2: TMPDA (0.25g)+ PEO(0.05g) Layer3: TiO_2(0.5g) + PEO(0.05g) Layer4: DMSO (1ml) Layer5: Cl_4BQ(0.25g) + PEO(0.05g) Layer6: TiO_2(0.5g) + PEO(0.05g) Al----------	1 h	28 °C 35 °C	0.886 0.916	5.633 8.909	0.436 0.508	2.841 4.464	1.239 2.267	0.248 0.278
		48 h	35 °C	0.942	7.401	0.372	3.614	1.343	0.193
		96 h	35 °C	0.892	2.373	0.316	1.062	0.335	0.158

Table ES3 TiO_2 in edge layer,Cl_4BQ in middle layers, DMSO used as solvent.

Cell Configuration 6 (Figure 7) (Cl_4BQ in 4 layers)

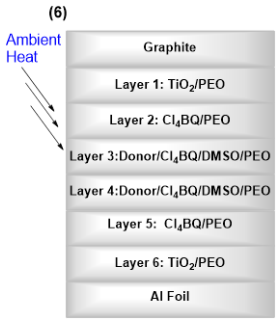

(Entries 15-16)

Cell Configuration 7 (Figure 8) (Cl_4BQ in 4 layer)

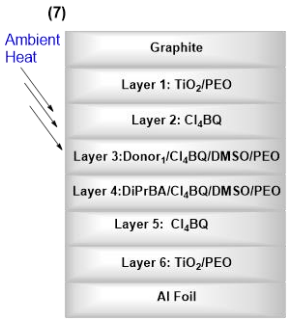

(Entries 17-21)

Cell Configuration 8 (Figure 9) (Cl_4BQ in 4 layer)

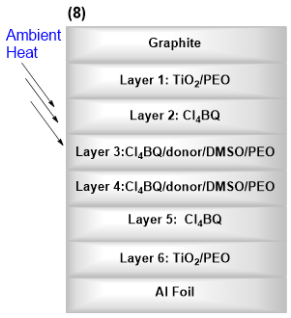

(Entries 22-24)

Entry	Cell Configuration	Time after packing	T °C[c]	Voc (V)	Isc (mA)	Vmax (V)	Imax (mA)	Pmax (mW)	Fill Factor
15	Gr---------- Layer1:TiO_2(0.5g) + PEO(0.05g) Layer2: Cl_4BQ(0.25g) + PEO(0.05g) Layer3: Cl_4BQ (0.025g) + DiPrBA (0.1g) + DMSO (0.5ml) + PEO(0.05g) Layer4: Cl_4BQ (0.025g) + DiPrBA (0.1g) +DMSO (0.5ml) + PEO(0.05g) Layer5: Cl_4BQ(0.25g) + PEO(0.05g) Layer6: TiO_2(0.5g) + PEO(0.05g) Al----------	1 h	28 °C	1.082	20.31	0.46	10.05	4.618	0.21
			35 °C	1.106	26.55	0.503	13.47	6.77	0.231
		48 h	35 °C	1.15	17.86	0.454	9.053	4.112	0.2
		96 h	35 °C	1.147	10.5	0.46	5.26	2.418	0.201
16	Gr---------- Layer1:TiO_2(0.5g) + PEO(0.05g) Layer2: Cl_4BQ(0.25g) + PEO(0.05g) Layer3: Cl_4BQ (0.025g) + TMPDA (0.1g) + DMSO (0.5ml) + PEO(0.05g) Layer4: Cl_4BQ (0.025g) + TMPDA (0.1g) +DMSO (0.5ml) + PEO(0.05g) Layer5: Cl_4BQ(0.25g) + PEO(0.05g) Layer6: TiO_2(0.5g) + PEO(0.05g) Al----------	1 h	28 °C	1.033	9.101	0.461	5.298	2.443	0.26
			35 °C	1.049	14.33	0.526	8.588	4.515	0.301
		48 h	35 °C	1.049	6.957	0.443	3.389	1.501	0.206
		96 h	35 °C	0.971	2.651	0.402	1.161	0.466	0.181
17	Gr---------- Layer1:TiO_2(0.75g) + PEO(0.05g) Layer2: Cl_4BQ(0.12g) Layer3: Cl_4BQ(0.12g) + DIPEA (0.1ml) + DMSO (0.7ml)+ PEO(0.05g) Layer4: Cl_4BQ(0.12g) + DiPrBA (0.1g) + DMSO (0.7ml)+ PEO(0.05g) Layer5: Cl_4BQ(0.12g) Layer6: TiO_2(0.75g) + PEO(0.05g) Al----------	1 h	28 °C	1.065	29.18	0.442	15.29	6.758	0.218
			35 °C	0.984	30.33	0.482	15.68	7.554	0.253
			40 °C	1.036	29.39	0.515	15.4	7.933	0.261
		48 h	40 °C	1.125	12.04	0.496	6.215	3.084	0.228
		96 h	40 °C	1.125	12.59	0.497	6.994	3.478	0.246
18	Gr---------- Layer1:TiO_2(0.75g) + PEO(0.05g) Layer2: Cl_4BQ(0.12g) Layer3: Cl_4BQ(0.12g) + DABCO (0.055g) + DMSO (0.7ml)+ PEO(0.05g) Layer4: Cl_4BQ(0.12g) + DiPrBA (0.1g) + DMSO (0.7ml)+ PEO(0.05g) Layer5: Cl_4BQ(0.12g) Layer6: TiO_2(0.75g) + PEO(0.05g) Al----------	1 h	28 °C	1.018	38.0	0.43	18.67	8.026	0.208
			35 °C	1.062	31.03	0.506	16.9	8.544	0.259
			40 °C	1.011	39.36	0.473	20.52	9.699	0.244
		48 h	40 °C	1.115	13.14	0.522	7.02	3.664	0.25
		96 h	40 °C	1.043	11.76	0.516	7.114	3.671	0.299

19	Gr---------- Layer1:TiO_2(0.75g) + PEO(0.05g) Layer2: Cl_4BQ(0.12g) Layer3: Cl_4BQ(0.12g) + PhNEt2 (0.1ml) + DMSO (0.7ml)+ PEO(0.05g) Layer4: Cl_4BQ(0.12g) + DiPrBA (0.1g) + DMSO (0.7ml)+ PEO(0.05g) Layer5: Cl_4BQ(0.12g) Layer6: TiO_2(0.75g) + PEO(0.05g) Al----------	1 h	28 ºC	1.038	21.22	0.492	10.9	5.357	0.243
			35 ºC	1.004	27.8	0.443	14.45	6.403	0.229
			40 ºC	1.005	28.73	0.484	14.76	7.144	0.248
		48 h	40 ºC	1.11	20.74	0.559	11.28	6.304	0.274
		96 h	40 ºC	1.094	10.99	0.55	6.3	3.465	0.288
20	Gr---------- Layer1:TiO_2(0.75g) + PEO(0.05g) Layer2: Cl_4BQ(0.12g) Layer3: Cl_4BQ(0.12g) + TPA (0.12g) + DMSO (0.7ml)+ PEO(0.05g) Layer4: Cl_4BQ(0.12g) + DiPrBA (0.1g) + DMSO (0.7ml)+ PEO(0.05g) Layer5: Cl_4BQ(0.12g) Layer6: TiO_2(0.75g) + PEO(0.05g) Al----------	1 h	28 ºC	0.98	5.708	0.5	2.914	1.457	0.261
			35 ºC	0.985	7.004	0.53	3.839	2.036	0.295
			40 ºC	1.001	7.444	0.565	4.487	2.535	0.34
		48 h	40 ºC	1.069	7.54	0.497	4.715	2.342	0.291
		96 h	40 ºC	1.103	5.686	0.527	3.264	1.719	0.27
21	Gr---------- Layer1:TiO_2(0.75g) + PEO(0.05g) Layer2: Cl_4BQ(0.12g) Layer3: Cl_4BQ(0.12g) + TMPDA (0.08g) + DMSO (0.7ml)+ PEO(0.05g) Layer4: Cl_4BQ(0.12g) + DiPrBA (0.1g) + DMSO (0.7ml)+ PEO(0.05g) Layer5: Cl_4BQ(0.12g) Layer6: TiO_2(0.75g) + PEO(0.05g) Al----------	1 h	28 ºC	1.027	14.39	0.575	7.261	4.172	0.282
			35 ºC	1.036	18.12	0.734	7.845	5.758	0.307
			40 ºC	1.046	18.86	0.759	8.39	6.37	0.323
		48 h	40 ºC	1.059	20.35	0.603	14.28	8.603	0.399
		96 h	40 ºC	0.982	12.1	0.467	7.98	3.727	0.314
22	Gr---------- Layer1:TiO_2(0.75g) + PEO(0.05g) Layer2: Cl_4BQ(0.12g) Layer3: Cl_4BQ(0.12g) + N,N-Diethyl benzamide (0.1g) + DMSO (0.7ml)+ PEO(0.05g) Layer4: Cl_4BQ(0.12g) + N,N-Diethyl benzamide (0.1g) + DMSO (0.7ml)+ PEO(0.05g) Layer5: Cl_4BQ(0.12g) Layer6: TiO_2(0.75g) + PEO(0.05g) Al----------	1 h	28 ºC	0.929	15.76	0.375	8.13	3.045	0.208
			35 ºC	0.966	17.79	0.436	9.225	4.018	0.234
			40 ºC	0.989	18.4	0.458	10.04	4.6	0.253
		48 h	40 ºC	1.142	8.688	0.533	4.934	2.631	0.265
		96 h	40 ºC	1.111	4.559	0.508	2.646	1.345	0.266
23	Gr---------- Layer1:TiO_2(0.75g) + PEO(0.05g) Layer2: Cl_4BQ(0.12g) Layer3: Cl_4BQ(0.12g) + N,N-Diisopropyl benzamide (0.1g) + DMSO (0.7ml)+ PEO(0.05g) Layer4: Cl_4BQ(0.12g) + N,N-Diisopropyl benzamide (0.1g) + DMSO (0.7ml)+ PEO(0.05g) Layer5: Cl_4BQ(0.12g) Layer6: TiO_2(0.75g) + PEO(0.05g) Al----------	1 h	28 ºC	0.953	16.39	0.433	8.711	3.768	0.241
			35 ºC	0.972	17.26	0.474	10.04	4.754	0.283
			40 ºC	0.992	16.63	0.494	10.15	5.009	0.304
		48 h	40 ºC	1.141	9.966	0.557	5.915	3.292	0.29
		96 h	40 ºC	1.124	8.952	0.545	5.688	3.098	0.308
24	Gr---------- Layer1:TiO_2(0.75g) + PEO(0.05g) Layer2: Cl_4BQ(0.12g) Layer3: Cl_4BQ(0.12g) + N,N-Dimethyl benzamide (0.1g) + DMSO (0.7ml)+ PEO(0.05g) Layer4: Cl_4BQ(0.12g) + N,N-Dimethyl benzamide (0.1g) + DMSO (0.7ml)+ PEO(0.05g) Layer5: Cl_4BQ(0.12g) Layer6: TiO_2(0.75g) + PEO(0.05g) Al----------	1 h	28 ºC	0.926	9.216	0.354	4.642	1.641	0.192
			35 ºC	0.936	12.35	0.39	6.486	2.529	0.219
			40 ºC	0.954	12.56	0.42	6.89	2.896	0.242
		48 h	40 ºC	1.106	8.01	0.426	4.024	1.712	0.199
		96 h	40 ºC	1.082	5.931	0.442	3.263	1.442	0.225

Table ES4 TiO_2 in edge layer,Cl_4BQ in middle layers, DMSO used as donor in PC solvent.

Cell Configuration 9 (Figure 10) (Cl_4BQ in 4 layers)

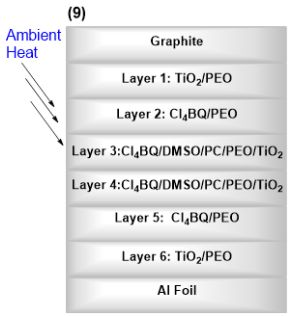

(Entries 25)

Cell Configuration 10 (Figure 11) (Cl_4BQ and BQ in 4 layer)

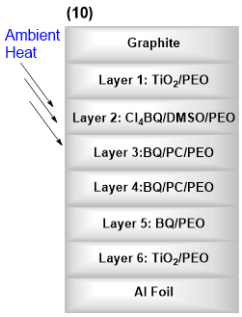

(Entries 26)

Cell Configuration 11 (Figure 12) (Cl_4BQ and BQ in 4 layer)

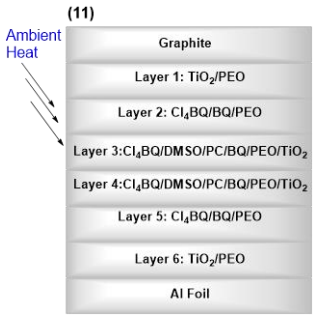

(Entries 27)

Entry	Cell Configuration	Time after packing	T °C[c]	Voc (V)	Isc (mA)	Vmax (V)	Imax (mA)	Pmax (mW)	Fill Factor
25	Gr---------- Layer1:TiO_2(0.5g) + PEO(0.05g) Layer2: Cl_4BQ(0.1g) + PEO(0.05g) Layer3: Cl_4BQ(0.025g)+DMSO(0.078g) + PC (0.5g) + PEO(0.05g)+ TiO_2(0.25g) Layer4: Cl_4BQ(0.025g)+DMSO(0.078g) + PC (0.5g) + PEO(0.05g)+ TiO_2(0.25g) Layer5: Cl_4BQ(0.1g) + PEO (0.05g) Layer6: TiO_2(0.5g) + PEO(0.05g) Al----------	1 h	28 °C	0.961	23.15	0.503	12.19	6.135	0.276
			35 °C	0.953	22.8	0.533	12.83	6.833	0.315
			40 °C	0.964	20.77	0.57	12.84	7.318	0.366
		48 h	28 °C	1.019	15.96	0.508	10.86	5.511	0.339
			35 °C	1.01	18.65	0.567	12.63	7.159	0.38
			40 °C	0.989	17.59	0.602	12.73	7.669	0.441
		96 h	40 °C	1.03	11.2	0.503	8.466	4.256	0.369
26	Gr---------- Layer1:TiO_2(0.5g) + PEO(0.05g) Layer2: Cl_4BQ(0.5g) + DMSO (0.156g)+ PEO(0.05g) Layer3: BQ(0.11g) + PC (0.5ml)+ PEO(0.05g) Layer4: BQ(0.11g) + PC (0.5ml)+ PEO(0.05g) Layer5: BQ(0.22g) + PEO(0.05g) Layer6: TiO_2(0.5g) + PEO(0.05g) Al----------	1 h	28 °C	1.166	13.91	0.461	5.346	2.462	0.159
			35 °C	1.128	14.69	0.485	6.268	3.04	0.183
			40 °C	1.14	15.31	0.526	6.638	3.488	0.2
		48 h	28 °C	1.175	8.864	0.41	3.634	1.491	0.143
			35 °C	1.17	11.04	0.462	4.834	2.231	0.173
			40 °C	1.173	10.5	0.489	4.585	2.241	0.182
		96 h	40°C	1.059	14.66	0.448	6.752	3.027	0.195
27	Gr---------- Layer1:TiO_2(0.5g) + PEO(0.05g) Layer2: Cl_4BQ(0.1g) + BQ(0.1g) + PEO(0.05g) Layer3: Cl_4BQ(0.025g)+DMSO(0.078g) + PC (0.5g) + BQ(0.1g) + PEO(0.05g)+ TiO_2(0.25g) Layer4: Cl_4BQ(0.025g)+DMSO(0.078g) + PC (0.5g) + BQ(0.1g) + PEO(0.05g)+ TiO_2(0.25g) Layer5: Cl_4BQ(0.1g) + BQ(0.1g) + PEO (0.05g) Layer6: TiO_2(0.5g) + PEO(0.05g) Al----------	1 h	28 °C	1.07	20.17	0.44	8.794	3.867	0.179
			35 °C	1.071	25.27	0.374	11.45	4.28	0.158
			40 °C	1.074	24.96	0.445	11.48	5.109	0.191
		48 h	28 °C	1.085	22.42	0.492	11.06	5.439	0.224
			35 °C	1.094	27.53	0.525	13.76	7.223	0.24
			40 °C	1.095	31.23	0.466	15.69	7.312	0.214
		96 h	40 °C	1.102	16.87	0.496	8.887	4.403	0.237

Table ES5 TiO_2 in edge layer,Cl_4BQ in middle layers, DMSO used as donor in PC solvent.

Cell Configuration 12 (Figure 13) (Cl_4BQ and BQ in 4 layer)

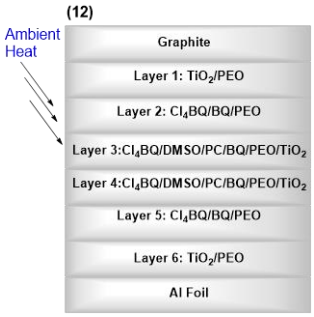

(Entries 28)

Cell Configuration 13 (Figure 14) (Cl_4BQ in 4 layer)

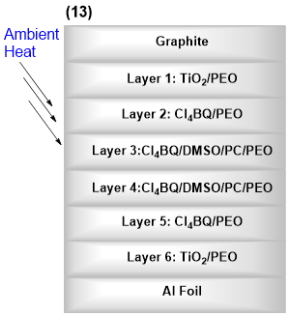

(Entries 29)

Cell Configuration 14 (Figure 15) (Cl_4BQ in 4 layer)

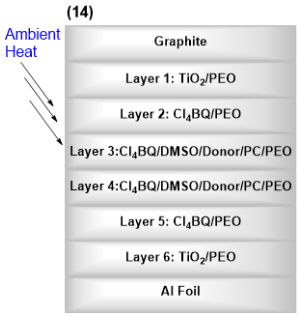

(Entries 30-32)

Entry	Cell Configuration	Time after packing	T °C[c]	Voc (V)	Isc (mA)	Vmax (V)	Imax (mA)	Pmax (mW)	Fill Factor
28	Gr---------- Layer1:TiO_2(1.0g) + PEO(0.1g) Layer2: Cl_4BQ(0.1g) +BQ(0.1g) +PEO(0.05g) Layer3: Cl_4BQ(0.025g)+DMSO(0.078g) + PC (0.5g) + BQ(0.1g) +PEO(0.05g)+ TiO_2(0.25g) Layer4: Cl_4BQ(0.025g)+DMSO(0.078g) + PC (0.5g) + BQ(0.1g) + PEO(0.05g)+ TiO_2(0.25g) Layer5: Cl_4BQ(0.1g) + BQ(0.1g) +PEO (0.05g) Layer6: TiO_2(1.0g) + PEO(0.1g) Al----------	1 h	28 °C	1.182	9.697	0.46	4.427	2.035	0.178
			35 °C	1.184	11.62	0.5	5.346	2.674	0.194
			40 °C	1.185	13.45	0.521	6.31	3.284	0.206
		48 h	28 °C	1.187	12.61	0.47	6.622	3.114	0.208
			35 °C	1.179	15.86	0.512	8.855	4.53	0.242
			40 °C	1.165	16.48	0.507	9.64	4.89	0.255
		96 h	40 °C	1.181	12.45	0.499	8.405	4.194	0.285
29	Gr---------- Layer1:TiO_2(0.75g) + PEO(0.025g) Layer2: Cl_4BQ(0.25g) + PEO(0.025g) Layer3: Cl_4BQ(0.05g) + DMSO (0.1ml) + PC (0.5ml) + PEO(0.05g) Layer4: Cl_4BQ(0.05g) + DMSO (0.1ml) + PC (0.5ml) + PEO(0.05g) Layer5: Cl_4BQ(0.25g) + PEO(0.025g) Layer6: TiO_2(0.75g) + PEO(0.05g) Al----------	1 h	28 °C	1.042	20.63	0.411	10.32	4.244	0.197
			35 °C	1.037	24.29	0.437	12.0	5.245	0.208
			40 °C	1.088	29.67	0.458	15.33	7.015	0.217
		48 h	28 °C	1.129	16.27	0.492	7.86	3.869	0.211
			35 °C	1.113	19.26	0.493	9.487	4.679	0.218
			40 °C	1.116	25.31	0.517	12.5	6.463	0.229
		96 h	28 °C	1.128	18.22	0.509	9.525	4.846	0.236
30	Gr---------- Layer1:TiO_2(0.75g) + PEO(0.025g) Layer2: Cl_4BQ(0.25g) + PEO(0.025g) Layer3: Cl_4BQ(0.1g) + DMSO (0.1ml) + PC (0.5ml) + DIPEA(0.1ml) + PEO(0.05g) Layer4: Cl_4BQ(0.1g) + DMSO (0.1ml) + PC (0.5ml) + DIPEA(0.1ml) + PEO(0.05g) Layer5: Cl_4BQ(0.25g) + PEO(0.025g) Layer6: TiO_2(0.75g) + PEO(0.05g) Al----------	1 h	28 °C	1.155	37.66	0.463	19.45	8.998	0.207
			35 °C	1.113	52.85	0.529	27.45	14.53	0.247
			40 °C	1.156	54.24	0.567	29.33	16.63	0.265
		48 h	28 °C	1.17	28.88	0.497	16.04	7.97	0.236
			35 °C	1.146	31.71	0.527	17.91	9.428	0.259
			40 °C	1.153	38.83	0.575	22.58	12.99	0.29
		96 h	28 °C	1.162	26.95	0.525	17.19	9.018	0.288
31	Gr---------- Layer1:TiO_2(0.75g) + PEO(0.05g) Layer2: Cl_4BQ(0.25g) + PEO(0.025g) Layer3: Cl_4BQ(0.1g) + DMSO (0.1ml) + PC (0.5ml) +	1 h	28 °C	1.075	28.42	0.402	13.72	5.509	0.18
			35 °C	1.064	36.3	0.421	16.94	7.131	0.185

	DiPrBA (0.1g) + PEO(0.05g) Layer4: Cl_4BQ(0.1g) + DMSO (0.1ml)+PC(0.5ml)+ DiPrBA (0.1g) + PEO(0.05g) Layer5: Cl_4BQ(0.25g) + PEO(0.025g) Layer6: TiO_2(0.75g) + PEO(0.05g) Al----------		40 °C	1.104	38.57	0.455	18.35	8.341	0.196
		48 h	28 °C	1.14	22.17	0.455	10.86	4.935	0.195
			35 °C	1.127	24.93	0.498	12.56	6.254	0.223
			40 °C	1.146	33.82	0.561	17.26	9.673	0.25
		96 h	28 °C	1.144	22.57	0.507	12.23	6.195	0.24
32	Gr---------- Layer1:TiO_2(0.75g) + PEO(0.05g) Layer2: Cl_4BQ(0.25g) + PEO(0.025g) Layer3: Cl_4BQ(0.1g) + DMSO (0.1ml) + PC (0.5ml) + TMPDA(0.1g) + PEO(0.05g) Layer4: Cl_4BQ(0.1g) + DMSO (0.1ml) + PC (0.5ml) + TMPDA(0.1g) + PEO(0.05g) Layer5: Cl_4BQ(0.25g) + PEO(0.025g) Layer6: TiO_2(0.75g) + PEO(0.05g) Al----------	1 h	28 °C	1.129	33.16	0.563	20.11	11.31	0.302
			35 °C	1.122	33.79	0.645	19.13	12.35	0.326
			40 °C	1.135	32.76	0.675	18.98	12.81	0.345
		48 h	28 °C	1.07	10.88	0.529	5.425	2.869	0.247
			35 °C	1.05	12.15	0.504	6.407	3.228	0.253
			40 °C	1.045	14.23	0.528	7.739	4.082	0.275
		96 h	28 °C	1.019	8.869	0.431	4.847	2.089	0.231

Table ES6 TiO_2 in edge layer,Cl_4BQ in edge layers, DMSO used as donor in PC solvent.

Cell Configuration 15 (Figure 16)

(Cl_4BQ in 2 layers)

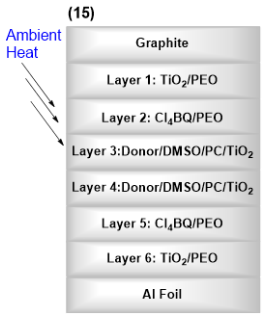

(Entries 33-34)

Cell Configuration 16 (Figure 17)

(Cl_4BQ in 1 layer & BQ in 1 layer)

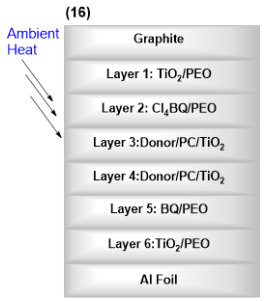

(Entries 35-37)

Entry	Cell Configuration	Time after packing	T °C[c]	Voc (V)	Isc (mA)	Vmax (V)	Imax (mA)	Pmax (mW)	Fill Factor
33	Gr---------- Layer1:TiO_2(0.5g) + PEO(0.05g) Layer2: Cl_4BQ(0.25g) + PEO(0.05g) Layer3: DIPEA(0.13g) + DMSO (0.188g)+ PC (0.5g)+ TiO_2(0.25g) Layer4: DIPEA(0.13g) + DMSO (0.188g)+ PC (0.5g)+ TiO_2(0.25g) Layer5: Cl_4BQ(0.25g) + PEO(0.05g) Layer6: TiO_2(0.5g) + PEO(0.05g) Al----------	1 h	28 °C	1.101	27.69	0.466	15.4	7.181	0.235
			35 °C	1.109	32.69	0.517	18.28	9.45	0.261
			40 °C	1.115	32.3	0.55	19.46	10.7	0.297
		48 h	28 °C	1.165	23.98	0.502	14.35	7.202	0.258
			35 °C	1.145	30.33	0.536	18.03	9.67	0.278
			40 °C	1.142	30.2	0.651	19.32	10.75	0.312
		96 h	40 °C	1.181	25.85	0.49	13.65	6.69	0.219
34	Gr---------- Layer1:TiO_2(0.5g) + PEO(0.05g) Layer2: Cl_4BQ(0.25g) + PEO(0.05g) Layer3: DiPrBA(0.205g) + DMSO (0.188g)+ PC (0.5g)+	1 h	28 °C	1.113	21.16	0.491	9.769	4.794	0.204
			35 °C	1.116	25.06	0.495	12.19	6.03	0.216

	TiO_2(0.25g) Layer4: DiPrBA (0.205g) + DMSO (0.188g)+ PC (0.5g)+ TiO_2(0.25g) Layer5: Cl_4BQ(0.25g) + PEO(0.05g) Layer6: TiO_2(0.5g) + PEO(0.05g) Al----------		40 ºC	1.115	23.4	0.502	11.96	6.005	0.23
		48 h	28 ºC	1.167	16.61	0.506	8.695	4.395	0.227
			35 ºC	1.156	22.65	0.535	11.73	6.271	0.239
			40 ºC	1.147	22.06	0.539	11.63	6.271	0.248
		96 h	40 ºC	1.183	8.575	0.507	4.322	2.192	0.216
35	Gr---------- Layer1:TiO_2(0.5g) + PEO(0.05g) Layer2: Cl_4BQ(0.25g) + PEO (0.05g) Layer3: DIPEA(0.26g) + PC (0.5g) + TiO_2(0.25g) Layer4: DIPEA(0.26g) + PC (0.5g) + TiO_2(0.25g) Layer5: BQ (0.44g)+ PEO(0.05g) Layer6: TiO_2(0.5g) + PEO(0.05g) Al----------	1 h	28 ºC	1.077	9.375	0.552	5.454	3.012	0.298
			35 ºC	1.087	12.14	0.534	6.849	3.656	0.277
			40 ºC	1.08	12.72	0.529	7.529	3.983	0.29
		48 h	28 ºC	1.116	4.265	0.520	2.241	1.166	0.245
			35 ºC	1.101	5.034	0.527	2.611	1.375	0.248
			40 ºC	1.108	5.247	0.516	2.740	1.412	0.243
		96 h	40 ºC	1.09	4.206	0.513	2.135	1.095	0.239
36	Gr---------- Layer1:TiO_2(0.5g) + PEO(0.05g) Layer2: Cl_4BQ(0.25g) + PEO (0.05g) Layer3: DMSO (0.188g) + PC (0.5g) + TiO_2(0.25g) Layer4: DMSO(0.188g) + PC (0.5g) + TiO_2(0.25g) Layer5: BQ (0.44g)+ PEO(0.05g) Layer6: TiO_2(0.5g) + PEO(0.05g) Al----------	1 h	28 ºC	1.016	24.38	0.396	9.338	3.7	0.149
			35 ºC	0.926	35.34	0.376	15.0	5.641	0.172
			40 ºC	1.033	37.48	0.38	16.19	6.156	0.159
		48 h	28 ºC	1.075	21.64	0.428	10.92	4.668	0.201
			35 ºC	1.071	27.76	0.460	14.78	6.805	0.229
			40 ºC	1.079	29.27	0.451	15.30	6.899	0.218
		96 h	40 ºC	1.074	16.62	0.503	9.403	4.725	0.265
37	Gr---------- Layer1:TiO_2(0.5g) + PEO(0.05g) Layer2: Cl_4BQ(0.25g) + PEO (0.05g) Layer3: DABCO(0.224g) + PC (0.5g) + TiO_2(0.25g) Layer4: DABCO(0.224g) + PC (0.5g) + TiO_2(0.25g) Layer5: BQ (0.44g)+ PEO(0.05g) Layer6: TiO_2(0.5g) + PEO(0.05g) Al----------	1 h	28 ºC	0.975	5.115	0.472	1.624	0.766	0.154
			35 ºC	0.98	7.103	0.456	2.844	1.297	0.186
			40 ºC	0.979	6.553	0.467	3.073	1.434	0.224
		48 h	28 ºC	0.852	3.742	0.414	1.658	0.685	0.215
			35 ºC	0.832	5.035	0.350	2.314	0.808	0.143
			40 ºC	0.855	5.431	0.388	2.492	0.967	0.208
		96 h	40 ºC	0.833	5.127	0.375	2.176	0.815	0.191

4.5 References

1 Yao, B.; Song, R.-J.; Liu, Y.; Xie, Y.-X.; Li, J.-H.; Wang, M.-K.; Tang, R.-Y.; Zhang, X.-G.; Deng, C.-L.; *Adv. Synth. Catal.* **2012**, *354*, 1890.

2 (a) Jiang, X.; Wang, C. Wei, Y.; Xue, D. Liu, Z.; Xiao, J. *Chem. Eur. J.* **2014**, *20*, 58.(b) Atkinson, B. N.; Williams, J. M. J. *ChemCatChem* **2014**, *6*, 1860.

3 Sun, K.; Wang, X.; Jiang, Y.; Lv, Y.; Zhang, L.; Xiao, B.; Li, D.; Zhu, Z.; Liu, L. *Chem. Asian. J.* **2015**, *10*, 536.

4 Sun, K.; Lv, Y.; Zhu, Z.; Zhang, L.; Wu, H.; Liu, L.; Jiang, Y.; Xiao, B.; Wang, X. *RSC. Adv.* **2015**, *5*, 3094.

5 Wang, J.; Rochon, F. D.; Yang, Y.; Hua, L.; Kayser, M. M. *Tetrahedron. Asymmetry* **2007**, *18*, 1115.

6 Mahajan, P. S.; Tanpure, S. D.; More, N. A.; Gajbhiye, J. M.; Mhaske, S. B. *RSC. Adv.*. **2015**, *5*, 101641.

7 Lv, Y.; Li, Y.; Xiong, T.; Pu, W.; Zhang, H.; Sun, K.; Liu, Q.; Zhang, Q. *Chem. Commun.* **2013**, *49*, 6439.

8 Pan, X.; Liu, Q.; Chang, L.; Yuan, G. *RSC. Adv.*. **2015**, *5*, 51183.

9 Wang, F.; Shen, J.; Cheng, G.; Cui, X. *RSC. Adv.*. **2015**, *5*, 73180.

10 Fei, H.; Yu, J.; Jiang, Y.; Guo, H.; Cheng, J.; *Org. Biomol. Chem.* **2013**, *11*,7092.

11 (a) Qian, J.; Zhang, Z.; Liu, Q.; Liu, T.; Zhang, G.; Adv. *Synth. Catal.* **2014**, *356*, 3119.

12 Cao, H.; Lei, S.; Li, N.; Chen, L.; Liu, J.; Cai, H.; Qiuaand, S.; Tan, J. *Chem. .Commun.* **2015**, *51*, 1823.

13 Chu, L.; Yue, X.; Qing, F. L.; *Org. Lett.* **2010**, *12*, 1644.

14 Xu, Y.; Cong, T.; Liu, P.; Sun, P. *Org. Biomol. Chem.* **2015**, *13*, 9742.

15 Liu, F.-L.; Chen, J.-R.; Zou, Y.-Q.; Wei, Q.; Xiao, W.-J. *Org. Lett.* **2014**, *16*, 3768.

16 Yuan, G.; Zheng, J.; Gao, X.; Li, X.; Huang, L.; Chen, H.; Jiang, H. *Chem. Commun.* **2012,** *48*, 7513.

17 Jiang, Y.; Loh, T.-P. *Chem. Sci*. **2014**, *5*, 4939.

18 Ren, X.; Chen, J.; Chen, F.; Cheng, J *Chem. Commun.* **2011**, *47*, 6725.

19 Shen, T.; Huang, X.; Liang, Y.-F.; Jiao, N. *Org. Lett.* **2015**, *17*, 6186.

20 Carlsen, L.; Egsgaard, H. *J. Am. Chem. Soc.* **1988**, *110*, 6701.

21 Roy, A. K.; Sarkar, B. K.; Sanyal, S. *Pramana- J. Phys.* **1990**, *35*, 389.

22 Shanmugaraja, M. Ph.D. Thesis **2018**, School of chemistry, University of Hyderabad.

23 Chernyak, Y. *J. Chem. Eng.* **2006**, *51*, 416.

24 Puranik, S. M.; Kumbharkhane, A. C.; Mehrotra, S. C. *J. Chem. Soc. Faraday Trans.* **1992**, *88*, 433.

Appendix I

(Representative Spectra)

Spectrum No. 1 (Chapter 2), ^{1}H NMR Spectrum (400 MHz, $CDCl_3$)

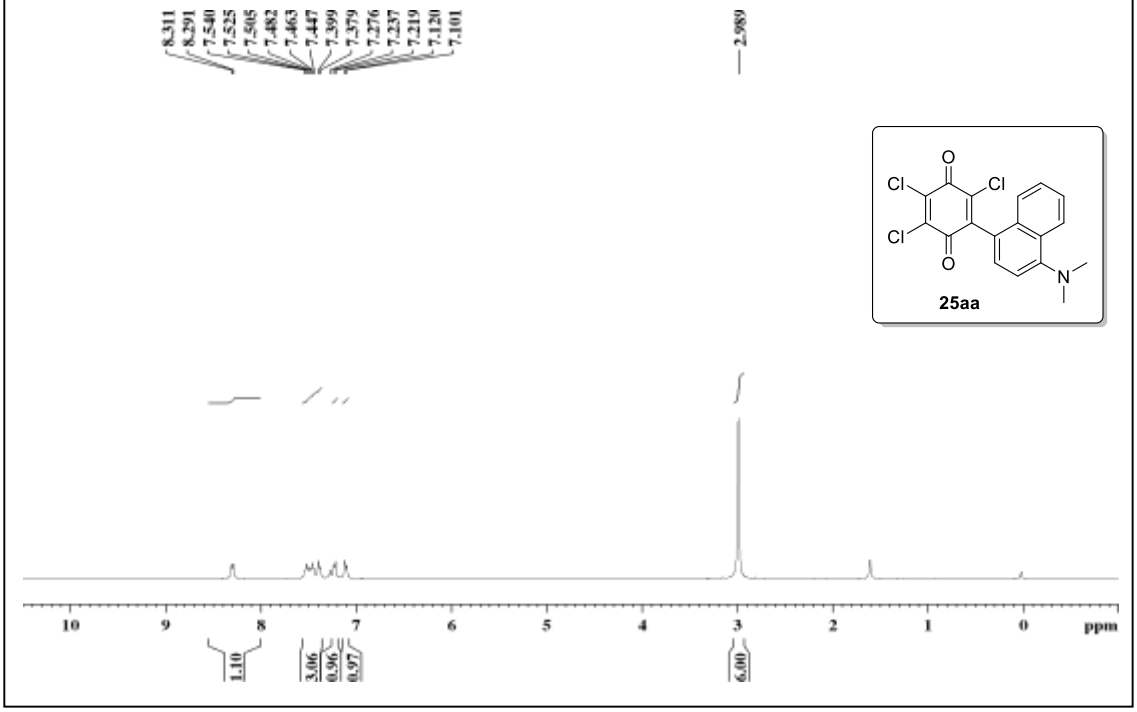

Spectrum No. 2 (Chapter 2), ^{13}C NMR Spectrum (100 MHz, $CDCl_3$)

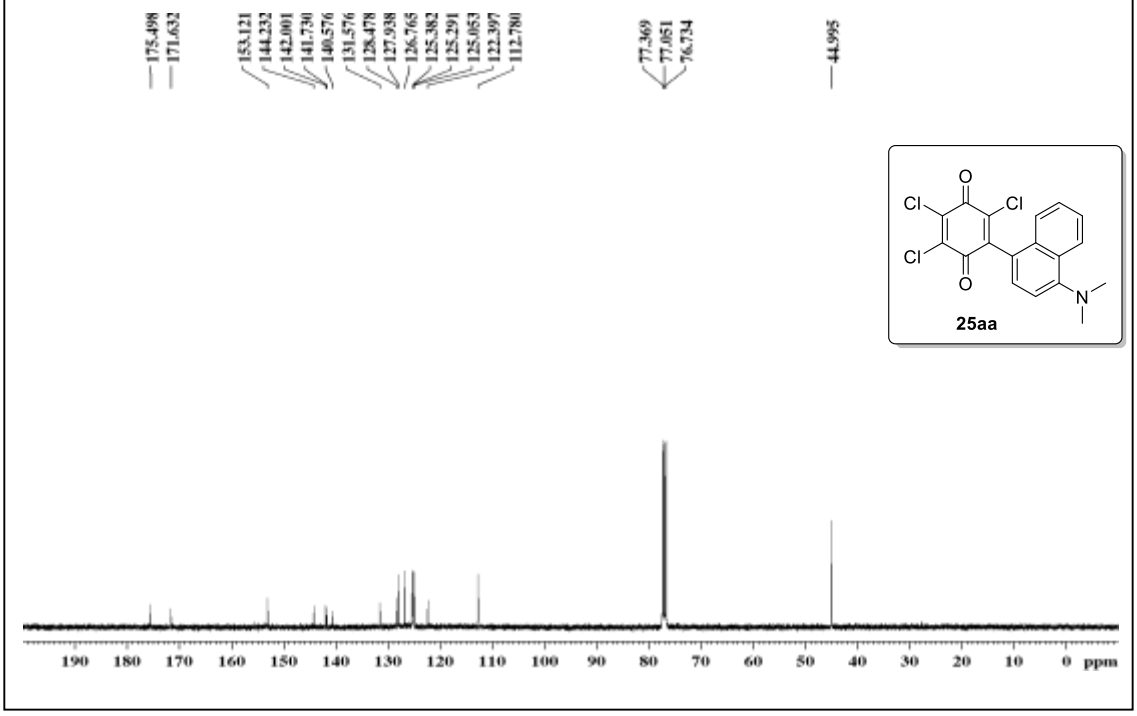

Spectrum No. 3 (Chapter 2), ^{1}H NMR Spectrum (400 MHz, $CDCl_3$)

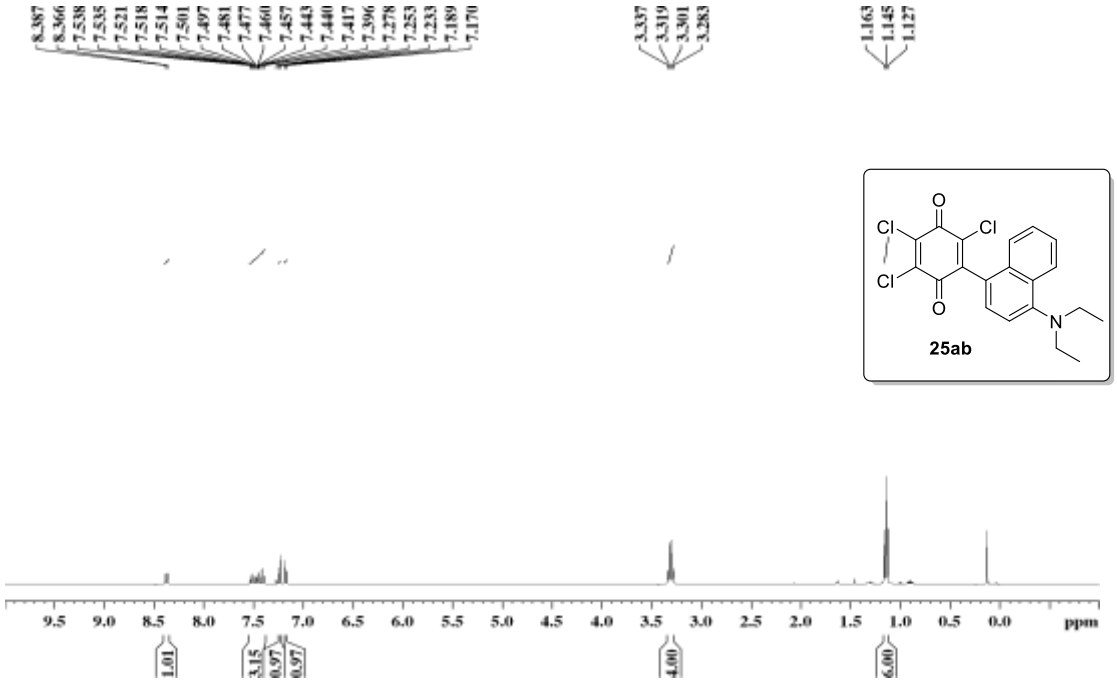

Spectrum No. 4 (Chapter 2), ^{13}C NMR Spectrum (100 MHz, $CDCl_3$)

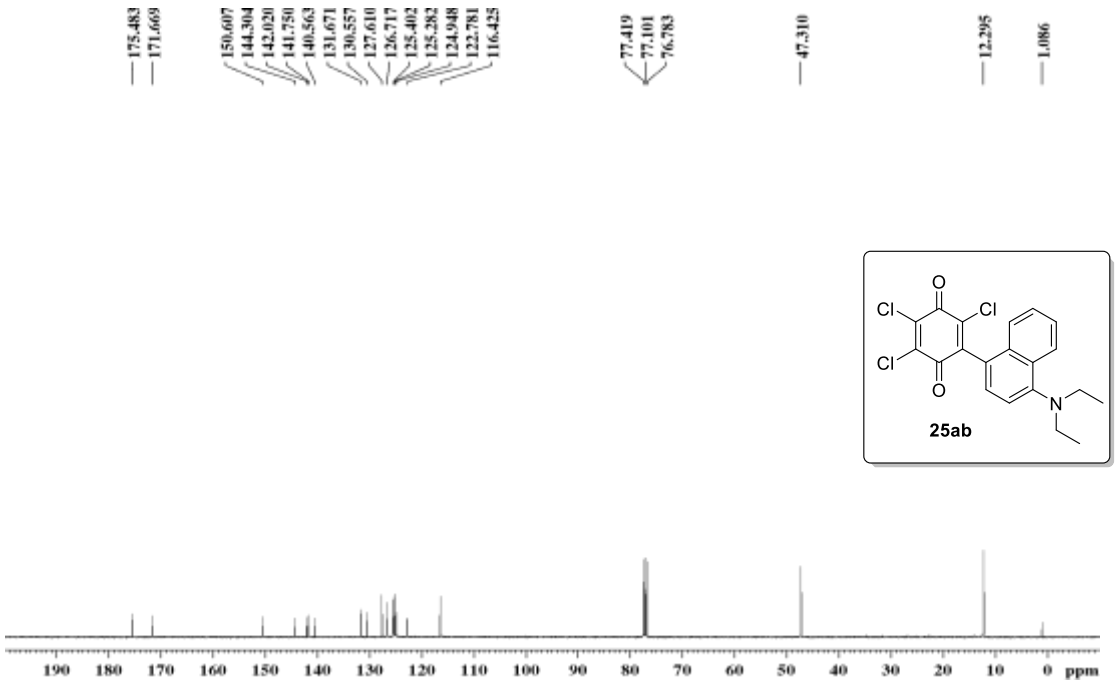

Spectrum No. 5 (Chapter 2), ^{1}H NMR Spectrum (400 MHz, $CDCl_3$)

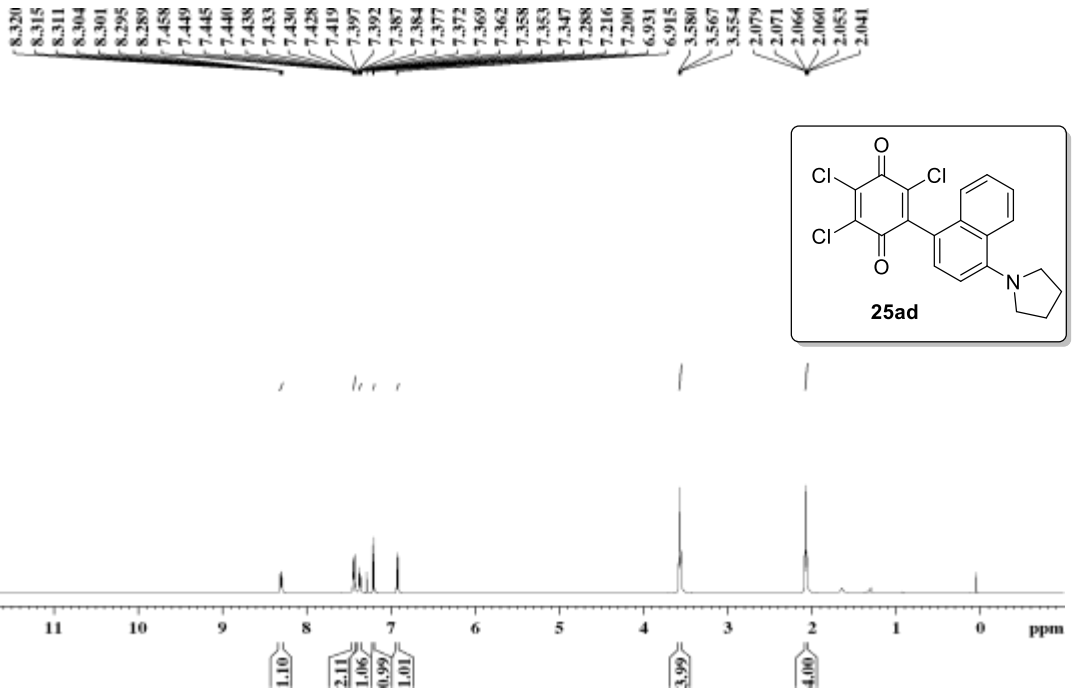

Spectrum No. 6 (Chapter 2), ^{13}C NMR Spectrum (100 MHz, $CDCl_3$)

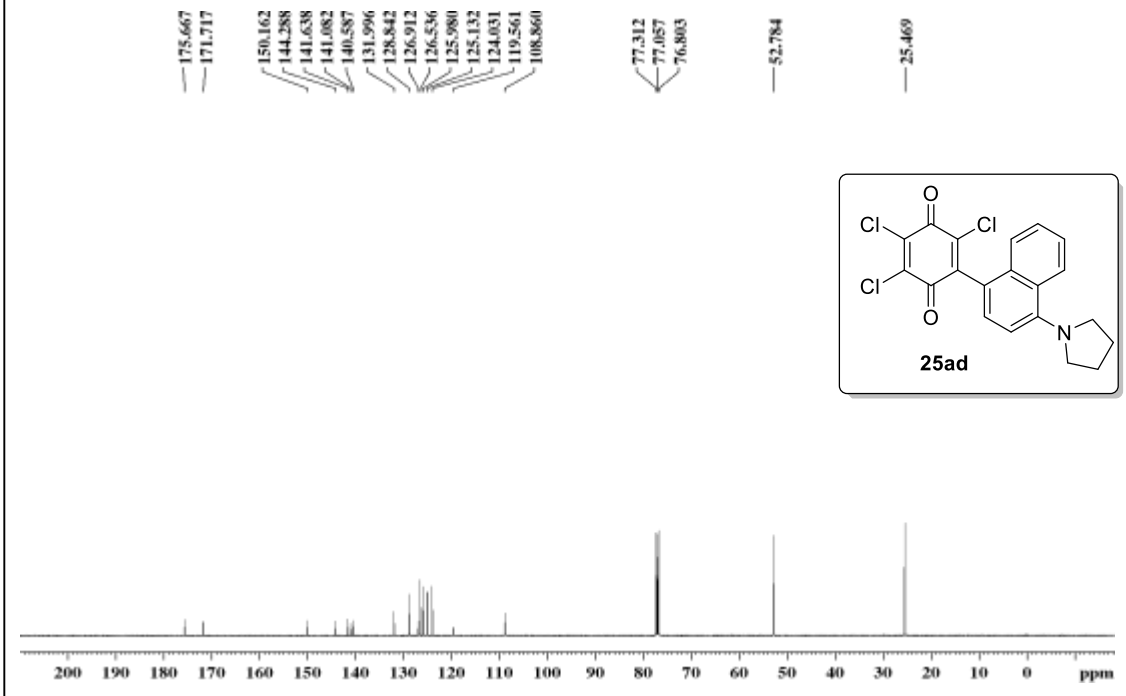

Spectrum No. 7 (Chapter 2), ^{1}H NMR Spectrum (400 MHz, $CDCl_3$)

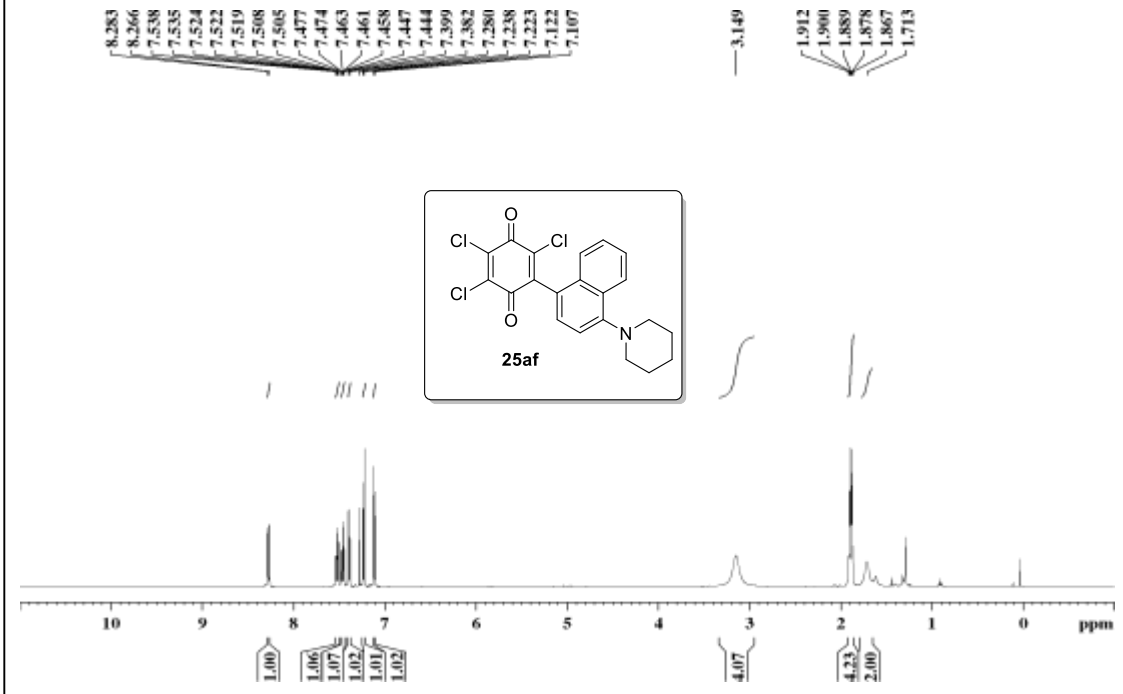

Spectrum No. 8 (Chapter 2), ^{13}C NMR Spectrum (100 MHz, $CDCl_3$)

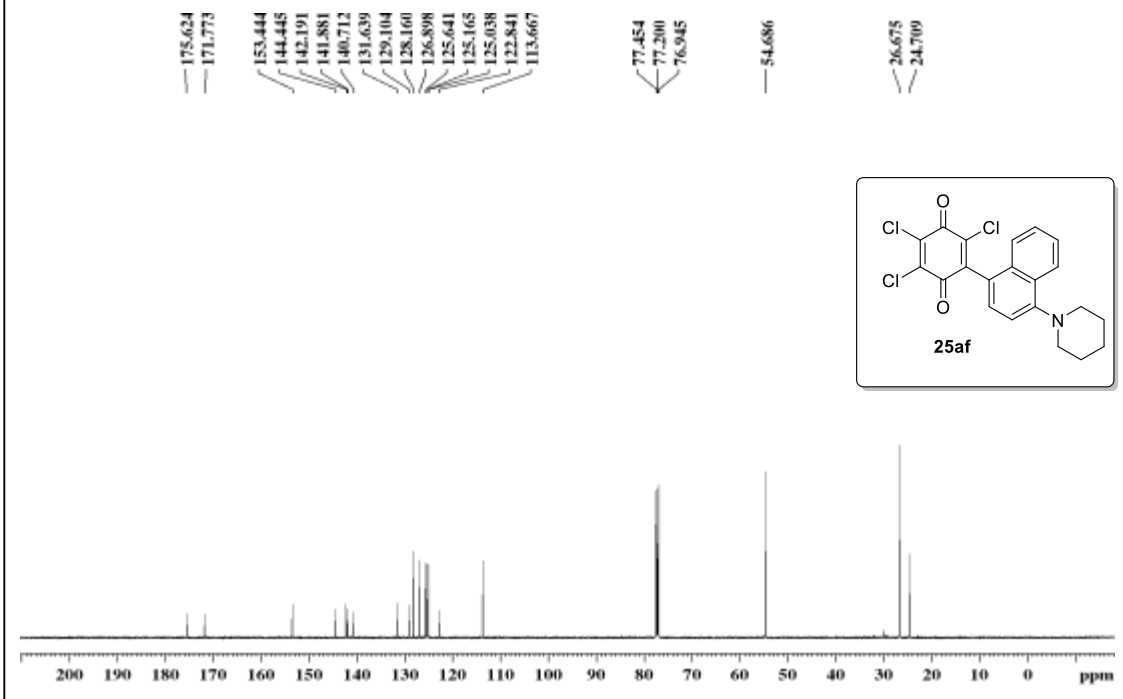

Spectrum No. 9 (Chapter 2), ^{1}H NMR Spectrum (400 MHz DMSO d_6)

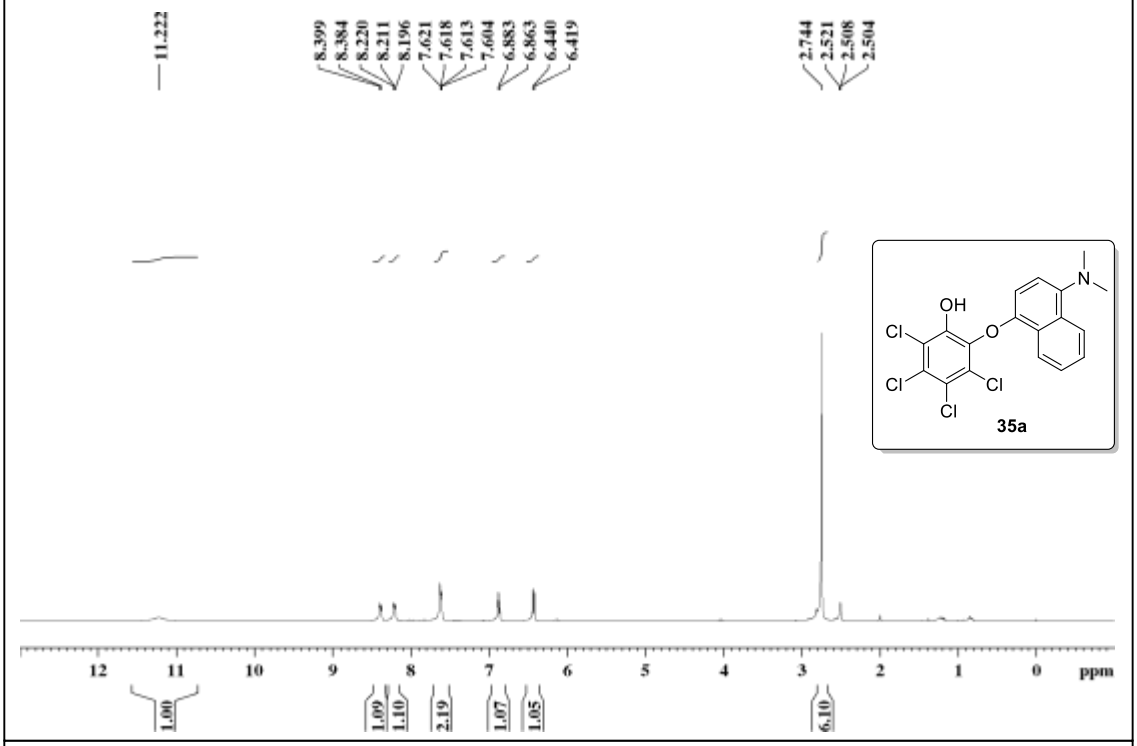

Spectrum No. 10 (Chapter 2), ^{13}C NMR Spectrum (100 MHz, DMSO d_6)

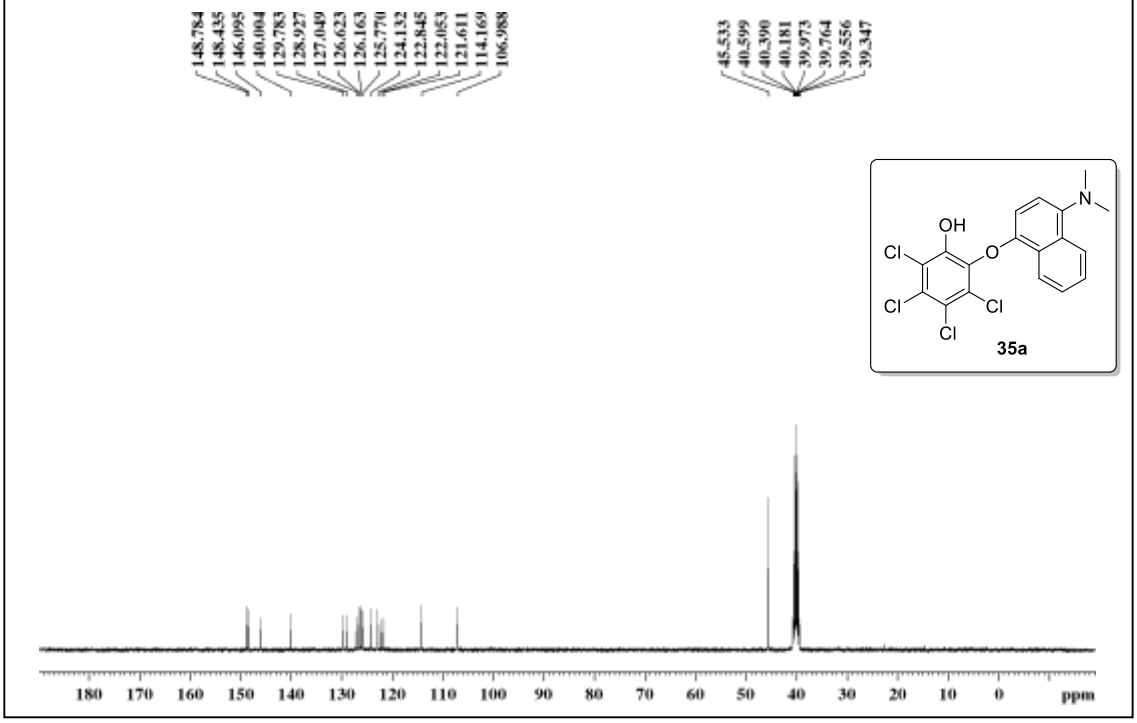

Spectrum No. 11 (Chapter 2), ^{1}H NMR Spectrum (400 MHz, DMSO d_6)

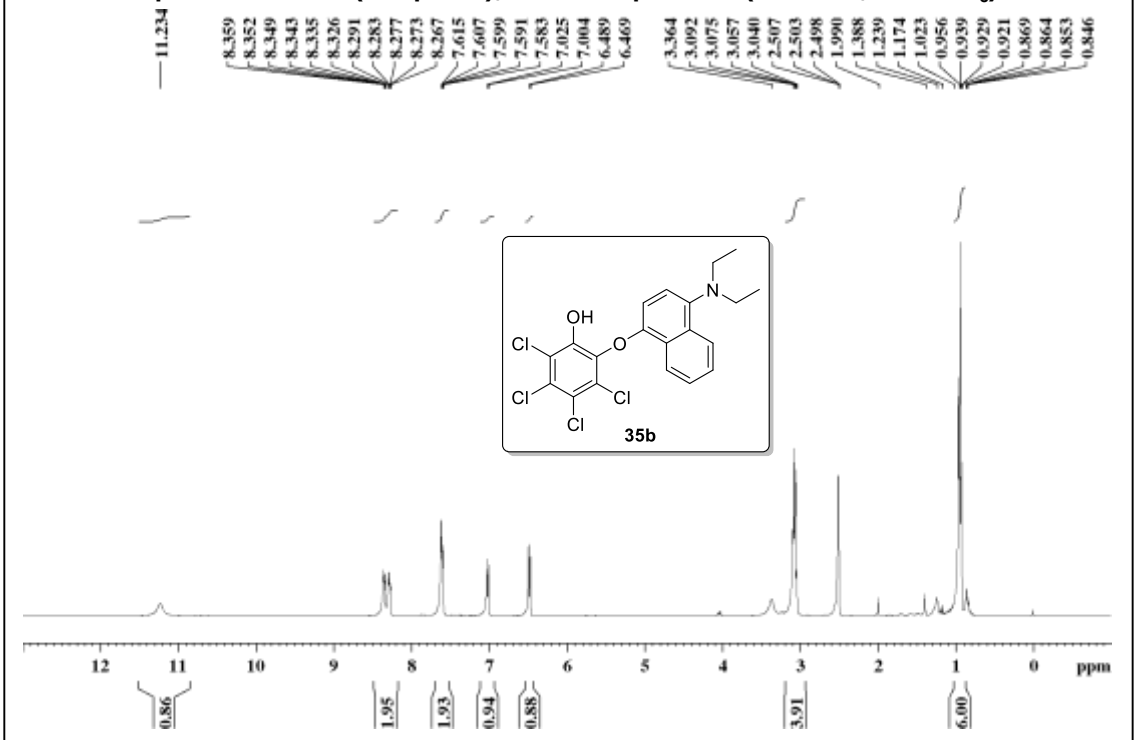

Spectrum No. 12 (Chapter 2), ^{13}C NMR Spectrum (100 MHz, DMSO d_6)

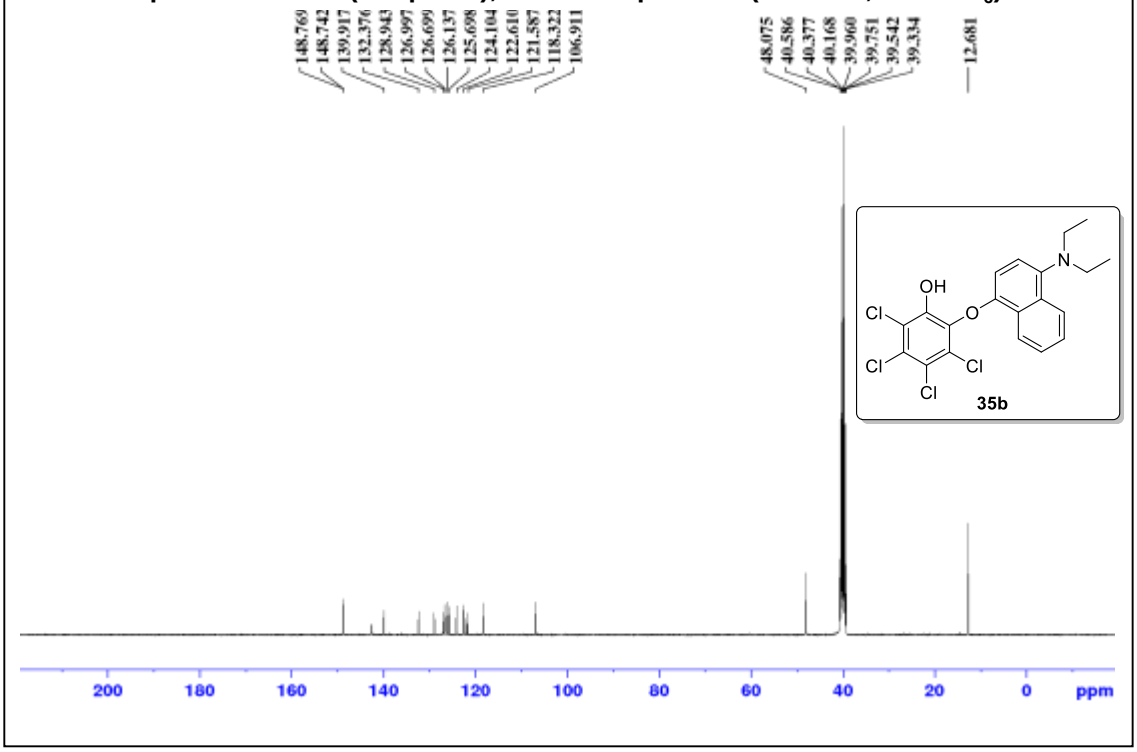

Spectrum No. 13 (Chapter 2), ^{1}H NMR Spectrum (400 MHz, DMSO d_6)

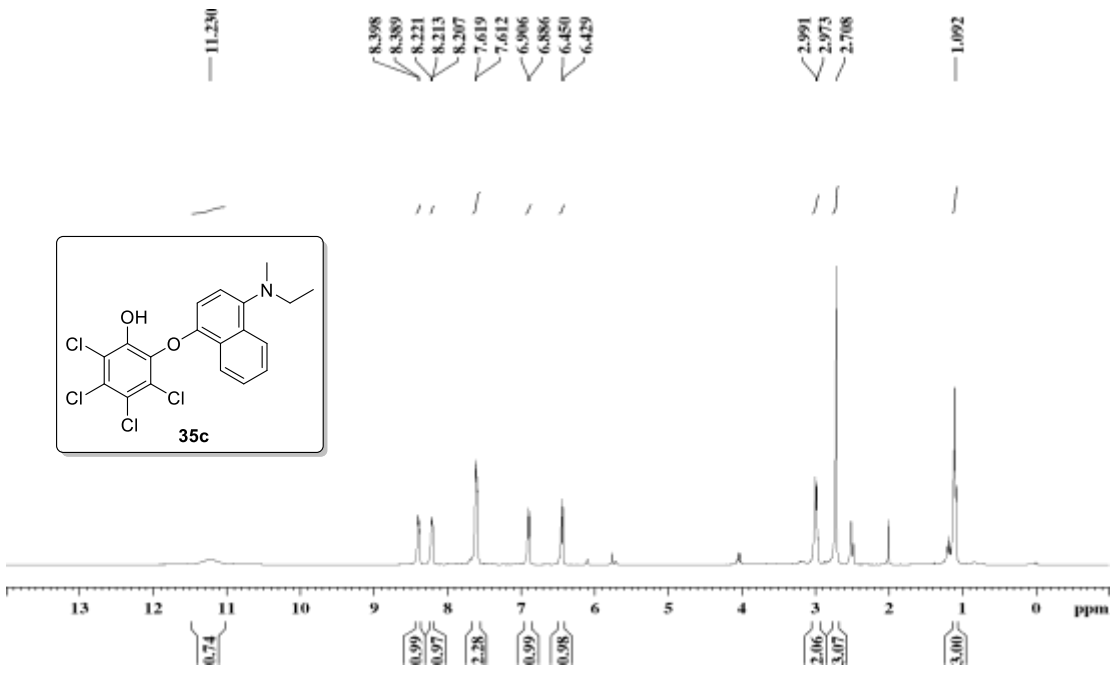

Spectrum No. 14 (Chapter 2), ^{13}C NMR Spectrum (100 MHz, DMSO d_6)

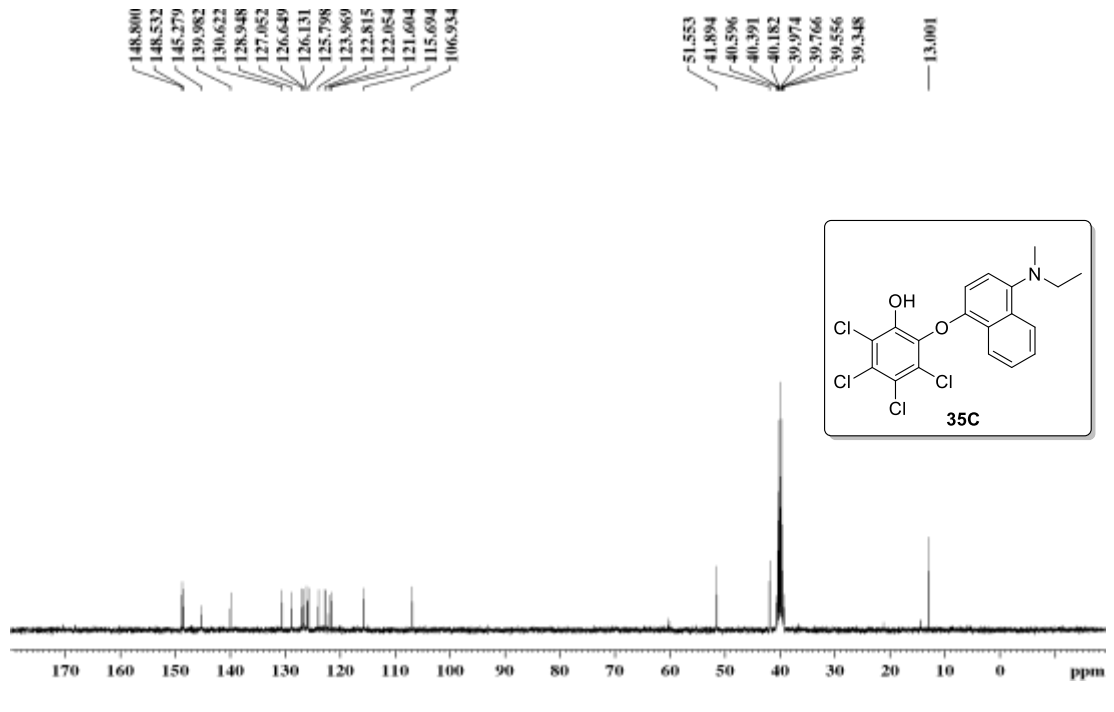

Spectrum No. 15 (Chapter 2), ^{1}H NMR Spectrum (400 MHz, $CDCl_3$)

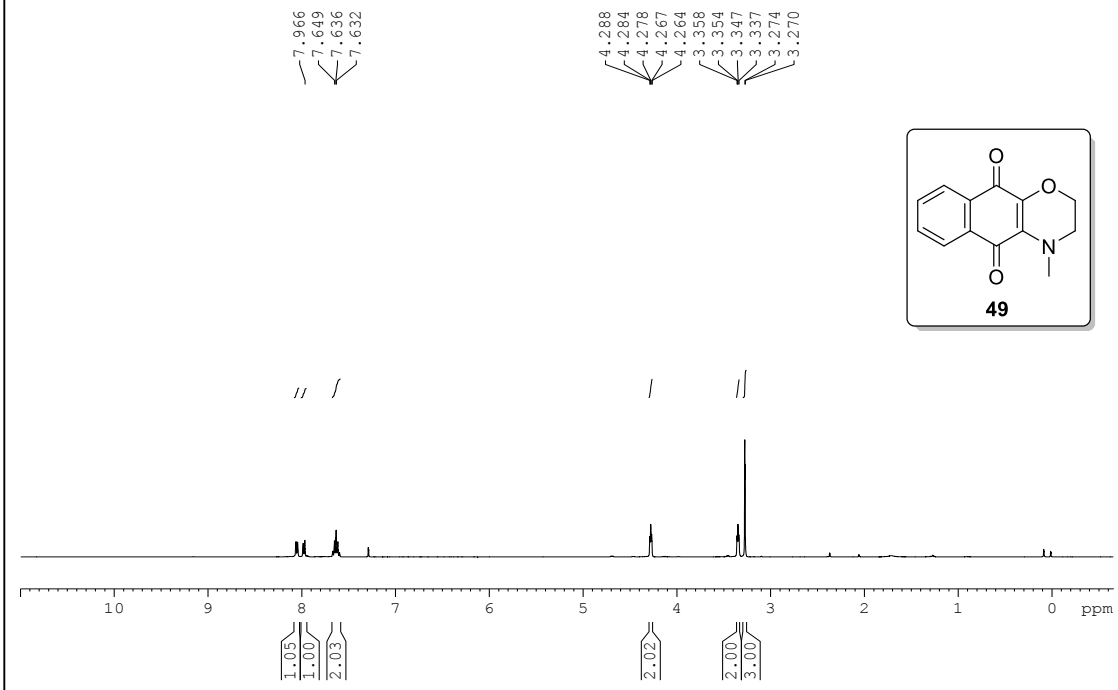

Spectrum No. 16 (Chapter 2), ^{13}C NMR Spectrum (100 MHz, $CDCl_3$)

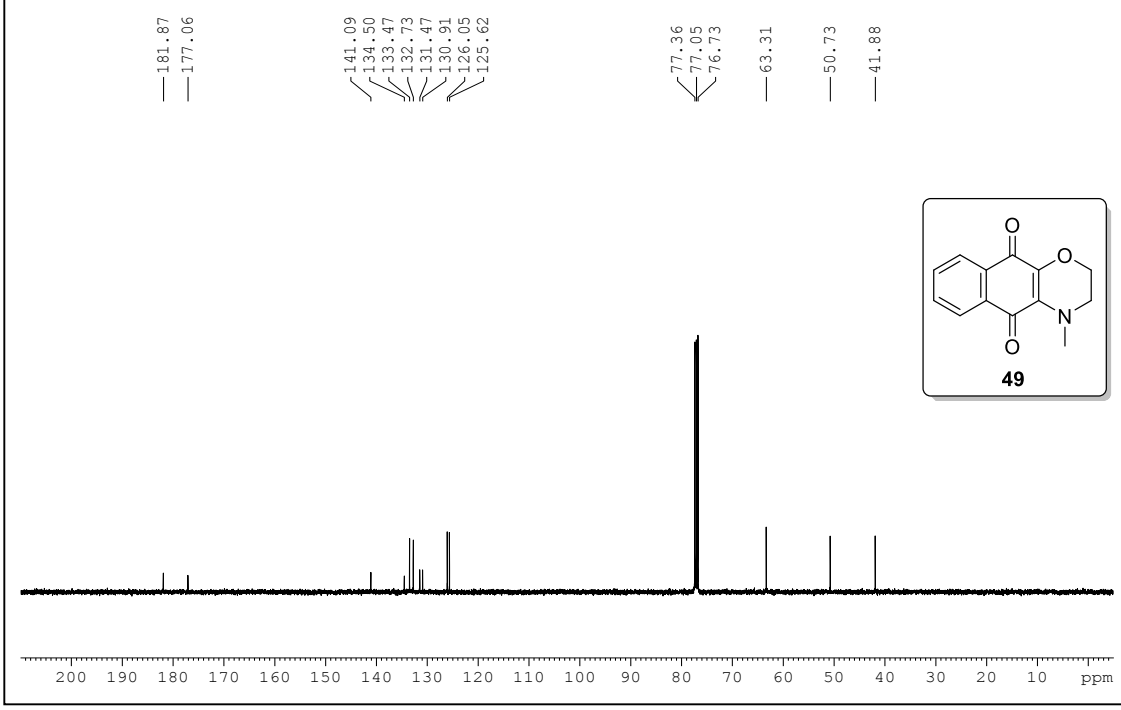

Spectrum No. 17 (Chapter 2), ^{11}H NMR Spectrum (400 MHz, $CDCl_3$)

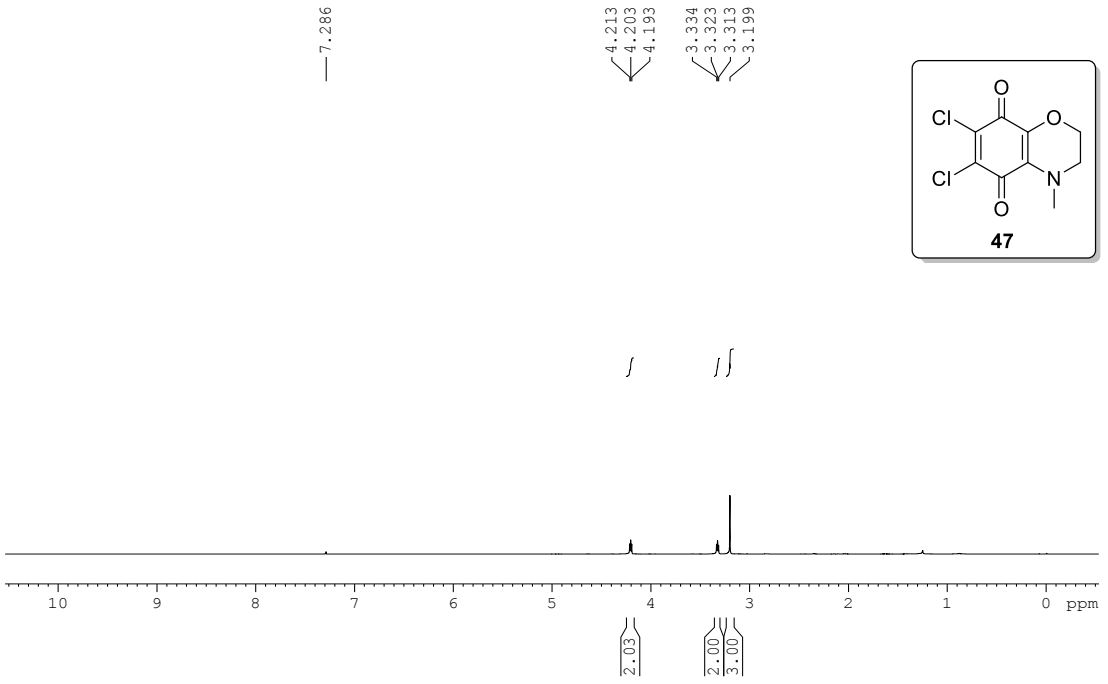

Spectrum No. 18 (Chapter 2), ^{1}H NMR Spectrum (100 MHz, $CDCl_3$)

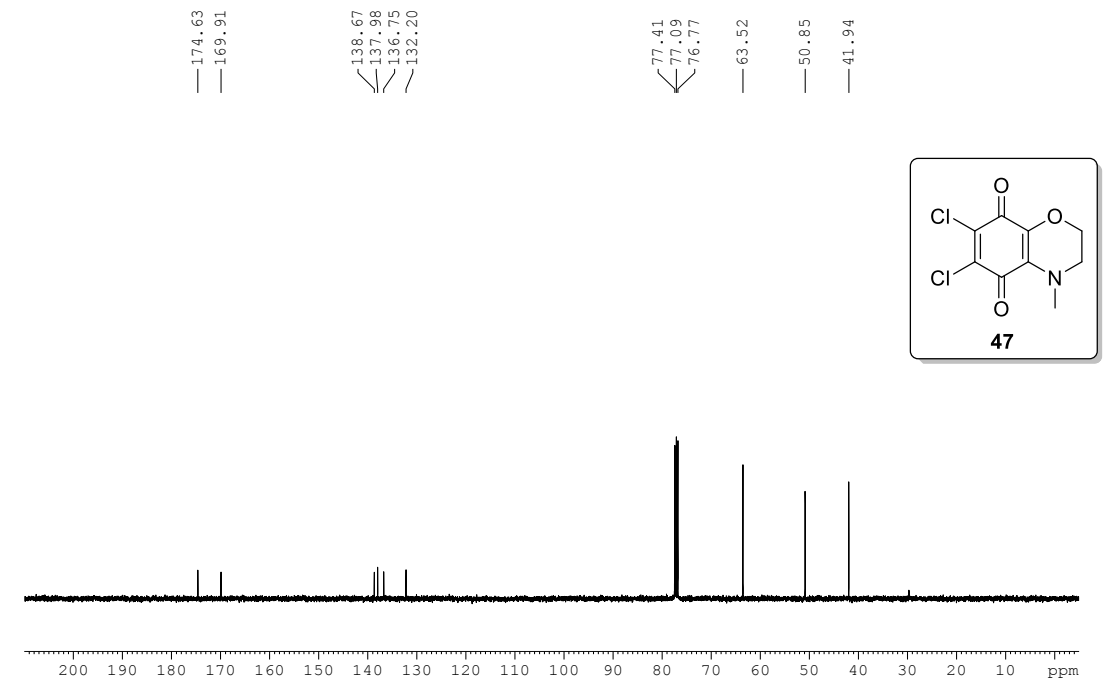

Spectrum No. 19 (Chapter 2), ^{1}H NMR Spectrum (400 MHz, $CDCl_3$)

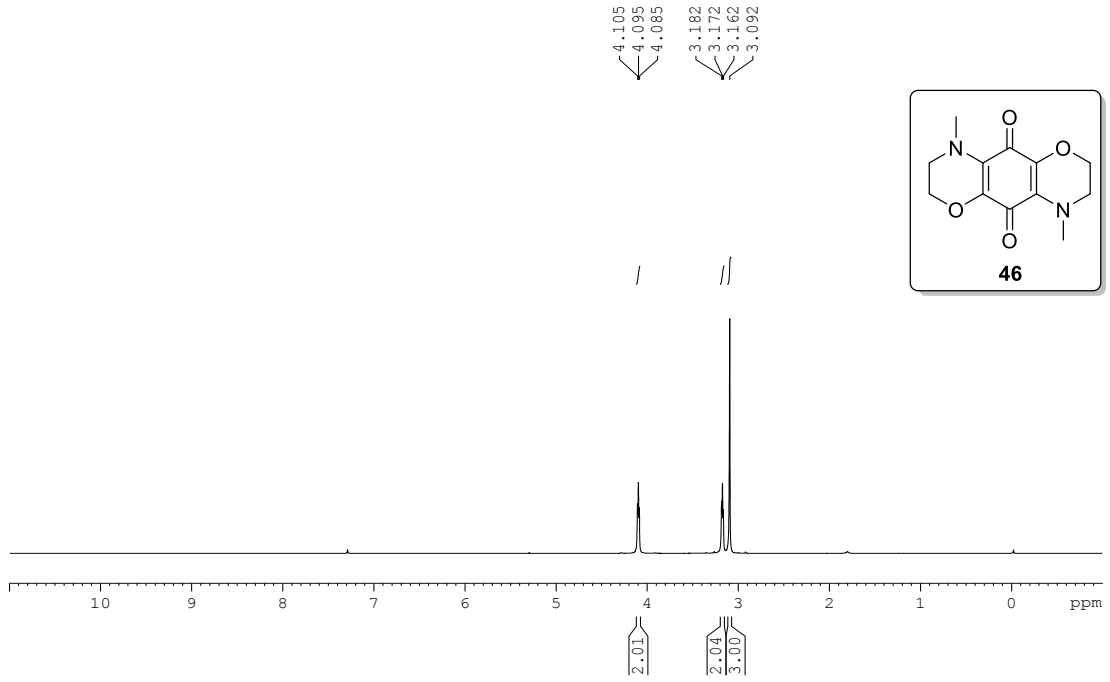

Spectrum No. 20 (Chapter 2), ^{13}C NMR Spectrum (100 MHz, $CDCl_3$)

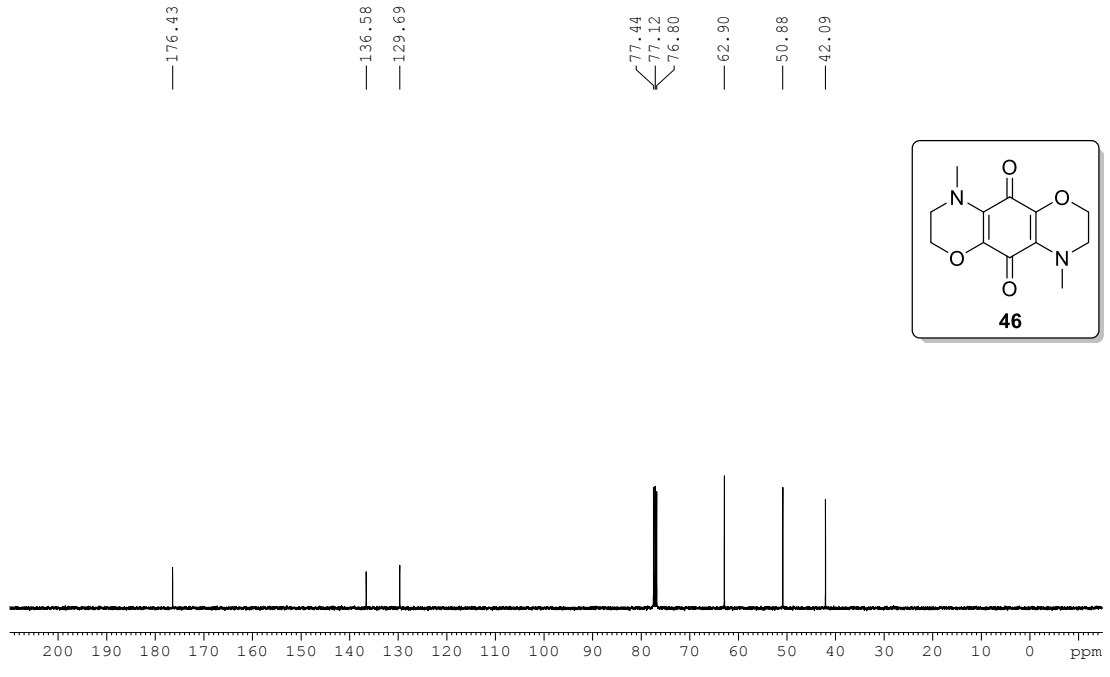

Spectrum No. 21 (Chapter 2), ^{1}H NMR Spectrum (400 MHz, $CDCl_3$)

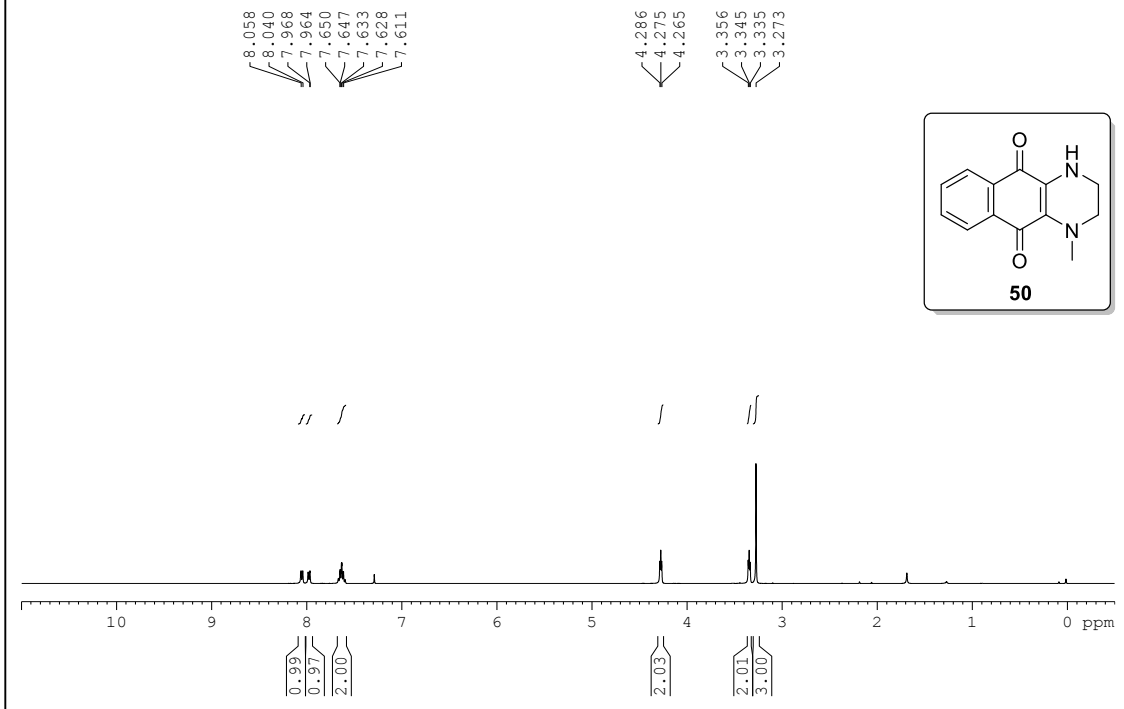

Spectrum No. 22 (Chapter 2), ^{13}C NMR Spectrum (100 MHz, $CDCl_3$)

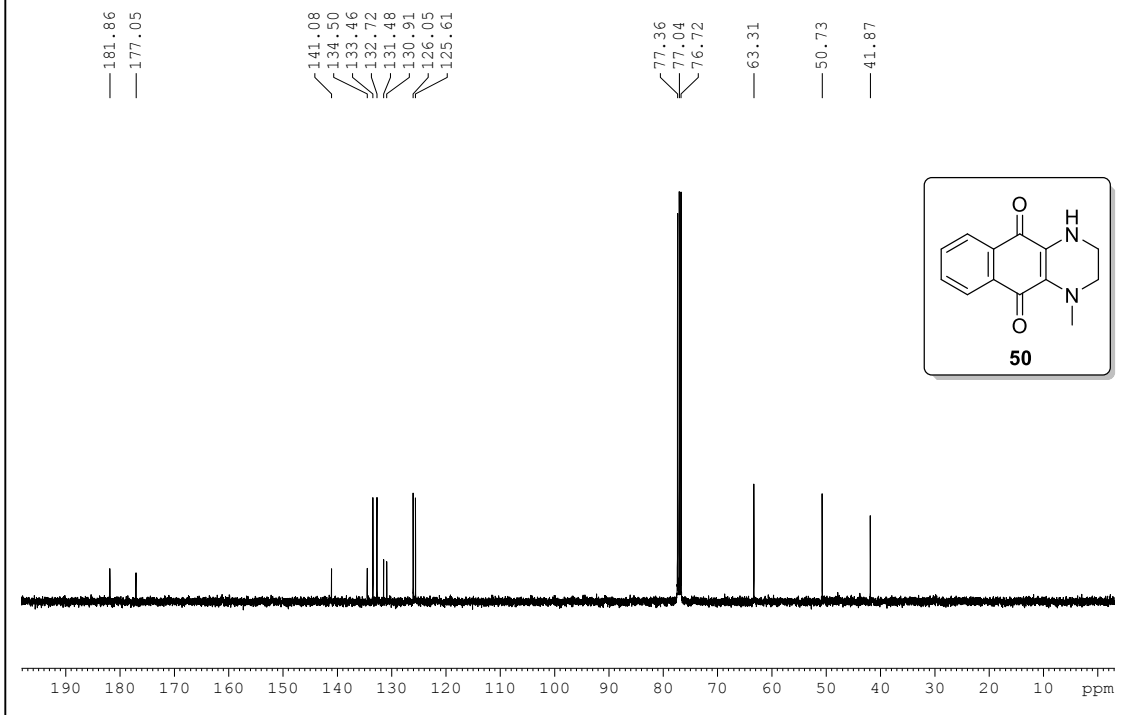

Spectrum No. 23 (Chapter 2), ^{1}HNMR Spectrum (400 MHz, $CDCl_3$)

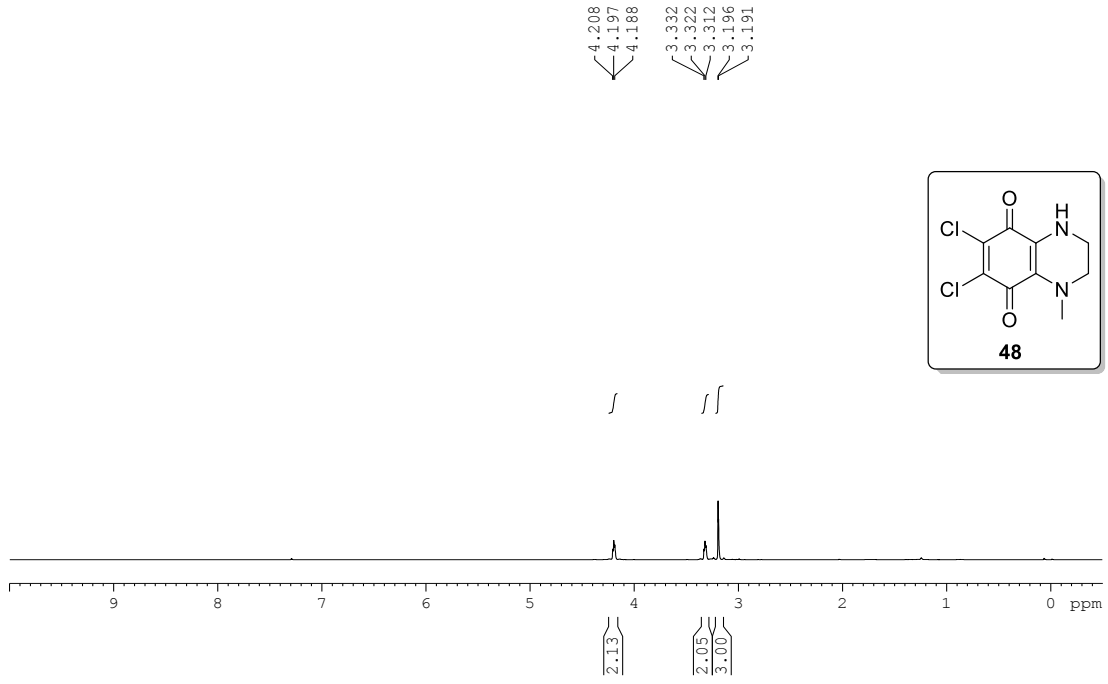

Spectrum No. 24 (Chapter 2), ^{13}C NMR Spectrum (100 MHz, $CDCl_3$)

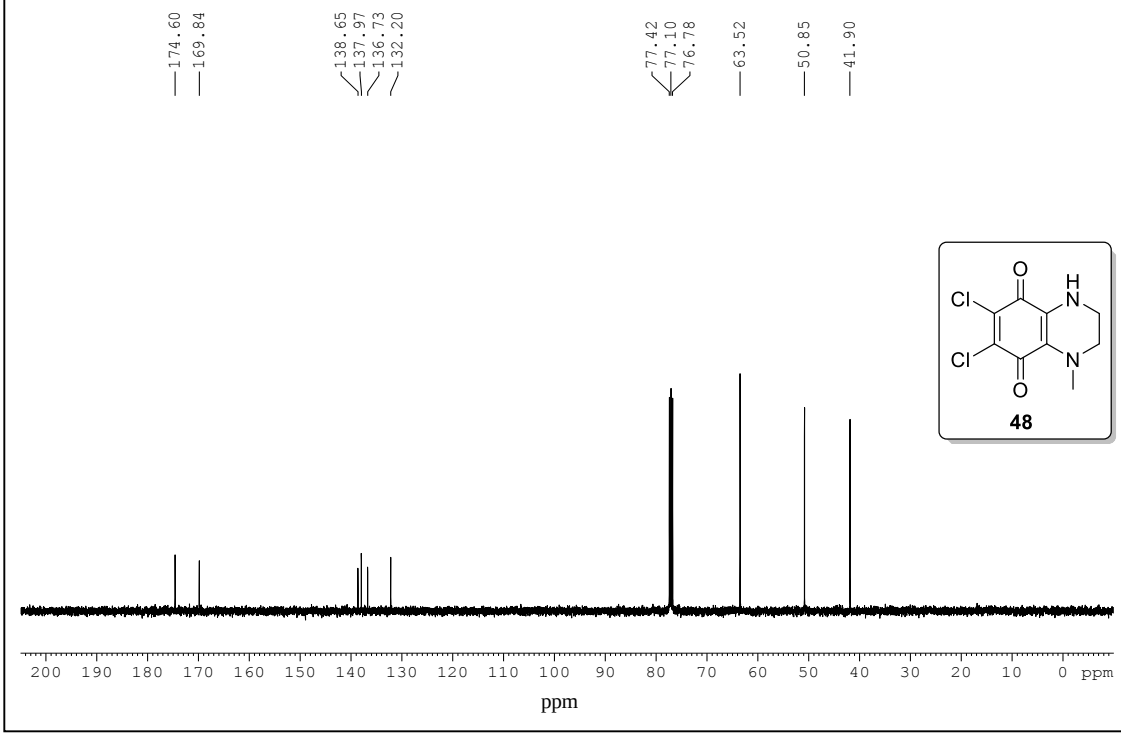

Spectrum No. 25 (Chapter 2), ^{1}H NMR Spectrum (400 MHz, $CDCl_3$)

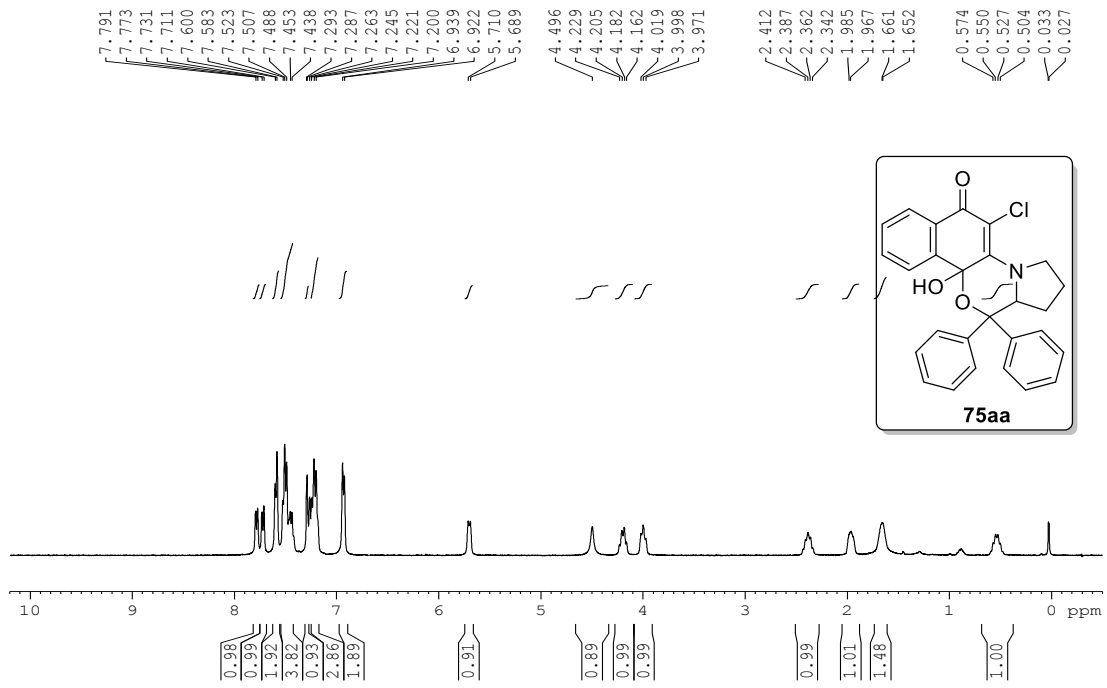

Spectrum No. 26 (Chapter 2), ^{13}C NMR Spectrum (100 MHz, $CDCl_3$)

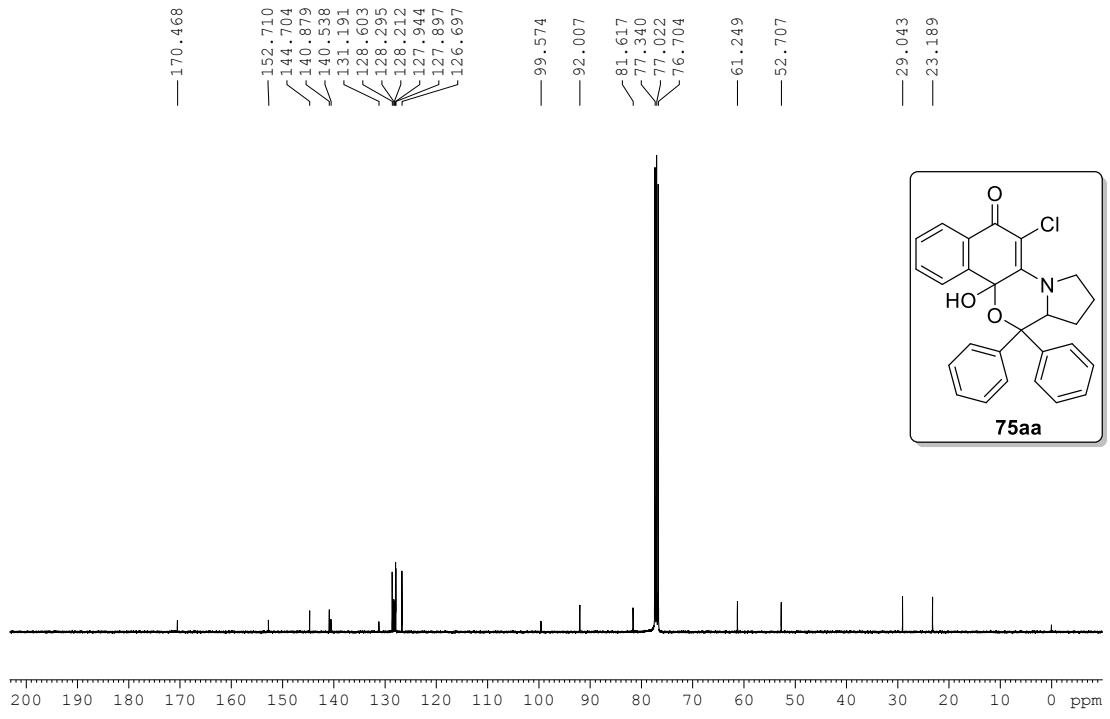

Spectrum No. 27 (Chapter 2), ^{11}H NMR Spectrum (400 MHz, $CDCl_3$)

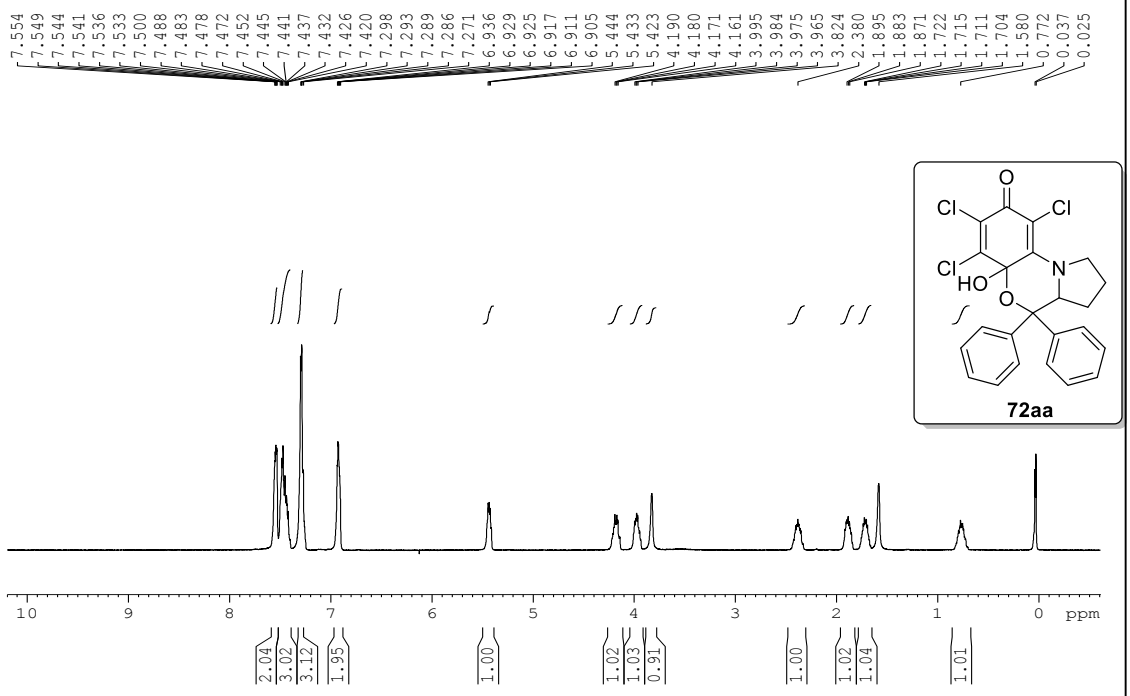

Spectrum No. 28 (Chapter 2), ^{11}C NMR Spectrum (100 MHz, $CDCl_3$)

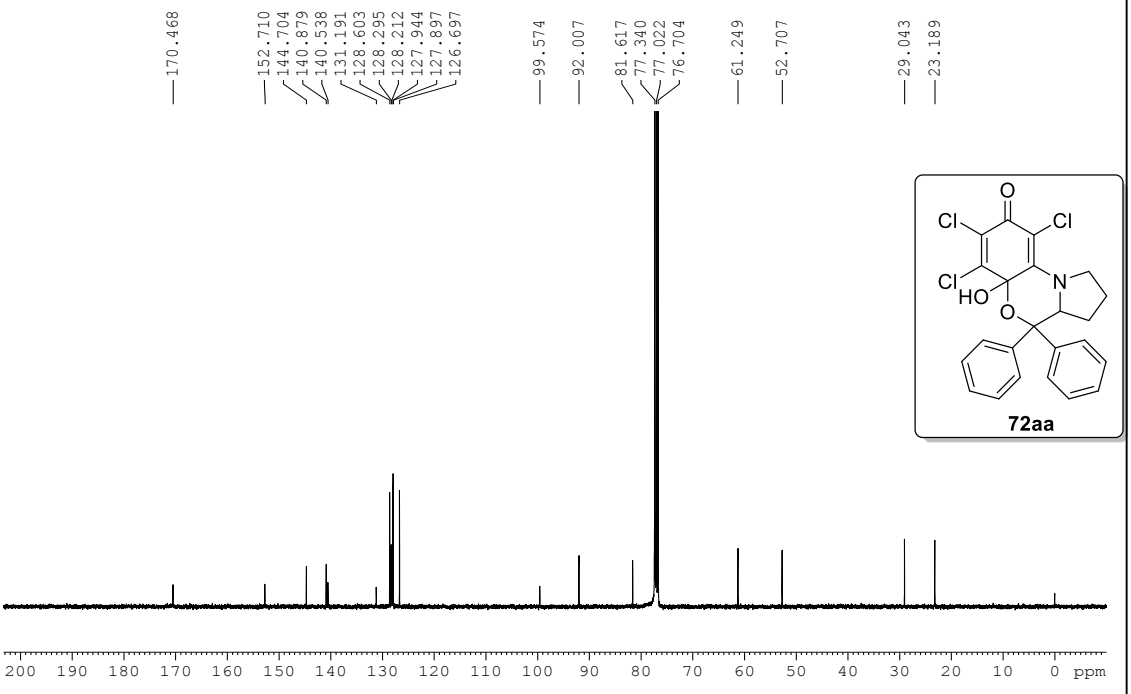

Spectrum No. 29 (Chapter 2), ^{1}H NMR Spectrum (400 MHz, DMSO d_6)

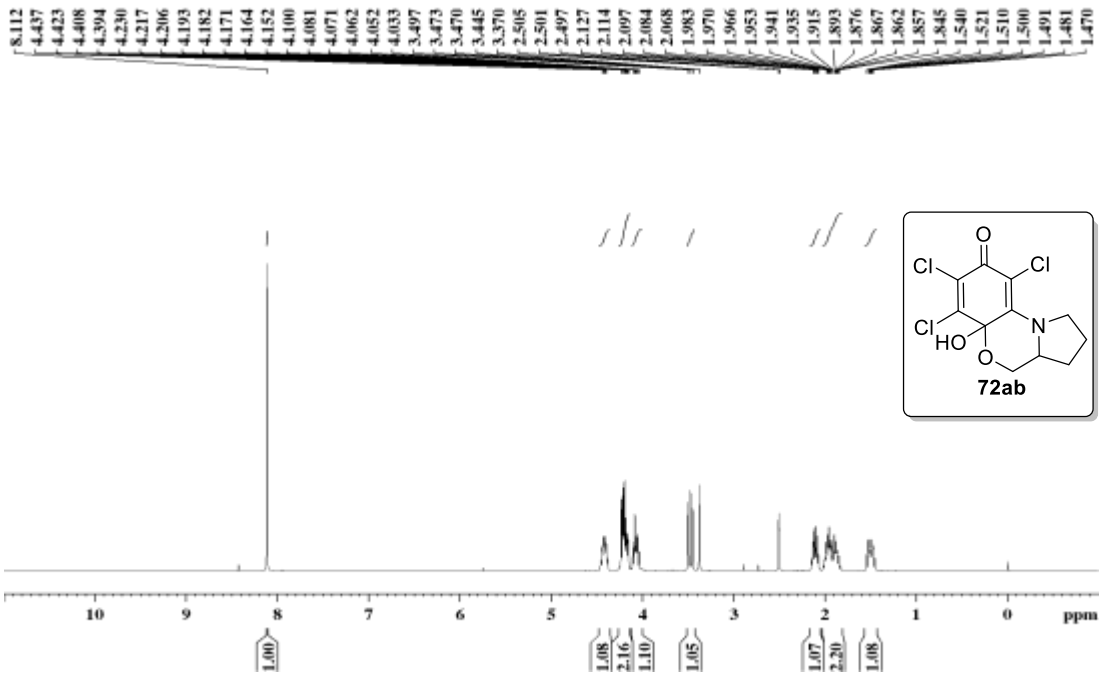

Spectrum No. 30 (Chapter 2), ^{13}C NMR Spectrum (100 MHz, DMSO d_6)

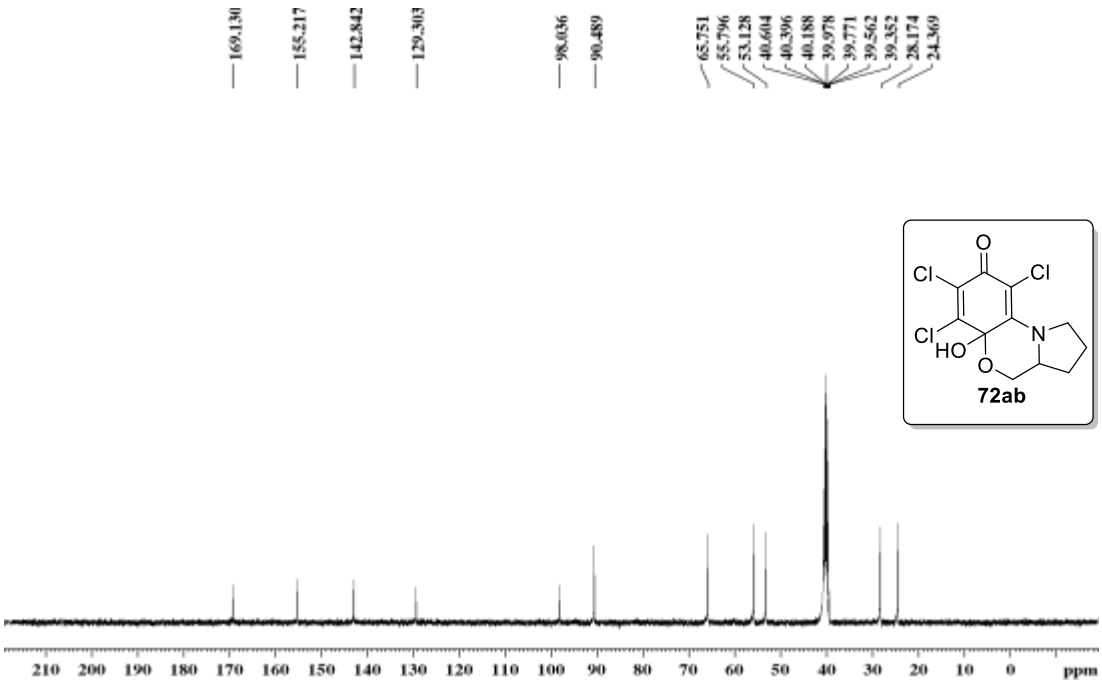

Spectrum No. 31 (Chapter 2), ^{11}H NMR Spectrum (400MHz, DMSO d_6)

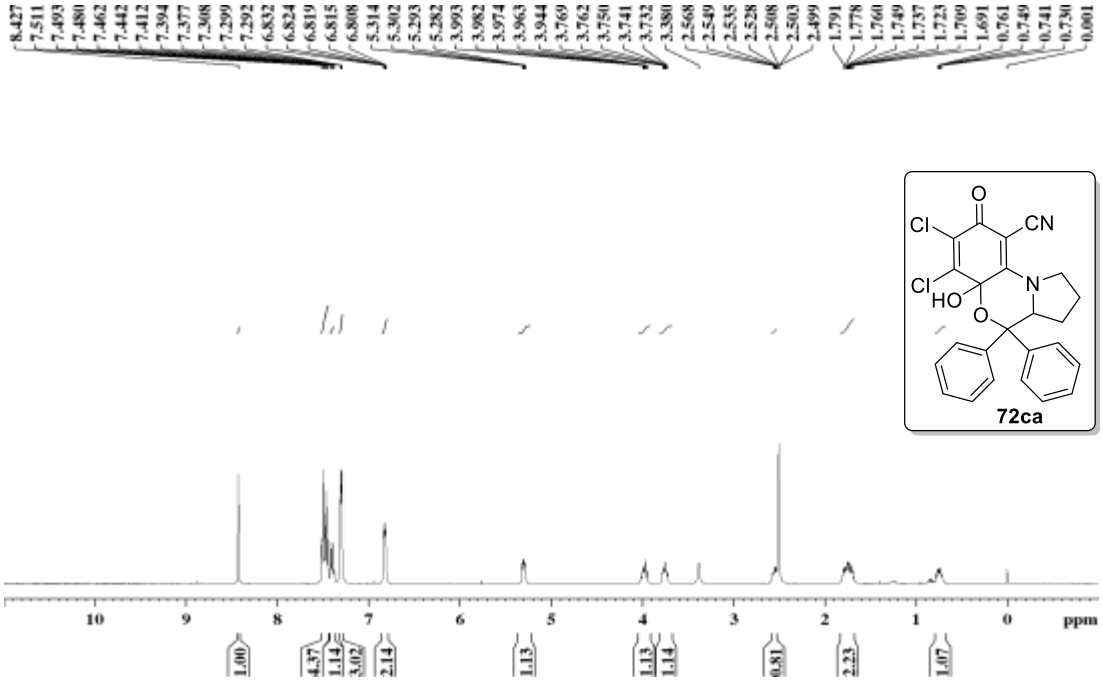

Spectrum No. 32 (Chapter 2), ^{11}C NMR Spectrum (100 MHz, DMSO d_6)

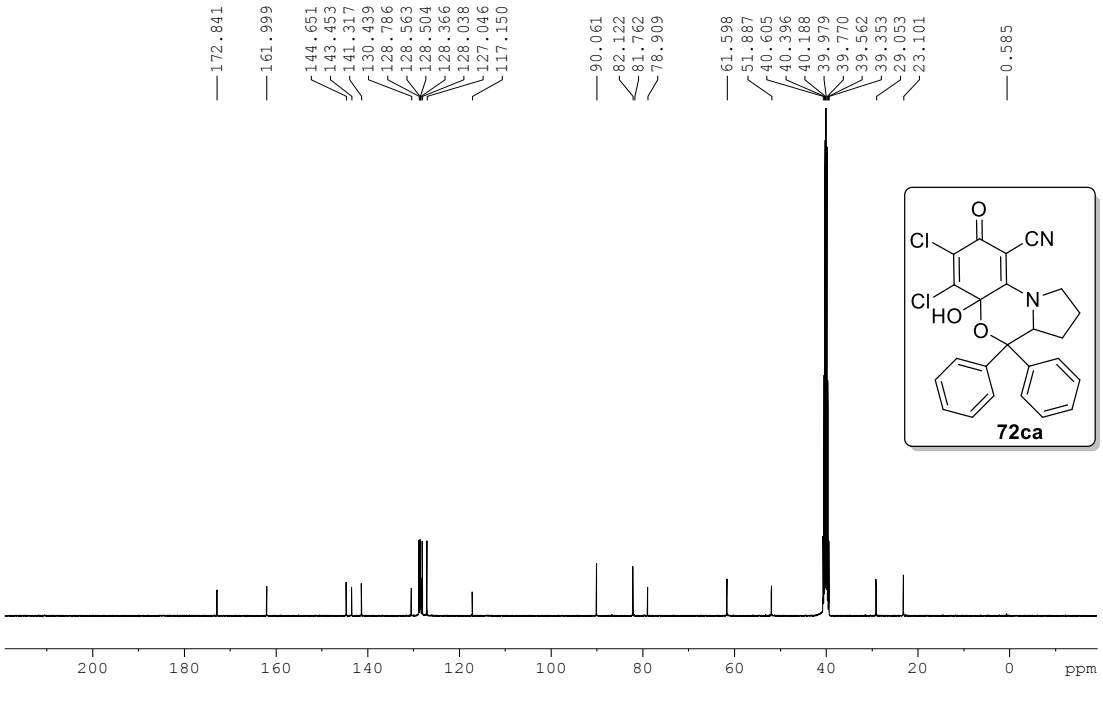

Spectrum No. 33 (Chapter 2), ^{1}H NMR Spectrum (400 MHz, $CDCl_3$)

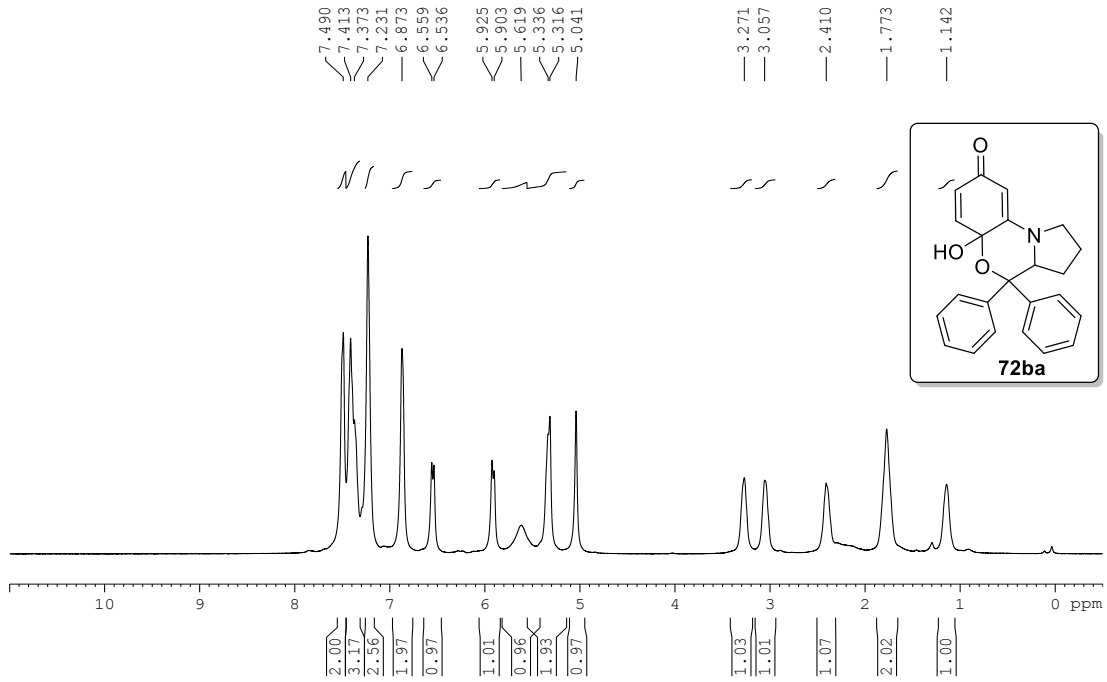

Spectrum No. 34 (Chapter 2), ^{13}C NMR Spectrum (100 MHz, $CDCl_3$)

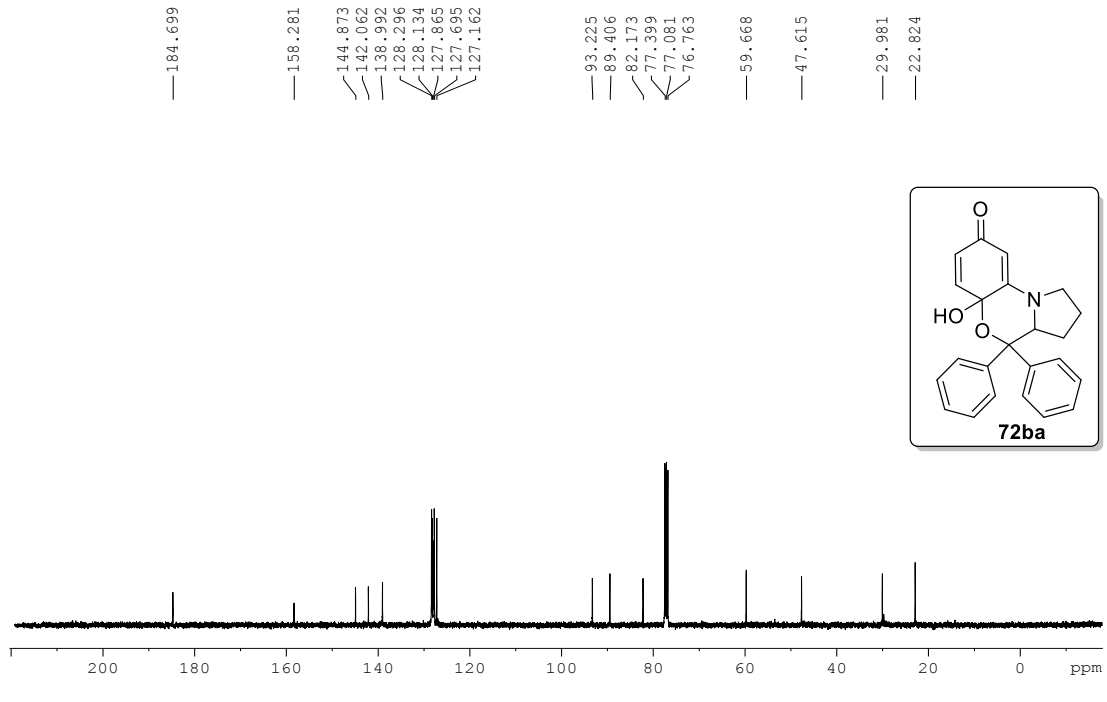

Spectrum No. 35 (Chapter 2), ^{1}H NMR Spectrum (400 MHz, DMSO d_6)

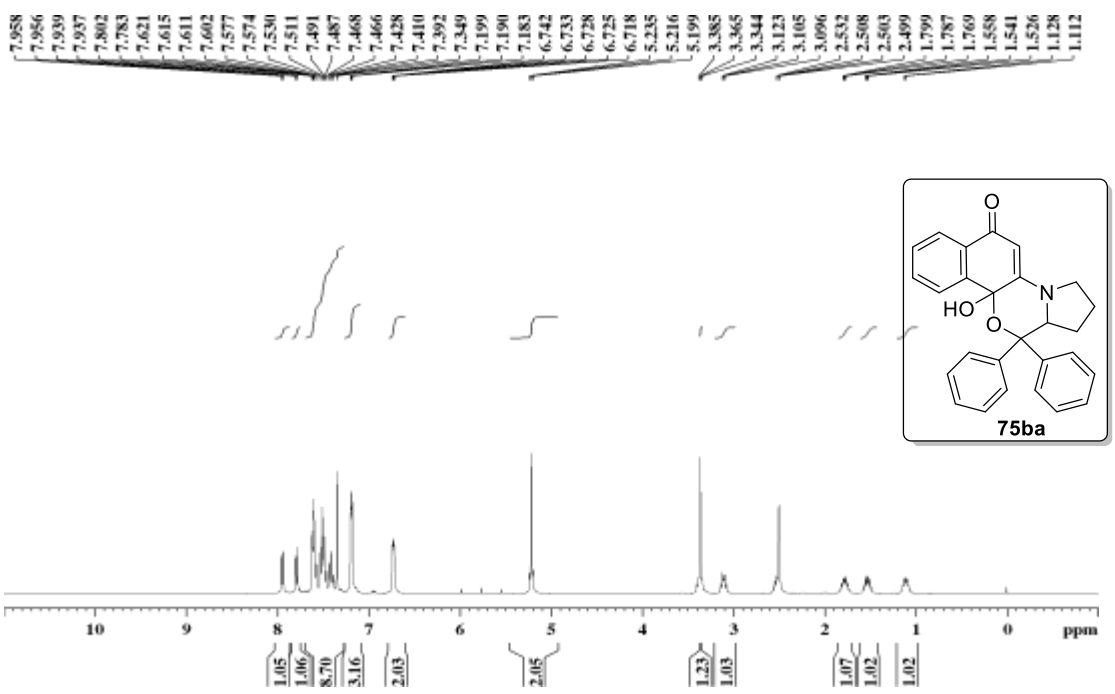

Spectrum No. 36 (Chapter 2), ^{13}C NMR Spectrum (100 MHz, DMSO d_6)

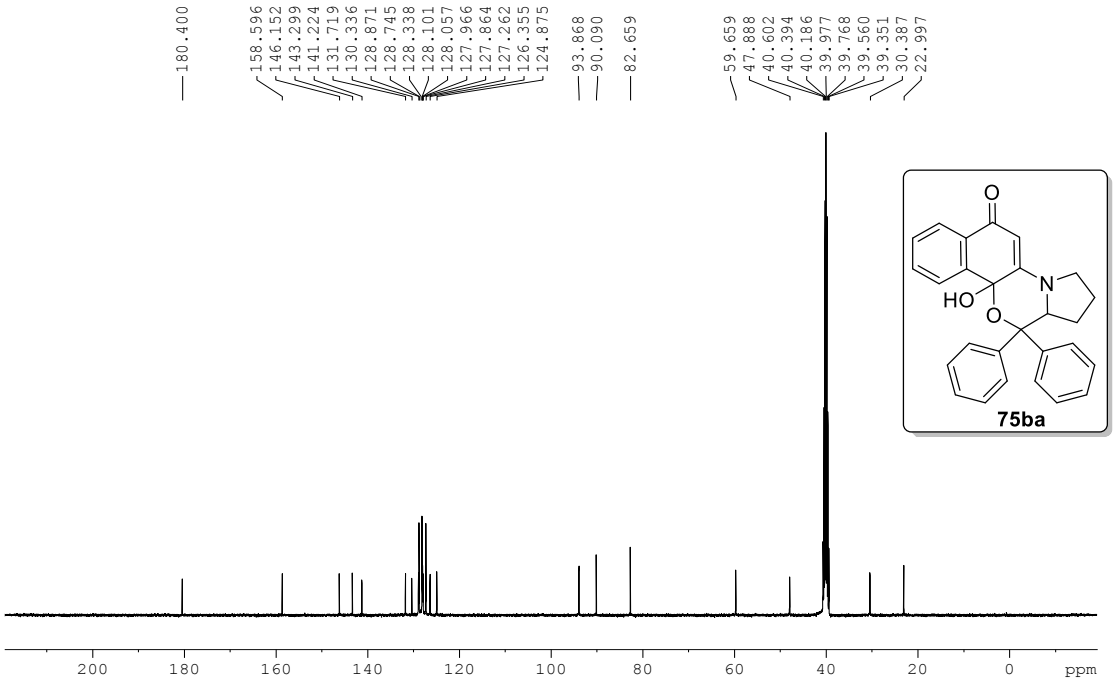

Spectrum No. 37 (Chapter 2), ^{1}H NMR Spectrum (400 MHz, $CDCl_3$)

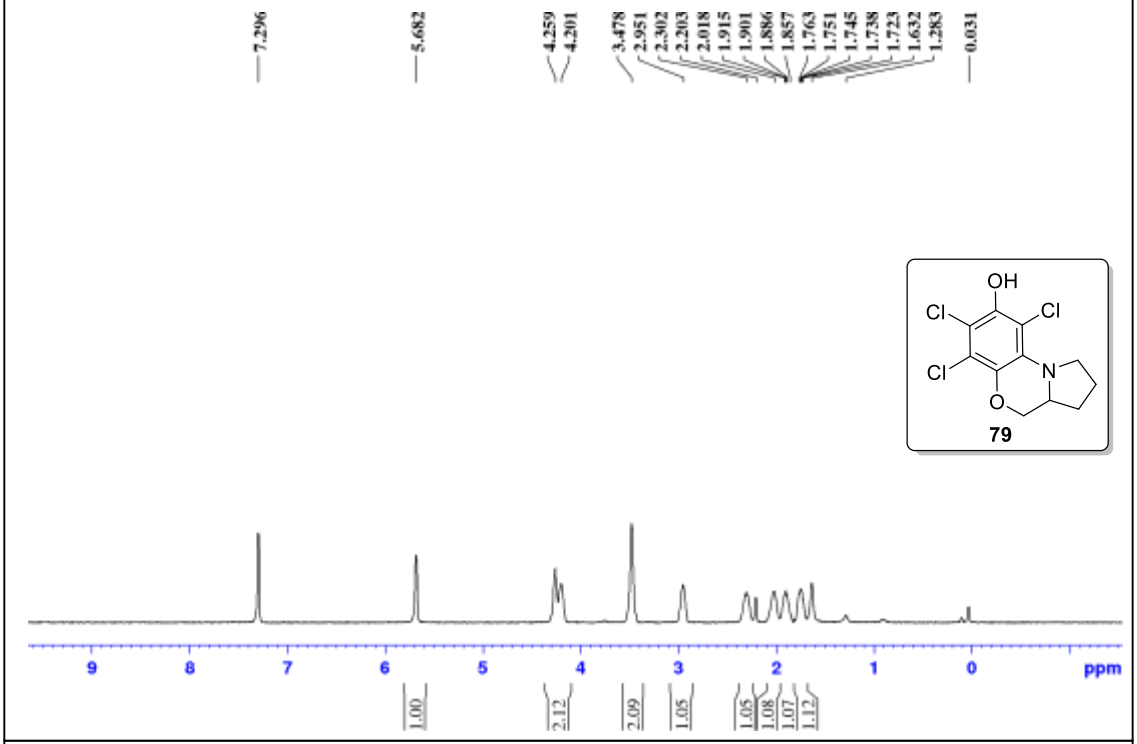

Spectrum No. 38 (Chapter 2), ^{13}C NMR Spectrum (100 MHz, $CDCl_3$)

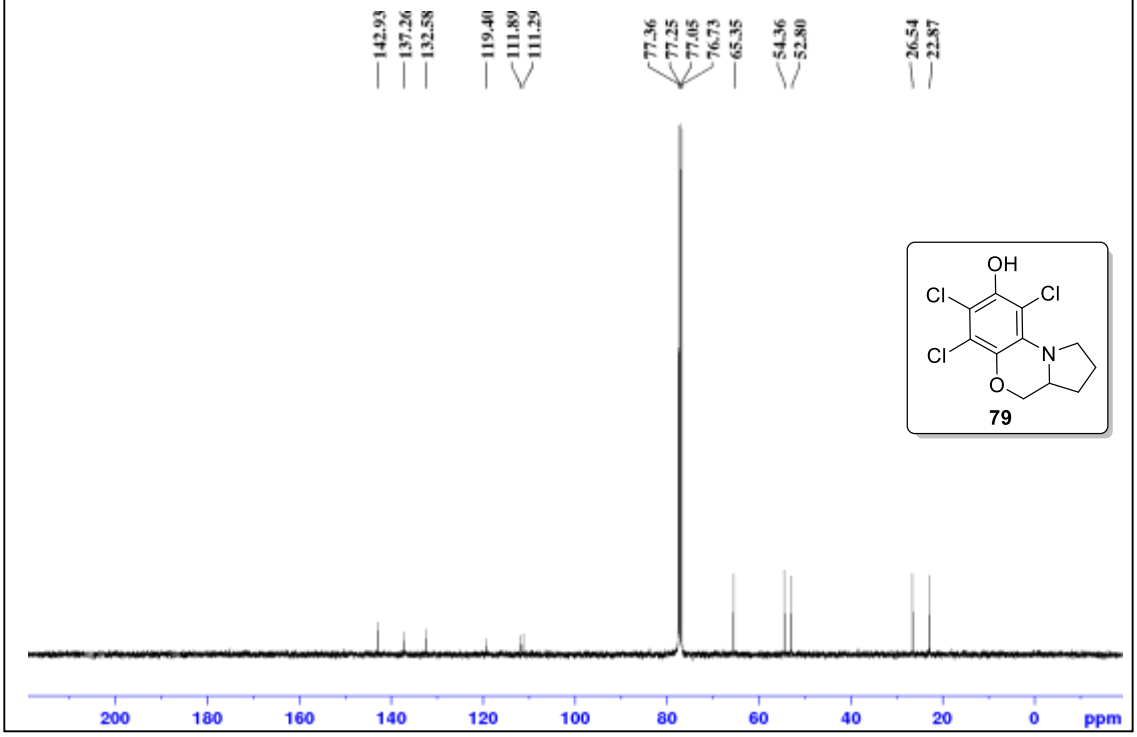

Spectrum No. 39 (Chapter 2), ^{1}H NMR Spectrum (400 MHz, $CDCl_3$)

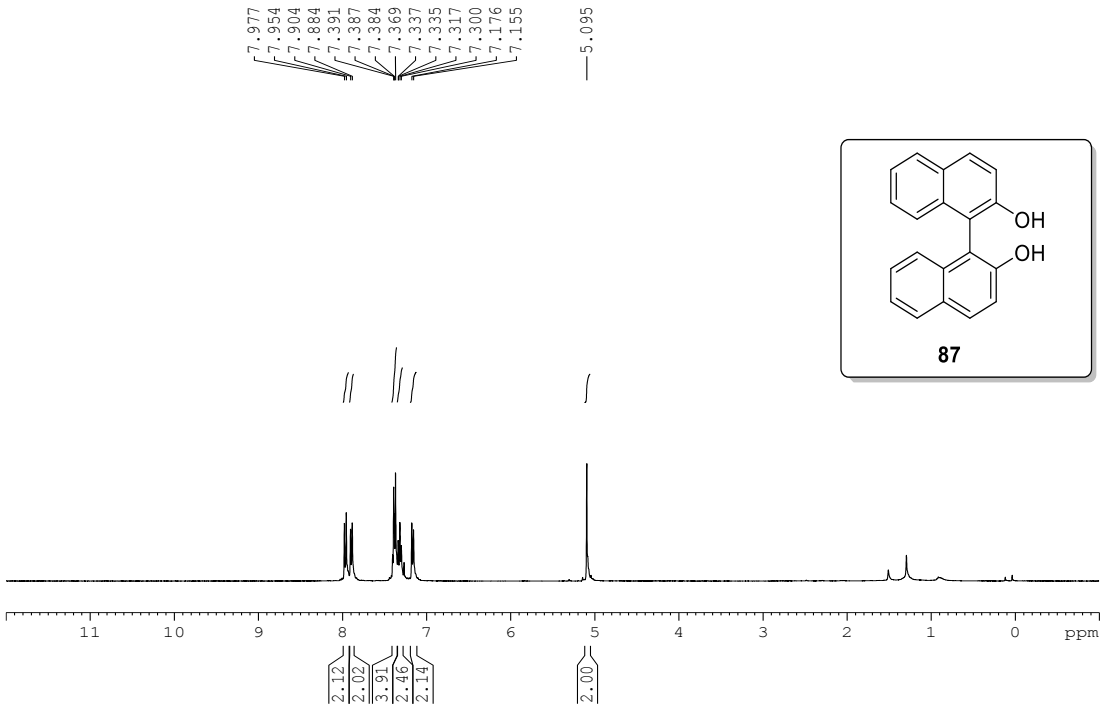

Spectrum No. 40 (Chapter 2), ^{13}C NMR Spectrum (100 MHz, $CDCl_3$)

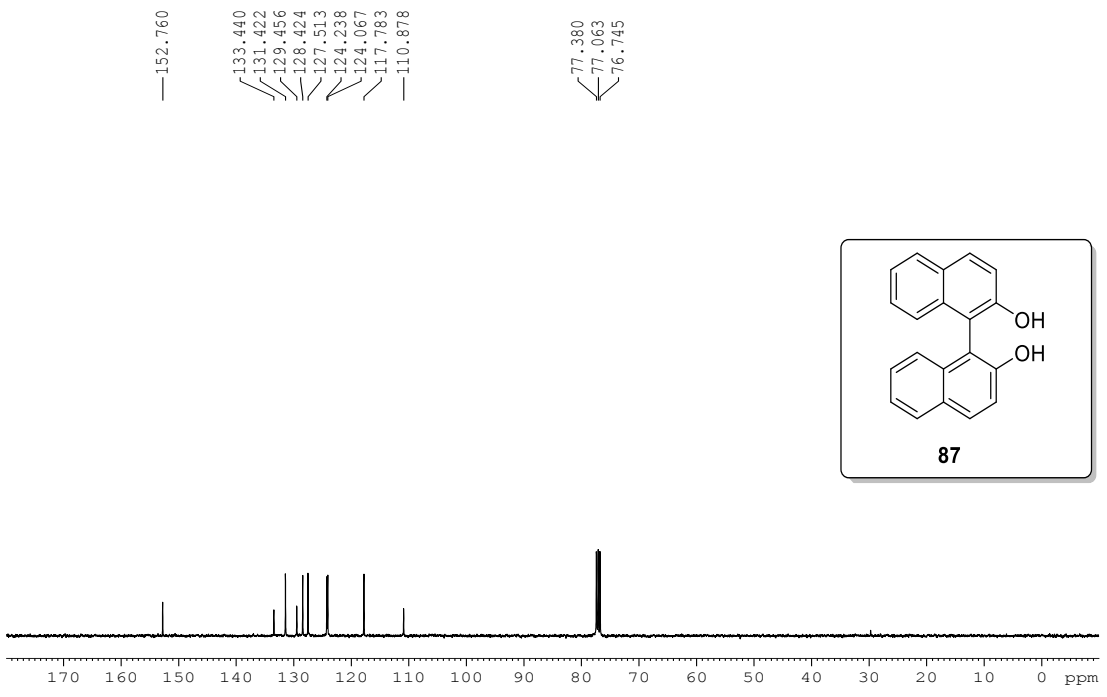

Appendix II

(X-ray Crystallographic Data)

Table 4. Atomic coordinates (x 10^4) and equivalent isotropic displacement parameters ($Å^2$x 10^3)
for compound **35c**. U(eq) is defined as one third of the trace of the orthogonalized U^{ij} tensor.

	x	y	z	U(eq)
Cl(2)	-3318(1)	3950(1)	-30(1)	56(1)
Cl(1)	-827(1)	1537(1)	485(1)	61(1)
Cl(4)	1328(1)	8269(1)	2477(1)	62(1)
Cl(3)	-2293(1)	7329(1)	1016(1)	67(1)
O(1)	3432(2)	5720(2)	2733(1)	49(1)
O(2)	2373(2)	2725(2)	1828(1)	55(1)
N(1)	4452(2)	7533(2)	6943(1)	41(1)
C(5)	5488(3)	7400(2)	5360(2)	35(1)
C(1)	3578(3)	6171(2)	3767(2)	37(1)
C(6)	5188(3)	6968(2)	4294(2)	36(1)
C(17)	-1358(3)	4493(3)	801(2)	39(1)
C(4)	4134(3)	7065(2)	5862(2)	37(1)
C(15)	1349(3)	3821(3)	1675(2)	39(1)
C(10)	7138(3)	8115(3)	5877(2)	45(1)
C(16)	-251(3)	3415(2)	1014(2)	39(1)
C(2)	2329(3)	5845(3)	4255(2)	45(1)
C(14)	1798(3)	5326(3)	2129(2)	40(1)
C(18)	-903(3)	5991(3)	1258(2)	42(1)
C(7)	6508(3)	7309(3)	3791(2)	45(1)
C(19)	690(3)	6410(3)	1923(2)	42(1)
C(3)	2608(3)	6311(3)	5302(2)	44(1)
C(9)	8395(3)	8395(3)	5373(2)	54(1)
C(12)	4369(3)	9196(3)	7201(2)	53(1)
C(8)	8076(3)	8000(3)	4324(2)	54(1)
C(11)	3289(3)	6713(3)	7425(2)	60(1)
C(13)	5056(4)	9840(3)	8311(2)	69(1)

Table 7. Atomic coordinates (x 10^4) and equivalent isotropic displacement parameters ($Å^2$x 10^3)
for compound **46**. U(eq) is defined as one third of the trace of the orthogonalized U^{ij} tensor.

	x	y	z	U(eq)
C(1)	6110(6)	5489(2)	3886(2)	24(1)
C(2)	6116(6)	6011(2)	5111(2)	23(1)
C(3)	5258(6)	5568(2)	6205(2)	22(1)
C(4)	5984(7)	7582(2)	6078(3)	30(1)
C(5)	6869(7)	7091(2)	7376(3)	29(1)
C(6)	5706(11)	5601(2)	8620(3)	46(1)
N(1)	5443(6)	6076(2)	7359(2)	28(1)
O(1)	7265(7)	5893(2)	2968(2)	45(1)
O(2)	7231(5)	6990(1)	5074(2)	31(1)

Table 9. Atomic coordinates (x 10^4) and equivalent isotropic displacement parameters ($Å^2$x 10^3)
for compound **72aa**. U(eq) is defined as one third of the trace of the orthogonalized U^{ij} tensor.

	x	y	z	U(eq)
Cl(1)	1951(1)	9135(1)	170(1)	56(1)
Cl(2)	1508(1)	6664(1)	745(1)	59(1)
Cl(3)	9523(2)	9201(1)	2484(1)	69(1)
O(1)	4865(3)	6096(2)	2555(2)	34(1)
O(2)	6050(5)	9833(2)	825(2)	57(1)
N(4)	8587(4)	6770(3)	3059(2)	46(1)
C(5)	5857(5)	8946(3)	1211(2)	42(1)
C(6)	5499(4)	6687(3)	1725(2)	35(1)
C(7)	3900(5)	8379(3)	895(2)	39(1)
C(8)	7313(4)	7356(3)	2300(2)	36(1)
C(9)	6035(5)	6246(3)	4872(3)	43(1)
C(10)	3706(5)	7355(3)	1153(2)	37(1)
C(11)	5962(4)	5272(3)	4313(2)	35(1)
C(12)	7431(5)	8410(3)	2003(3)	42(1)
C(13)	5762(5)	4334(3)	4866(2)	43(1)
C(14)	5952(5)	6263(3)	5983(3)	48(1)
C(15)	5642(6)	4358(3)	5972(3)	50(1)
C(16)	6222(4)	5272(3)	3120(2)	37(1)
C(17)	3617(7)	4013(4)	2015(3)	63(1)
C(18)	5765(5)	5319(4)	6529(3)	52(1)
C(19)	5613(6)	4196(3)	2535(2)	49(1)
C(20)	3027(11)	3054(4)	1470(4)	90(2)
C(21)	6955(9)	3380(4)	2500(4)	71(1)
C(22)	8389(5)	5589(3)	3084(3)	48(1)
C(23)	10711(6)	6246(6)	4738(4)	84(2)
C(24)	10074(6)	5237(5)	4079(4)	69(1)
C(25)	6305(13)	2411(4)	1933(5)	93(2)
C(26)	4342(13)	2261(5)	1427(4)	89(2)
C(27)	10358(6)	7140(5)	3893(4)	72(1)

O(3)	6135(4)	6045(2)	960(2)	44(1)

Table 10. Atomic coordinates (x 10^4) and equivalent isotropic displacement parameters ($Å^2$x 10^3)
for compound **72ab**. U(eq) is defined as one third of the trace of the orthogonalized U^{ij} tensor.

	x	y	z	U(eq)
C(1)	5900(3)	3558(3)	3297(1)	29(1)
C(2)	4183(3)	3742(3)	3078(1)	31(1)
C(3)	2861(3)	4636(3)	3512(2)	30(1)
C(4)	3502(3)	5209(3)	4202(1)	27(1)
C(5)	5212(3)	4935(2)	4485(1)	25(1)
C(6)	6693(3)	4281(2)	3982(1)	24(1)
C(7)	8361(4)	3524(3)	5067(2)	37(1)
C(8)	7746(3)	4986(3)	5352(1)	29(1)
C(9)	7820(4)	5093(4)	6194(2)	42(1)
C(10)	5921(5)	4636(4)	6443(2)	49(1)
C(11)	4673(4)	5299(4)	5858(2)	40(1)
N(1)	5789(3)	5174(2)	5174(1)	29(1)
O(1)	7602(2)	3152(2)	4359(1)	31(1)
O(2)	7843(2)	5423(2)	3788(1)	31(1)
O(3)	1306(3)	4809(3)	3276(1)	46(1)
Cl(1)	7423(1)	2533(1)	2801(1)	44(1)
Cl(2)	3333(1)	2942(1)	2291(1)	50(1)
Cl(3)	1959(1)	6294(1)	4675(1)	43(1)

List of publications

1 Synthesis and desymmetrization of meso-2,3-diphenylpiperazine for application in asymmetric transformations; Periasamy, M.; Edukondalu, A.; **Ramesh, E**. *ChemistrySelect*. **2017**, *2*, 3937.

2 Synthesis of iodoallenes from trisubstituted propargylamines using simple methyl iodide; Periasamy, M.; Edukondalu, A.; **Ramesh, E**. *(.to be communicated*).

3 Ambient Heat Harvesting Organic Electrochemical cell Constructed using Tertiary amines, Amide donors and *p*-chloranil acceptor. Periasamy, M.; Shanmugaraja, M.; Ramusagar, M.; Ramesh, E. (Communicated).

4 Ambient Heat Harvesting Organic Electrochemical cell Constructed using DMSO donor and *p*-chloranil acceptor. Periasamy, M.; Ramesh, E.; Shanmugaraja, M.; Ramusagar, M. (*to be Communicated*).

5 Oxidative Coupling of 2-naphthol and 1-naphthylamines using the I_2/O_2 Reagent System.; Periasamy, M.; Ramusagar, M.; Ramesh E. (*to be communicated*).

6 Synthesis of fused aminoquinones. Periasamy, M.; Ramesh E,; Ramusagar, M. (*to be communicated*).

7 Synthesis of chiralaminoquinones. Periasamy, M.; Ramesh E,; Ramusagar, M. (*to be communicated*).

8 Synthesis of *N*,*N*'-dialkylnaphthylaminoquinones and aryloxy compounds. Periasamy, M.; Ramesh E,; Ramusagar, M. (*to be communicated*).

Posters/Papers presented in symposia

1. Synthesis of Aminoquinone derivatives via Electron Transfer Reactions; Poster Presentation in the *Chemfest-2017* held at School of Chemistry, University of Hyderabad, INDIA.
2. Oxidative Coupling of 2-Naphthols using I_2/O_2 Reagent; Poster Presentation in the *Chemfest-2018* held at School of Chemistry, University of Hyderabad, INDIA.

Synthesis of Aminoquinone Derivatives and Development of Electricity Harvesting Cells using Electron Transfer Reactions

by Ramesh Eagala

Submission date: 28-Dec-2018 05:18PM (UTC+0530)
Submission ID: 1060751814
File name: 2.pdf (9.06M)
Word count: 15722
Character count: 76618

Synthesis of Aminoquinone Derivatives and Development of Electricity Harvesting Cells using Electron Transfer Reactions

ORIGINALITY REPORT

10%	5%	8%	4%
SIMILARITY INDEX	INTERNET SOURCES	PUBLICATIONS	STUDENT PAPERS

PRIMARY SOURCES

1	Submitted to University of Nevada Reno Student Paper	1%
2	Submitted to Jawaharlal Nehru Technological University Student Paper	1%
3	wiredspace.wits.ac.za Internet Source	1%
4	Ana Rocha. "Investigation of exudation from marsh plants and microorganisms and their role on bioavailability and remediation of pollutants", Repositório Aberto da Universidade do Porto, 2013. Publication	1%
5	www.docstoc.com Internet Source	1%
6	Jones-Mensah, Ebenezer, Megha Karki, and Jakob Magolan. "Dimethyl Sulfoxide as a Synthon in Organic Chemistry", Synthesis, 2016.	1%

Publication

7	Liu, Chin, and James K. Coward. "A facile and highly stereoselective synthesis of (R)- and (S)-[2-(phenylmethoxy)ethyl]oxirane", The Journal of Organic Chemistry, 1991. Publication	1%
8	Ertl, Cathrin D., Henk J. Bolink, Catherine E. Housecroft, Edwin C. Constable, Enrique Ortí, José M. Junquera-Hernández, Markus Neuburger, Nail M. Shavaleev, Mohammad Khaja Nazeeruddin, and David Vonlanthen. "Bis-Sulfone- and Bis-Sulfoxide-Spirobifluorenes: Polar Acceptor Hosts with Tunable Solubilities for Blue-Phosphorescent Light-Emitting Devices", European Journal of Organic Chemistry, 2016. Publication	<1%
9	Submitted to Thapar University, Patiala Student Paper	<1%
10	en.wikipedia.org Internet Source	<1%
11	vts.uni-ulm.de Internet Source	<1%
12	repository.ubn.ru.nl Internet Source	<1%
13	B. Lee. "Hydrothermal Preparation of BaTiO 3	